Design, Synthesis, and Application of Stimuli-Responsive Block Copolymers

by

MUHAMMAD RABNAWAZ

A thesis submitted to the Department of Chemistry

in conformity with the requirements for

the degree of Doctor of Philosophy

Queen's University

Kingston, Ontario, Canada

(April, 2013)

Abstract

This thesis reports the preparation of novel multi-responsive and multiply stimulable triblock copolymers. The resultant polymers were used to coat cotton fabrics and glass to render them amphiphobic. Further, a method was developed for the preparation of poly(ethylene glycol)-*block*-poly(hydroxyethyl methacrylate) (PEG-*b*-PHEMA) via anionic polymerization.

The multi-responsive copolymer refers to poly(ethylene glycol)-*orthonitrobenzyl*-poly[2-(perfluorooctyl)ethyl methacrylate)-*block*-poly(2-cinnamoloxyethyl methacrylate) (PEG-*ONB*-PFOEMA-*b*-PCEMA, or P1). P1 was synthesized via sequential atom transfer radical polymerization (ATRP) of FOEMA and a precursory monomer of CEMA using a PEG macroinitiator. The copolymer was multi-responsive or dual light-responsive because the *ONB* junction cleaves and PCEMA block becomes crosslinked upon UV photolysis. The multiply stimulable copolymers are a series of poly(ethylene glycol)-*disulfide*-poly[2-(perfluorooctyl)ethyl methacrylate)-*block*-poly(2-cinnamoloxyethyl methacrylate) (PEG-S_2-PFOEMA-*b*-PCEMA) copolymers. These polymers were synthesized by the end-coupling Py-S_2-PFOEMA-*b*-PHEMA and PEG-SH, and subsequent cinnamation of the PHEMA block. These polymers are multiply stimulable because the S_2 junction and PCEMA block respond to different stimulations, such as reducing agents and light, respectively. These synthetic strategies will advance the field of stimuli-responsive polymers by providing novel functional polymers for the generation of durable self-cleaning surfaces.

The above polymers form micelles in water or water/organic solvent mixtures because of the water-soluble PEG blocks. Polymer-coated cotton was obtained by immersing cotton in micellar copolymer solutions before subsequent drying and annealing treatment. Upon

photolysis, the PEG block was cleaved and the PCEMA anchoring layer became crosslinked. Such a crosslinked and stable layer was rendered amphiphobic because of the exposed PFOEMA block. A similar coating can be obtained from P2. Two types of stimulations including photolysis and reduction treatment need to be applied to yield amphiphobic textiles. This coating strategy is unique and environmentally friendly because the water- and oil-repellent coatings were prepared from an aqueous solution for the first time.

In a further study, a novel and long-sought method was developed for the anionic polymerization of PEG-*b*-PHEMA. A PEG-DPE macroinitiator was synthesized and subsequently converted into an active initiator by reaction with *sec*-butyl lithium. Consequently, the active initiator underwent polymerization with HEMA-TMS to yield PEG-*b*-P(HEMA-TMS). Upon post-polymerization modification, PEG-*b*-PHEMA was obtained with a low polydispersity of 1.08.

Acknowledgements

First and foremost, I am highly thankful to my supervisor Dr. Guojun Liu for providing me with the opportunity to work in his research group. This allowed me to accomplish my dreams. All of this became possible due to his able guidance and consistent support since the very beginning of my Ph.D. programme.

I am indebted to the contributions by members of the Liu group, both past and present, including Dr. Gabriel Njikang, Dr. Dehui Han, Dr John Dupont, Dr. Zhihan Zhou, Dr Yang Gao, Dr Dean Xiong, Xiaoyu Li, Qiliang Peng, Heng Hu, Wejiee, Jiang, and Yu Wang. Due to these amazing people, I enjoyed an excellent working environment for performing research in our laboratory. Also, I received many valuable suggestions over the years that were extremely helpful for achieving my goals.

I am also thankful to Jian Wang for AFM analysis, Xiaoyu Li for TEM analysis, and Dr Francoise Sauriol for NMR analysis. I am also thankful to Ian Wyman for his help with proofreading my thesis and providing valuable suggestions.

Special thanks also go to my parents, Khan Raziq and Afsari Begum (deceased) as well as my siblings, Nizakat Bibi, Muhammad Riaz, Israj Bibi, Muhammad Imtiaz, and Muhammad Mumtaz. I sincerely appreciate the love and support provided by my wife, Saira Naz. I don’t think I could have gone through this challenging time without you.

Finally, I would like to acknowledge the financial assistance from NSERC, Queen´s University, Faculty of Graduate Studies and the Department of Chemistry.

Statement of Originality

I hereby certify that all of the work described within this thesis is the original work of the author. Any published (or unpublished) ideas and/or techniques from the work of others are fully acknowledged in accordance with the standard referencing practices.

(Muhammad Rabnawaz)

(March, 2013)

Table of Contents

Abstract ..... **i**
Acknowledgments ..... **iii**
Statement of Originality ..... **iv**
Table of Contents ..... **v**
List of Tables ..... **ix**
List of Figures ..... **x**
List of Schemes ..... **xv**
List of Abbreviations ..... **xvii**

Chapter 1 – Introduction
1.1 Block Copolymers **01**
1.1.1 Block Copolymer Self-Assembly in Block-Selective Solvents 02
1.2 Synthesis of Block Copolymers **04**
1.2.1 Free Radical Polymerization 06
1.2.2 End-Coupling of Homopolymers 06
1.2.3 Living Anionic Polymerization 07
1.2.4 Cationic Polymerization 09
1.2.5 Controlled Radical Polymerization 10
1.2.5.1 Nitroxide Mediated Polymerization 10
1.2.5.2 Reversible Addition-Fragmentation Chain Transfer (RAFT) Polymerization 12
1.2.5.3 Atom Transfer Radical Polymerization (ATRP) 14
1.2.5.3.1 Scope of ATRP in Block Copolymer Synthesis 16
1.2.6 Post-Polymerization Modifications 17
1.3 Stimuli-Responsive Block Copolymers… 18
1.3.1 Thermoresponsive Polymers 19
1.3.2 pH-Responsive Polymers 19
1.3.3 Photo-Responsive Polymer 20
1.4 Superamphiphobic Surfaces…… 20
1.5 Polymer Characterization Techniques 22
1.5.1 Nuclear Magnetic Resonance Spectroscopy (NMR) 22
1.5.2 Size Exclusion Chromatography (SEC) 24
1.5.3 Transmission Electron Microscopy (TEM) 26
1.5.4 Atomic Force Microscopy (AFM) 27
1.6 Thesis Objectives **29**
1.7 References **33**

Chapter 2 - Design, Synthesis and Application of a Dual Light-Responsive Triblock Terpolymer
2.1 Preface **40**
2.2 Introduction **40**
2.2.1 Objectives 42
2.2.2 Experimental Design Considerations 43
2.3 Experimental Section **44**

2.4 Results and Discussion 51
2.4.1 PEG-*ONB*-Br 51
2.4.2 PEG-*ONB*-PFOEMA-Br 53
2.4.4 PEG-*ONB*-PFOEMA-*b*-PHEMA 57
2.4.5 PEG-*ONB*-PFOEMA-*b*-PCEMA 59
2.4.6 P1 Micelles 60
2.4.7 Absorption Characteristics of *ONB* and PCEMA 62
2.4.8 Micelle Photolysis 64
2.4.9 PEG-Cleft Particles 68
2.4.10 AFM Analysis of P1 Films Cast onto Glass Surfaces 71
2.5 Conclusions 72
2.6 References 73

Chapter 3 - Synthesis of Doubly Stimulable Triblock Terpolymers and their Applications for Preparing Amphiphobic Films
3.1 Preface 76
3.2 Introduction 76
3.2.1 Objectives 78
3.2.2 Experimental Design Considerations 79
3.3 Experimental 80
3.4 Results and Discussion 89
3.4.1 PEG_{113}-SH 89
3.4.2 3-(Pyridin-2-yldisulfanyl)propyl 2-bromo-2-methylpropanoate (Py-S_2-Br) 94
3.4.3 Py-S_2-$PFOEMA_{12}$-*b*-$PHEMA_{60}$ 96
3.4.4 Test for the Presence of Activated Sulfide (Py-S_2-) Among Batches of the Py-S_2-PFOEMA-*b*- PHEMA Copolymer 98
3.4.5 PEG_{113}-S_2-$PFOEMA_{12}$-*b*-$PHEMA_{60}$ 100
3.4.6 PEG_{113}-S_2-$PFOEMA_{12}$-*b*-$PCEMA_{60}$ (P2) 103
3.4.7 Synthesis of PEG_{113}-S_2-$PFOEMA_{10}$-*b*-$PCEMA_{20}$ (P3) 105
3.4.8 Reductive Cleavage of P2 and P3 107
3.4.9 Micellization of P2 109
3.4.10 Micellar Crosslinking and Coronal Chain Cleavage 112
3.4.11 PEG-Cleft Particles 113
3.4.12 PEG-Cleft Particle Films 115
3.4.13 AFM Analysis of P3-Derived Films Cast onto Glass 115
3.5 Conclusions 116
3.6 References 117

Chapter 4 – Superhydrophobic and Oleophobic Cotton Coatings Prepared from Aqueous Solutions of Block Copolymers

4.1 Preface 121
4.2 Introduction 121
4.2.1 Objectives 124
4.2.2 Experimental Design Considerations 124
4.3 Experimental 125

4.4 Results and Discussion **130**
4.4.1 Polymer Characteristics 130
4.4.2 Criteria for Selecting Polymers for the Coating Studies 131
4.4.3 Preparation of Cotton Coatings and Assessment of their Properties 132
4.4.4 Kinetics of P1-Based Coatings from Various Solvent Systems 134
4.4.5 Coating Durability Tests against Washing 138
4.4.6 Reasons for the Poor Performance of the Coatings Prepared from Water 141
4.4.7 Effect of Varying the Polymer Concentration on the Coating Performance 144
4.4.8 Effect of Varying the Photolysis Time 146
4.4.9 Effect of PEG Rinsing on Contact Angles 147
4.4.10 XPS Surface Analysis 148
4.4.11 Determination of the Copolymer Grafting Densities 150
4.4.12 Plastron Layer Formation 153
4.4.13 Application of P1 Coatings onto Semi-Cotton 154
4.5 Conclusions **155**
4.6 References **157**

Chapter 5 - Synthesis of Poly(ethylene glycol)-*block*-poly(2-hydroxyethyl methacrylate) via Anionic Polymerization
5.1 Preface **160**
5.2 Introduction 160
5.2.1 Objectives 162
5.2.2 Experimental Design Considerations 163
5.3 Experimental Section **164**
5.4 Results and Discussion **170**
5.4.1 Diphenylethylene End-Capped Polyethylene Glycol (PEG_{113}-DPE) Macroinitiator 170
5.4.2 Synthesis of PEG_{113}-*b*-$PHEMA_{260}$ from the PEG_{113}-DPE Macroinitiator 173
5.4.3 Vinylbenzyl End-Capped Polyethylene Glycol (PEG_{228}-VB) Initiator 176
5.4.4 Synthesis of PEG_{228}-*b*-PHEMA from the PEG_{228}-VB Macroinitiator 178
5.5 Conclusions **180**
5.6 References **181**

Chapter 6 – Conclusions and Future Work
6.1 Conclusions **183**
6.2 Future Work **186**

6.2.1 Facile Coating Strategy with Non-Cleavable PEG-*b*-PFOEMA-*b*-PCEMA and PCEMA-*b*-PEG-*b*-PFOEMA Copolymers 187
6.2.2 Fabrication of Cotton Coatings using PEG_{113}-CH=N-$PFOEMA_{12}$-*b*-$PCEMA_{25}$ as a pH- and Light-Responsive Triblock Copolymer 188

6.2.3 Non-Polymeric Substances as Potential Candidates for Cotton Coatings 189
6.2.4 Proposed Chemical Grafting of PFOEMA onto Cotton using PAA as a Crosslinker 190
6.3 References 192

Appendix A – Cotton Coating with PS-*b*-PCEMA, P*t*BA-*b*-PCEMA and Py-S_2-PFOEMA-*b*-PCEMA

A1. PS-*b*-PCEMA (P4), P*t*BA-*b*-PCEMA (P5) and Py-S_2-PFOEMA-*b*-PCEMA (P6) 193
A2. Preparation of Cotton Coatings from P4 and P5 193
A3. Preparation of Cotton Coatings from P6 193
A4. Assessment of the Coatings Obtained from P4 and P5 Solutions 194
A5. Assessment of the Coatings Obtained from P6 Solutions 195

A6. References 198

Appendix B – AFM Analysis of P1 Coated Fibers 199

Appendix C - List of Publications 202

List of Tables

Table 2.1. Characterization of PEG-*ONB*-PFOEMA samples collected at various intervals during the polymerization of FOEMA. 57

Table 2.2. Characteristics of P1 and its precursors at various stages of the preparation. 59

Table 3.1. Characterization of P2 and its precursors at various stages of the Preparation. ..105

Table 3.2. Molecular properties of P3 and its precursors at various stages of the preparation. 106

Table 4.1. Different polymers used in the coating studies. 130

Table 5.1. Molecular properties of polymers prepared in this study. 176

Table A1. Properties of cotton samples that had been coated with P4 and P5. 195

Table A2. Compositional analysis of the solutions prepared from P6. 196

Table A3. Properties of P6-coated cotton samples those were prepared under various conditions. 197

List of Figures

Figure 1.1. Schematic diagram of various architectural block copolymers: (a) star, (b) branched, (c) ladder, (d) bicyclic, (e) theta-ring, and (f) tadpole-shaped polymers. ……...2

Figure 1.2. Common morphologies produced by an AB diblock copolymer; (A) spheres of PS_{500}-*b*-PAA_{58}, (B) rod-like micelles of PS_{190}-*b*-PAA_{20}, (C) vesicles of PS_{410}-*b*-PAA_{20}, and (D) large compound micelles of PS_{200}-*b*-PAA_4. From Zhang, L.; Eisenberg, A. *Science,* 1995, *268*, 1728. Reprinted with permission from AAAS. 4

Figure 1.3. Common persistent radicals used for NMP. 12

Figure 1.4. Schematic illustration of the separation of a polymer mixture using a SEC column. Higher and lower molecular weight components of the mixture are shown as larger and smaller dots, respectively. A typical SEC chromatogram showing hypothetical curves corresponding to these components are also plotted as signal intensity vs. retention time. 26

Figure 1.5. A schematic diagram showing the components of an AFM system. 28

Figure 1.6. Structure of PEG-*ONB*-PFOEMA-*b*-PCEMA. 30

Figure 1.7. Chemical structure of PEG-S_2-PFOEMA-*b*-PCEMA. 31

Figure 1.8. Chemical structure of PEG-*b*-PHEMA, which was synthesized via anionic polymerization. 32

Figure 2.1. Chemical structure of PEG_l-*ONB*-$PFOEMA_m$-*b*-$PCEMA_n$ (P1). 41

Figure 2.2. ^{1}H NMR spectrum of PEG-*ONB*-OH in $CDCl_3$ at 300 MHz along with integration of the signals. 53

Figure 2.3. ^{1}H NMR spectra of PEG-*ONB*-Br (top) and PEG-*ONB*-PFOEMA (bottom) recorded in $CDCl_3$ at 300 MHz. 54

Figure 2.4. Comparison of SEC traces of PEG-*ONB*-Br, PEG-*ONB*-PFOEMA, and PEG-*ONB*-PFOEMA-*b*-PCEMA. 55

Figure 2.5. SEC traces of PEG_{113}-*ONB*-Br (and PEG_{113}-*ONB*-*b*-$PFOEMA_m$) samples collected at various intervals during the polymerization of FOEMA. 56

Figure 2.6. ^{1}H NMR spectra of PEG-*ONB*-PFOEMA-*b*-PHEMA measured in CD_3OD (top) and PEG-*ONB*-PFOEMA-*b*-PCEMA measured in $CDCl_3$ (bottom). 58

Figure 2.7. AFM topography images of P1 micelles (a), photolyzed P1 micelles (c), and a TEM image of the P1 micelles (b). The micelles were aero-sprayed from THF/water at f_{H2O} = 80%. 61

Figure 2.8. UV absorption spectra; (a) PEG-*ONB*-Br, (b) PEG-*b*-PCEMA, and (c) P1. 63

Figure 2.9. Comparision of UV absorption spectra of P1 at different photolysis times (a). Also shown are the variations in the relative absorbances at 274 and 306 nm as a function of the irradiation time (b). 65

Figure 2.10. Comparison of SEC traces of P1 containing PEG-550 that were irradiated for 0, 10, 20, and 180 min (a). Also shown is the change in the degree of PEG cleavage as a function of the photolysis time (b). 67

Figure 2.11. ^{1}H NMR spectrum of the PEG-cleft P1 particles recorded in $CDCl_3$ at 400 MHz. 69

Figure 2.12. ^{19}F NMR spectra (recorded in $CDCl_3$ at 400 MHz) of PEG_{113}-*ONB*-PFOEMA-*b*-$PCEMA_{25}$ (A), and of the PEG-cleft particles (B). 69

Figure 2.13. Photographs of H_2O droplets impregnated with rhodamine B (a and b) and CH_2I_2 droplets (c and d) on films of P1 micelles (a and c) and photolyzed P1 particles (b and d). Also shown are the variations in the contact angles of H_2O and CH_2I_2 droplets as functions of PEG cleavage (e). 70

Figure 2.14. AFM topography images showing films of photolyzed nanoparticles that were cast onto a glass plate from TFT at a smaller (left) and larger (right) scales. The root-mean square roughnesses for the two images were 8.5 and 154.0 nm, respectively.....72

Figure 3.1. Chemical structure of PEG_l-S_2-$PFOEMA_m$-*b*-$PCEMA_n$. 78

Figure 3.2. SEC traces of PEG_{113}-SH synthesized via Method 1. DMF salted with tetrabutylammonium bromide (0.25 wt.%) was used as the mobile phase. 91

Figure 3.3. ^{1}H NMR (300 MHz, recorded in $CDCl_3$) spectra of PEG_{113}-OTs (A), PEG_{113}-SAc (B), and PEG_{113}-SH (C). 93

Figure 3.4. Combined SEC traces of P2 and its precursors, Py-S_2-$PFOEMA_{12}$-*b*-$PHEMA_{60}$ and PEG_{113}-SH. The SEC traces were recorded using DMF as the eluent. 94

Figure 3.5. ^{1}H NMR (300 MHz in $CDCl_3$) spectra of 3-(pyridine-2-yldisulfanyl)propan-1-ol (bottom) and the initiator Py-S_2-Br (top). 95

Figure 3.6. ^{1}H NMR spectra of the initiator Py-S_2-Br (bottom) and the diblock copolymer Py-S_2-$PFOEMA_{12}$-*b*-$PHEMA_{60}$ (top). The spectra were recorded in $CDCl_3$ using a 300 MHz ^{1}H NMR spectrometer. 98

Figure 3.7. Plot of the absorbance vs. wavelength for the reduction of Py-S_2-$PFOEMA_{12}$-*b*-$PHEMA_{60}$ using DTT at various intervals. In the in-set, a plot of the absorbance for 2-pyridothione at 375 nm vs. reaction time is shown. The UV-visible spectra were recorded in DMF. 100

Figure 3.8. UV-visible spectra recorded during the coupling reaction between PEG-SH and Py-S_2-PFOEMA-*b*-PHEMA (a) and a plot of the absorbance at ~375 nm vs. reaction time (b). 102

Figure 3.9. ^{1}H NMR (500 MHz, $CDCl_3$) spectrum of P2, with labelled peaks. 104

Figure 3.10. SEC traces for PEG_{113}-S_2-$PFOEMA_{10}$-*b*-$PCEMA_{20}$ (P3), PEG_{113}-SH, and Py-S_2-$PFOEMA_{10}$-*b*-$PCEMA_{20}$. 106

Figure 3.11. SEC plots of a P2 solution (in DMF) recorded before (dotted line) and after (solid line) DTT addition. After 3 h of reaction with DTT, the disulfide bond had been cleaved. Signals corresponding to PEG_{113}-SH and HS-$PFOEMA_{12}$-*b*-$PCEMA_{60}$ are also visible. 107

Figure 3.12. SEC traces of Py-S_2-$PFOEMA_{12}$-*b*-$PHEMA_{60}$ and Py-S_2-$PFOEMA_{12}$-*b*-$PCEMA_{60}$. The samples were recorded using DMF as the eluent at a flow rate of 0.9mL/min. 108

Figure 3.13. SEC traces of P3 before (dotted line) and after (solid line) reaction with DTT. The samples were recorded using DMF as the eluent. 109

Figure 3.14. AFM topography (a) and TEM (b) images of P2 micelles obtained from a THF/water solution at f_{H2O} = 80%. An AFM topography image recorded after the P2 micelles underwent crosslinking and PEG-cleavage is also shown (c). The arrow in image (b) highlights a larger particle. The upper arrow in image (c) highlights an aggregate of smaller particles, while the lower arrow in that image highlights an individual particle. 111

Figure 3.15. ^{1}H NMR (300 MHz in $CDCl_3$) spectrum of the PEG-cleft particles obtained from P2. 114

Figure 3.16. AMF analysis of a glass surface that had been coated with PEG-cleft P3 particles. 116

Figure 4.1. Chemical structure of P1. 131

Figure 4.2. The images show water droplets that were placed on cotton samples that were coated with P1 using: (a) 100% aqueous solution (CA = 141 ± 1^o), (b) THF/water with f_{H2O} = 15 % (CA = 143 ± 1^o), (c) 95% ethanol (CA = 148^o ± 1^o), and (d) an aqueous DMP-containing solution (CA = 150 ± 1^o) as the dispersion solvent. The abbreviation CA refers to contact angles, while water droplets were impregnated with Rhodamine B for visual clarity…. 133

Figure 4.3. Water contact angles vs. equilibration time observed for P1 coatings prepared using 100% water, water/DMP, water/THF (at f_{H2O} = 15%), and water/ethanol (at f_{H2O} = 5%) as the solvent systems. 145

Figure 4.4. Plots of diiodomethane contact angles vs. equilibration time observed for P1 coatings prepared using 100% water, water/THF at f_{H2O} = 15%, water/ethanol at f_{H2O} = 5% and water/DMP as the solvent systems.....137

Figure 4.5. The images at the top show water droplets placed on cotton samples that were coated with P1 using (a) 100% aqueous solution (CA = 141 ± 1^o), (b) THF/water with f_{H2O} = 15 % (CA = 143 ± 1^o), (c) 95% ethanol (CA = 148 ± 1^o), and (d) water + 10 wt.% DMP (CA = 150 ± 1^o, d) as the dispersion solvent. The bottom images were recorded after 24 h washing cycles had been performed. They show water droplets placed on the washed cotton surfaces that were coated using (a1) 100% aqueous solution (CA = 0.0^o), (b1) THF/water with f_{H2O} = 15 %, (CA = 140 ± 1^o), (c1) 95% ethanol (CA = 144 ± 1^o), and (d1) water + 10 wt.% DMP (CA = 148 ± 1^o) as the P1 dispersion solvent. 139

Figure 4.6. Plots comparing the contact angles of water (A) and diiodomethane (B) droplets placed on P1-coated cotton samples before and after washing treatment. These samples were coated using aqueous solutions of P1 containing the DMP additive (10 wt.%). 140

Figure 4.7: Figure 4.7: AFM image of P1 micelles from (a) 100% aqueous solution, and (b) aqueous solution with DMP. 141

Figure 4.8. An SEM image of uncoated cotton (A). Also shown are SEM images of a cotton sample that had been coated with P1 using an aqueous solution containing the DMP additive both before (B), and after (C) annealing treatment. An AFM image (D) is also shown of a cotton fiber that had been coated with an aqueous P1 solution containing no DMP and subsequently annealed. 144

Figure 4.9. Plot showing the variation of the contact angles for water and diiodomethane droplets with changes in the concentrations of the P1 coating solutions. The cotton samples were immersed into various solutions for 40 min, and photo-crosslinked for 1 h. 145

Figure 4.10. Plot of the changes in the contact angles of water and diiodomethane droplets vs. the duration of photo-crosslinking. 146

Figure 4.11. Plot of the water and diiodomethane contact angles vs. the rinsing time employed to remove the cleaved PEG chains from P1-coated cotton samples. 148

Figure 4.12. XPS spectra of PFOEMA, an uncoated cotton sample, a P1-coated cotton sample, and a "P1-coated-washed" cotton sample. The term P1-Coated-Washed means that the samples had been coated with P1 and subsequently extracted with THF for 2 h to remove the cleft PEG chains and other loosely held polymer residues. 149

Figure 4.13. Comparison of TGA curves for P1, uncoated cotton, and cotton samples that were coated with P1 and subsequently washed with THF. In the legend above cotton is abbreviated as C.). 151

Figure 4.14. Plot comparing water and diiodomethane droplet contact angles vs. P1 content (wt.%) among cotton samples prepared using DMP-containing 100% aqueous P1 dispersions. 152

Figure 4.15 Pictures of an uncoated cotton fabric (a) and a P1-coated cotton sample (b) upon immersion into water. The coated cotton sample formed a plastron layer upon immersion into water, as evidenced by the reflections visible on its surface (b).....154

Figure 4.16 Water (left) and diiodomethane (right) droplets placed onto coated samples of pure cotton (a) and semi-cotton (b). The pictures were taken 2 min after the droplets had been applied onto the surfaces. The P1 coatings were prepared using 100% aqueous dispersions containing DMP. The droplets were impregnated with Rhodamine B for visual clarity……155

Figure 5.1. Structures of PEG_{113}-DPE and PEG_{113}-*b*-$PHEMA_{260}$. 163

Figure 5.2. ^1H NMR spectra (recorded at 300 MHz in $CDCl_3$) of 4-(3-bromopropyl) benzophenone (bottom) and DPE-Br (top). 171

Figure 5.3. ^1H NMR spectra of PEG_{113}-DPE ($CDCl_3$, 300 MHz, top) and PEG_{113}-*b*-$PHEMA_{260}$ (CD_3OD, 300 MHz, bottom). 173

Figure 5.4. SEC traces for PEG_{113}-*b*-$PHEMA_{260}$ and PEG_{113}-DPE. The samples were recorded using DMF as the mobile phase at a flow rate of 0.9 mL/min. 175

Figure 5.5. ^1H NMR spectrum (300 MHz in $CDCl_3$) of PEG_{228}-VB. 177

Figure 5.6 SEC traces of PEG_{228}-VB before the addition of *sec*-butyllithium addition and PEG_{228} after *sec*-butyllithium had been added and the VB group had been lost. 179

Figure 6.1. Possible chain packing patterns of two different systems. Scheme A depicts an ABC triblock copolymer in which the A and C blocks are more compatible with each other than with the middle B block. Scheme B depicts an ABC block copolymer in which the A and B blocks are more miscible with each other than with the terminal C block. Reprinted from Synthesis and morphological studies of polyisoprene-*b lock*-polystyrene-*b lock*-poly(vinylmethyl ether) triblock terpolymer, Yamauchi, K.; Hasegawa, H.; Hashimoto, T.; Kohler, N.; Knoll, K. *Polymer,* vol. 43, p. 3563, 2002, with permission from Elsevier.…..188

Figure A1. Images of water droplets placed on uncoated cotton (a), a cotton sample that was coated with P4 (b), and a cotton sample that was coated with P5. Images were recorded 2 min after application of the water droplet. 194

Figure A2. Images of solutions a, b, and c, which were prepared for coating experiments using P6. 196

Figure B1. AFM images of aqueous P1 solutions (a), P1-coated cotton before annealing treatment (b), and a P1-coated cotton sample after annealing treatment (c). 200

Figure B2: AFM images for P1 aqueous solutions with DMP, (a), coated cotton after annealing. 201

List of Schemes

Scheme 1.1. Flow-chart diagram showing various categories of synthetic strategies for the preparation of block copolymers 5

Scheme 1.2. End-coupling of pre-made polymer chains to form an AB diblock copolymer. ..7

Scheme 1.3. A generalized synthetic pathway for an anionic polymerization.....8

Scheme 1.4. Resonance stabilization of an anion during polystyrene synthesis. 9

Scheme 1.5. A generalized cationic polymerization mechanism. 10

Scheme 1.6. An equilibrium favoring polymer growth in an NMP reaction. Reprinted from Controlled/living radical polymerization: Features, developments, and perspectives, Braunecker, W.A.; Matyjaszewski, K. *Prog. Polym. Sci.* vol. 32, 2007, with permission from Elsevier. 11

Scheme 1.7. Initiation and chain transfer steps occurring in a RAFT polymerization. Reprinted from Stimuli-responsive amphiphilic (co)polymers via RAFT polymerization, Smith, A.E.; Xu, X.; McCormick. C.L. *Prog. Polym. Sci.* vol. 35, p. 47, 2010, with permission from Elsevier. 13

Scheme 1.8. Key equilibrium process in an ATRP reaction. Reprinted with permission from Matyjaszewski, K.; Xia, J.H. *Chem. Rev.* **2001,** *101*, 2921. Copyright (2001) American Chemical Society. 14

Scheme 1.9. Hydrolysis of P*t*BA, yielding PAA through the cleavage of the *tert*-butyl group. 17

Scheme 1.10. Post-polymerization modifications of P(HEMA-TMS) to prepare PCEMA. 18

Scheme 1.11. The [2+2] cycloaddition of two 2-cinnamoyloxyethyl methacrylate units upon exposure to UV light. 18

Scheme 2.1. Schematic representation of P1 micelles before and after photolysis treatment. The photograph in the inset shows a water droplet placed onto a film that had been cast from a dispersion of the PEG-cleft particles. 43

Scheme 2.2. Reactions used to synthesize PEG_l-*ONB*-Br.....52

Scheme 2.3. Schematic depiction of the *ONB* rearrangement.....
.....64

Scheme 3.1. Schematic representation of the preparation of PEG_{l}-$\mathit{S_2}$-$PFOEMA_{\mathit{m}}$-*b*-$PCEMA_{\mathit{n}}$ via an end-coupling reaction, and its subsequent micellization in a THF/water solvent mixture. The steps involving photo-crosslinking of the micelles as well as cleavage of the PEG chains are also shown. 79

Scheme 3.2. Synthetic pathway toward PEG_{113}-SH via Method 2. 90

Scheme 3.3. Synthetic strategy for the preparation of the Py-$\mathit{S_2}$-Br initiator. 95

Scheme 3.4. Various reactions involved in the preparation of Py-$\mathit{S_2}$-$PFOEMA_{12}$-*b*-$PHEMA_{60.}$ 96

Scheme 3.5. Cleavage of Py-$\mathit{S_2}$-PFOEMA-*b*-PHEMA upon reaction with DTT. 99

Scheme 3.6. Synthetic pathway for preparing PEG_{113}-$\mathit{S_2}$-$PFOEMA_{12}$-*b*-$PHEMA_{60}$ by the end-coupling of PEG_{113}-SH with Py-$\mathit{S_2}$-$PFOEMA_{12}$-*b*-$PHEMA_{60}$. 102

Scheme 3.7. Schematic representation of P3 micelles before and after crosslinking and DTT treatment. Water and diiodomethane droplets placed on a film cast from a dispersion of the PEG-cleft P3 particles are also shown. 113

Scheme 4.1. Illustration of steps involved in the preparation of cotton coatings from micellar P1 solutions. 123

Scheme 5.1. Synthetic pathway for the preparation of 1-(4-(3-bromopropyl)phenyl)-1-phenylethylene (DPE-Br). 171

Scheme 5.2. Synthetic pathway followed for the preparation of PEG_{113}-*b*-$PHEMA_{260}$. 172

Scheme 5.3. Synthesis of PEG_{228} from EO, and subsequent reaction with VBC. 177

Scheme 5.4. Attempted synthesis of PEG_{228}-VB-*b*-PHEMA via anionic polymerization with PEG_{228}-VB as the macroinitiator. 179

Scheme 6.1. The preparation of a dynamic pH- and light-responsive triblock terpolymer ..189

Scheme 6.2. Steps required for the synthesis and grafting of fluorinated molecules onto cellulose. 190

Scheme 6.3. Grafting of PFOEMA onto cellulose using PAA as a crosslinking reagent. …191

List of Abbreviations

^{1}H NMR	proton nuclear magnetic resonance
σ	standard deviation
χ	Flory-Huggins interaction parameter
η	viscosity
[η]	intrinsic viscosity
3-D	three dimensional
Å	angstrom (1 Å = 10^{-10} m)
Ac	acetyl group
AFM	atomic force microscopy
AIBN	azobisisobutyronitrile
ATRP	atom transfer radical polymerization
BC	block copolymer
cmc	critical micellization concentration
CO_2H	carboxylic acid
CRP	controlled radical polymerization
CP	cationic polymerization
cp	cyclopentane
CuBr	cuprous bromide
$CuBr_2$	cupric bromide
CTA	chain transfer agent
d_1	relaxation time
DCC	*N*,*N'*-dicyclohexylcarbodiimide
DMAP	4-dimethylaminopyridine
D_h	hydrodynamic diameter
DLS	dynamic light scattering
DMF	*N*,*N*-dimethylformamide
DMP	dimethyl phthalate
DPE	diphenylethylene
dn_r/dc	refractive index increments
DTBA	(2S)-2-amino-1,4-dimercaptobutane (dithiobutylamine)
DTT	dithiothreitol
EtOH	ethanol
f	volume fraction
^{19}F NMR	fluorine-19 nuclear magnetic resonance
FID	free induction decay
M_w	weight average molecular weight
H_o	magnetic field
HCl	hydrochloric acid
LCST	lower critical solution temperature
LS	light scattering

M	mol/litre
MA	micelle-like aggregate
mg	milligram
MHz	megahertz
mL	millilitre
MMA	methyl methacrylate
mol%	molar percentage
$NaOH_{aq}$	aqueous sodium hydroxide
nm	nanometre (1 nm = 10^{-9} m)
NMP	nitroxide mediated polymerization
NMR	nuclear magnetic resonance
ONB	*ortho*-nitrobenzyl
OsO_4	osmium tetraoxide
PAA	poly(acrylic acid)
PCL	poly(caprolactone)
PCEMA	poly(2-cinnamoyloxyethyl methacrylate)
PCEMA-*b*-P*t*BA	poly(2-cinnamoyloxyethyl methacrylate)-*block*-poly(*tert*-butyl acrylate)
PDI or M_w/M_n	polydispersity index
PDMA	poly(*N*,*N*-dimethylacrylamide)
PDMAEMA	poly(*N*,*N*-dimethylaminoethyl methacrylate)
PEG	poly(ethylene glycol)
PEGA-*b*-PFBA	poly[oligo(ethylene glycol) monomethyl ether acrylate]-*block*-poly(1H,1H-perfluorobutyl acrylate)
PEG-CHO	aldehyde-end-functionalized PEG
PEG-OCH_3	poly(ethylene glycol) monomethyl ether
PEG-DPE	diphenylethylene-end-functionalized PEG
PEO-OH	poly(ethylene oxide)
PEG-OAc	thioacetate-end-functionlized PEG
PEG-OTs	α-methoxy-ω-toluenesulfonyl-PEG
PEG-SH	thiol-end-functionlized PEG
PEO-*b*-PS	poly(ethylene oxide)-*block*-poly(styrene)
PEG-VB	vinylbenzyl-end-functionalized PEG
PFOEMA	poly(perfluorooctylethyl methacrylate)
PFOEMA-*b*-PCEMA	Poly(perfluorooctylethyl methacrylate)-*block*-poly(2-cinnamoloxyethyl methacrylate)
PHEMA	poly(2-hydroxyethyl methacrylate)
P(HEMA-TMS)	poly(trimethylsiloxyethyl methacrylate)
PL	poly(lactide)
PMA	poly(methacrylate)
PMDETA	*N,N,N′,N″,N″*-pentamethyldiethylenetriamine
PMMA	poly(methyl methacrylate)
PMAA	poly(methacrylic acid)

PNIPAM	poly(*N*-isopropylacrylamide
POEGA	poly(oligoethylene glycol acrylate)
POEOMA	poly(oligo(ethylene glycol) monomethyl ether methacrylate)
PPO	poly(propylene glycol)
PS	polystyrene
PS-*b*-PAA	poly(styrene)-*block*-poly(acrylic acid)
P2VP	poly(2-vinyl pyridine)
P4VP	poly(4-vinyl pyridine)
PVCL	poly(*N*-vinylcaprolactone)
ppm	parts per million
PS-*b*-PAA	poly(styrene)-*block*-poly(acrylic acid)
P*t*BA	poly(*tert*-butyl acrylate)
Py-S_2-Br	3-(pyridin-2-yldisulfanyl)propyl 2-bromo-2-methylpropanoate
r	molar ratio
$R^{\bullet}$	free radical
RAFT	reversible addition-fragmentation chain transfer polymerization
R_h	hydrodynamic radius
RI	refractive index
SEC	size exclusion chromatography
SEM	scanning electron microscopy
t-BA	*tert*-butyl acrylate
TEA	triethylamine
TEM	transmission electron microscopy
TFT	α,α,α-trifluorotoluene
T_g	glass transition temperature
TGA	thermogravimetric analysis
TMS	trimethylsilyl
TsCl	*p*-toluenesulphonyl chloride
μm	micrometer (1 μm = 10^{-6} m)
UV	ultraviolet
VBC	vinylbenzyl chloride
V_h	hydrodynamic radii
Vol.%	volume percentage
VP	poly(2-vinyl pyridine)
vs.	versus
W	watt
wt.%.	weight percentage
XPS	X-ray photoelectron spectroscopy

Chapter 1 – Introduction

The aim of the research described in this thesis was to develop synthetic methodologies for the preparation of stimuli-responsive block copolymers. In this thesis, Chapter 2 will discuss the preparation and application of a dual light responsive copolymer, poly(ethylene glycol)-*orthonitrobenzyl*-poly[2-(perfluorooctyl)ethyl methacrylate]-*block*-poly(2-cinnamoyloxyethyl methacrylate) (PEG-*ONB*-PFOEMA-*b*-PCEMA). In Chapter 3, the facile synthesis of a doubly stimulable copolymer, poly(ethylene glycol)-*disulfide*-poly[2-(perfluorooctyl)ethyl methacrylate]-*block*-poly(2-cinnamoyloxyethyl methacrylate) (PEG-S_2-PFOEMA-*b*-PCEMA), will be discussed. Chapter 4 will describe a novel and facile approach that uses micellar block copolymer solutions to coat cotton fabrics, thus imparting these fabrics with superhydrophobic and oleophobic properties. A new method for the synthesis of poly(ethylene glycol)-*block*-poly(2-hydroxyethyl methacrylate) (PEG-*b*-PHEMA) via anionic polymerization will be discussed in Chapter 5. Concluding remarks and proposed future work will be provided in Chapter 6. Meanwhile, Sections 1.1-1.4 of this chapter will provide a general introduction to block copolymers, the strategies for their preparation, and will also describe the fundamental concepts of stimuli-responsive copolymers and superamphiphobic surfaces. Various techniques used to characterize the copolymers described in this thesis are summarized in Section 1.5. Subsequently, the objectives of this thesis are defined in Section 1.6.

1.1 Block Copolymers

Macromolecules consisting of two or more homogeneous and chemically distinct polymer chains that are covalently linked together are called block copolymers, with each polymer chain corresponding to a block.[1] Block copolymers can be described as diblock,

triblock, tetrablock and multiblock copolymers, respectively, depending on whether they incorporate two, three, four, or multiple blocks. Consequently, polystyrene-*block*-poly(ethylene oxide) (PS-*b*-PEO) is an example of an AB diblock copolymer, since it consists of two chemically distinct polymer chains connected together by a covalent bond. Block copolymers are also classified according to their architecture, which can include linear polymers, star polymers, branched chain polymers, ladder chain polymers, and macrocyclic polymers (examples of which include monocyclic, bicyclic, tadpole-shaped, and theta-ring polymers) are illustrated in Figure 1.1.[2] Interest in block copolymers continues to grow, with the combined efforts from polymer chemists, polymer physicists and computational experts.[3] This field is a broad discipline, ranging from the development of new synthetic methodologies to the preparation of intricate and useful nanostructures with wide range of applications.[4]

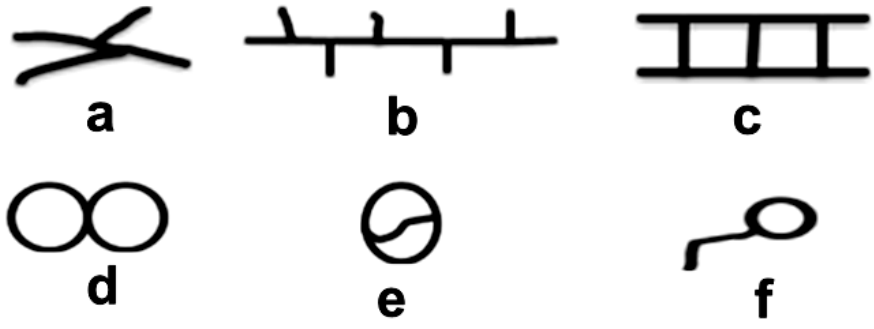

Figure 1.1. Schematic diagram of various architectural block copolymers: a) star, b) branched, c) ladder, d) bicyclic, e) theta-ring, and f) tadpole-shaped polymers.

1.1.1 Block Copolymer Self-Assembly in Block-Selective Solvents

As mentioned earlier, block copolymers consist of more than one chemically distinct polymer chains. Each of these chains may have different solubility in a particular solvent. A

good solvent for a block copolymer is one that solubilizes all blocks of that particular copolymer. Meanwhile, a block selective solvent dissolves one or more of the block(s) selectively over the other(s). Alternatively, a poor solvent is the one that cannot solubilize any blocks of a block copolymer. Dispersed aggregates are typically obtained by initially dissolving a block polymer into a good solvent and subsequently adding a selectively poor solvent for one or more blocks. For example, if an AB diblock copolymer is initially dissolved in a good solvent, the addition of a selectively poor solvent for the B block will trigger the less soluble B block to collapse while the soluble A block remains stretched out into the solvent. The collapse of the B block occurs in order to minimize the unfavourable interactions between the B block and the solvent. If the concentration of AB chains having collapsed B blocks is increased and reaches the critical micelle concentration (cmc), micelle formation occurs.[5] In general, micelles consist of an inner phase called a core domain that consists of insoluble blocks, and a soluble corona domain stretching outwardly into the solvent. In block selective solvents, block copolymers self-assemble to form aggregates of various shapes or morphologies. These morphologies are dependent on multiple factors that include the volume fractions of the individual blocks, nature of solvent, pH, and various other parameters.[6-7] For example, Eisenberg *et al.*[7] performed the very first systematic investigation of the self-assembled aggregates formed by poly(styrene)-*block*-poly(acrylic acid) (PS-*b*-PAA). By changing the volume fractions of the two blocks, they were able to tune the morphologies of these aggregates from spheres (Figure 1.2A), to cylinders (Figure 1.2B), to vesicles (Figure 1.2C), and to large compound micelles (Figure 1.2D).[8]

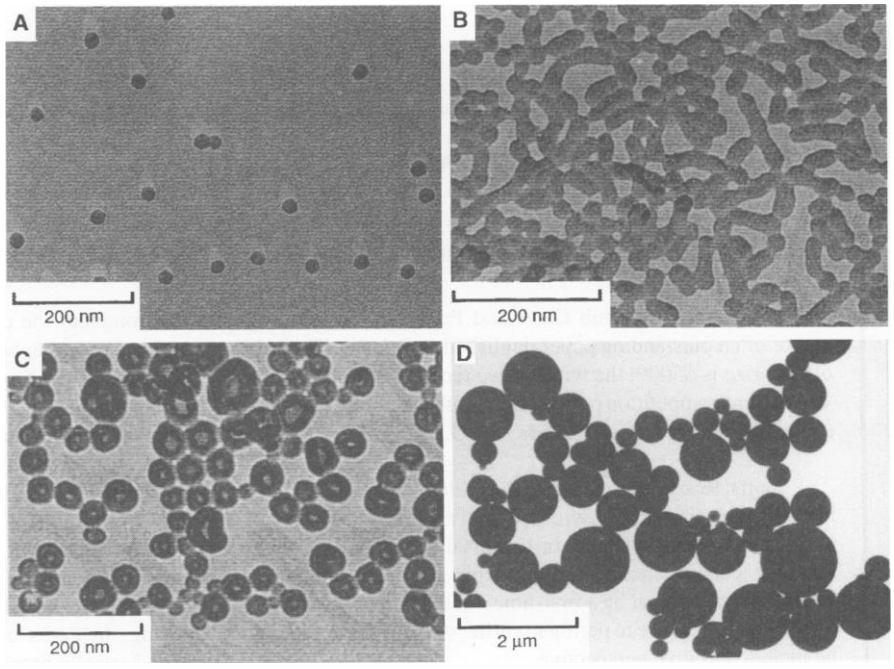

Figure 1.2. Common morphologies produced by an AB diblock copolymer; (A) spheres of PS_{500}-*b*-PAA_{58}, (B) rod-like micelles of PS_{190}-*b*-PAA_{20}, (C) vesicles of PS_{410}-*b*-PAA_{20}, and (D) large compound micelles of PS_{200}-*b*-PAA_4. From Zhang, L.; Eisenberg, A. *Science,* 1995, *268*, 1728. Reprinted with permission from AAAS.

Examples of block copolymer assemblies include spheres, cylinders, vesicles, hollow spheres, and hollow tubes with sizes ranging between 10 and 200 nm. These assemblies are thus referred to nanospheres, nanocylinders, polymersomes, and nanotubes, respectively.[9-10] Block copolymer nanostructures have a plethora of potential applications, such as drug delivery agents,[11-12] thin films,[13-14] and also in microelectronics and photovoltaic devices.[15]

1.2 Synthesis of Block Copolymers

Scheme 1.1 summarizes commonly used synthetic strategies employed for synthesizing block copolymers. In general, three major synthetic approaches are used for the preparation of

block copolymers, including radical polymerization, ionic polymerization and end-coupling of polymers.

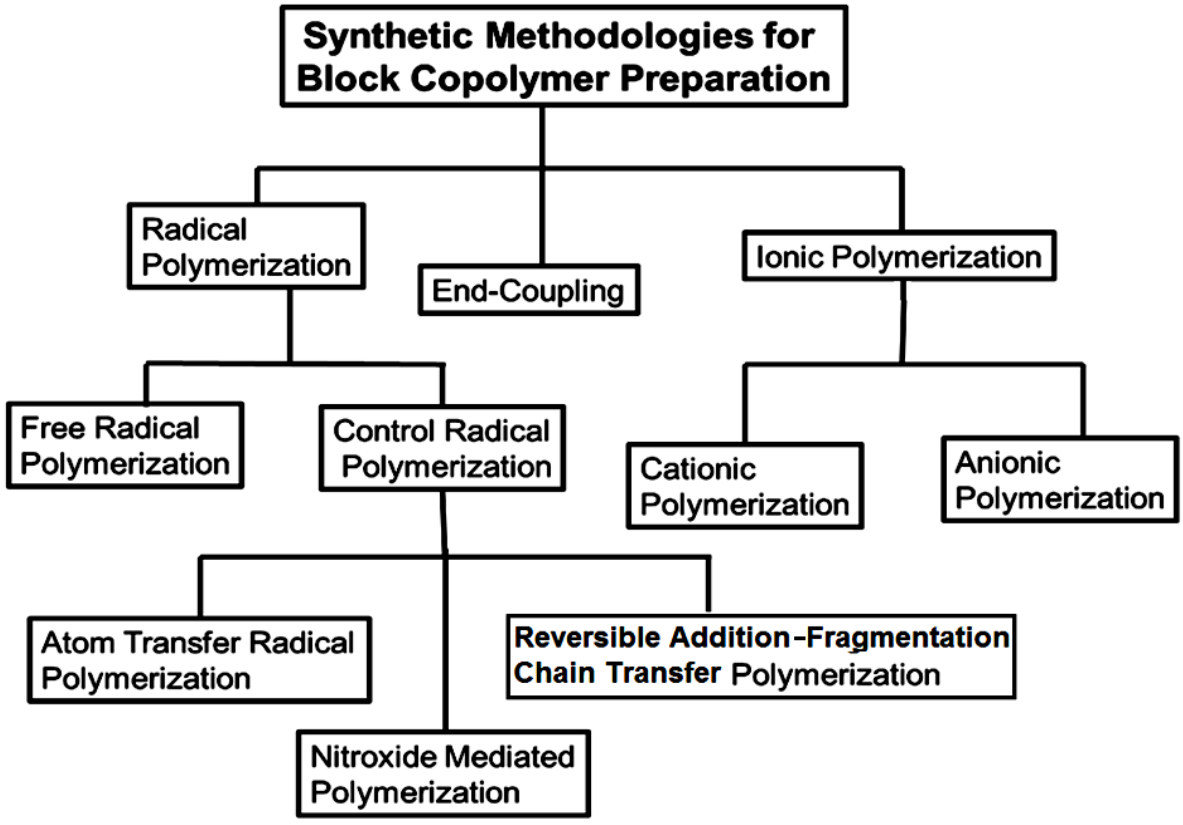

Scheme 1.1. Flow-chart diagram showing various categories of synthetic strategies for the preparation of block copolymers.

Radical polymerization refers to those reactions that are initiated by free radical species.[16] During this process, a radical species reacts with the C=C bond of a monomer in an addition-type reaction to carry out the polymerization. Radical polymerizations can be further classified into free radical polymerization and controlled radical polymerizations. On the other hand, ionic polymerization utilizes ions to initiate the polymerization. Depending on whether a cationic or anionic initiator is employed, this process can be classified as either cationic or

anionic polymerization.[17] The third approach is referred to as an end-coupling strategy, which involves a reaction between two polymers or copolymers to either produce block copolymers or to incorporate new blocks into an existing block copolymer. However, among all of these approaches, controlled radical polymerization has generated enormous interest in the synthesis of block copolymers. A detailed description of each method is provided below, along with leading examples from literature.

1.2.1 Free Radical Polymerization

Free radical polymerization is an important radical polymerization technique. It is called free radical polymerization because radical reactions are allowed to proceed uninterrupted. In a free radical polymerization, a radical reacts with the monomer at its C=C bond, which subsequently reacts with other monomers in an addition-type reaction to build the polymer chains. An approach to prepare block copolymers via free radical polymerization involves the use of a macroinitiator with a latent radical site that can initiate the block copolymerization of another monomer. This method was used for the synthesis of poly(ethylene oxide)-*block*-polystyrene (PEO-*b*-PS).[18] However, free radical results in side reactions, such as inter-chain radical coupling reaction and proton abstraction. Consequently, non-homogeneous polymers are produced, and thus this approach is unsuitable for block copolymer synthesis.[3]

1.2.2 End-Coupling of Homopolymers

An end-coupling strategy involves a reaction between end-functionalized polymer chains (or sometimes copolymer chains) to produce a block copolymer, as shown in Scheme 1.2.[19] This strategy initially involves the labelling of the end-groups of the polymer chains with certain reactive functional groups. The reactive end-groups of these labelled polymer chains are usually

different from those on the opposing chains. For example the chains may incorporate alkyne and azide groups to facilitate click chemistry.[20-22] Alternatively, these end-groups may be identical, with both chains incorporating C=C bonds to allow metathesis reactions.[23]

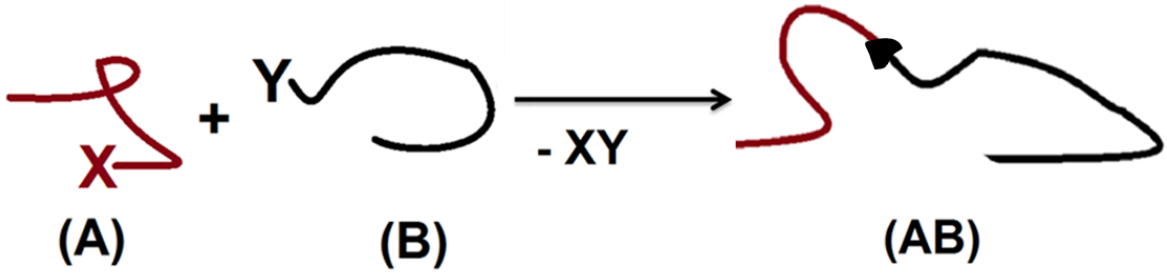

Scheme 1.2. End-coupling of pre-made polymer chains to form an AB block copolymer.

However, end-coupling strategies have certain disadvantages. These include the requirement of a suitable solvent as a reaction medium for the end-coupling reaction, post-reaction purification problems due to incomplete coupling, and the need for quantitive end-labelling of reactive functional groups on the polymer chains. For these reasons, the scope of end-coupling strategies in block copolymer synthesis is limited only to highly efficient and selective coupling reactions. More recently, pseudo di- and triblock copolymers have been generated via non-covalent interactions, such as through host-guest interactions between the end-labelled copolymers.[24]

1.2.3 Living Anionic Polymerization

The interest in block copolymers arose with the discovery of anionic polymerization by Michael Szwarc in 1956.[25] The era of anionic polymerization as the dominant method to synthesize block copolymers prevailed for ~45 years, until the emergence of controlled radical polymerizations.[26] A generalized mechanism for a typical anionic polymerization is depicted in

Scheme 1.3. This process involves three steps, including initiation, propagation and termination. Initiators can include carbanions (such as *n*-butyl lithium and *sec*-butyl lithium) or oxyanions (such as *tert*-butoxide and methoxide), depending on the nature of the monomer. Monomers suitable to smoothly undergo anionic polymerization must be able to stabilize the negative charge on the growing polymer chain. This charge stabilization is achieved either through conjugation (Scheme 1.3) or via resonance (Scheme 1.4). According to Fetter's theory, anionic polymerizations are performed in a particular monomer sequence, which is based on the principle of the basicity of growing polymeric anion.[27] For example, poly(styrene)-*block*-poly(methyl methacrylate) (PS-*b*-PMMA) is synthesized by initially polymerizing styrene and subsequently polymerizing methyl methacrylate (MMA). However, the reverse order, polymerization of MMA prior to styrene polymerization, is not applicable because styrenenyl anion is more basic than MMA anion. In general, the following sequence exists for various classes of monomers in anionic polymerization: butadiene/styrene > methacrylate > oxiranes> siloxane.[3]

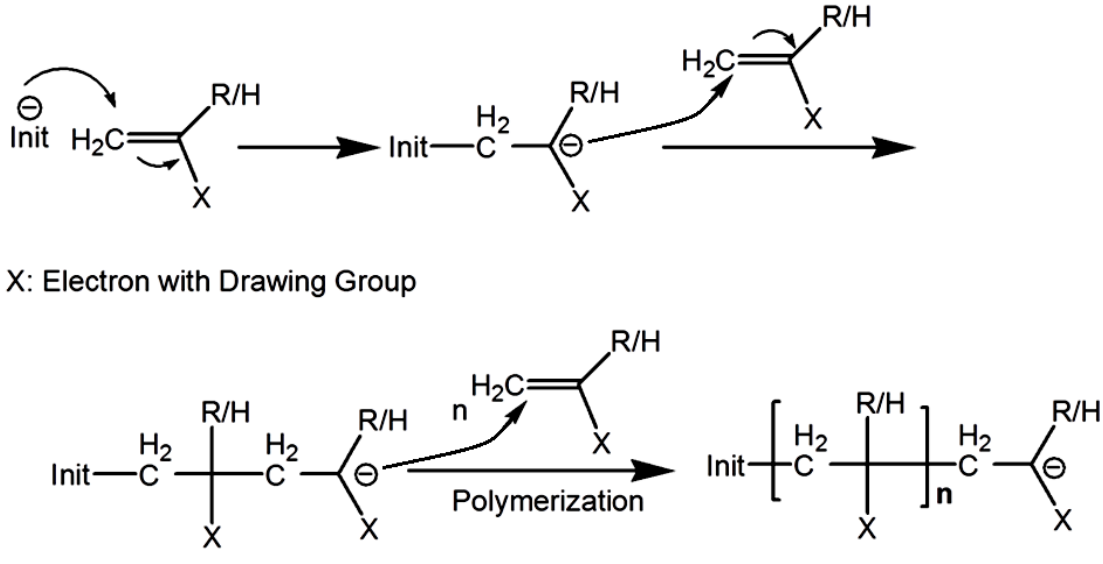

Scheme 1.3. A generalized synthetic pathway for an anionic polymerization.

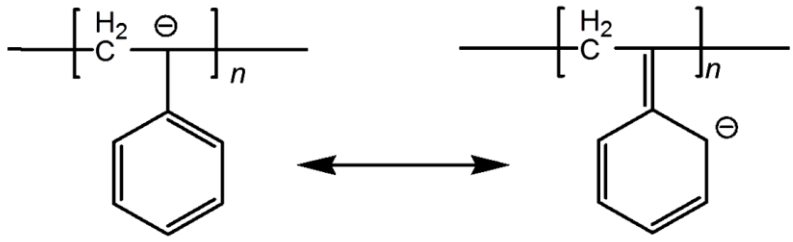

Scheme 1.4. Resonance stabilization of an anion during polystyrene synthesis.

1.2.4 Cationic Polymerization

Living cationic polymerization was developed in 1984. This method provides a useful tool for controlled polymerization with low PDIs and controlled molecular weights.[28] Generally, cationic polymerization is considered as a complimentary technique to anionic polymerization because monomers that cannot be polymerized via anionic polymerization, are often suitable for cationic polymerization.[29] Scheme 1.5 describes the mechanism for a cationic polymerization reaction. Contrary to anionic polymerization, this polymerization is initiated by a positively charged species, such as a carbenium ion or an oxonium ion. Styrene, isobutene, vinyl ethers and tetrahydrofuran are some representative monomers of different classes that undergo living cationic polymerization.[3]

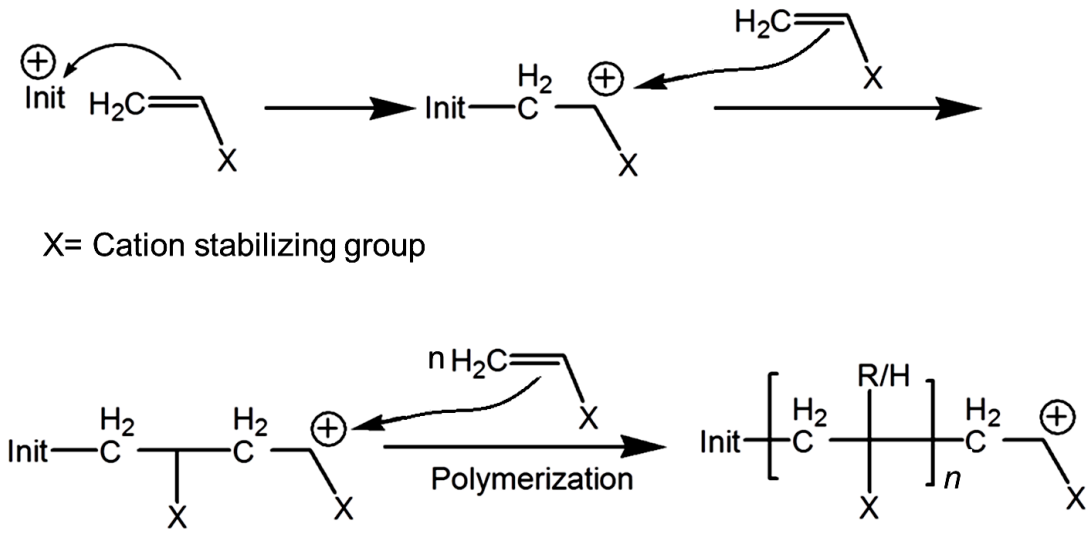

Scheme 1.5. A generalized cationic polymerization mechanism.[26]

1.2.5 Controlled Radical Polymerization

The term controlled radical polymerization (CRP) refers to a radical polymerization that is performed in the presence of reagents that control the rate of polymerization.[30] In the 15 years, since its discovery, CRP has totally changed the synthetic landscape of polymer chemistry. This dramatic impact can be attributed to the fact that this strategy facilitates the synthesis of architectural block copolymers that were not available through classical techniques, such as anionic polymerization and cationic polymerization.[30] Among CRP methods, nitroxide mediated polymerization (NMP), reversible addition-fragmentation chain transfer (RAFT) polymerization and atom transfer radical polymerization (ATRP) have been widely studied.[31-32]

1.2.5.1 Nitroxide Mediated Polymerization

Nitroxide mediated polymerization (NMP) is an important class of controlled radical polymerization reactions that was developed in the 1990s.[33] Polymers obtained via NMP exhibit well-defined molecular weights and low polydispersity indices (PDIs) that typically range

between 1.1 and 1.2.[34] A generalized mechanism for NMP is illustrated in Scheme 1.6. First, homolysis of a C-O bond in an alkoxy amine occurs, thus generating two radicals. One radical species incorporates a transient carbon free radical that acts as an initiator, while the other species possesses a persistent secondary amine oxide radical. As shown in Scheme 1.6, a transient radical can either react reversibly with the persistent radical to form a dormant species, or it can react with the monomer to start polymerization.[35] On the other hand, persistent radicals are more stable than transient carbon radicals, due to the resonance of the single electron between the nitrogen and oxygen of the secondary amine oxide radical. To inhibit intermolecular coupling between the transient radicals and the persistent radicals, highly substituted amines or macrocyclic amines are used. Figure 1.3 shows the most commonly used persistent radicals in NMP, including 2,2,6,6-tetramethylpiperidinyloxy (TEMPO), *N*-tert-butyl-*N*-[1-diethylphosphono-(2,2-dimethylpropyl)]nitroxide (DEPN) and 2,2,5-trimethyl- 4-phenyl-3-azahexane-3-oxy (TIPNO). Also, it has been established that the rate of transient radical generation from alkoxy amine oxides is dependent on the bulkiness of the substituent groups and/or the size of the ring (cyclic alkoxy amines). For example, a smaller angle between the C-O-N bonds of a cyclic amine oxide generates greater steric hindrance, which in turn increases the rate of C-O cleavage and subsequently the rate of transient radical generations.[36]

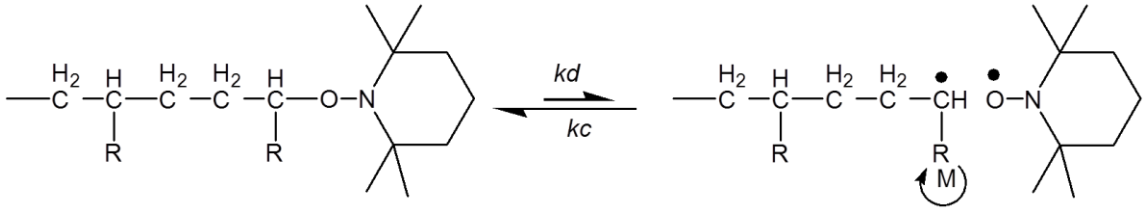

Scheme 1.6. An equilibrium favoring polymer growth in an NMP reaction. Reprinted from Controlled/living radical polymerization: Features, developments, and perspectives, Braunecker, W.A.; Matyjaszewski, K. *Prog. Polym. Sci.* vol. 32, 2007, with permission from Elsevier.[37]

Currently, NMP is widely used for the synthesis of block copolymers. Various classes of monomers, including styrene, isoprene and acrylate monomers have been successfully copolymerized.[37-39] Furthermore, block copolymers consisting of different classes of monomers such as P*t*BA-*b*-PS, where P*t*BA corresponds to poly(*tert*-butyl acrylate), have been reported by this method.[40]

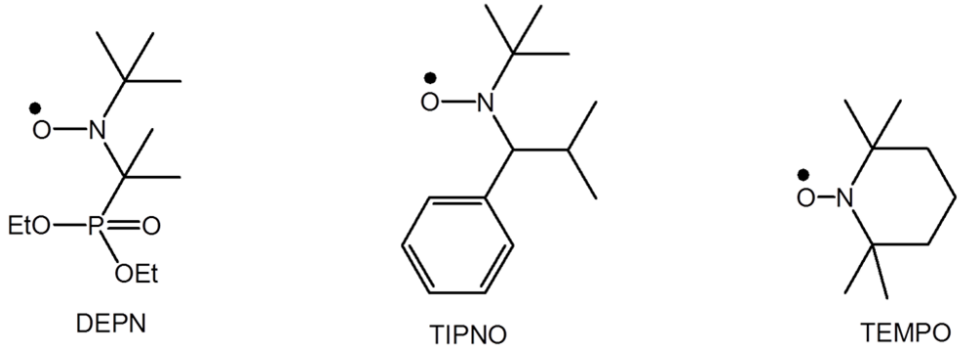

Figure 1.3. Common persistent radicals used for NMP.[37]

1.2.5.2 Reversible Addition-Fragmentation Chain Transfer (RAFT) Polymerization

The reversible addition-fragmentation chain transfer (RAFT) process is another important class of controlled radical polymerization reactions. This technique was discovered in 1998 by John Chiefari *et al*.[41] Recently, various features of the RAFT process, including mechanistic aspects and applications in block copolymer synthesis have been thoroughly reviewed by Smith *et al*.[42] The chemistry involved in a RAFT reaction is shown in Scheme 1.7. Briefly, a RAFT process consists of three basic components, which include an initiator, a monomer, and a RAFT agent. An initiator is generated by the decomposition of a latent initiator using heat or light to initiate the polymerization. A chain transfer agent (CTA), also called a RAFT agent, controls the reactivity of the free radical. For example, thiocarbonylthio compounds substituted with various alkyl/aryl groups are used as CTAs. As depicted in Scheme

1.7, the growing polymer chain ($P_n^{\bullet}$) reacts with the CTA at the C=S bond, and undergoes rearrangement to generate another radical ($R^{\bullet}$). The newly formed $R^{\bullet}$ initiates a new polymer chain. The main equilibrium involved in the RAFT process is the reaction between the polymeric-CTA (dormant $P_n^{\bullet}$) and the polymeric growing free radical ($P_m^{\bullet}$), which in turn generates a dormant species and an active growing free radical. A faster equilibrium between a dormant species and an active species ensures the synthesis of well-defined polymers with narrow molecular weight distributions.[33]

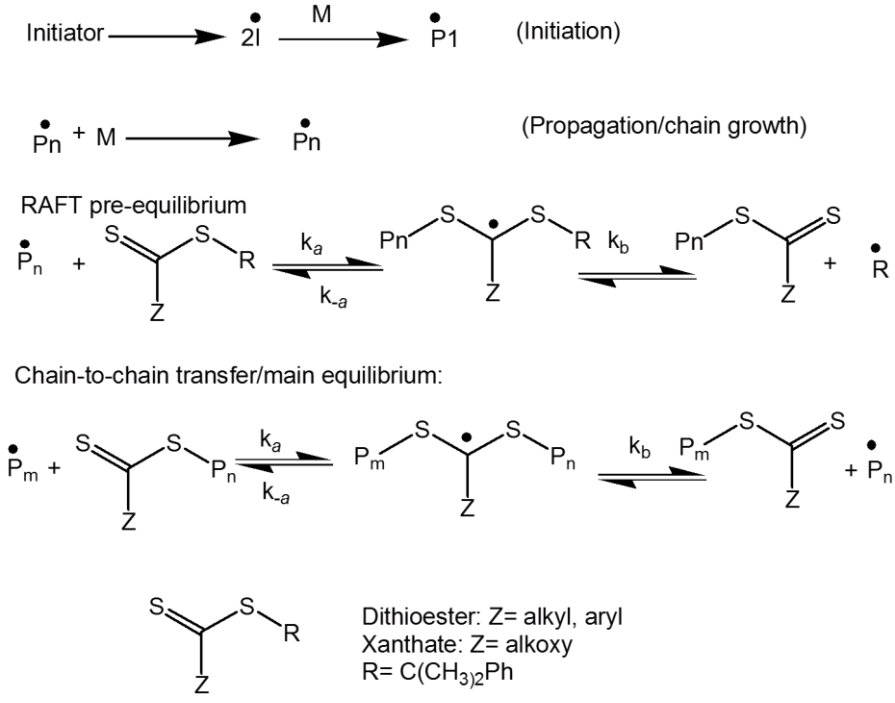

Scheme 1.7. Initiation and chain transfer steps occurring in a RAFT polymerization. Reprinted from Stimuli-responsive amphiphilic (co)polymers via RAFT polymerization, Smith, A.E.; Xu, X.; McCormick. C.L. *Prog. Polym. Sci.* vol. 35, p. 47, 2010, with permission from Elsevier.[42]

Currently, a wide range of monomers are polymerized via the RAFT technique; examples include those from the styrene, acrylate, acrylamide, and vinyl families.[43-44] For example, the synthesis of the poly(*N*-isopropylacrylamide)-*block*-poly(dimethylacrylamide)

(PNIPAM-*b*-PDMA) and poly(dimethylacrylamide)-poly(*N*-isopropylacrylamide)-*block*-poly(dimethylacrylamide) (PDMA-*b*-PNIPAM-*b*-PDMA) have been successfully executed via the RAFT process.[45] Additionally, the RAFT process has a unique advantage over the contemporary polymerization methods for the polymerization of acidic monomers such as acrylic acid.[46-47]

1.2.5.3 Atom Transfer Radical Polymerization (ATRP)

Another important generation of controlled radical polymerization is atom transfer radical polymerization (ATRP). ATRP was discovered independently by Mitsuo Sawamoto *et al.*[48] and by Jin-Shan Wang and Krzysztof Matyjaszewski in 1995.[49] In a short period of time, it became a vital tool allowing synthetic polymer chemists to prepare a diverse range of architectural copolymers.

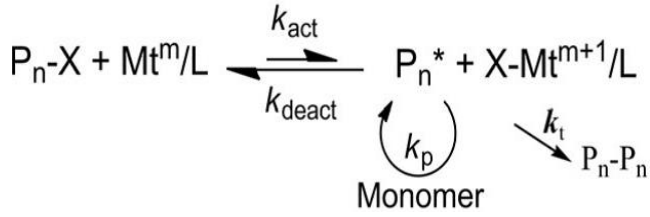

Scheme 1.8. Key equilibrium process in an ATRP reaction. Reprinted with permission from Matyjaszewski, K.; Xia, J.H. *Chem. Rev.* **2001,** *101,* 2921. Copyright (2001) American Chemical Society.

A simple picture of ATRP chemistry is drawn in Scheme 1.8. First, halides reversibly reacts with transition metal-complexes such as Cu^IX/L to form a free radical P_n^* and $Cu^{II}X_2/L$. The equilibrium remains in the reverse direction in an ATRP reaction, and thus the active radical species P_n^* exists as a minor species, while the dormant species P_n-X remains dominant. This

leads to low PDI polymers as all polymer chains grow at equal rates. Also, the number of radicals during polymerization remains smaller and hence radical combination is minimal.[49]

An ATRP system consists of various components, such as the monomer, initiator, catalyst, ligand, and/or solvent. These components are described in the following paragraphs.

Various classes of monomers, such as styrenes, acrylates, methacrylates, acrylamides, methacrylamides, and acrylonitriles are polymerized via ATRP.[51-52] However, acidic monomers cannot be polymerized by ATRP, as organic acids can poison a catalyst and consequently inhibit the ATRP reaction.

Another component of an ATRP system is the initiator. An ATRP initiator consists of a halo functional group that can reversibly exchange halides with transition metal complexes. This exchange involves a single electron process, and the resultant alkyl radical generated through halide exchange is capable of initiating the polymerization. Among halogens, only bromine and chlorine are commonly used for ATRP reactions. However, the use of alkyl iodides as initiator has also been reported.[50,53]

An ATRP reaction also utilizes a catalyst. In principle, transition metals with two stable oxidation states that differ by a single electron can be used to catalyze ATRP reactions. For this reason, a wide range of transition metals have been investigated. However, copper is the most commonly used transition metal catalyst for ATRP reactions, because of its affinity for halogens. Among other metals, molybdenum,[54] chromium,[55] rhenium,[56] ruthenium,[46] and iron[57] have also been used to catalyze ATRP reactions.

Ligands and solvents are also components of an ATRP reaction. Fundamentally, ligands perform two equally important roles in an ATRP reaction.[58] First, ligands are organic in nature and undergo complexation with inorganic transition metals, thus helping metals become solubilized in organic solvents. Second, the rate of an ATRP reaction is highly dependent on the

binding strength between the ligand and the metal. Stronger ligands yield a faster polymerization rate and vice versa. Meanwhile, solvent also plays a significant role in ATRP, especially for polymers with higher glass transition temperatures (T_g). For example, polymerization rates are higher in aprotic and polar solvents in comparison with those conducted in non-polar solvents. Additionally, the use of solvent decreases the viscosity, especially at the later stages of a reaction. Consequently, the polymer chains can grow in a uniform manner. Nevertheless, bulk phase (solvent free) ATRP techniques are sometimes used in polymer synthesis, especially for preparing polymers with lower T_g.[59-61]

1.2.5.3.1 Scope of ATRP in Block Copolymer Synthesis

As mentioned earlier, ATRP is the most widely used technique for the synthesis of block copolymers with diverse architectures. ATRP is compatible with many functional groups, except for some acidic groups.[50] A wide range of block copolymers have been prepared via ATRP.[62] Monomers from the same class as well as from different classes have been polymerized to build block copolymers. For example, the use of methacrylate-based monomers to prepare block copolymers such as poly(butyl methacrylate)-*block*-poly(methyl methacrylate) and poly(methyl methacrylate)-*block*-poly(butyl methacrylate)-*block*-poly(methyl methacrylate) via ATRP have been reported.[48] Alternatively, different members of the styrenic class of monomers have been used to prepare copolymers such as polystyrene-*block*-poly(4-acetoxystyrene)-*block*-polystyrene and poly(4-acetoxystyrene)-*block*-polystyrene-*b*-poly(4-acetoxystyrene).[63] Similarly, different classes of monomers have been used to synthesize copolymers such as polystyrene-*block*-poly(methacrylic acid) and polystyrene-*block*-poly(*N*-butyl methacrylamide) via ATRP, where each block belongs to a different class of polymers.[64] Currently, ATRP is at the interface between industry and academia. For this technique to

become viable at commercial scales, the issue of toxic metallic residues associated with this technique needs to be resolved.[65] This challenge has been addressed to a great extent by various innovative methods, including the invention of non-classical ATRP (reverse ATRP), which uses only parts per million quantities of transition metal catalysts. In reverse ATRP, azobisisobutyronitrile (AIBN) is used as a radical source in the presence of higher oxidation state metal catalysts.[66-68]

1.2.6 Post-Polymerization Modifications

Polymers synthesized via radical polymerization and ionic polymerization techniques are generally used directly. However, in certain cases, block copolymers whose direct synthesis is not feasible with the available methods, are treated with further chemical reactions.[69-70] These treatments are known as post-polymerization chemical modifications. Some classical examples of post-polymerization treatments include hydrolysis, quaternization, and crosslinking reactions.[69-70] For example, hydrolysis can be used to convert hydrophobic P*t*BA blocks into hydrophilic PAA blocks, as shown in Scheme 1.9. Meanwhile, nitrogen-bearing polymers such as P4VP and P2VP can be subjected to quaternization treatment.[69-70]

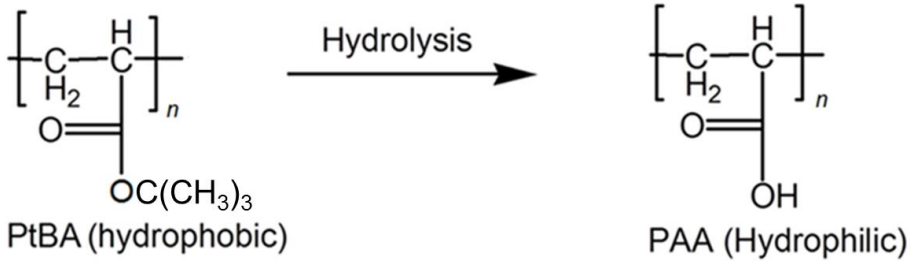

Scheme 1.9. Hydrolysis of P*t*BA, yielding PAA through the cleavage of the *tert*-butyl group.

Similarly, Scheme 1.10 highlights two post-synthetic modifications frequently used in the research described in this thesis. In the first step, a trimethylsilyl (TMS) group is hydrolyzed from the poly(2-trimethylsilyloxyethyl methacrylate) or P(HEMA-TMS) block. Subsequently, PHEMA is reacted with cinnamoyl chloride to prepare poly(2-cinnamoyloxyethyl methacrylate) (PCEMA). Here PCEMA is hydrophobic in nature and is also photo-crosslinkable. PCEMA-based block copolymers can be used to prepare permanent nanostructures because PCEMA can undergo crosslinking upon exposure to light.[71] Scheme 1.11 describes a [2+2] cycloaddition reaction between the C=C bonds of the two CEMA units.

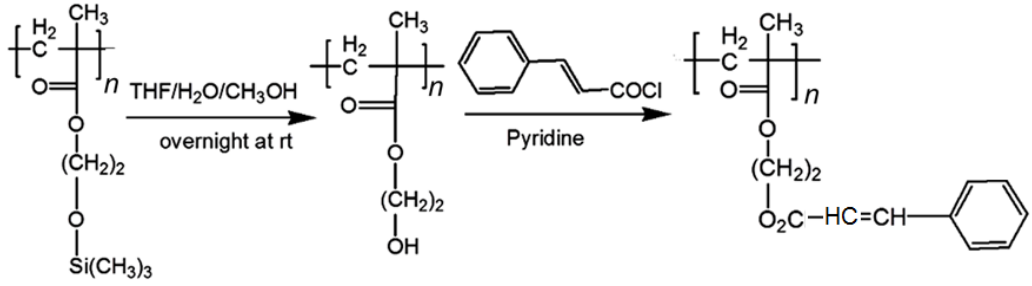

Scheme 1.10. Post-polymerization modifications of P(HEMA-TMS) to prepare PCEMA.

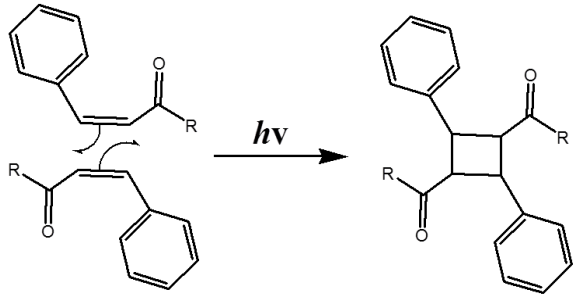

Scheme 1.11. [2+2] cycloaddition of two 2-cinnamoyloxyethyl methacrylate units upon exposure to UV light.[71]

1.3 Stimuli-Responsive Block Copolymers

Chapters 2, 3, and 4 of this thesis deal with the preparation and applications of stimuli-responsive triblock polymers. Therefore, a brief introduction to stimuli-responsive polymers

with relevant examples will be described in this section. Stimuli-responsive polymers are sensitive to a number of stimuli or external conditions, which can be classified into two categories. These categories include chemical stimuli (such as changes in pH, electrochemical conditions, or ionic strength) and physical stimuli (such as changes in temperature, light, or the magnetic field).[72] This topic is thus very broad, and to review all of these stimuli individually is beyond the scope of this thesis. Therefore, only temperature-, pH- and light-responsive polymers will be discussed here.

1.3.1 Thermoresponsive Polymers

Thermoresponsive polymers undergo changes at particular temperatures. The most widely investigated thermoresponsive polymer is poly(*N*-isopropylacrylamide) (PNIPAM). In aqueous media, PNIPAM undergoes a coil-to-globule phase transition at a temperature of 32 ^{o}C.[73] Consequently, it becomes insoluble above 32 ^{o}C in aqueous solution. However, this transition temperature is tunable and can be increased by the attachment of a hydrophilic block. For this reason, block copolymers incorporating a PNIPAM block are considered as ideal candidates for drug delivery systems.[73] Poly(*N*-vinylcaprolactone) (PVCL),[74] and poly(*N*-(dl)-(1-hydroxymethyl) propylmethacrylamide) are other examples of thermoresponsive polymers.[75-76]

1.3.2 pH-Responsive Polymers

Polymers capable of undergoing protonation and deprotonation are described as pH-responsive polymers. P4VP and P2VP are examples of electron donating polymers, while PAA is an example of a proton donating polymer. In principle, acidic polymers such as PAA[77] and poly(methacrylic acid) (PMAA)[78] are soluble in basic media, while polymers with basic functionalities, such as poly(*N*,*N*-dimethyl aminoethyl methacrylate) (PDMAEMA), P2VP, and

P4VP are soluble in acidic media.[79] Therefore, a change in the pH determines the solubility of a pH-responsive polymer.

1.3.3 Photo-Responsive Polymers

Photo-responsive polymers undergo changes driven by exposure to light. A telling example of a light sensitive polymer is PCEMA. Block copolymers incorporating a PCEMA block have been thoroughly studied by Liu and coworkers.[80-81] More recently, the photo-cleavable *ortho*-nitrobenzyl (*ONB*) group has found many applications in polymer science, particularly as a photo-responsive junction between polymer blocks.[82]

Currently, multiple responsive polymers are of great interest and can be classified into two categories. The first category includes multiply stimulable block polymers that undergo multiple changes in response to more than one stimuli.[83] For example, a block copolymer incorporating both PNIPAM and PCEMA blocks is both thermo-responsive and light sensitive, respectively.[84] The other category is multi-responsive block copolymers, which undergo several changes in their properties or structures when subjected to a single stimulus.[85] Both multiply stimulable block copolymers and multi-responsive block copolymers have received considerable attention and they are considered as an exciting research area, with a wide range of applications in biomedical science, drug delivery systems, sensors, and for various other systems.[86-88]

1.4 Superamphiphobic Surfaces

A superamphiphobic surface is defined as a "surface on which water and oil contact angles exceeds 150^{o}".[89] The creation of superhydrophobic surfaces has been studied for many decades.[90] Recently, however, interest in superamphiphobic surfaces has grown significantly.[91] It has been found that both plants and insects, such as the leaves of lotus plants and cicada

wings, display superhydrophobic properties because of their surface roughness.[92] Inspired by nature, researchers have also prepared superhydrophobic surfaces.[93] It is relatively easy to prepare superhydrophobic surfaces because of the higher surface tension of water (72.3 mN/m).[93-94] Meanwhile, creating superoleophobic surfaces is a highly challenging task due to the very low surface tension of oils. Fluorinated polymers are known for their low surface energy and inert chemical nature, and they are thus considered as ideal materials for creating superoleophobic coatings.

Theoretically, two mathematical equations are used to describe contact angles of a given surface. The first of these is Wenzel's equation that defines homogenous wetting regimes (Eq. 1.1).[95]

$$\cos\theta' = r\cos\theta \qquad \text{(Eq 1.1)}$$

Where θ' is the apparent contact angle on a rough surface, θ is the contact angle on an ideal surface and r is the roughness ratio, which is equal to the ratio of the actual area of the surface to the apparent area. Another equation that describes contact angles is Cassie's equation, which describes heterogeneous wet surfaces and is expressed as Eq. 1.2.[96]

$$\cos\theta' = f\cos\theta - (1-f) \qquad \text{(Eq. 1.2)}$$

Where θ' represents the apparent contact angle on a rough surface, f represents the fraction of a solid/liquid interface, and $(1-f)$ represents the fraction of an air/liquid interface (trapped air on a rough surface and liquid on the surface). On wet surfaces, $f = 1$, and hence the Cassie-Baxter equation takes the form of the Wenzel equation.

1.5 Polymer Characterization Techniques

1.5.1 Nuclear Magnetic Resonance Spectroscopy (NMR)

Nuclear magnetic resonance (NMR) spectroscopy is a powerful characterization technique for the structural determination of organic compounds and polymers. The nucleus of an atom is composed of both proton(s) and (with hydrogen being an exception) neutron(s). These particles have an intrinsic spin property. The spin of a nucleus is represented by the spin quantum number(s) of that nucleus. Nuclei having non-zero spin quantum numbers behave as tiny magnets. In the absence of an external magnetic field, all of the spinning nuclei are degenerate and randomly oriented.[97] However, under the influence of a strong magnetic field (H_o), these nuclei rearrange into different orientations.[98] The number of orientations obtained is dependent on the spin quantum number and is calculated by the formula 2s + 1, where s represents the spin quantum number. For example, both ^{1}H and ^{13}C have spin quantum numbers of ½, and they thus have two possible orientations: parallel (lower in energy) and antiparallel (higher in energy). The lower energy state has a slight excess of nuclei than the higher energy state, which is known as the Boltzmann excess.[98] In the presence of strong magnetic field, the sample is irradiated with electromagnetic radiation. If the irradiation frequency matches the frequency required for the excitation of the nuclei from low energy state to higher energy states, excitation occurs. This phenomenon is described as nuclear magnetic resonance.[98] Beside other factors, the frequency required for the excitation of nuclei are dependent on the strength of the applied magnetic field and the magnetogyric ratio as shown in Eq. 1.3.[97]

$$\nu_o = \gamma H_o/2\pi \qquad \text{(Eq. 1.3)}$$

Where ν_o represents the Larmor frequency and γ represents the magnetogyric ratio, which is an intrinsic property of each nuclei.[99] However, the effective magnetic field experienced by a given nucleus is influenced by the electron density, and thus the density of electrons,

surrounding the nucleus. This phenomenon is referred to as the shielding effect.[98] A nucleus surrounded by a dense electron cloud is said to be shielded. Meanwhile, a nucleus that is only covered by a thin electron cloud, and is thus relatively exposed to the applied field, is said to be deshielded. The extent of the shielding or deshielding is heavily influenced by the chemical environment surrounding the nucleus. Therefore, nuclei of an atom that is bound to different neighbours having different electronegativities will be placed in different electronic environments and hence appears at different chemical shifts in the NMR spectrum.[96] This phenomenon of shielding and deshielding has made it possible to differentiate between different functional groups of a molecule. Therefore, NMR has become a vital tool for the structural analysis of organic compounds.

Modern NMR spectrometers are equipped with superconducting magnets that generate strong and stable magnetic fields ranging from 4.7 to 14 Tesla.[98] Also, radio frequency in short pulses are applied to induce nuclei resonance, while the interval between these pulses allows the nuclei to relax back to their lower spin states to maintain the initial Boltzmann excess. The obtained relaxation decay signal is known as free induction decay (FID), because the signal decays with time due to relaxation. The time domain signal (the FID) is converted into frequency domain signal through a mathematical process called Fourier transformation.[100] This conversion provides the frequency domain signals appearing in a typical NMR spectrum.

Proton NMR (^{1}H NMR) is used as a first hand tool for the structural characterization of the polymers described in this thesis. ^{1}H NMR provides information regarding block composition ratios, the nature of the functional groups, and is useful for obtaining an end-group analysis of a block copolymer. There are two obvious differences in the ^{1}H NMR spectra of polymers in comparison with those of small organic molecules. Firstly, protons of a polymer generate broader signals than those of smaller molecules due to the lower chain mobility that

inhibit the net magnetic dipole surrounding a nuclei to get zero.[101] Secondly, a relaxation delay of 3s (>5T_1) is typically used for the polymers investigated in this thesis, rather than the shorter relaxation delay of 1 s typically used for recording ^{1}H NMR spectra of small organic molecules. This longer relaxation delay is used due to the low chain mobilities encountered among macromolecules or polymers.

1.5.2 Size Exclusion Chromatography (SEC)

The characteristics of a polymer, such as its weight average molecular weight (M_w), number average molecular weight (M_n), molecular weight distributions M_w/M_n, and its purity are determined by size exclusion chromatography (SEC). SEC is based on the entropic exclusion mechanism, and the elution time of a polymer passing through a SEC column is dependent on its hydrodynamic radius. Eq. 1.4 correlates the relationship between the molecular weight M, the hydrodynamic volume V_h and the intrinsic viscosity $[\eta]$:[102]

$$[\eta]M \sim V_h \qquad \text{(Eq. 1.4)}$$

Typically, a SEC instrument consists of three basic components, including a solvent pump and solvent reservoir, a set of chromatographic columns, and a detector. To achieve an unperturbed flow rate through the SEC columns, mechanical pumps are employed. SEC columns are packed with cross-linked polymer gels, made of a crosslinked polymer such as polystyrene, having different pore sizes. A polymer chain with smaller hydrodynamic volumes diffuses into the pores to a larger extent and hence takes a longer time to elute through the column. Meanwhile, polymers with larger hydrodynamic volumes have shorter elution times, as illustrated in Figure 1.4.

An SEC instrument may be equipped with a single detector or alternatively with multiple detectors that monitor the composition of the solution eluting from the column. The most commonly used detectors are refractive index (RI) detectors, which measure the difference in the refractive indices of the solvent and the polymer solution. As polymer solution has different refractive index than the solvent alone, these differences are plotted as the RI intensity versus the retention time. Generally, SEC peaks appear as positive signals, since the refractive indices of most polymer solutions are higher than those of solvents. In some cases, however, a polymer may generate a negative signal in case of polymers having smaller refractive indices than the eluent itself such as fluorinated polymers. Modern instruments are equipped with two or even three detector systems, such as those using a combination of differential refractive index (DRI) and light scattering (LS) detectors.[103]

The value of M_w calculated by SEC is relative rather than absolute. For this purpose, the SEC system is first calibrated using standards such as samples of PS or PMMA of known molecular weights. For polymers where calibration curves are not available, universal calibration techniques are used to estimate the molar masses of these polymers.[105] However, a detail description of this topic is beyond the scope of this section.

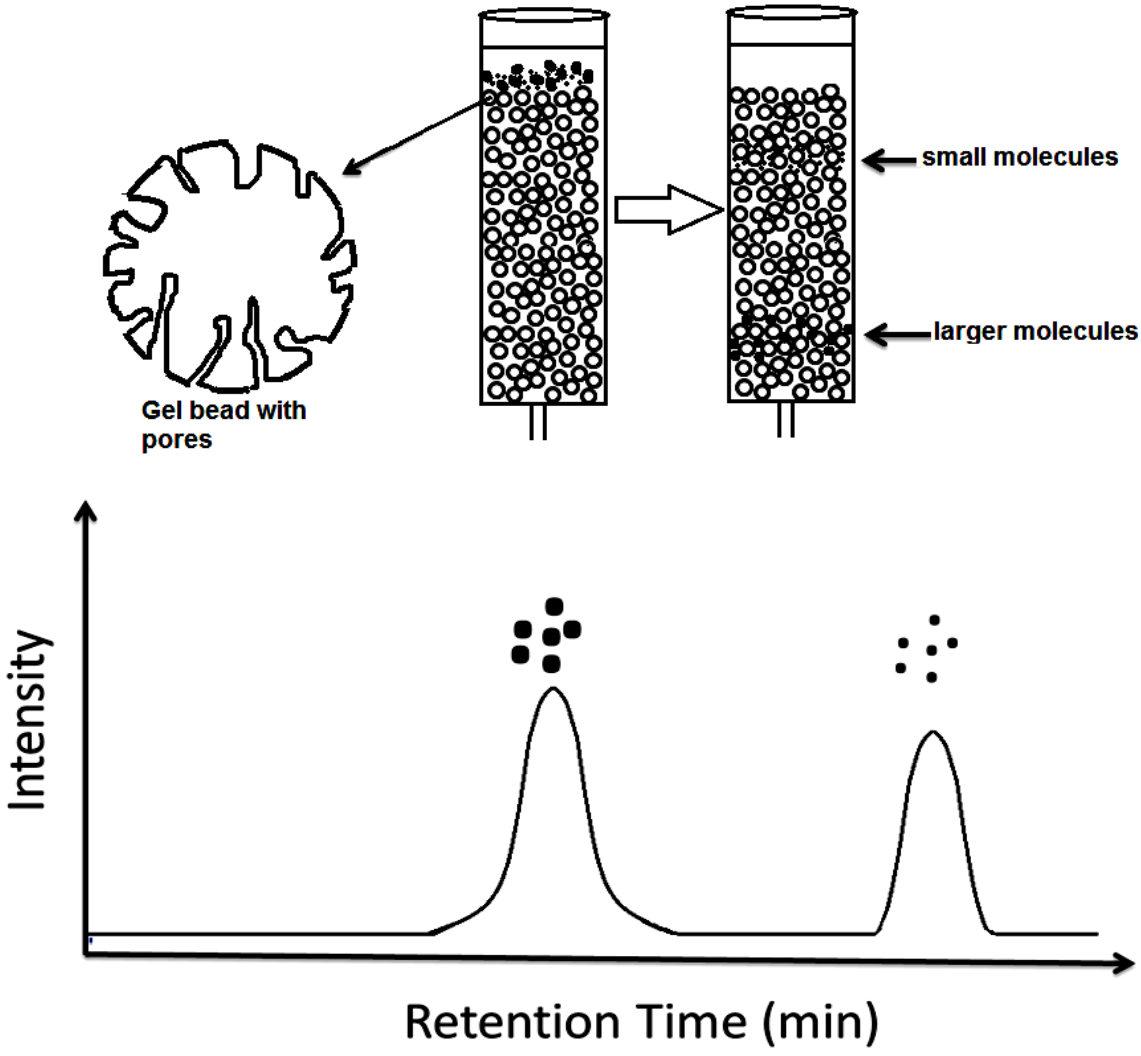

Figure 1.4. Schematic illustration of the separation of a polymer mixture using a SEC column. Higher and lower molecular weight components of the mixture are shown as larger and smaller dots, respectively. A typical SEC chromatogram showing hypothetical curves corresponding to these components are also plotted as signal intensity vs. retention time.[104]

1.5.3 Transmission Electron Microscopy (TEM)

Transmission electron microscopy (TEM) is used to directly observe self-assembled aggregates of block copolymers on the nanometer scale. According to the Rayleigh criterion, the resolution of any imaging instrument is roughly half of the wavelength of the radiation

source.[106] As TEM utilizes electrons as a bombardment source, the resolution of the TEM images thus reaches down to a few nanometers in scale.[106] Depending on the nature and thickness of the specimen, electrons impacting a specimen may either become scattered, they may become absorbed by the sample, or alternatively they may pass through the sample. In TEM analysis, the transmitted electrons are captured on a fluorescent screen and the generated TEM images reveal the relative electron density captured on the screen.

Block copolymer self-assemblies often do not provide good contrast for TEM images, because the transmitted electron densities usually differ only slightly between the different organic polymer domains. Therefore, selective staining of one domain over the other is achieved by using heavy metal complexes such as osmium tetroxide and uranyl acetate as staining agents for C=C bonds and carboxyl groups, respectively. These staining agents impart a greater electron density to the domain with which they selectively bind, and they thus provide better contrast for the resultant TEM image. TEM specimens are prepared by aero-spraying polymer solutions from block selective solvents onto ultrathin carbon/cellulose films. These films are supported on copper grids. These aero-sprayed specimens are subsequently equilibrated with a staining agent such as OsO_4 before TEM analysis.

1.5.4 Atomic Force Microscopy (AFM)

Atomic force microscopy is an important tool for the 3D imaging of nanostructures, and has enabled polymer chemists to probe the morphologies of block copolymer assemblies.[107] As shown in Figure 1.5, a typical AFM instrument consists of three main components, including a cantilever, a sample holder, and a signal detector. A tip is placed at the end of the cantilever, and the resonance of the cantilever is monitored with the detector. The tip serves as a probe, and it is scanned over the surface of the sample. Three types of scanning modes are common,

including contact mode, tapping mode, and non-contact mode.[107-110] In the contact mode, the tip is held sufficiently close to the sample so that interactions between the sample and the probe fall in the repulsive regime. However, the surface features of samples that are scanned via contact mode may become deformed due to the close proximity of the tip, particularly if these samples are soft materials. In the tapping mode, the tip is kept at an intermediate distance from the sample surface, so that interactions between the tip and sample remain in the attractive regime. These forces can cause the tip to touch the surface as the cantilever oscillates. The tapping mode is widely used for the characterization of soft materials such as polymers, because significantly less deformation occurs in this mode in comparison with the contact mode. Meanwhile, in the non-contact mode the tip oscillates at a certain distance above the surface, but never actually touches the surface. Advantages of the AFM technique are that it can be applied equally for characterizing conducting and insulating materials, it provides a high resolution down to a few nanometers, and it allows operation under ambient conditions.

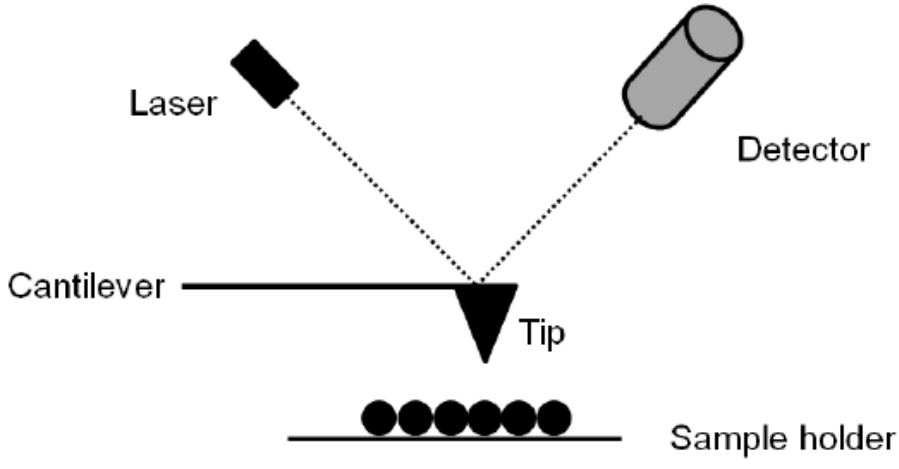

Figure 1.5. A schematic diagram showing the components of an AFM.[111]

1.6 Thesis Objectives

The aim of this study is to design and synthesize novel stimuli-responsive block copolymers and to investigate their applications. The first part of the study, which covers Chapters 2-4, deals with the preparation of novel, multi-stimuli responsive and multiply stimulable block copolymers and their applications as coating materials for glass and cotton. Meanwhile, the second part of the study described in Chapter 5 involves developing a new method for the synthesis of PEG-based block copolymers via anionic polymerization.

Chapter 2 describes the preparation of a dual light responsive triblock copolymer. Stimuli-responsive block copolymers are anticipated to fill a central role as biomedical materials.[112-113] However, the synthesis and applications of stimuli-responsive block copolymers are currently not well-explored. In particular, stimuli-responsive triblock copolymers incorporating a central fluorinated block are highly challenging to synthesize. For this purpose, a novel dual light-responsive triblock terpolymer, PEG-*ONB*-PFOEMA-*b*-PCEMA, as shown in Figure 1.6 was designed. The synthesis of PEG-*ONB*-PFOEMA-*b*-PCEMA was executed via ATRP, the first of its kind in terms of block sequences and compositions. The PEG block is water-soluble, the PCEMA block is both hydrophobic and photo-crosslinkable, and the PFOEMA block possesses a low surface tension. Meanwhile, *ONB* denotes a photo-cleavable *ortho*-nitrobenzyl unit placed at the junction between the PEG and PFOEMA blocks. In this study, the reaction conditions for the preparation of PEG-*ONB*-PFOEMA and PEG-*ONB*-PFOEMA-*b*-PHEMA were optimized using ATRP. Post-polymerization modifications yielded the dual light-responsive PEG-*ONB*-PFOEMA-*b*-PCEMA triblock copolymer. The micellar morphologies of this copolymer were prepared in tetrahydrofuran/water mixture and examined via AFM and TEM techniques. In these dispersions, PEG formed the micellar corona, PFOEMA formed an intermediate shell domain,

while PCEMA formed a central core. We also investigated the changes in the properties of the micellar dispersions upon exposure to UV light. This UV light exposure triggered the crosslinking of the PCEMA block and induced the cleavage of the PEG block. The crosslinked PFOEMA-*b*-PCEMA nanoparticles were screened for their water- and oil-repellent properties due to the exposure of the initially masked PFOEMA block. The synthesis of this novel PEG-*ONB*-PFOEMA-*b*-PCEMA copolymer will open new doors for the synthesis of novel functional polymers.

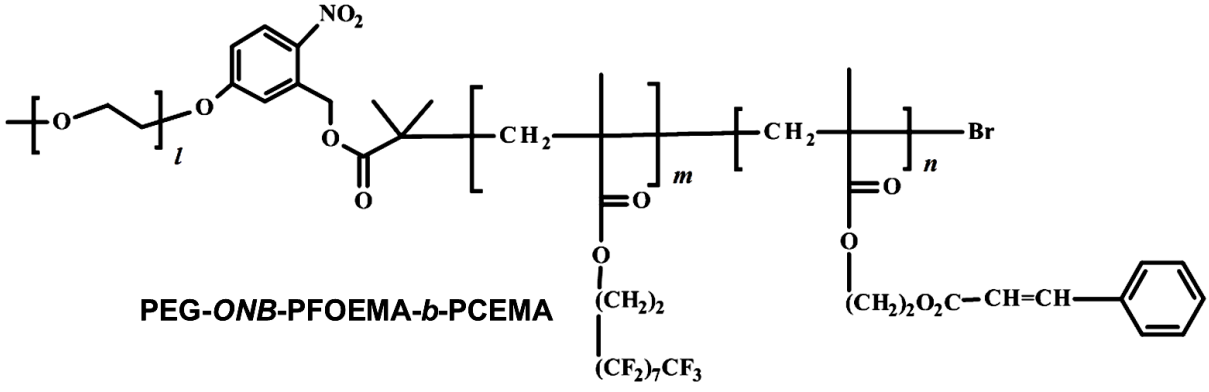

Figure 1.6. Structure of PEG_l-*ONB*-$PFOEMA_m$-*b*-$PCEMA_n$.

Chapter 3 deals with the synthesis of doubly stimulable triblock copolymer PEG-S_2-PFOEMA-*b*-PCEMA, which is shown in Figure 1.7. This copolymer incorporates a reducing agent cleavable disulfide group located at the junction between the PEG and PFOEMA blocks. Upon PEG cleavage at this junction, the PFOEMA chains will become exposed. Two PEG-S_2-PFOEMA-*b*-PCEMA triblock copolymers with different molecular weights were prepared by ATRP and end-coupling methods. The micellization in tetrahydrofuran/water solvent mixtures at different solvent compositions were investigated. In these dispersions, PEG formed the

micellar corona, PFOEMA formed an intermediate shell domain, while PCEMA formed a central core. In addition, the aggregates after crosslinking and PEG cleavage were studied. We also investigated the cleavage of the PEG corona upon exposure to reducing agent dithiothreitol (DTT), and studied the amphiphobic properties of the crosslinked PEG-cleft nanoparticles. This synthetic strategy will help to prepare new stimuli-responsive polymers especially to block copolymers having central PFOEMA or other fluorinated blocks for future applications.

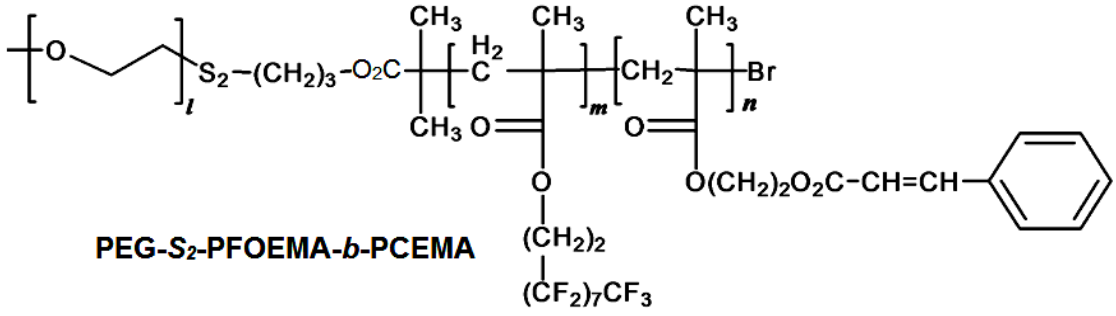

Figure 1.7. Chemical structure of PEG_{l}-S_2-$PFOEMA_{m}$-*b*-$PCEMA_{n}$.

Chapter 4 will discuss the preparation of cotton coatings from solutions of block copolymers, especially the dual light responsive copolymer PEG-*ONB*-PFOEMA-*b*-PCEMA. To the best of our knowledge, there have been no reports of cotton being coated by the use of block copolymer micellar dispersions. The aim of this project was to develop a facile method for the preparation of amphiphobic cotton coatings from aqueous PEG-*ONB*-PFOEMA-*b*-PCEMA solutions. Furthermore, another goal of this study was to optimize the coating conditions by adjusting parameters such as the concentration, soaking time, and solvent composition to determine which protocols provided the best results. To demonstrate that the PCEMA block was anchored onto the cotton surface and the PFOEMA chains indeed formed top layer, we analysed the coated cotton surfaces via XPS, AFM, and also TGA analysis. Additionally, the applicability of this method was also extended to semi-cotton samples.

Chapter 5 describes the synthesis of PEG-*b*-PHEMA by anionic polymerization. The structure of PEG-*b*-PHEMA is shown in Figure 1.8. The synthesis of block copolymers incorporating both PEG and polymethacrylate blocks via anionic polymerization was attempted in the past, but those attempts did not yield desirable results.[114] As a proof of concept, diphenylethylene end-functionalized PEG (PEG-DPE) was synthesized as a latent macroinitiator for the block copolymerization of HEMA-TMS. The conditions of this reaction were also optimized in this investigation.

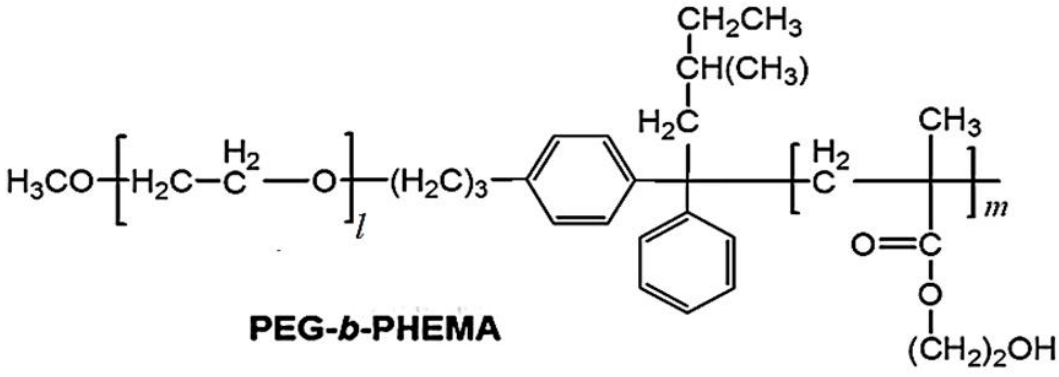

Figure 1.8. Chemical structure of PEG_l-*b*-$PHEMA_m$, which was synthesized via anionic polymerization.

1.7 References

1. Jenkins, A. D.; Kratochvil, P.; Stepto, R.F.T.; Suter, U.W. IUPAC. Pure & Appl. Chem. **1996,** *68*, 2287.
2. Endo. K. *Adv. Polym. Sci.* **2008**, *217*, 121.
3. Lazzari, M.; Liu, G.J.; Lecommandoux, S. *Block Copolymers in Nanoscience*. Wiley-VCH: Weinheim, Germany, 2006.
4. Lodge, T.P. *Macromol. Chem. Phys.* **2003,** *204*, 265.
5. Riess, G. *Prog. Polym. Sci.* **2003,** *28*, 1107.
6. Lysenko, E.; Bronich, T.; Slonkina, E.; Eisenberg, A.; Kabanov, V.; Kabanov, A. *Macromolecules*, **2002,** *35*, 6351.
7. Zhang, L.; Eisenberg, A. *Polym. Adv. Technol.* **1998**, *9*, 677.
8. Zhang, L.; Eisenberg, A. *Science*, **1995,** *268*, 1728.
9. Cameron, N.S.; Corbierre M.; Eisenberg, A. *Can. J. Chem.* **1999,** *77*, 1311.
10. Ding, J.F; Liu, G.J; Yang, M. *Polymer*, **1997,** *38*, 5497.
11. Adams, M.; Lavansanifar, A.; Kwon, G. *J. Pharm. Sci*. **2003,** *92*, 1343.
12. Kataoka, A.; Harada, A.; Nagasaki, Y. *Adv. Drug Deliver. Rev.* **2001,** *47*, 113.
13. Lee, J.S; Hirao, A.; Nakahama, S. *Macromolecules*, **1989,** *22*, 2602.
14. Segalman, R. A.; Yokoyama, H.; Kramer, E. J. *Adv. Mater.* **2001,** *13*, 1152.
15. Krausch, G.; Magerle, R. *Adv. Mater.* **2002,** *14*, 1479.
16. Matyjaszewski, K.; Davis, T. *Handbook of Radical Polymerization*, John Wiley: Chichester, 2002.
17. Blackeley, D.; Twaits, R. Ionic Polymerization. *Addition Polymers: Formation and Characterization*, Plenum Press: New York, 1968.

18. Ladousse, A.; Filliatre, C.; Mallard, B. ; Maillard, B. ; Manigand, C.; Villenvae, J.J. *Eur. Polym. J.* **1979,** *15*, 987.

19. Xu, X.; Flores, J.D.; McCormick, C.L. *Macromolecules,* **2011,** *44,* 1327.

20. Zhang W.; Zhang, W.; Zhang, Z.B.; Zhu, J.; Pan, Q.; Zhu X.L. *Polym. Bull.* **2009,** *63,* 467.

21. Ladmiral, V.; Mantovani, G.; Clarkson, G. J.; Cauet, S.; Irwin, J. L.; Haddleton, D. M. *J. Am. Chem. Soc.* **2006,** *128,* 4823.

22. Ding, L.; Xie, M.; Yang, D.; Song, C. *Macromolecules,* **2010,** *43*, 10336.

23. Herndon, J.W. *Coord. Chem. Rev*. **2012,** *256,* 1281.

24. Zeng, J.; Shi, K.; Zhang, Y.; Sun, X.; Zhang, B. *Chem. Commun*. **2008,** *32,* 3753.

25. Szwarc, M.; Levy, M.; Milkovich, R. *J. Am. Chem. Soc.* **1956,** *78,* 2656.

26. Fetters, L.J. *J. Poly. Sci. Part C,* **1969,** *26*, 1.

27. Hsieh, H.L; Quirk, R.P. *Anionic Polymerization: Principles and Practical Applications.* Marcel Dekker, New York, 1996.

28. Goethals, E, J.; Prez, F. D. *Prog. Polym. Sci.* **2007,** *32*, 220.

29. Matyjaszewski, K. *Cationic Polymerizations: Mechanisms, Synthesis and Applications,* New York, 1996.

30. Jizheng, Q.; Bernadette, C.; Matyjaszewski, K. *Prog. Polym. Sci.* **2001,** *26,* 2083.

31. Matyjaszewski, K. *Controlled Radical Polymerization.* ACS symposium Series 685. Washington, DC: American Chemical Society, 1998.

32. Schue, F. *Controlled/Living Radical Polymerization. Progress in ATRP, NMP, and RAFT.* ACS symposium Series 768. Washington, DC: American Chemical Society, 2000.

33. Sciannamea, V.; Jerome, R.; Detrembleur, C. *Chem. Rev.* **2008,** *108*, 1104.

34. Fisher, H. *Chem. Rev.* **2001,** *101*, 3581.

35. Tebben, L.; Studer, A. *Angew. Chem. Int. Ed.* **2011,** *50*, 5034.

36. Moad, G.; Rizzardo, E. *Macromolecules*, **1995,** *28*, 8722.

37. Braunecker, W.A.; Matyjaszewski, K. *Prog. Polym. Sci.* **2007**, *32*, 93.

38. Hawker, C.J.; Bosman, A.W.; Harth, E. *Chem. Rev*. **2001,** *101*, 3661.

39. Robin S.; Gnanou, Y. *Controlled Radical Polymeriation*, ACS Symposium Series, 768, Washington, DC: American Chemical Society 2000.

40. Chong, Y.K.; Le, T.P.T.; Ercole, F.; Moad, G.; Rizzardo, E.; Thang, S.H.;. *Macromolecules*, **1999,** *31*, 7559.

41. Chiefari, J.; Chong, Y. K.; Ercole, F.; Kristina, J.; Jeffery, J.; Le, P. T. T.; Mayadunne, R.T. A.; Meijs, G.F.; Moad, C.L.; Moad, G.; Rizzardo, E.; Thang, S.H. *Macromolecules*, **1998,** *31*, 5559.

42. Smith, A.E.; Xu, X.; McCormick. C.L. *Prog. Polym. Sci.* **2010,** *35*, 45.

43. Moad, G.; Rizzardo, E.; Thang, S.H. *Aust. J. Chem.* **2005,** *58*, 379.

44. Perrier, S.; Takolpuckdee, P. *J. Polym. Sci. A: Polym. Chem.* **2005,** *43*, 5347.

45. Convertine, A. J.; Lokitz, B. S.; Vasileva, Y.; Myrick, L. J.; Scales, C. W.; Lowe, A. B.; McCormick, C. L. *Macromolecules*, **2006,** *39*, 1724.

46. Taton, D.; Wilczewska, A.Z.; Destarac, M. *Macromol. Rapid. Commun.* **2001**, *22*, 1497.

47. McCormack, C.L.; Lowe, A.B. *Acc. Chem. Res.* **2004,** *37*, 312.

48. Kato, M.; Kamigaito, M.; Sawamoto, M.; Higashimura, T. *Macromolecules*, **1995,** *28*, 1721.

49. Wang, J.S; Matyjaszewski, K. *J. Am. Chem. Soc.* **1995,** *117*, 5614.

50. Matyjaszewski, K.; Xia, J.H. *Chem. Rev.* **2001,** *101*, 2921.

51. Patten, T. E.; Matyjaszewski, K. *Adv. Mater.* **1998,** *10*, 901.

52. Matyjaszewski, K. *Chem. Eur. J.* **1999,** *5*, 3095.

53. Davis, K.; O'Malley, J.; Paik, H.J.; Matyjaszewski, K. *Polym.Prepr. (Am. Chem. Soc., Div. Polym. Chem.).* **1997,** *38,* 687.

54. Stump, M. A.; Haddleton, D. M.; McCamley, A.; Duncalf, D.; Segal, J. A.; Irvine, D. J. *Polym. Prepr. (Am. Chem. Soc., Div. Polym. Chem.).* **1997,** *38,* 508.

55. Brandts, J. A. M.; van de Geijn, P.; van Faassen, E. E.; Boersma, J.; Van Koten, G. *J. Organomet. Chem.* **1999,** *584,* 246.

56. Kotani, Y.; Kamigaito, M.; Sawamoto, M. *Macromolecules,* **1999,** *32,* 2420.

57. Ando, T.; Kamigaito, M.; Sawamoto, M. *Macromolecules,* **1997,** *30,* 4507.

58. Xia, J.; Zhang, X.; Matyjaszewski, K. *ACS Symp. Ser.* **2000,** *760,* 207.

59. Wang, X.; Luo, N.; Ying, S. *Polymer,* **1999,** *40,* 4157.

60. Wang, X. S.; Armes, S. P. *Macromolecules,* **2000,** *33,* 6640.

61. Perrier, S.; Armes, S. P.; Wang, X. S.; Malet, F.; Haddleton, D.M. *J. Polym. Sci. Part A: Polym. Chem.* **2001,** *39,* 1696.

62. Matyjaszewski, K.; Coca, S.; Gaynor, S. G.; Nakagawa, Y.; Jo, S. M. *WO Patent* 9801480, U.S. Pat. 5, 1998.

63. Gao, B.; Chen, X.; Ivan, B.; Kops, J.; Batsberg, W. *Polym. Bull.* **1997,** *39,* 559.

64. Liu, Y.; Wang, L.X.; Pan, C.Y. *Macromolecules,* **1999,** *32,* 8301.

65. Shen, Y.Q.; Tang, H.D.; Ding, S.J. *Prog. Polym. Sci.* **2004,** *29,* 1053.

66. Wang, J. S.; Matyjaszewski, K. *Macromolecules,* **1995,** *28,* 7572.

67. Wang, W. X.; Dong, Z. H.; Xia, P.; Yan, D. Y.; Zhang, Q. *Macromol. Rapid Commun.* **1998,** *19,* 647.

68. Wang, W.; Yan, D. *Controlled/Living Radical Polymerisation. ACS Symp. Ser.* **2000,** *768,* 263.

69. Hadjichristidis N.; Pispas S.; Fluodas G.A. *Block Copolymers: Synthetic Strategies, Physical Properties, and Applications.* Wiley Interscience, John Wiley &Sons. Hoboken New Jersey, 2003.

70. Gauthier, M.A.; Gibson, M.I.; Klok, H.A. *Angew. Chem. Int. Ed. Engl.* **2009,** *48*, 48.

71. Zheng, R. H.; Liu, G.J.; Yan X. H. *J. Am. Chem. Soc.*, **2005,** *127*, 15358.

72. Urban, M. W. *Prog. Polym. Sci.* **2009,** *34*, 679.

73. Fujishige, S.; Kubota, K.; Ando, I. *J. Phys. Chem.* **1989,** *93*, 3311.

74. Maeda, Y.; Nakamura, T.; Ikeda, I. *Macromolecules,* **2002,** *35*, 217.

75. Aoki, T.; Muramatsu, M.; Torii, T.; Sanui, K.; Ogata, N. *Macromolecules,* **2001,** *34*, 3118.

76. Liu, F.; Urban, M.W. *Macromolecules,* **2008,** *41*, 352.

77. Connal, L. A.; Li, Q.; Quinn, J. F.; Tjipto, E.; Caruso, F.; Qiao, G.G. *Macromolecules,* **2008,** *41*, 2620.

78. He, E.; Yue, C. Y.; Tam, K. C. *Langmuir*, **2009,** *25*, 4892.

79. Hu, L.; Chu, L.Y.; Yang, M.; Wang, H.D.; Hui, N.C. *J. Colloid. Interf. Sci.* **2007,** *311*, 110.

80. Guo, A.; Liu, G. J.; Tao, J. *Macromolecules*, **1996,** *29*, 2487.

81. Liu, G. J.; Qiao, L. J.; Guo, A. *Macromolecules,* **1996**, *29*, 5508.

82. Kang, M.; Moon, B. *Macromolecules,* **2009**, *42*, 455.

83. Hirao, A.; Sugiyama, K.; Yokoyama, H. *Progr. Polym. Sci.* **2007,** *32*, 1393.

84. Zhaou, Z. H.; Liu, G. J.; Hong, L. Z. *Biomacromolecules,* **2011,** *12*, 813.

85. Roy, D.; Cambre, J.N.; Sumerlin, B.S. *Chem. Commun.* **2009,** *16*, 2106.

86. Wang, J. S.; Matyjaszewski, K. *J. Am. Chem. Soc.* **1995,** *117*, 5614.

87. Schumers, J.M; Fustin, C.A.; Gohy, J. F. *Macromol. Rapid. Commun.* **2010**, *31*, 1588.

88. Liu, F.; Urban, M. W. *Prog. Polym. Sci.* **2010**, *35*, 3.

89. Brun-Graeppi, A.K.A.S.; Richard, C.; Bessodes, M.; Scherman, D.; Merten, O. *Prog. Polym. Sci.* **2010**, *35*, 1311.

90. Li, X. M.; Reinhoudt, D.; Crego-Calama, M. *Chem. Soc. Rev.* **2007**, *36*, 1350.

91. Feng, L.; Yang, Z.; Zhai, J.; Song, Y.; Ma, Y.; Yang, Z.; Jiang, L.; Zhu, D. *Angew. Chem. Int. Ed.* **2003,** *42*, 7.

92. Tuteja, A.; Choi, W.; Ma, M.; Mabry, M.J.; Mazella, S.A.; Rutledge, G. C.; Mckinley, G.H.; Cohen, R.E. *Science*, **2007,** *318*, 1618.

93. Lide, D. R. Ed. *Handbook of Chemistry and Physics.* 76th Ed. CRC Press: Boca Raton, FL (US), 1995.

94. Lafuma, A.; Quere, D. *Nat. Mater*. **2003,** 2, 457.

95. Wenzel, R. N. *Ind. Eng. Chem.* **1936,** *28*, 988.

96. Cassie, A. B. D.; Baxter, S. *T. Faraday Soc.* **1944,** *40*, 0546.

97. Staurt, B. H. *Polymer Analysis*; Wiley: Chichester, **2002**.

98. McMurry, J. *Organic Chemistry*. 4th Ed. Brooks/Cole Pacific Grove, USA, 1996.

99. Fawcett, A.H. *Polymer Spectroscopy.* Wiley, Chichester England, 1996.

100. Duer, M.J. *Introduction to Solid-State NMR Spectroscopy*. Blackwell Publishing, 2004.

101. Koenig, J. L. *Spectroscopy of Polymer* 2nd Ed. Elsevier, Amsterdam, New York, 1999.

102. Wu, C.S. *Handbook of Size Exclusion Chromatography and Related Techniques.* Ed. Marcel Dekker Inc. New York, 2004.

103. Trathnigg, B. *Prog. Polym. Sci.* **1995,** *20*, 615.

104. Chromatography. San Diego State University, accessed 3 March 2013. <http://www.sci.sdsu.edu/TFrey/Bio750/Chromatography.html>.

105. Grubisic, Z.; Rempp, R.; Benoit, H. *J. Polym. Sci. B.* **1967,** *5*, 753.

106. Born, M.W.E. *Principles of Optics*. Cambridge Univ. Press: Cambridge, U.K., 1999.

107. Magonov, S. N. W., M.H. *Surface Analysis with STM and AFM*; VCH: Weinheim, 1996.

108. Chowdhury, S.; Laugier, M. T. *Nanotechnology*, **2004**, *15*, 1017.

109. Bar, G.; Thomann, Y.; Brandsch, R.; Cantow, H.J.; Whangbo, M.H. *Langmuir*, **1997**, *13*, 3807.

110. Wang, J.; Horton, J. H.; Liu, G.; Lee, S.; Shea, K. J. *Polymer*, **2007**, *48*, 4123.

111. Gao, Yang. (2011). *Polymolecular and Unimolecular Micelles of Triblock Copolymers*. Ph.D. Thesis. Queen's University, Canada.

112. de Las Heras, A. C.; Pennadam, S.; Alexander, C. *Chem. Soc. Rev.* **2005,** *34*, 276.

113. Galaev, I. Y.; Mattiasson, B. *Trends Biotechnol.* **1999,** *17*, 335.

114. Suzuki, T.; Muarakami, Y.; Takegami, Y. *Polym. J.* **1980,** *12*, 183.

Chapter 2 - Design, Synthesis and Application of a Dual Light-Responsive Triblock Terpolymer

2.1 Preface

The material described in this chapter has been published as: Rabnawaz, M.; Liu, G. **Preparation and Application of a Dual Light-Responsive Triblock Terpolymer**, *Macromolecules*, **2012**, *45*(13), 5586–5595 **(DOI:** 10.1021/ma3006476).

2.2 Introduction

Light-responsive block copolymers have various applications.[1] For example, the photo-crosslinking of poly(2-cinnamoyloxyethyl methacrylate)- (or PCEMA)-bearing micelles[2-6] stabilizes their structures to yield "permanent" nanostructures. Some examples of these permanent nanostructures include nanofibers,[3,4,7] nanotubes,[8-10] nanospheres,[2] and hollow nanospheres.[11-13] Subjecting thin films of a diblock copolymer to photo-cleavage at its block junction and subsequently removing the minority block via solvent extraction yielded membranes with controlled and uniformly-sized permeating nanochannels.[14-19] Furthermore, photo-induced dissociation of block copolymer micelles has been tested *in vitro* for triggering drug release from carrier micelles.[20-22] Last but not least, block copolymers bearing azobenzene units that undergo a photo-induced reversible *trans-cis* isomerisation have been studied extensively for their potential applications in optical information storage and other areas.[1]

Reported in this chapter is the synthesis of a triblock copolymer that bears a photo-crosslinkable block and a photo-cleavable block junction. Upon UV irradiation, photo-crosslinking and cleavage of the triblock copolymer occurs concurrently. While there have been many reports describing the synthesis of multiply stimulable block copolymers capable of

responding to multiple stimuli,[23,24,25,26] reports on multi-responsive block copolymers have been rare.[27] Aside from the system reported by Zhao and coworkers,[27] this represents the second report of a block copolymer possessing dual light responses.

The targeted polymer consists of poly(ethylene glycol)-*orthonitrobenzyl*-poly[2-(perfluorooctyl)ethyl methacrylate)-*block*-poly(2-cinnamoloxyethyl methacrylate) (PEG-*ONB*-PFOEMA-*b*-PCEMA or P1), as shown in Figure 2.1. Here the PEG block is water soluble, the fluorinated PFOEMA block possesses low surface tension,[28] and the PCEMA block is photo-crosslinkable.[2,29] Meanwhile, *ONB* denotes a photo-cleavable *ortho*-nitrobenzyl unit. Also reported is the preparation of micelles from P1 in THF/water mixtures at a water volume fraction (f_{H2O}) of 80%, in which only the PEG block was soluble. Exposure to light caused the PCEMA domains to undergo crosslinking and the PEG coronas to become cleaved from the micelles, resulting in a photo-induced particle precipitation. Coatings prepared from these photolyzed particles were strongly water- and oil-repellent due to the exposure of the originally masked or hidden PFOEMA block.

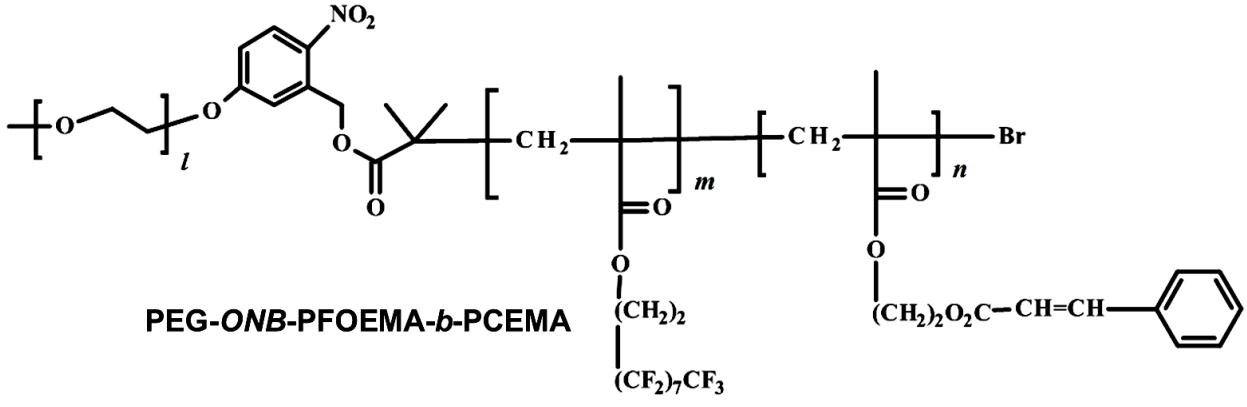

Figure 2.1. Chemical structure of PEG_l-*ONB*-$PFOEMA_m$-*b*-$PCEMA_n$ (P1).

While the copolymer composition disclosed in this chapter is new, atom transfer radical polymerization (ATRP),[30,31,32] reversible addition-fragmentation chain transfer polymerization (RAFT),[33,34] and anionic polymerization[35,36] have been used to prepare copolymers containing fluorinated blocks. Such diblock copolymers have included poly[oligo(ethylene glycol) monomethyl ether acrylate]-*block*-poly(1H,1H-perfluorobutyl acrylate),[37] poly(butyl methacrylate)-*block*-poly(perfluoroalkyl acrylate),[38] poly(4-fluorostyrene)-*block*-poly(methyl acrylate) and poly(perfluorooctyl acrylate)-*block*-poly(methyl methacrylate),[39] PEGA-*b*-PFOEMA,[40] and poly(styrene)-*block*-poly(2,2,3,3,4,4,4-heptafluorobutyl methacrylate).[41] Examples of fluorinated triblock copolymers prepared in this manner have included poly(ethylene glycol)-*block*-polystyrene-*block*-poly(perfluorohexylethyl acrylate)[42] and poly[4-methyl-4-(4-vinylbenzyl)morpholin-4-ium chloride]-*block*-polystyrene-*block*-poly(pentafluorophenyl 4-vinylbenzyl ether).[43] Triblock copolymers have also been prepared through different monomer addition sequences, where fluorinated blocks such as poly(1H,1H-perfluorobutyl acrylate) (PFBA)[37] and poly(perfluorooctylethyl methacrylate) (PFOEMA)[40] were incorporated as the last block.

2.2.1 Objectives

This chapter describes the design and synthesis of a novel dual light-responsive triblock copolymer, P1. For the first time, a synthetic methodology for preparing a dual light responsive polymer with this novel composition has been established. Also, the aim of this study was to explore the formation of micelles of P1 in THF/water solutions and their light-responsive behaviour. Exposure to light induced both crosslinking of PCEMA domains and cleavage of PEG chains. In addition, the wetting properties of the PEG-cleft particles (bearing exposed PFOEMA chains on their surfaces) were investigated.

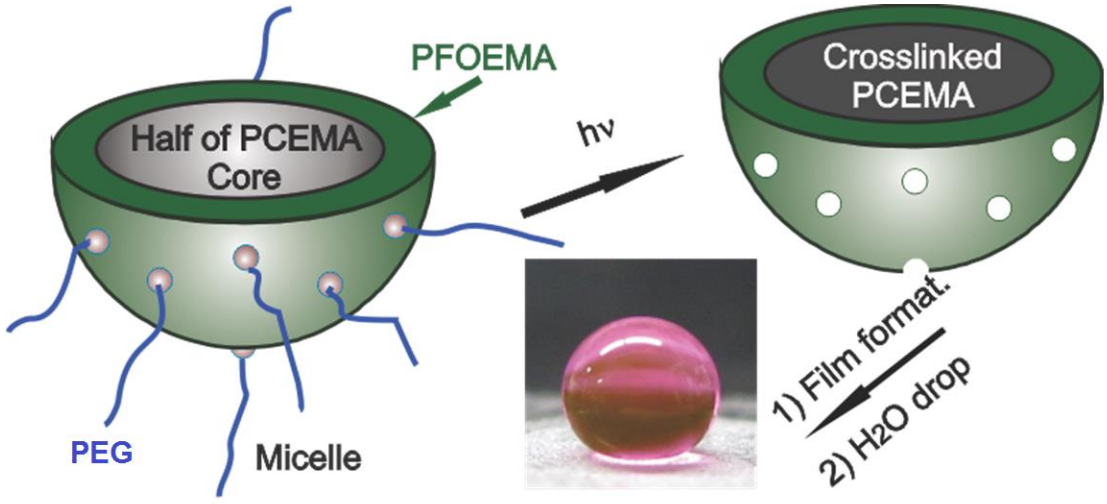

Scheme 2.1. Schematic representation of P1 micelles before and after photolysis treatment. The photograph in the inset shows a water droplet placed onto a film cast from a dispersion of the PEG-cleft particles.

2.2.2 Experimental Design Considerations

In this study, the synthesis of a dual light-responsive triblock copolymer P1 is reported. P1 was chosen mainly for two reasons. Firstly, the block sequence of P1 is such that the envisioned micelles formed in aqueous solutions incorporate PEG chains as the corona, a cross-linkable PCEMA block as the inner core and PFOEMA chains forming a central shell, as shown in Scheme 2.1. Secondly, the ONB linker is placed strategically at PFOEMA and PEG junction. Upon exposure to light, simultaneous crosslinking of the PCEMA block and rearrangement of the *ONB* group will occur, thus yielding PEG-cleft crosslinked particles bearing exposed PFOEMA chains. Cast films of PEG-cleft particles should be both water- and oil-repellent due to the exposure of the initially hidden PFOEMA chains.

2.3 Experimental Section

2.3.1 Materials

2-Trimethylsiloxyethyl methacrylate (HEMA-TMS) was synthesized according to a literature method[44] and was distilled over calcium hydride before use. Prior to use, poly(ethylene glycol) monomethyl ether (Aldrich, M_n = 5,000 g/mol) was vacuum-dried for 3 d at 55 ^oC, pyridine (ACS reagent, Fisher Scientific) was refluxed and distilled over CaH_2 under nitrogen, and tetrahydrofuran (THF) was distilled over sodium and a small amount of benzophenone. Cinnamoyl chloride (98%, Aldrich), 5-hydroxy-2-nitrobenzaldehyde (98%, Aldrich), *p*-toluenesulphonyl chloride (99.0%, TCI), and 2-bromoisobutyryl bromide (98%, Aldrich), triethylamine (> 99.5%, Sigma-Aldrich), α,α,α-trifluorotoluene (TFT, 99+%, Acros), anisole (99%, Sigma-Aldrich), CuBr (Aldrich, 99.999%), $CuBr_2$ (Aldrich, 99.999%), bipyridine (Acros, 99+%), and poly(ethylene glycol) monomethyl ether (PEG-550, Fluka, M_n = 550 g/mol) were used as received.

2.3.2 Characterization

Size exclusion chromatography (SEC) was performed at 70 °C on a Waters 515 system equipped with a Waters 2410 refractive index detector. The three columns were packed by American Polymer Standards Corporation with 5-μm AM 1000, 10,000, and 100,000 Å gels. The system was calibrated using monodisperse polystyrene (PS) standards. The eluent used was a dimethylformamide (DMF) solution containing tetrabutylammonium bromide at 2.5 g/L. The flow rate was 0.9 mL/min. ^1H NMR measurements were performed using Bruker Avance-300, Avance-400 or Avance-500 instruments using deuterated pyridine-d_5, methanol-d_4 or chloroform-*d* as solvents and a 3 s relaxation delay.

2.3.3 Synthesis of the Macroinitiator

The ATRP macroinitiator PEG_{113}-*ONB*-Br bearing an *ONB* unit between PEG and the initiating site was synthesized in three steps following a literature method.[18] The overall yield for the macroinitiator was 40% and this product was characterized by ^{1}H NMR in $CDCl_3$: δ 8.2 (*d*, *J* = 9 Hz, 1H), 7.2 (*s*, 1H), 6.98 (*dd*, *J* = 9.0 Hz and 2.2 Hz, 1H), 5.6 (*s*, 2H), 4.24 (*t*, *J* = 5 Hz, 2H), 3.8-3.4 (*br*, -O*CH*$_2$*CH*$_2$, 456H), 3.3 (*s*, CH_3, 3H), 2.0 (*s*, 6H) ppm.

2.3.4 Synthesis of PEG-*ONB*-PFOEMA

PEG-*ONB*-Br (0.30 g, 5.6×10^{-2} mmol) and FOEMA (0.31 mL, 9.6×10^{-1} mmol) were mixed in a two neck flask. To this mixture were added anisole (0.7 mL), TFT (0.7 mL), bipyridine (17.6 mg, 1.13×10^{-1} mmol), and $CuBr_2$ (1.2 mg, 5.3×10^{-3} mmol). The flask was purged with N_2 before CuBr (8.14 mg, 5.60×10^{-2} mmol) was added under nitrogen. The flask was then degassed by three freeze-pump-thaw-N_2 refill cycles before it was immersed into a pre-heated oil bath at 85 ^{o}C. The polymerization was quenched after 1 h by immersing the reaction flask into a liquid nitrogen bath and the introduction of air. The crude mixture was warmed to room temperature, and then passed through an alumina column using THF as the eluent to remove ligated copper. This mixture was subsequently concentrated to 2.0 mL via rotary evaporation, and then added into 20 mL of diethyl ether to precipitate the polymer. The precipitate was re-dissolved into 2.0 mL of THF, and the resultant solution was added into another 20 mL of diethyl ether to precipitate the polymer. This precipitation procedure was repeated once more before the polymer was dried under vacuum for 24 h to yield 0.61g of product in 86% yield. ^{1}H NMR ($CDCl_3$, 500 MHz): δ 4.4 (*br*, -COO*CH*$_2$, 24H), 3.8-3.4 (*br*, *CH*$_2$*CH*$_2$O, 456H,), 2.3 (*br*, -CH_2*CH*$_2$$CF_2$, 24H), 0.8-1.4 (*br*, CH_3, 36H) ppm.

2.3.5 FOEMA Polymerization Kinetics

The synthetic procedure discussed above in Section 2.3.4 was also used here to synthesize PEG-*ONB*-PFOEMA, except that samples (~0.05 mL each) were collected from the reaction mixture at 1.0, 2.0, and 3.0 h. The crude mixture was exposed to air in a vial that was placed in liquid nitrogen to stop the reaction. Subsequently, 0.5 mL of $CDCl_3$ was added to each sample for ^1H NMR analysis. The decrease in the area of the FOEMA signal at 4.4 ppm was compared with that of the main PEG signal at 3.4-3.8 ppm to determine the FOEMA conversion. For SEC analysis, samples were prepared by initially passing the crude mixture over a short pad of alumina to remove residual copper. The solvent was subsequently evaporated, and the crude mixture was then dissolved into DMF at a concentration of 5 mg/mL.

2.3.6 Synthesis of PEG-*ONB*-PFOEMA-*b*-PHEMA.

PEG-*ONB*-*b*-PFOEMA was placed into a dialysis tube with a cut-off molecular weight of 12,000 g/mol and dialysed against distilled THF. The solvent was changed 4 times over 36 h to remove low molecular weight impurities. The dialysed PEG-*ONB*-PFOEMA sample was dried (0.68 g, 5.9×10^{-2} mmol), transferred into a two-neck flask, and subsequently re-dissolved in a solvent mixture of anisole/TFT (4.0 mL, v/v = 1/1). After 20 min of stirring at room temperature, HEMA-TMS monomer (0.80 mL, 3.8×10^{-1} mmol), bipyridine ligand (35 mg, 2.2×10^{-1} mmol) and $CuBr_2$ (2.0 mg, 8.1×10^{-3} mmol) were added. CuBr (15.1 mg, 1.05×10^{-1} mmol) was added only after the system was purged with N_2. The flask was subjected to four freeze-pump-thaw-N_2 refill cycles, and subsequently immersed into a pre-heated oil bath at 65 ^oC. After 3 h, the reaction flask was quenched in liquid N_2 and opened to introduce air. Ligated copper was removed by passing the crude mixture through a short pad of alumina using THF as

the eluent. At the end of the elution, methanol and water were added to reach volume ratios of 3/0.5/0.1 for THF, methanol, and water, respectively. The TMS group was removed after the mixture was stirred overnight at room temperature. The crude polymer was dissolved into THF (4.0 mL) and precipitated from 50 mL of diethyl ether. This sequence was repeated another time. The product was subsequently centrifuged at 3900 rpm (2600 *g*) for 10 min to yield a compact precipitate. This precipitate was dried under vacuum for 16 h, yielding 0.71 g of the target polymer in 82% yield. ^{1}H NMR (CD_3OD, 500 MHz): δ 4.2 (*br*, -COO*CH*$_2$, 50H), (*br*, -*CH*$_2$OH, 50H), 3.4-3.7 (*br*, -*CH*$_2$*CH*$_2$O, 456H), 0.9-1.4 (*br*, -CH_3, 75H) ppm.

2.3.7 Synthesis of PEG-*ONB*-PFOEMA-*b*-PCEMA (P1)

PEG-*ONB*-PFOEMA-*b*-PHEMA (0.20 g, 1.1×10^{-2} mmol containing 2.8×10^{-1} mmol of hydroxyl groups) was dissolved into 4.0 mL of dry pyridine and stirred for 30 min before cinnamoyl chloride (302 mg, 1.80 mmol, 6.50 molar equivalents) was added. After stirring the mixture in the dark overnight at room temperature, the reacted mixture was centrifuged at 3900 rpm (2600 *g*) for 10 min to settle the pyridinium salt. The supernatant was concentrated to ~2.5 mL via rotary evaporation and added into 50 mL of diethyl ether to precipitate the polymer. The precipitate was briefly dried before it was re-dissolved into 3.0 mL of THF. The resultant solution was added into another 50 mL of diethyl ether to precipitate the polymer. This procedure was repeated once again. The resultant solid was dried at room temperature in a vacuum oven overnight to yield 0.20 g of polymer in 82% yield. ^{1}H NMR ($CDCl_3$, 500 MHz): δ 7.8-7.2 (aromatic protons, 5H), 4.25 (*br*, -COO*CH*$_2$CH$_2$CF$_2$, 24H), 4.2 (*br*, -COO*CH*$_2$, 50H), 4.05 (*br*, -COOCH$_2$*CH*$_2$, 50H), 3.5-3.6 (*br*, -*CH*$_2$*CH*$_2$O, 456H), 2.4 (*br*, -*CH*$_2$CF$_2$, 24H), δ 1.8-2.2 (*br*, CH$_2$, 74H), 0.8-1.4 (*br*, CH_3, 3H, 111H) ppm.

2.3.8 Synthesis of the PEG-Br Macroinitiator

The PEG-Br macroinitiator was prepared by reacting poly(ethylene glycol) monomethyl ether with 2-bromoisobutyryl bromide using the protocol used to prepare PEG-*ONB*-Br. ^{1}H NMR (300 MHz, $CDCl_3$): δ 4.24 (-CH_2OOC, 2H), 3.35-3.80 (*br*, -CH_2CH_2O, 456H), 3.38 (3H, -OCH_3, 3H), 2.03 (CH_3, 6H) ppm.

2.3.9 Synthesis of PEG-*b*-PHEMA

The polymerization procedure was similar to that used to prepare PEG-*ONB*-PFOEMA-*b*-PHEMA from PEG-*ONB*-PFOEMA-Br, except that PEG-Br was used as the macroinitiator. The crude product was filtered through an aluminum pad to remove the catalyst, and subsequently dissolved into THF (2.0 mL). This solution was then added into 40 mL of diethyl ether to precipitate the polymer. This procedure was repeated once again. The polymer was centrifuged at 3900 rpm (2600 *g*) and dried under vacuum for 24 h, producing 0.31 g of the product in 60% yield. ^{1}H NMR (CD_3OD, 500 MHz): δ 4.2 (*br*, -COOCH_2, 2H), 3.8 (*br*, -$COOCH_2CH_2$, 2H), 3.8-3.4 (*br*, -OCH_2CH_2, 4H), 1.0-1.4 (*br*, -CH_3, 3H) ppm.

2.3.10 PEG-*b*-PCEMA.

A cinnamation reaction was performed to convert PEG-*b*-PHEMA into PEG-*b*-PCEMA following the procedure described above in Section 2.3.7 for the cinnamation of PEG-*ONB*-PFOEMA-*b*-PHEMA. PEG-*b*-PCEMA was obtained in 88% yield. ^{1}H NMR ($CDCl_3$, 500 MHz): δ 7.8-7.2 (aromatic protons), 4.25 (*br*, -COOCH_2, 2H), δ 4.15 (*br*, -$COOCH_2CH_2$CO, 2H), 3.5-3.6 (*br*, -CH_2CH_2O, 4H), 1.8-2.2 (*br*, -CH_2, 2H), δ 0.8-1.4 (*br*, CH_3, 3H) ppm.

2.3.11 PEG-*ONB*-PFOEMA-*b*-PCEMA Micelles

P1 (2.0 mg) was dissolved into 2.0 mL of THF and stirred for 4 h at room temperature. Water (8.0 mL) was added at a rate of 6-7 drops per minute to the solution until f_{H2O} reached 80%. The final solution had a concentration of ~0.1 mg/mL and was stirred at 500 rpm at room temperature until analysis.

2.3.12 TEM Measurements

Transmission electron microscopy (TEM) specimens were prepared by aero-spraying samples via a homemade atomizer onto cellulose-coated copper grids.[45] The specimens were further dried under vacuum for 4 h before they were stained with OsO_4 vapour for 1.5 h. The specimens were analysed using a Hitachi H-7000 instrument operated at 75 kV.

2.3.13 AFM Measurements

Specimens were prepared by aero-spraying samples onto freshly cleft sheet mica surfaces. Tapping mode atomic force microscopy (AFM) was performed using a Veeco Multimode microscope equipped with a Nanoscope IIIa controller. The silicon cantilevers used had a force constant of ~40 N/m and an oscillating frequency of ~300 kHz.

2.3.14 Micellar Photolysis

A P1 solution (3.0 mL at 0.06 mg/mL in THF/water at f_{H2O} = 80%) was irradiated in a 1.00 cm thick Hellma quartz cell. The contents of the cell were magnetically stirred to ensure a uniform photolysis treatment. The photolysis was performed using a focused beam generated by a 500 W mercury lamp in an Oriel 6140 lamp housing powered by an Oriel 6128 power supply.

This beam of light was passed through a 300 nm cut-off filter before it reached the sample. To monitor the reaction progress, UV absorption spectra were recorded at different times.

In order to monitor the photolysis progress via SEC, P1 (16 mg) was initially dissolved into 0.40 mL of THF before water was added at a rate of 6-7 drops/minute until the total volume reached 2.0 mL. This was followed by the addition of PEG-550 (11.8 mg) as an internal standard. At pre-designated times 0.15 mL of the irradiated sample was collected, dried in a vacuum oven, and then dissolved in 0.02 mL of DMF for SEC analysis.

2.3.15 Contact Angle Measurements

The P1 particles that were photolyzed for 3 h were found to have exposed PFOEMA domains. The photolyzed particles were settled from the solvation medium via centrifugation for 10 min at 2500 rpm (1250 *g*). The settled particles (~1.0 mg) were then stirred with 10 mL of methanol for 1 h before the particles were settled by centrifugation for 10 min at 1250 *g*. The methanol rinsing step was repeated three times, and the final particles (~0.75 mg) were dispersed again into TFT (2.0 mL). Two droplets of this dispersion were then dispensed onto a glass plate to cover an area of ~5-6 mm^2. After the TFT had evaporated from these droplets, another 2 droplets were applied to the same area. This procedure was repeated once again. The particulate film was allowed to dry for 14 h before contact angle measurements were performed using 5 μL test droplets.

2.4 Results and Discussion

The first aspect of this study involved the preparation of the triblock copolymer PEG-*ONB*-PFOEMA-*b*-PCEMA, which is also abbreviated as P1. To prepare P1, a PEG-*ONB*-Br macro-initiator bearing an *ONB* unit between the PEG chain and an initiating site was first synthesized.[18,19] This preparation was followed by the sequential ATRP of FOEMA and 2-trimethylsilyloxyethyl methacrylate (HEMA-TMS) to yield the triblock copolymer PEG-*ONB*-PFOEMA-*b*-P(HEMA-TMS). The targeted P1 copolymer was obtained after the cleavage of the trimethylsilyl group and the cinnamation of the resultant PHEMA block with cinnamoyl chloride.[2] An overall yield of 23.1% was obtained for P1 with high degree of reproducibility.

2.4.1 PEG-*ONB*-Br

PEG-*ONB*-Br was synthesized according to a literature method using the reactions depicted in Scheme 2.2[18] The commercially-available 5-hydroxy-2-nitrobenzaldehyde was first reduced via treatment with $NaBH_4$ to yield 3-hydroxymethyl-4-nitrophenol. The latter reagent was then reacted with α-methoxy-ω-toluenesulfonyl-PEG, to yield PEG chains bearing a terminal hydroxyl group. This hydroxyl group was further reacted with 2-bromoisobutyryl bromide to yield the targeted macroinitiator.

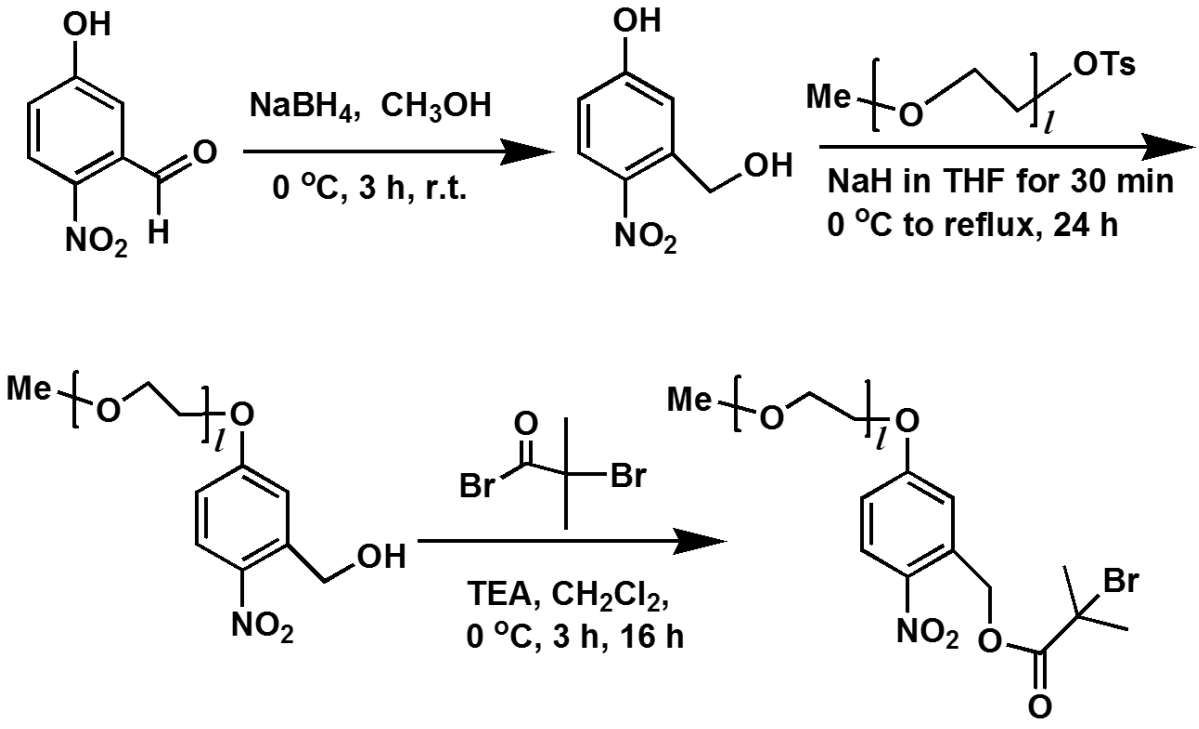

Scheme 2.2. Reactions used to synthesize PEG$_l$-*ONB*-Br.

Figure 2.3 shows a ^{1}H NMR spectrum of PEG-*ONB*-Br in $CDCl_3$ and its peak assignments. Our analysis suggested that PEG was quantitatively labelled by 3-hydroxymethyl-4-nitrophenol, as shown in Figure 2.2. The singlet with an integration corresponding to two protons at 5.0 ppm was derived from the benzyl protons. Meanwhile, the protons of the main PEG chain were responsible for the signal appearing between 3.5 and 3.8 ppm. The ratio between the two signal integrations was 477.05/2.09, which equalled 228. Theoretically, this ratio should be 226. A quantitative end-capping was important, because the incomplete end-capping of the PEG terminal hydroxyl groups by 3-hydroxymethyl-4-nitrophenol would lead to their capping by 2-bromoisobutyryl bromide in the subsequent step and eventually yield PEG-*b*-PFOEMA-*b*-PCEMA. Unlike PEG-*ONB*-PFOEMA-*b*-PCEMA, PEG-*b*-PFOEMA-*b*-PCEMA would not undergo photochemical cleavage.

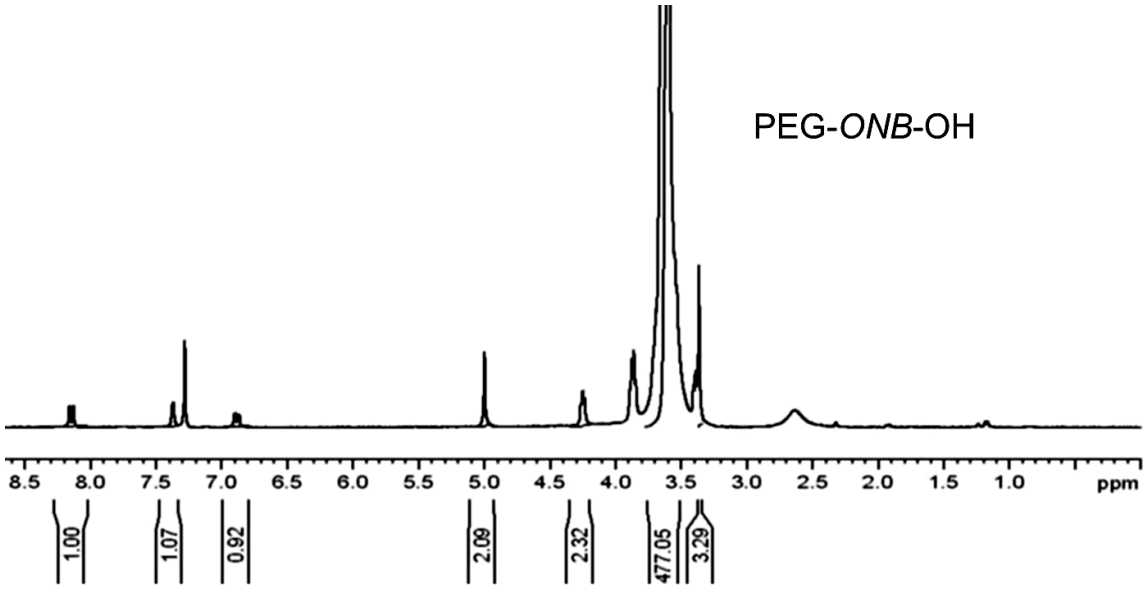

Figure 2.2. ^{1}H NMR spectrum of PEG-*ONB*-OH in $CDCl_3$ at 300 MHz along with integration of the signals.

2.4.2 PEG-*ONB*-PFOEMA-Br

PEG-*ONB*-PFOEMA-Br was synthesized by ATRP of FOEMA, using PEG-*ONB*-Br as the macroinitiator. FOEMA was polymerized at different temperatures and using different solvents such as toluene, hexafluorobenzene, TFT, and mixtures of TFT and toluene. In addition, different ligands such as bipyridine and *N,N,N′,N″,N″*-pentamethyldiethylenetriamine were used. These experiments eventually established that the use of TFT/anisole at v/v = 1/1 as the solvent and bipyridine as the ligand yielded samples with the lowest polydispersity of 1.08.

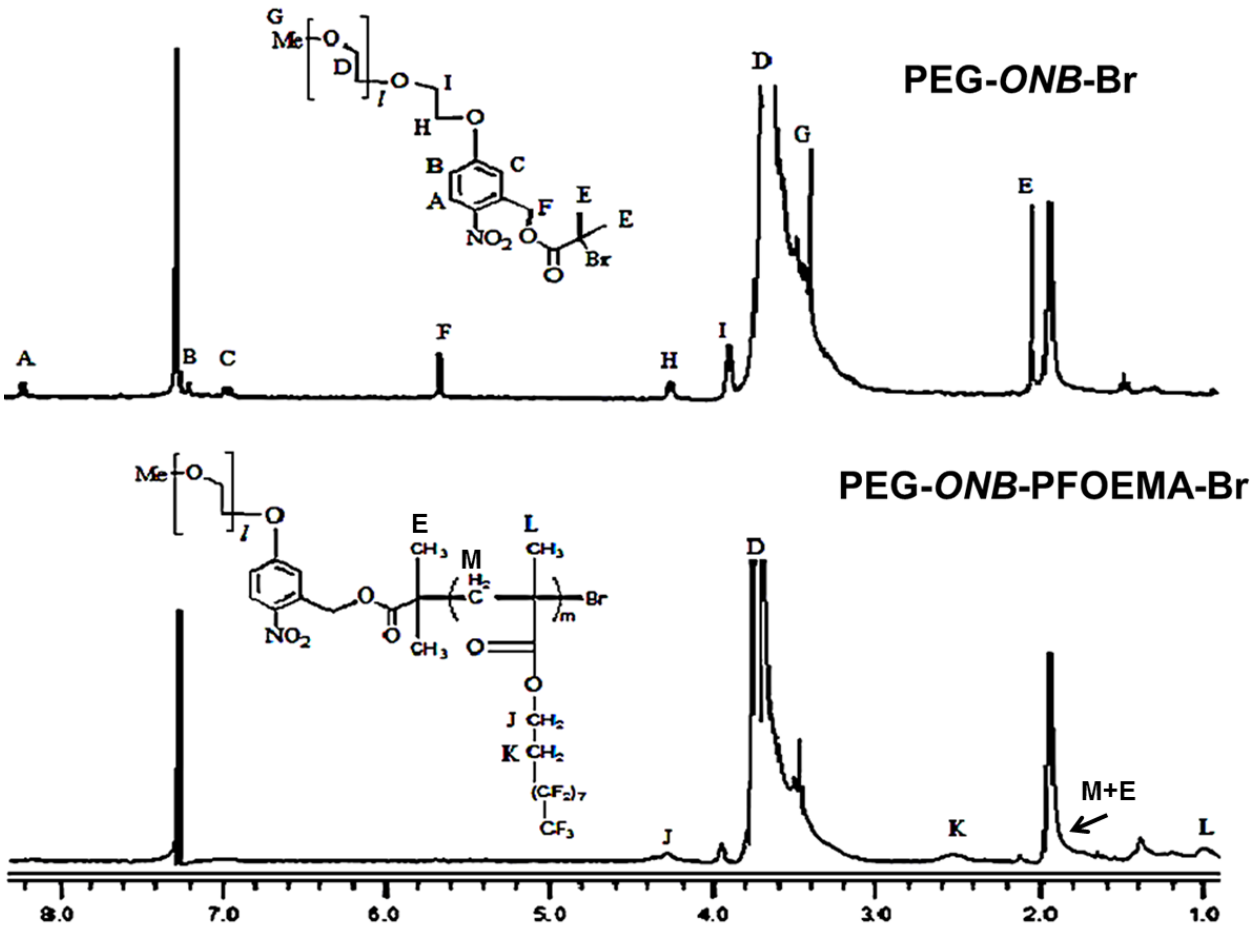

Figure 2.3. ^{1}H NMR spectra of PEG-*ONB*-Br (top) and PEG-*ONB*-PFOEMA (bottom) recorded in $CDCl_3$ at 300 MHz.

SEC analysis of PEG-*ONB*-Br was performed using a DMF solution containing tetrabutylammonium bromide as the mobile phase, an eluent that we use routinely. Figure 2.4 shows the SEC trace for PEG-*ONB*-Br. The trace consisted of a main peak at 27.8 min and a small impurity peak at 26 min. The polydispersity of the main peak was 1.04 in terms of polystyrene standards. Both of these peaks were essentially identical to those observed for the precursory PEG sample.

Figure 2.4 also shows a SEC trace for PEG-*ONB*-PFOEMA. The polydispersity index M_w/M_n in terms of PS standards was low, at 1.08. While the apparent M_n for PEG-*ONB*-Br in terms of PS standards was 13,300 g/mol, the value for PEG-*ONB*-PFOEMA was ~15,000 g/mol. This small increase in M_n was most likely due to the poor solubility and the compact conformation of the PFOEMA block in DMF. The prepared PEG-*ONB*-PFOEMA-Br copolymer was filtered through an alumina column to remove ligated copper and was purified by repeated precipitation from diethyl ether. Figure 2.3 also shows the ^{1}H NMR spectrum of PEG-*ONB*-PFOEMA-Br. From the comparison between the integrations of the PEG and the PFOEMA signals and based on the repeat unit number of 113 for PEG, the PFOEMA repeat unit number was calculated to be 12.

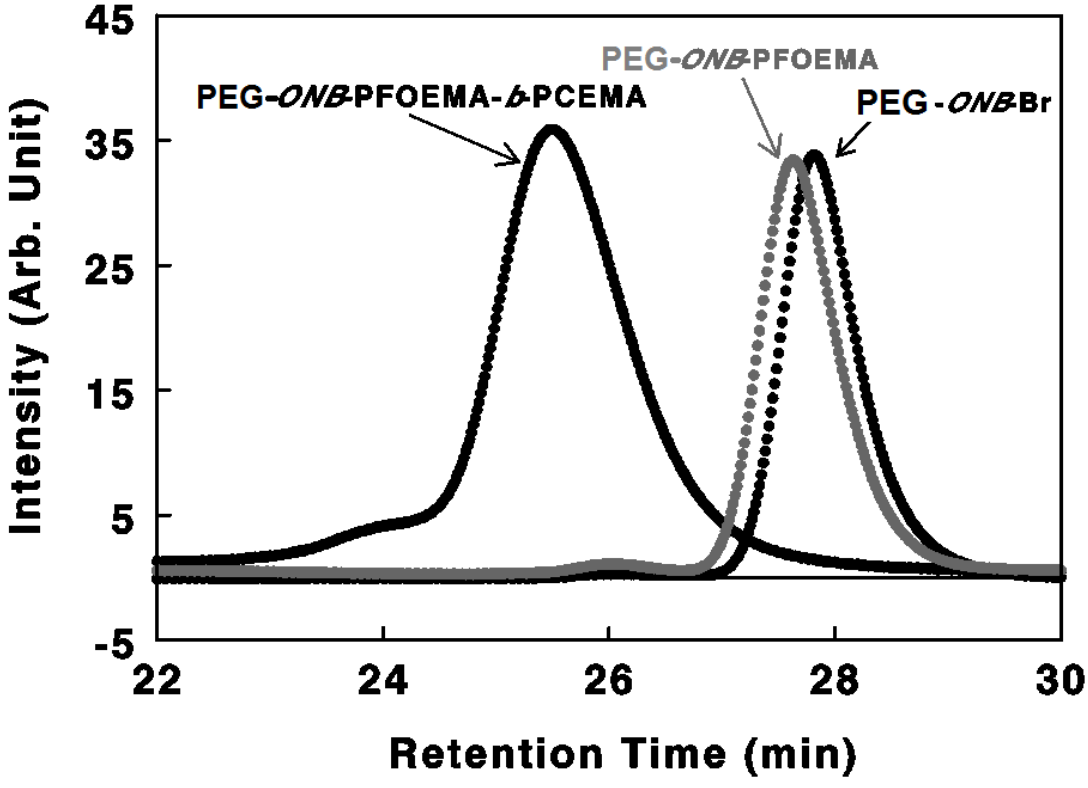

Figure 2.4. Comparison of SEC traces of PEG-*ONB*-Br, PEG-*ONB*-PFOEMA, and PEG-*ONB*-PFOEMA-*b*-PCEMA.

2.4.3 Kinetics of the PEG-*ONB*-PFOEMA Polymerization

The polymerization of FOEMA in TFT/anisole at v/v = 1/1 was monitored by collecting samples at different times during the reaction and analyzing these samples via ^{1}H NMR and SEC. Our ^{1}H NMR analyses indicated that the monomer conversions at the polymerization times of 1, 2, and 3 h were 67%, 90%, and 100%, respectively. Figure 2.5 compares the SEC traces of samples collected at these times. At 1 h, the diblock copolymer exhibited a symmetric peak at 27.8 min and a very small shoulder at 26 min. At 2 h, the shoulder peak at 26 min increased in intensity. Subsequently, at 3 h, an extra peak appeared at 25.2 min. The high molecular weight shoulder peaks might be due to the coupling between different chains at the latter stages of polymerization. The characteristic features of PEG-*ONB*-PFOEMA at different intervals of polymerization are highlighted in Table 2.1. Based on these results, a FOEMA polymerization time of 1 h was chosen for the preparation of PEG-*ONB*-PFOEMA.

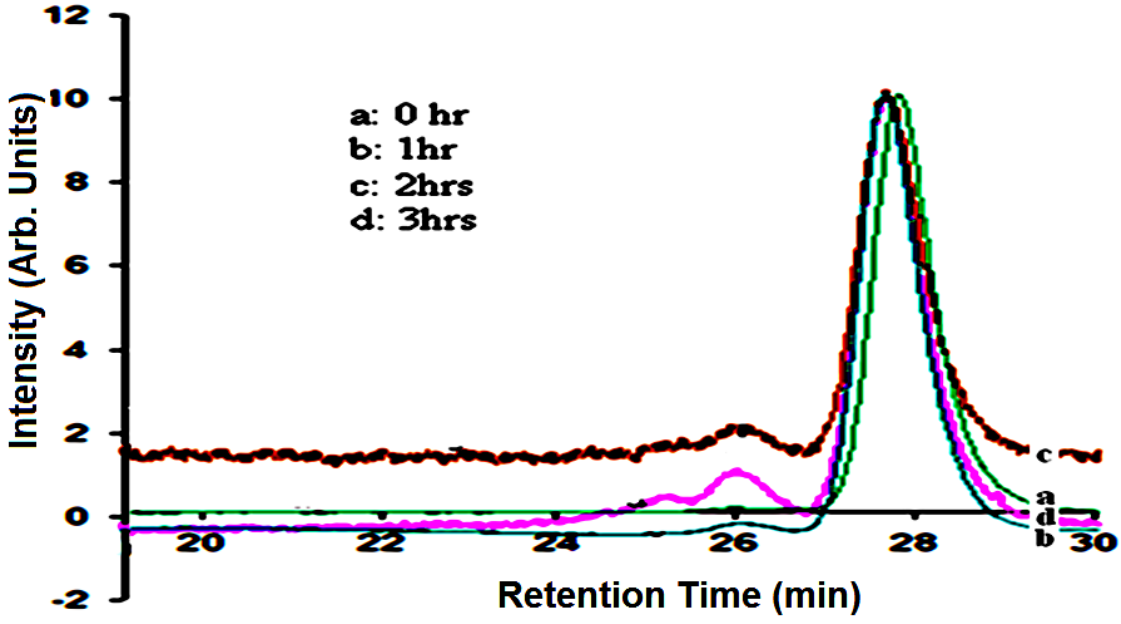

Figure 2.5. SEC traces of PEG_{113}-*ONB*-Br (and PEG_{113}-*ONB*-*b*-$PFOEMA_m$) samples collected at various intervals during the polymerization of FOEMA.

Table 2.1. Characterization of PEG-*ONB*-PFOEMA samples collected at various intervals during the polymerization of FOEMA.

Polymerization time(min)	Degree of conversion (%)	Peak shape (See Figure S1)	PDI	Number of units PEG: PFOEMA (*l* : *m*)
0	0	Single peak (a)	1.04	113:0
50	54	Single peak	Not calculated	113:10
60	68	Single peak (b)	1.08	113:12
120	90	Main peak+ two shoulder peak(c)	Not calculated	113:~16
180	~100	Main peak+ two shoulder peaks (d)	Not calculated	113:~18

2.4.4 PEG-*ONB*-PFOEMA-*b*-PHEMA

HEMA was not directly polymerized using PEG-*ONB*-PFOEMA-Br as the macroinitiator, because the PFOEMA block was insoluble in polar solvents that solubilised PHEMA. Therefore, a detour was taken by first polymerizing HEMA-TMS using PEG-*ONB*-PFOEMA-Br in TFT/anisole at v/v = 1/1, in which both the short PFOEMA and P(HEMA-TMS) blocks were soluble. PHEMA was obtained via the hydrolysis of P(HEMA-TMS) under mild conditions in the presence of water and methanol in THF.

At the beginning of the HEMA-TMS polymerization, the reaction mixture was foaming, probably due to bubble stabilization by PEG-*ONB*-PFOEMA-Br. This foaming behaviour

gradually diminished with time. The reaction progress was again monitored by ^{1}H NMR and SEC analysis of samples collected at different times. The optimized polymerization time was found to be 3 h at 65 ^{o}C when bipyridine was used as the ligand.

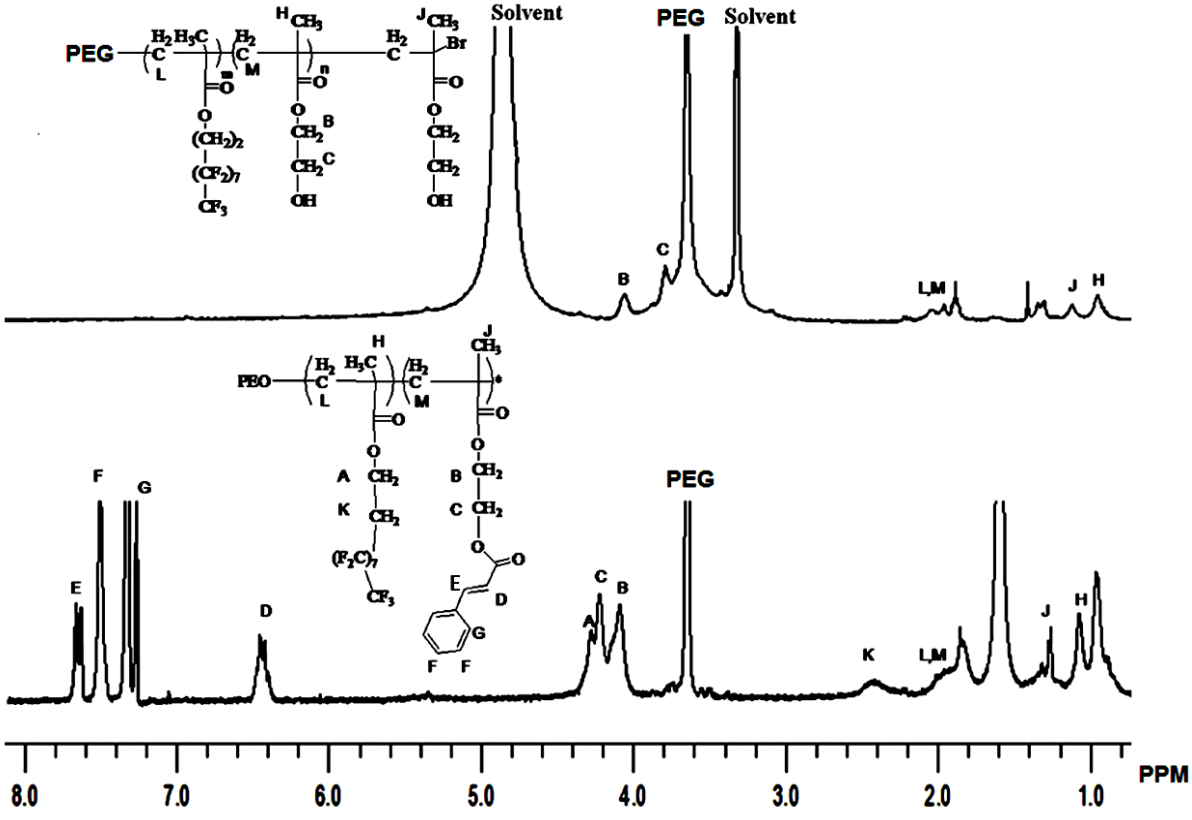

Figure 2.6. ^{1}H NMR spectra of PEG-*ONB*-PFOEMA-*b*-PHEMA measured in CD_3OD (top) and PEG-*ONB*-PFOEMA-*b*-PCEMA measured in $CDCl_3$ (bottom).

PEG-*ONB*-PFOEMA-*b*-PHEMA was freed of the ligated copper again by filtration through an alumina column and was purified by repeated precipitation. A ^{1}H NMR spectrum was obtained in CD_3OD, which dissolved only the PEG and PHEMA blocks, and not the PFOEMA block. Figure 2.6 shows the ^{1}H NMR spectrum together with the peak assignments. The signals at 4.2 and 3.8 ppm corresponded to ethylene protons of the hydroxyethyl group,

confirming the production of the PHEMA block. Our quantitative analysis based on ^{1}H NMR indicated that the PEG/PHEMA molar ratio was 113/25, thus indicating that the PHEMA block had a repeat unit number of 25.

2.4.5 PEG-*ONB*-PFOEMA-*b*-PCEMA (P1)

Reacting the hydroxyl groups of PEG-*ONB*-PFOEMA-*b*-PHEMA with an excess of cinnamoyl chloride in pyridine at room temperature yielded PEG-*ONB*-PFOEMA-*b*-PCEMA.[2,46,47] The resultant copolymer was easily purified by repeated precipitation into diethyl ether and was analyzed by ^{1}H NMR in $CDCl_3$. Figure 2.6 also shows a ^{1}H NMR spectrum of P1 together with the peak assignments. All of the anticipated signals for PEG, PFOEMA, and PCEMA were observed. A quantitative peak integration analysis confirmed that the repeat unit numbers for the PEG, PFOEMA, and the PCEMA blocks (or *l*, *m*, and *n*, respectively) were 113, 12, and 25, respectively.

Table 2.2. Characteristics of P1 and its precursors at various stages of the preparation.

Sample	SEC M_w (g/mol)	SEC M_w/M_n	NMR *l*/*m*/*n*	NMR M_n	*l*	*m*	*n*
PEG-*ONB*-Br	14,000	1.04		5000 [a]	113		
PEG-*ONB*-PFOEMA-Br	15,000	1.08	113/12	11,500	113	12	
P1	38,000	1.10	113/12/25	18,200	113	12	25

[a]:Calculated based on the supplier's nominal molecular weight of 5,000 g/mol for PEG.

The SEC trace of P1 is shown in Figure 2.4. Despite its apparent width, the polydispersity of the peak including the high-molecular-weight shoulder was confirmed to be only 1.10. The apparent width of this peak might have two contributing factors. Firstly, the mobile phase had a flow rate of 0.90 mL/min, which was lower than the ordinarily-used flow rate of 1.00 mL/min. Secondly, the 1000 and 10,000 Å columns used should have good resolution in this molecular weight range.

2.4.6 P1 Micelles

P1 micelles were prepared in several steps. Firstly, P1 was dissolved in THF. While THF is a good solvent for PCEMA, it does not dissolve high-molecular weight PFOEMA or PEG chains. Despite this, it did effectively dissolve the PFOEMA and PEG blocks of P1 due to their low molecular weights. Secondly, water was added as a selective solvent for PEG to a volume fraction (f_{H2O}) of 80% to yield micelles with PEG forming the corona and PFOEMA and PCEMA as the core.

The aqueous micellar solution was atomized or aero-sprayed onto freshly-cleft mica using a home-built device[45] for tapping-mode AFM analysis and onto a cellulose-covered grid for TEM analysis. Before TEM analysis, the PCEMA block of the sample was selectively stained by OsO_4. Aero-spraying was used because it sped up solvent evaporation from the atomized liquid droplets. Under these conditions, THF should have evaporated as it travelled from the spraying nozzle to the silicon wafer and water should have evaporated within ~3 s after the landing of the atomized aqueous droplets. The purpose of this fast solvent evaporation was to minimize the chances for the micelles to undergo morphological transitions during specimen preparation.

Figures 2.7a and 2.7b show AFM height and TEM images of the aero-sprayed P1 micelles. The particles seemed to have a bimodal distribution. The smaller particles had average AFM and TEM diameters of 31 ± 5 and 18 ± 4 nm, respectively. Meanwhile, the larger particles had respective AFM and TEM diameters of 47 ± 7 and 33 ± 6 nm, individually.

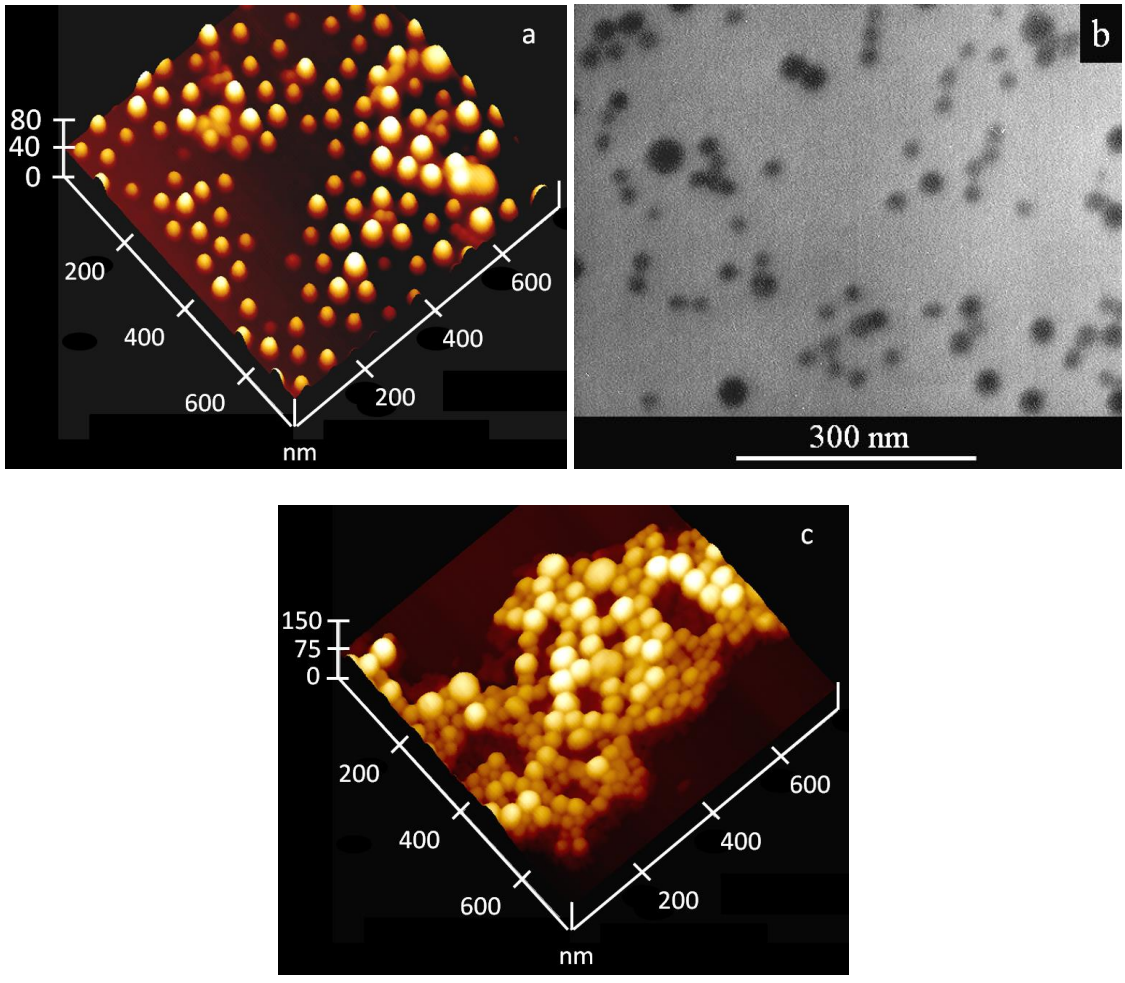

Figure 2.7. AFM topography images of P1 micelles (a), photolyzed P1 micelles (c), and a TEM image of the P1 micelles (b). The micelles were aero-sprayed from THF/water at f_{H2O} = 80%.

Our suspicion is that the smaller particles were core-shell-corona spherical micelles, where PCEMA, PFOEMA, and PEG formed the core, shell, and corona, respectively. The AFM diameter was larger than the TEM diameter, because AFM probed the whole particles, including

the PEG and PFOEMA layers. Meanwhile, TEM only probed the OsO_4-stained PCEMA core. Also, the AFM diameter likely had some contribution from the finite size of the tip used.

Evidently, the larger particles could not be the simple core-shell-corona micelles, because the PCEMA core chains, with an average of 25 repeat units, could not be stretched to 33 ± 6 nm. We initially contemplated that the larger particles were vesicles. This was, however, not supported by the TEM or the AFM results. If they were vesicles, the larger particles would have appeared in the TEM image as a circle with a dark rim and a gray center. Instead, the larger circles in Figure 2.7b appeared increasingly dark towards the center, suggesting that they were solid particles. Also, some of these vesicles would normally collapse after solvent evaporation, leaving behind a Kippah-like structure.[48] This Kippah-like (Skull-cap) structure was not observed in the AFM image shown in Figure 2.7a.

While the nature of this study does not demand a detailed clarification of the chain packing in the larger particles, we suspect that the larger particles were still core−shell−corona particles formed from polymer chains with a PCEMA block that was substantially longer than 25 units. Despite its low apparent polydispersity index, P1 probably possessed substantial composition heterogeneity, or a fairly large distribution of FOEMA-to-CEMA repeat unit ratios, *m*/*n*. Also in P1 the PEG block is constant; therefore variations in FOEMA-to-CEMA ratios by 10-20% will not affect the colloidal properties of P1.

2.4.7 Absorption Characteristics of *ONB* and PCEMA

To facilitate the choice of photolysis conditions that would crosslink the PCEMA domains and cleave PEG simultaneously, the absorption properties of PEG-*ONB*-Br, P1, and PEG-*b*-PCEMA were compared. For this purpose PEG-*b*-PCEMA was prepared using PEG-Br as the macroinitiator for HEMA-TMS polymerization. The TMS groups were then removed and

the resultant PHEMA block was subjected to a cinnamation reaction. As was the case with P1, the number of repeat units for the PCEMA block of PEG-*b*-PCEMA was also 25.

Compared in Figure 2.8 are the UV absorption spectra of PEG-*ONB*-Br, PEG-*b*-PCEMA, and P1, which were recorded in distilled THF. Since PEG should absorb negligibly at wavelengths > 260 nm, the maxima observed at 306 and 274 nm should result from *ONB* and CEMA absorption, respectively. A quantitative analysis indicated that the *ONB* group in PEG-*ONB*-Br had a molar extinction coefficient (ε) of 8.2×10^3 $M^{-1}cm^{-1}$ at 306 nm. The molar extinction coefficient of PCEMA at its absorption maximum has been reported to be 2.8×10^4 M^{-1} cm^{-1} by Guo et al.[2] and 2.1×10^4 $M^{-1}cm^{-1}$ by Marusich et al.[49] Each CEMA unit absorbed much more strongly than each *ONB* unit, and each P1 chain contained 25 CEMA units but only 1 *ONB* unit. Therefore, it could be anticipated that the *ONB* group should only contribute noticeably to light absorption by P1 at longer wavelengths. This prediction was confirmed by comparing curves (b) and (c) of Figure 2.8.

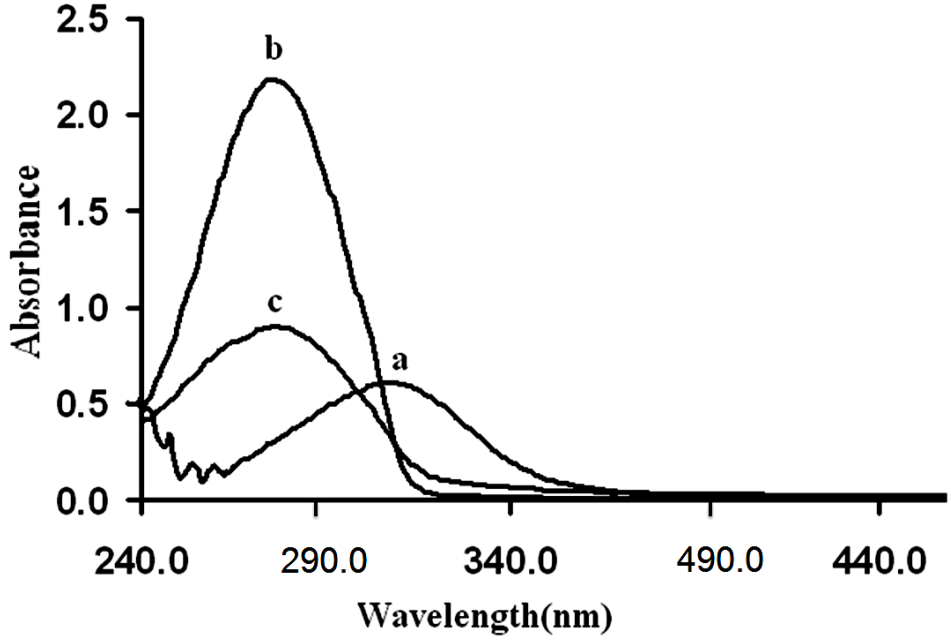

Figure 2.8. UV absorption spectra; (a) PEG-*ONB*-Br, (b) PEG-*b*-PCEMA, and (c) P1.

2.4.8 Micelle Photolysis

Based on the absorption characteristics of the PCEMA and *ONB*, P1 micelles were photolyzed in THF/water at f_{H2O} = 80% using light generated by a high-pressure mercury lamp and filtered by a 300 nm cut-off filter. Most of the light below 300 nm was removed to match the rates of *ONB* cleavage and PCEMA crosslinking. The micellar solution was clear before irradiation. Turbidity developed within 5 min and intensified with further irradiation. This phenomenon suggested that the cleavage of the corona-forming PEG block had occurred, resulting in photo-induced particle precipitation. Also, the settled particles were redispersed into $CDCl_3$ to yield a cloudy solution. Since samples of PFOEMA-*b*-PCEMA bearing uncrosslinked PCEMA blocks would have dissolved in this solvent to yield a clear solution, the cloudiness suggested the retention of the micellar structure in $CDCl_3$ and the crosslinking of the PCEMA core. The PEG chains were cleaved from the PFOEMA block through a Norrish II rearrangement (Scheme 2.3) of *ONB*.[50] Meanwhile, PCEMA became crosslinked due to the dimerization of CEMA units from the same and different P1 chains.[2] These photolysis processes were monitored by analyzing samples collected at different irradiation times using UV and SEC characterization techniques.

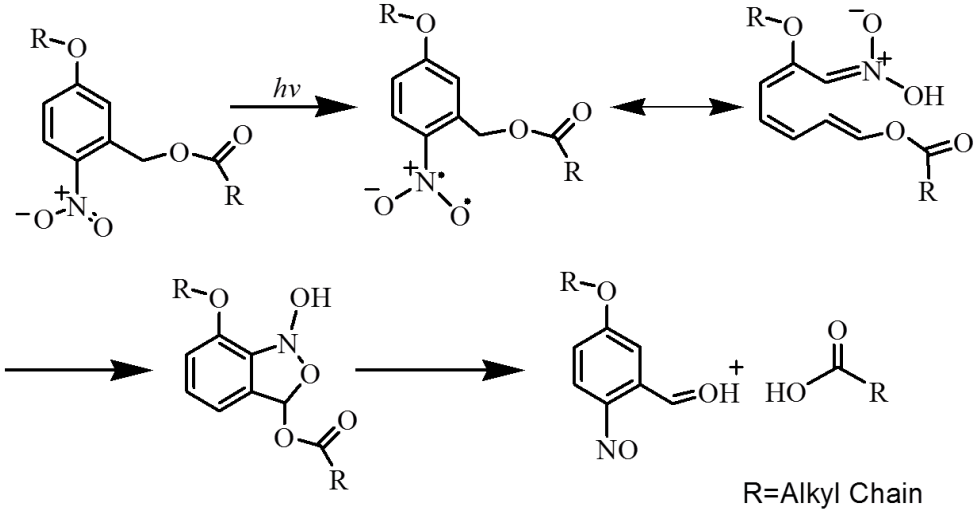

Scheme 2.3. Schematic depiction of the *ONB* rearrangement.

Figure 2.9a compares the UV absorption spectra of a 0.06 mg/mL solution of P1 in THF/water at f_{H2O} = 80% after it was irradiated for various time periods. Plotted in Figure 2.9b are the changes in the relative absorbances at 274 and 306 nm as a function of the photolysis time. The two curves almost coincided, with both curves showing a rapid initial absorbance decrease that was followed by a gradual change between 2 and 3 h. The observed absorbance decrease pattern was reasonable, as the rate of a reaction depended on the amount of light absorbed by the reacting species. As the conversion increased and less reactant remained, the amount of light absorbed by the reactant per unit time decreased, and thus the reaction rate decreased. The almost identical rate of absorbance decrease observed at 274 and 306 nm might be due to the fact that PCEMA absorption dominated over *ONB* absorption at 306 nm as well. Thus, UV absorption analysis apparently only allowed the monitoring of the rate of CEMA disappearance with photolysis. We also observed that the rate of photo-crosslinking and photo-cleavge for P1 are higher in normal solutions than colloidal solutions. It is due to the greater exposure of light sensitive groups in P1 solutions as compared to their colloidal solutions.

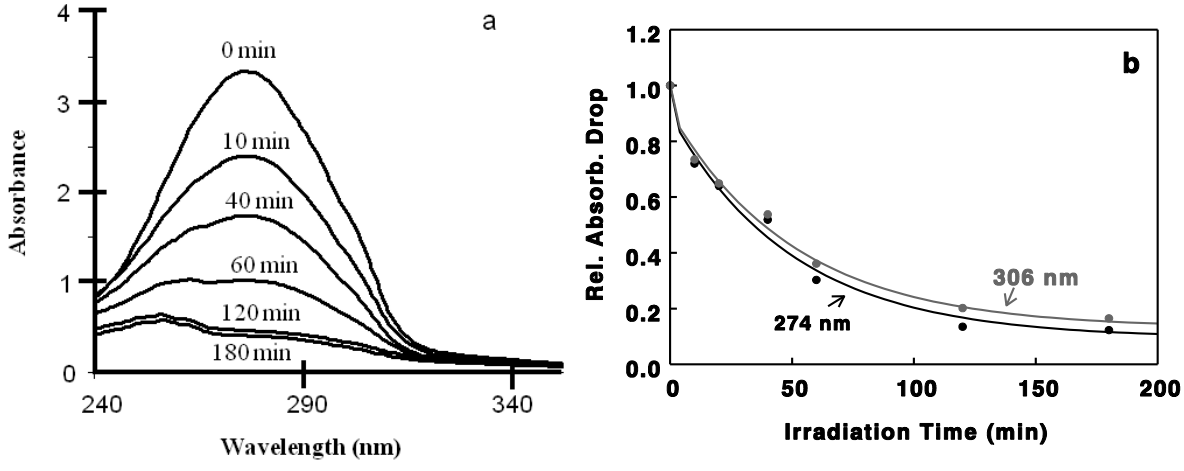

Figure 2.9. Comparision of UV absorption spectra of P1 at different photolysis times (a). Also shown are the variations in the relative absorbances at 274 and 306 nm as a function of irradiation time (b).

Meanwhile, SEC was better suited for monitoring PEG cleavage. As more sample was required for SEC analysis, the photolyzed polymer solution in this case had a higher initial concentration of 8 mg/mL. To quantify the amount of P1 lost or PEG formed, a PEG sample with M_n = 550 g/mol (PEG-550) was added into the photolysis mixture as an internal standard. This oligomer was used as the internal standard because it would remain inert during the photolysis. In addition, it was chosen because its elution peak appeared at 32 min, a position well-resolved from that of P1 and the cleft PEG block.

Solvent was removed from the photolyzed samples via rotary evaporation. They were then immediately redispersed into DMF, filtered, and analyzed by SEC. Figure 2.10 compares SEC traces of P1 that were irradiated for 0, 10, 20, and 180 min. Before the irradiation treatment, the peaks eluting at 25.5 and 32 min corresponded to P1 and PEG-550, respectively. After 10 min of irradiation, a shoulder emerged at ~24 min on the higher molecular weight side of P1 and the intensity of the P1 peak decreased. This suggested the production of a higher molecular weight species due to the photo-crosslinking of PCEMA. Although less noticeable, the shoulder on the lower-molecular-weight side at 27.8 min had also grown, suggesting PEG113 formation. At 20 min, the P1 peak had fully disappeared, leaving behind a very small peak at ~26 min. Meanwhile, the PEG-5k peak eluting at 27.8 nm became distinct. Further photolysis up to 180 min did not eliminate the small peak at 26 min but increased the intensity of the peak eluting at 27.8 min.

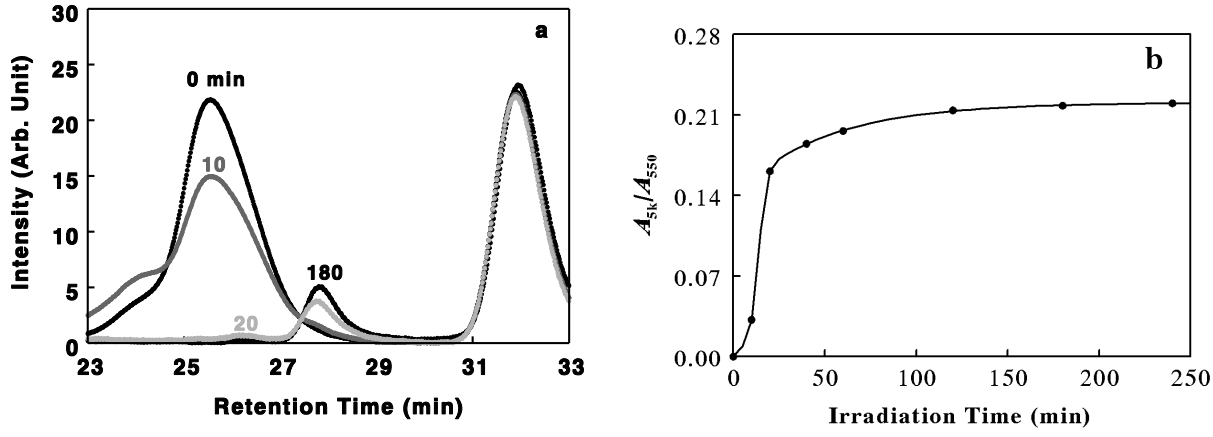

Figure 2.10. Comparison of SEC traces of P1 containing PEG-550 that were irradiated for 0, 10, 20, and 180 min (a). Also shown is the change in the degree of PEG cleavage as a function of photolysis time (b).

No peak was observed for the PFOEMA-*b*-PCEMA fragments after 20 min of photolysis time because this segment became locked into a crosslinked micellar structure. Crosslinked particles bearing a PFOEMA corona were not dispersible in DMF, the eluant used for SEC analysis, and thus were mostly removed during sample filtration. The small peak appearing at ~26 min must have been due to an impurity present in the original PEG precursor as the peak was seen in the SEC traces of both PEG-OH and PEG-*ONB*-Br.

The Peakfit® program was used to resolve the peak of the P1 sample that was irradiated for 10 min into three peaks that corresponded with crosslinked P1, P1, and photo-cleaved PEG-5k. The areas of the peak corresponding to PEG-5k and PEG-550 were calculated using the Peakfit® program to yield the area ratio A_{5k}/A_{550}, where A_{5k} and A_{550} represented the areas corresponding to PEG-5k and PEG-550, respectively. Since the PEG-5k peak was free of interference from P1 at other irradiation times, the determination of A_{5k}/A_{550} was straightforward. Figure 2.10b shows how A_{5k}/A_{550} varied with photolysis time.

Figure 2.10b clearly shows that much less PEG was cleft within the first 10 min of photolysis than in the next 10 min. This trend was probably due to the fact that PCEMA crosslinking dominated initially. It was only after the CEMA concentration and its absorption had decreased that the *ONB* rearrangement began to accelerate. The A_{5k}/A_{550} value levelled off after 120 min, suggesting the completion of the *ONB* rearrangement reaction at that point.

2.4.9 PEG-Cleft Particles

After a P1 solution at 8 mg/mL in THF/water at f_{H2O} = 80% was irradiated for 3 h, the solution became turbid. This solution was diluted to ~1 mg/mL with THF/water at f_{H2O} = 80% and then passed through a 3.1 μm filter to remove large aggregates. The smaller particles were then aero-sprayed for AFM analysis. Such an image is shown in Figure 2.7c.

The bimodal distribution of the particles was retained, and this phenomenon is evident in Figure 2.7c. The major difference between the particles shown in Figure 2.7a and 2.7c was that the particles in Figure 2.7c had formed aggregates and those in Figure 2.7a were mostly individual particles. The particles had aggregated together because they were free of the PEG corona and were not readily dispersible in THF/water.

After the photolysis treatment, the particles were centrifuged, separated from the supernatant, redispersed into methanol under vigorous stirring, and settled via centrifugation. This methanol rinsing step was repeated several times to remove the photo-cleft PEG chains. The particles were dried and then dispersed into $CDCl_3$ to yield a turbid solution. ^1H NMR analysis indicated the absence of any PEG peaks despite the solubility of PEG in $CDCl_3$, as shown in Figure 2.11. This phenomenon suggested the complete removal of the PEG coronal chains during photolysis. No PCEMA signals were observed either, because the PCEMA chains

were crosslinked and not mobile. However, the presence of the PFOEMA block in the photolyzed sample was confirmed by ^{19}F NMR analysis, as shown in Figure 2.12.

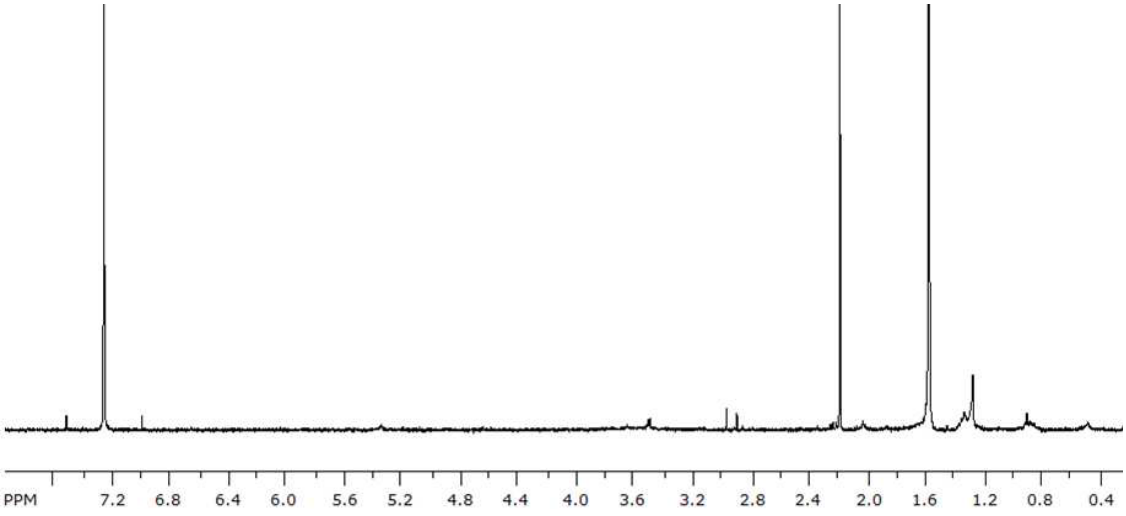

Figure 2.11. 400 MHz ^{1}H NMR spectrum of the PEG-cleft P1 particles recorded in $CDCl_3$.

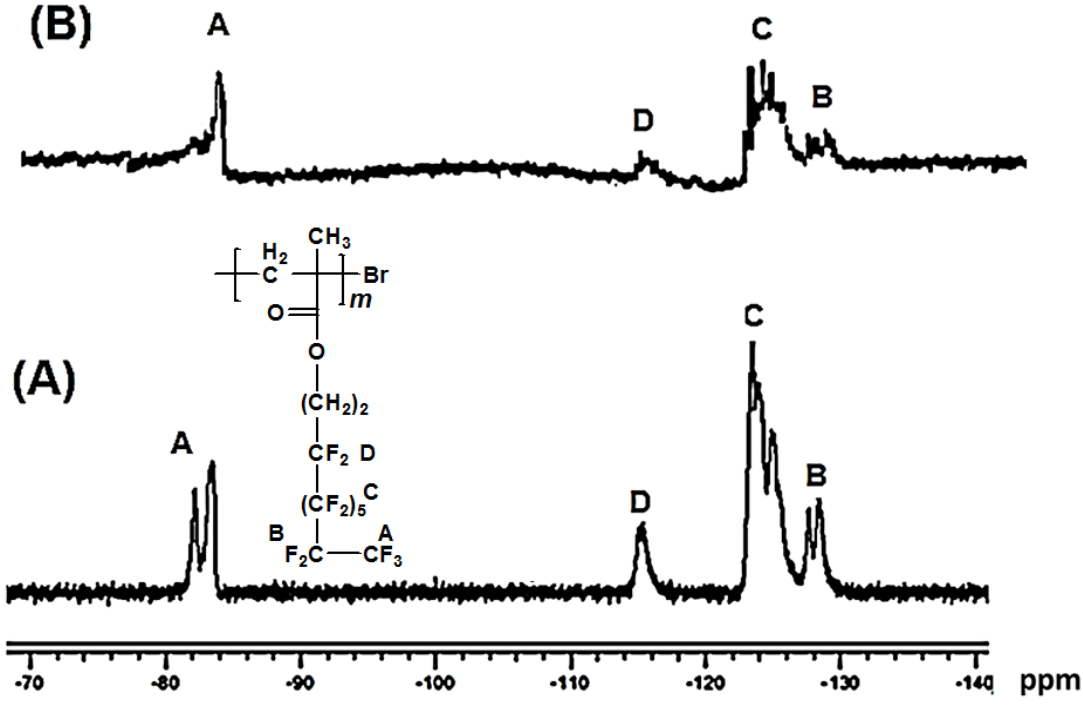

Figure 2.12. ^{19}F NMR (recorded in $CDCl_3$ at 400 MHz) of PEG_{113}-*ONB*-PFOEMA-*b*-$PCEMA_{25}$ (A) and ^{19}F NMR of the PEG-cleft particles (B).

Visual evidence for PEG cleavage was that the contact angles of H_2O and CH_2I_2 droplets placed on films made of non-photolyzed P1 micelles differed from those placed on films made from photolyzed P1 particles. Micellar P1 films were prepared by casting micellar P1 solutions (at f_{H2O} = 80%) onto glass plates. Meanwhile, films of the photolyzed P1 particles were prepared by casting the photolyzed P1 particles from TFT. Figure 2.13a-2.13d compares the shapes of H_2O and CH_2I_2 droplets on different films. While H_2O and CH_2I_2 contact angles on the micellar films were 52° and 32°, respectively, the corresponding values increased to 154° and 136° on films of the photolyzed samples. These large contact angles would be possible only if the particle surfaces were enriched by PFOEMA and if the particulate films were rough.[36,51,52]

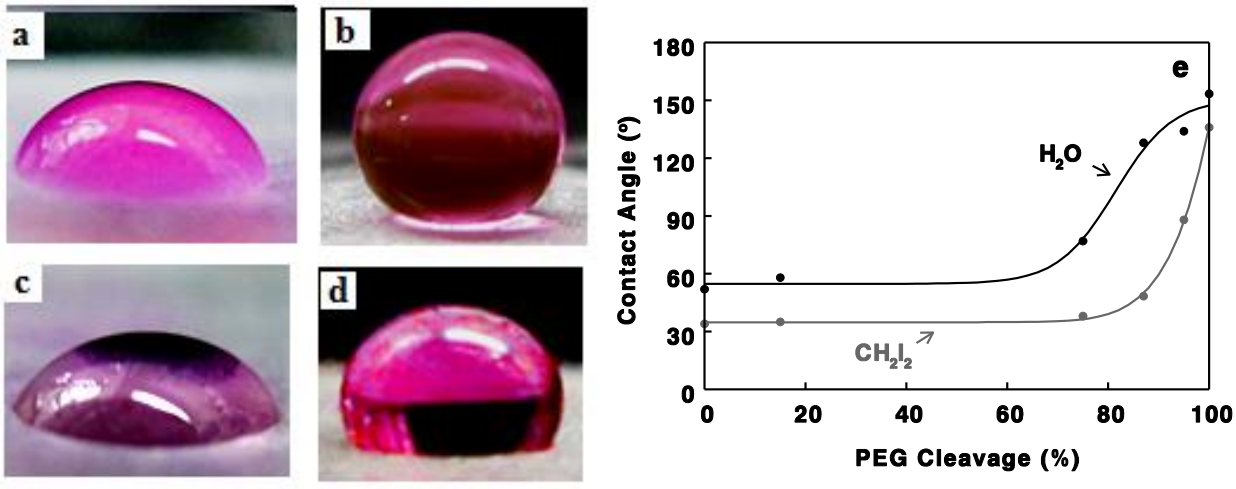

Figure 2.13. Photographs of H_2O droplets impregnated with rhodamine B (a and b) and CH_2I_2 droplets (c and d) on films of P1 micelles (a and c) and photolyzed P1 particles (b and d). Also shown are the variations in the contact angles of H_2O and CH_2I_2 droplets as functions of PEG cleavage (e).

While films of P1 micelles have been called micellar films, the micellar structure before photolysis was not locked and a structural rearrangement of the micelles might be possible during film formation. No other methods were attempted for preparing better micellar films because this structural rearrangement should not have changed the observed H_2O and CH_2I_2 contact angle variation trends for films made of micelles and photolyzed micelles. Plotted in Figure 2.13e are the variations in the H_2O and CH_2I_2 contact angles as functions of PEG cleavage. Significant increases in the contact angles occurred only when the degree of PEG cleavage exceeded 80%. This trend was consistent with our predictions, because the residual PEG chains might lie flat on the PFOEMA surface and help reduce the liquid contact angles. The PFOEMA chains were exposed only after the PEG chains were almost fully removed.

2.4.10 AFM Analysis of P1 Films Cast onto Glass

Glass surfaces were coated with films of the photolyzed P1 particles. These films were prepared by adding droplets of chloroform dispersions containing the crosslinked P1 particles onto the glass surface. The films were analyzed via AFM, and the image shown in Figure 2.14 (left), reveals a small region of the film with an area of 2.7μm^2 that had a mean roughness of 6.6nm. A larger scale (100 μm) image as shown in Figure 2.14 (right) was also recorded for the film. Calculations for a section with an area of 188 μm^2 revealed a mean roughness of 116.9 nm.

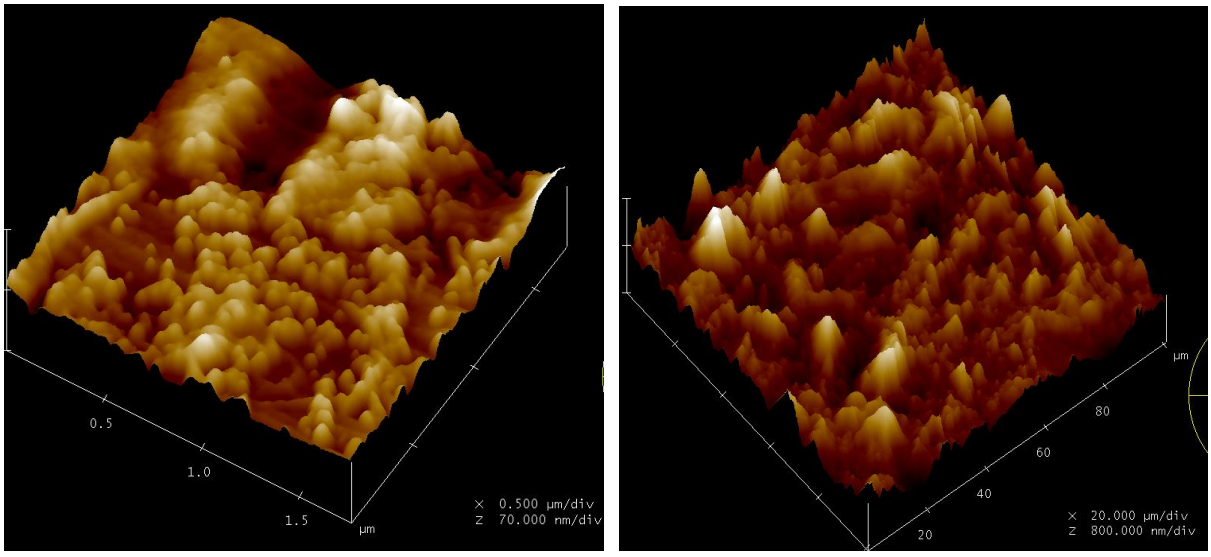

Figure 2.14. AFM topography images of films of photolyzed nanoparticles cast onto a glass plate from TFT at a smaller (left) and larger (right) scales. The root-mean square roughness for the two images were 8.5 and 154.0 nm, respectively.

2.5 Conclusions

In this study, ATRP has been used to produce a novel triblock copolymer P1. This copolymer has been carefully characterized by ^{1}H NMR and SEC analysis. The number of repeat units for the PEG, PFOEMA, and PCEMA blocks were 113, 12, and 25, respectively. In addition, the polydispersity of this copolymer was low, at 1.10 with respect to PS standards. The light absorption characteristics of the CEMA and *ONB* units were established by comparing the UV absorption spectra of PEG-*b*-PCEMA, PEG-*ONB*, and P1 samples. In THF/water dispersions at f_{H2O} = 80%, P1 formed core-shell-corona micelles. Irradiation using light with wavelengths >300 nm crosslinked the PCEMA core and cleft the PEG corona, yielding particles bearing exposed PFOEMA chains. Casting TFT dispersions of these photo-cleaved particles yielded films that were both superhydrophobic and oleophobic. The water and oil repellence of films of the crosslinked micelles improved as the degree of PEG cleavage increased.

2.6 References

1. Schumers, J. M.; Fustin, C. A.; Gohy, J. F. *Macromol. Rapid Commun.* **2010,** *31*, 1588.
2. Guo, A.; Liu, G. J.; Tao, J. *Macromolecules,* **1996,** *29*, 2487.
3. Liu, G. J.; Qiao, L. J.; Guo, A. *Macromolecules,* **1996,** *29*, 5508.
4. Liu, G. J. *Adv. Polym. Sci.* **2008,** *220*, 29.
5. Njikang, G.; Liu, G. J.; Hong, L. Z. *Langmuir,* **2011,** *27,* 7176.
6. Wyman, I.; Njikang, G.; Liu, G. J. *Progr. Polym. Sci.* **2011,** *36*, 1152.
7. Tao, J.; Stewart, S.; Liu, G. J.; Yang, M. L. *Macromolecules,* **1997,** *30*, 2738.
8. Stewart, S.; Liu, G. *Angew. Chem. Int. Ed.* **2000,** *39*, 340.
9. Yan, X. H.; Liu, G. J.; Liu, F. T.; Tang, B. Z.; Peng, H.; Pakhomov, A. B.; Wong, C. Y. *Angew. Chem. Int. Ed.* **2001,** *40*, 3593.
10. Yan, X. H.; Liu, G. J.; Haeussler, M.; Tang, B. Z. *Chem. Mater.* **2005,** *17*, 6053.
11. Ding, J. F.; Liu, G. J. *Chem. Mater.* **1998,** *10*, 537.
12. Stewart, S.; Liu, G. J. *Chem. Mater.* **1999,** *11*, 1048.
13. Ding, J. F.; Liu, G. J. *J. Phys. Chem. B,* **1998,** *102*, 6107.
14. Goldbach, J. T.; Lavery, K. A.; Penelle, J.; Russell, T. P. *Macromolecules,* **2004,** *37*, 9639.
15. Hillmyer, M. A. *Adv. Polym. Sci.* **2005,** *190*, 137.
16. Liu, G. J.; Ding, J. F.; Guo, A.; Herfort, M.; Bazett-Jones, D. *Macromolecules,* **1997,** *30*, 1851.
17. Liu, G. J.; Ding, J. F.; Hashimoto, T.; Kimishima, K.; Winnik, F. M.; Nigam, S. *Chem. Mater.* **1999,** *11*, 2233.
18. Kang, M.; Moon, B. *Macromolecules,* **2009,** *42*, 455.
19. Schumers, J. M.; Gohy, J. F.; Fustin, C. A. *Poly. Chem.* **2010,** *1*, 161.
20. Zhao, Y. *J. Mater. Chem.* **2009,** *19*, 4887.

21. Wang, G.; Tong, X.; Zhao, Y. *Macromolecules,* **2004,** *37*, 8911.

22. Jiang, J. Q.; Tong, X.; Zhao, Y. *J. Am. Chem. Soc.* **2005,** *127*, 8290.

23. Pasparakis, G.; Vamvakaki, M. *Polym. Chem.* **2011,** *2*, 1234.

24. Haag, S. F.; Fleige, E.; Chen, M.; Fahr, A.; Teutloff, C.; Bittl, R.; Lademann, J.; Schafer-Korting, M.; Haag, R.; Meinke, M. C. *Int. J. Pharm.* **2011,** *416*, 223.

25. Stuart, M. A. C.; Huck, W. T. S.; Genzer, J.; Muller, M.; Ober, C.; Stamm, M.; Sukhorukov, G. B.; Szleifer, I.; Tsukruk, V. V.; Urban, M.; Winnik, F.; Zauscher, S.; Luzinov, I.; Minko, S. *Nat. Mater.* **2010,** *9*, 101.

26. Hu, J. M.; Liu, S. Y. *Macromolecules,* **2010,** *43*, 8315.

27. He, J.; Tong, X.; Tremblay, L.; Zhao, Y. *Macromolecules,* **2009,** *42*, 7267.

28. Hirao, A.; Sugiyama, K.; Yokoyama, H. *Progr. Polym. Sci.* **2007,** *32*, 1393.

29. Zhou, Z. H.; Liu, G. J.; Hong, L. Z. *Biomacromolecules,* **2011,** *12*, 813.

30. Wang, J. S.; Matyjaszewski, K. *J. Am. Chem. Soc.* **1995,** *117*, 5614.

31. Matyjaszewski, K.; Xia, J. H. *Chem. Rev.* **2001,** *101*, 2921.

32. Kato, M.; Kamigaito, M.; Sawamoto, M.; Higashimura, T. *Macromolecules,* **1995,** *28*, 1721.

33. Chiefari, J.; Chong, Y. K.; Ercole, F.; Krstina, J.; Jeffery, J.; Le, T. P. T.; Mayadunne, R. T. A.; Meijs, G. F.; Moad, C. L.; Moad, G.; Rizzardo, E.; Thang, S. H. *Macromolecules,* **1998,** *31*, 5559.

34. Perrier, S.; Takolpuckdee, P. *J. Polym. Sci.: A: Polym. Chem.* **2005,** *43*, 5347.

35. Ishizone, T.; Sugiyama, K.; Sakano, Y.; Mori, H.; Hirao, A.; Nakahama, S. *Polym. J.* **1999,** *31*, 983.

36. Xiong, D.; Liu, G. J.; Hong, L. Z.; Duncan, E. J. S. *Chem. Mater.* **2011,** *23*, 4357.

37. Marsat, J. N.; Heydenreich, M.; Kleinpeter, E.; Berlepsch, H. V.; Bottcher, C.; Laschewsky, A. *Macromolecules,* **2011,** *44*, 2092.

38. Li, K.; Wu, P. P.; Han, Z. W. *Polymer,* **2002,** *43*, 4079.

39. Xia, J. H.; Johnson, T.; Gaynor, S. G.; Matyjaszewski, K.; DeSimone, J. *Macromolecules,* **1999,** *32*, 4802.

40. Skrabania, K.; von Berlepsch, H.; Bottcher, C.; Laschewsky, A. *Macromolecules,* **2010,** *43*, 271.

41. Zhou, Y. N.; Cheng, H.; Luo, Z. H. *J. Polym. Sci.: A: Polym. Chem.* **2011,** *49*, 3647.

42. Guo, W. J.; Tang, X. D.; Xu, J.; Wang, X.; Chen, Y.; Yu, F. Q.; Pei, M. S. *J. Polym. Sci.: A: Polym. Chem.* **2011,** *49*, 1528.

43. Kubowicz, S.; Baussard, J. F.; Lutz, J. F.; Thunemann, A. F.; von Berlepsch, H.; Laschewsky, A. *Angew. Chem. Int. Ed.* **2005,** *44*, 5262.

44. Hirao, A.; Kato, H.; Yamaguchi, K.; Nakahama, S. *Macromolecules,* **1986,** *19*, 1294.

45. Ding, J. F.; Liu, G. J. *Macromolecules,* **1999,** *32*, 8413.

46. Henselwood, F.; Liu, G. J. *Macromolecules,* **1997,** *30*, 488.

47. Wang, G. C.; Henselwood, F.; Liu, G. J. *Langmuir,* **1998,** *14*, 1554.

48. Azzam, T.; Eisenberg, A. *Langmuir,* **2010,** *26*, 10513.

49. Marusich, W. C.; Jensen, R. A.; Zamir, L. O. *J. Bacteriol.* **1981,** *146*, 1013.

50. Holmes, C. P. *J. Org. Chem.* **1997,** *62*, 2370.

51. Xia, F.; Jiang, L. *Adv. Mater.* **2008,** *20*, 2842.

52. Xiong, D. A.; Liu, G. J.; Zhang, J. G.; Duncan, S. *Chem. Mater.* **2011,** *23*, 2810.

Chapter 3 - Synthesis of Doubly Stimulable Triblock Terpolymers and their Applications for Preparing Amphiphobic Films

3.1 Preface

The work described in this chapter will be included in a manuscript that is currently under preparation.

3.2 Introduction

Polymers that change their structures responding to two types of stimuli are known as doubly stimulable polymers. Responsive polymers have many exciting applications in various areas of fundamental and industrial research.[1-13] For example, stimulable hydrogels have biomedical applications including drug delivery, scaffolds for the regeneration of tissues and bio-sensing materials.[14] Similarly, stimuli-responsive materials have been reported for switchable hydrophilic-superhydrophobic coatings, and self-cleaning surfaces.[15,16]

Light-responsive polymers have been widely explored over the years and have many interesting applications.[17] Poly(2-cinnamoyloxyethyl methacrylate) (PCEMA) is an eminent example of light responsive polymer that have been used to generate stable nanoscaled architectures.[18-24] PCEMA has also been used in combination with other stimuli-responsive functional groups in a single block copolymer to prepare multiply stimulable copolymers.[25,26] For example, light- and pH-responsive block copolymer polystyrene-*block*-poly(2-cinnamoyloxyethyl methacrylate-*block*-poly(acrylic acid) (PS-*b*-PCEMA-*b*-PAA) has been studied to develop intricate architectures through the coupling of photo-crosslinked nanotubes with nanospheres.[26]

Block copolymers incorporating a cleavable group at the junction between block segments have generated significant interest over the past few years.[27] These cleavable block copolymers are desirable for the selective removal of one block from a self-assembled nanostructure of block copolymers, such as the dissociation of micelles or the preparation of membranes.[28] Various methods have been explored for the cleavage of block copolymers at their junction points, including reduction reactions,[29] light bombardment techniques,[30] pH variation,[31] and oxidations reactions.[32] However, block copolymers that incorporate disulfide linkers have the advantage of being selectively cleavable under mild conditions when exposed to reducing agents such as dithiothreitol (DTT) and dithiobutylamine (DTBA).[33] Generally, disulfide linkers are incorporated into block copolymers through end-coupling reactions, such as the coupling of polymers that are end-labeled with activated disulfide groups.[29] Several block copolymers bearing disulfide linkers have been reported, such as poly(L-lactide)-*disulfide*-poly(oligo(ethylene glycol) monomethyl ether methacrylate (PL-S_2-POEOMA-Br),[34] and poly(*N*-(2-hydroxypropyl)methacrylamide-*disulfide*-*N*-(3-aminopropyl)methacrylamide (PHPMA-S_2-PAPMA).[35] Additionally, multiblock copolymers,[36] multiple polymer chains that are linked together via disulfide bridges, i.e. (–S_2–PMMA–S_2-)$_n$–,[37] and star polymers[38] have been studied that accommodate disulfide units at the junction of two blocks. However, reports on doubly stimulable block copolymers incorporating disulfide cleavable junctions along with some other responsive block/unit are rare.[39]

The synthesis of doubly stimulable block copolymers integrating light- and reduction-sensitive sensors into a single block copolymer have not been reported before. In this chapter, we disclose the synthesis of poly(ethylene glycol)$_l$-*disulfide*-poly[2-(perfluorooctyl)ethyl methacrylate)]$_m$-*block*-poly(2-cinnamoloxyethyl methacrylate)$_n$ (PEG$_l$-S_2-PFOEMA$_m$-*b*-PCEMA$_n$) by combining atom transfer radical polymerization (ATRP) and the end-coupling of

pre-made components. This novel copolymer contains a water-soluble PEG block, a fluorinated PFOEMA block as a low surface energy material, a light-responsive PCEMA block, and a cleavable disulfide linker, as shown in Figure 3.1.

Atom transfer radical polymerization (ATRP) and reversible addition-fragmentation chain transfer (RAFT) polymerization techniques are used to synthesize fluorinated block copolymers.[40] Examples of these copolymers include poly[oligo(ethylene glycol) monomethyl ether acrylate]-*block*-poly(1H,1H-perfluorobutyl acrylate),[41] poly(butyl methacrylate)-*block*-poly(perfluoroalkyl acrylate),[42] poly(4-fluorostyrene)-*block*-poly(methyl acrylate) and poly(perfluorooctyl acrylate)-*block*-poly(methyl methacrylate),[43] poly(styrene)-*block*-poly(2,2,3,3,4,4,4-heptafluorobutyl methacrylate),[44] and also poly(ethylene glycol)-*orthonitrobenzyl*-poly[2-(perfluorooctyl)ethyl methacrylate)]-*block*-poly(2-cinnamoloxyethyl methacrylate).[45]

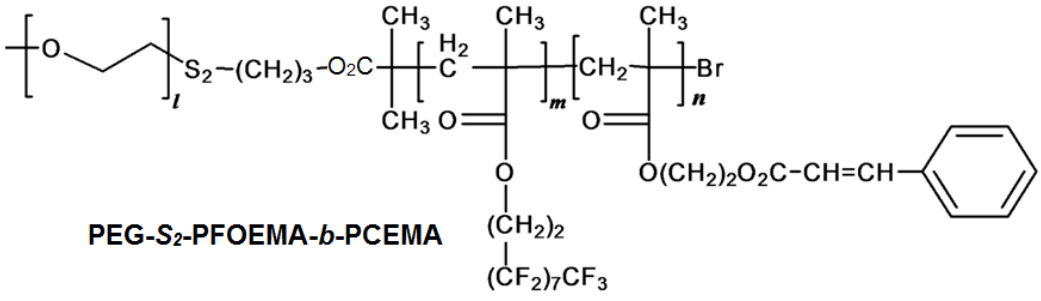

Figure 3.1. Chemical structure of PEG_l-S_2-$PFOEMA_m$-*b*-$PCEMA_n$.

3.2.1 Objectives

This chapter describes the synthesis of two novel doubly stimulable triblock copolymers. These copolymers were composed of PEG_l-S_2-$PFOEMA_m$-*b*-$PCEMA_n$ and were prepared by ATRP and end-coupling reactions as illustrated in Scheme 3.1. The formation of micelles by

PEG-S_2-PFOEMA-*b*-PCEMA was investigated in THF/water solvent mixtures. Also, these novel polymers were exposed to UV light and a reducing agent to assess their responsive properties. PEG$_l$-S_2-PFOEMA$_m$-*b*-PCEMA$_n$ is both light- and reducing agent responsive while P1 is light sensitive only.

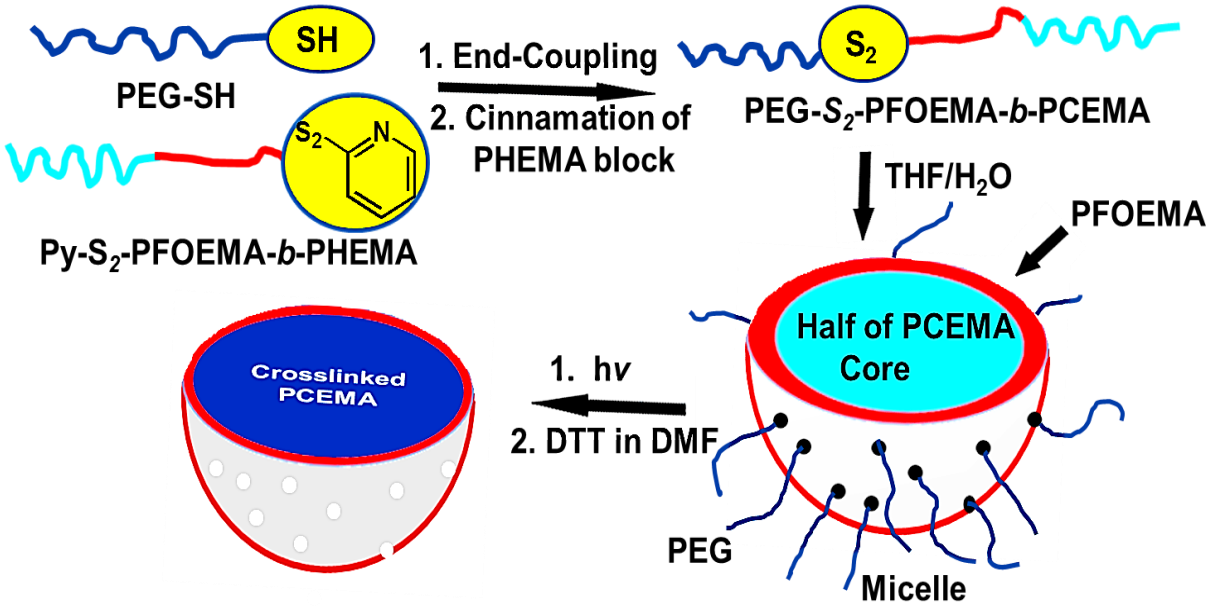

Scheme 3.1. Schematic representation of the preparation of PEG$_l$-S_2-PFOEMA$_m$-*b*-PCEMA$_n$ via an end-coupling reaction, and its subsequent micellization in a THF/water solvent mixture. The steps involving photo-crosslinking of the micelles as well as cleavage of the PEG chains are also shown.

3.2.2 Experimental Design Considerations

PEG$_l$-S_2-PFOEMA$_m$-*b*-PCEMA$_n$ (Figure 3.1) was chosen for many reasons. Firstly, PEG-SH can be conveniently prepared from commercially available PEG-OH and efficiently coupled with an activated disulfide (Py-S_2) end-functionalized diblock copolymer, i.e. Py-S_2-

PFOEMA-*b*-PHEMA. Secondly, PEG$_l$-S_2-PFOEMA$_m$-*b*-PCEMA$_n$ forms micelles in aqueous media because it is endowed with water soluble PEG block. Meanwhile, PCEMA is hydrophobic and will form the micellar core in aqueous media. Thirdly, the envisioned micelles will possess a photo-crosslinkable PCEMA core that upon UV light exposure will stabilize the micellar structure. Furthermore, S_2 is cleavable and is therefore placed at the junction between the PEG and PFOEMA blocks. This placement ensures that cleavage of the disulfide linker will unmask the fluorinated chains on the surface of the crosslinked micelles.

3.3 Experimental

3.3.1 Materials

2-Trimethylsiloxyethyl methacrylate (HEMA-TMS) was synthesized according to a literature method[46] and was distilled over calcium hydride before use. Pyridine (ACS reagent, Fisher Scientific) was refluxed and distilled over CaH_2 under nitrogen, and tetrahydrofuran (THF) was distilled over sodium and a small amount of benzophenone. Poly(ethylene glycol) monomethyl ether (M_n = 5,000 g/mol, Aldrich), cinnamoyl chloride (98%, Aldrich), *p*-toluenesulphonyl chloride (TsCl) (99.0%, TCI), triethylamine (99.5+%, Sigma-Aldrich), α,α,α-trifluorotoluene (TFT, 99+%, Acros), anisole (99%, Sigma-Aldrich), CuBr (99.999%, Aldrich), $CuBr_2$ (99.999%, Aldrich), and bipyridine (99+%, Acros) were used as received. Dithiothreitol (DTT), and potassium thioacetate (Aldrich, 98%) were used without purification.

3.3.2 Characterization

Size exclusion chromatography (SEC) was performed at 70 °C on a Waters 515 system equipped with a Waters 2410 refractive index detector. The three columns were repacked by

American Polymer Standards Corporation with 5-μm AM 1000, 10,000, and 100,000 Å gels, respectively. The system was calibrated using monodisperse polystyrene (PS) standards. The eluent used was dimethylformamide (DMF) containing 2.5 g/L of tetrabutylammonium bromide, and the flow rate was set to 0.9 mL/min. ^{1}H NMR measurements were performed using Bruker Avance-300, Avance-400 or Avance-500 instruments using deuterated pyridine-d_5, methanol-d_4 or chloroform-d_3 as solvents and a 3 s relaxation delay.

3.3.3 α-methoxy-ω-toluenesulfonyl-PEG (PEG-OTs)

PEG_{113}-OH (1.0 g, 2.0×10^{-1} mmol) was dissolved in 10 mL of THF and cooled down to 5-7 ^{o}C using an ice bath. An aqueous solution of NaOH (2.0 mL, 0.3 M) was added to the above solution and the mixture was stirred for 30 min at this temperature. A THF solution (2 mL) containing TsCl (57 mg, 1.5 equivalents) was added to the reaction mixture. The reaction flask was allowed to warm to 15-18 ^{o}C and stirred for ~7 h at this temperature. At regular intervals, 0.1 mL samples of the reaction mixture were collected. These samples were briefly extracted with chloroform before ^{1}H NMR analysis. After the reaction was completed, it was quenched with 20 mL of cold water and was subsequently extracted with chloroform (4 × 20 mL). The combined organic layers were rinsed with a brine solution (10 mL) and dried over magnesium sulfate. The solution was subsequently concentrated via rotary evaporation and the product was precipitated from diethyl ether (3 × 30 mL). The product was obtained as a white precipitate (0.84 g) in an 82% yield. ^{1}H NMR in $CDCl_3$: δ 7.88 (2H, Ar-), 7.32 (2H, Ar-), 3.9 (-CH_2OTs, 2H), 3.4-3.8 (*br*, -OCH_2CH_2, 456H), 3.3 (-OCH_3, 3H), 2.5 (CH_3, 3H) ppm.

3.3.3a Method 1: Direct synthesis of PEG_{113}-SH from PEG_{113}-OTs

PEG_{113}-OTs (500 mg, 9.58×10^{-2} mmol) was dissolved in anhydrous DMF (8.0 mL) in a 25 mL round-bottom flask. $NaSH\cdot H_2O$ (1.0 g, 10 equivalents) was then added to the reaction mixture. The color of the reaction mixture became greenish upon addition of $NaSH\cdot H_2O$, and remained unchanged during the course of the reaction. The reaction mixture was refluxed for 7 h at 80 ^oC, and was subsequently cooled to room temperature before the reaction was quenched with water (10 mL). DMF solution of the crude product was dialysed against THF (4 × 50 mL). The dialysed PEG-SH solution was concentrated via rotary evaporation to ~4 mL and was precipitated from diethyl ether, yielding 355 mg as a white precipitate in 71.0 % yield. ^{1}H NMR ($CDCl_3$ at 300 MHz): δ 3.9 ($CH_3OC\mathit{H_2}$-, 2H), 3.4-3.8 (*br*, -$O\mathit{CH_2CH_2}$, 456H), 3.3 (*s*, -OCH_3, 3H), 2.23 (HS-$\mathit{CH_2}$, 2H) ppm.

3.3.3b Method 2: Synthesis of PEG-SH via $SCOCH_3$

PEG_{113}-OTs (600 mg, 1.15×10^{-4} mol) was dissolved in anhydrous DMF (in 3.0 mL) in a 100 mL bottom flask and potassium ethanethioate (66.1 mg, 5.00 equivalents) was added to this solution. Immediately after the addition of potassium ethanethioate, the reaction mixture became dark-brown. After 16 h, the reaction mixture was analysed via ^{1}H NMR. Water (10 mL) was added to quench the reaction at this stage. The reaction mixture was extracted with dichloromethane (3 × 20 mL). The combined organic layers were washed with distilled water (20 mL) before the organic solvent was evaporated using a rotary evaporator. The crude product was dissolved into THF and was added drop wise into diethyl ether (4 × 20 mL). The resultant white precipitates were dried under vacuum at room temperature, yielding 0.51 g in an 85%

yield. ^{1}H NMR ($CDCl_3$ at 300 MHz): δ 3.9 (*s*, CH_3OCH_2-, 2H), 3.4-3.8 (*m*, -OCH_2CH_2, 456H), 3.03 (*s*, -OCH_3, 3H), 3.03(*m*, -CH_2SAc, 2H), 2.23 (*s*, S*Ac*, 3H) ppm.

In the next step, PEG_{113}-$SCOCH_3$ was converted into PEG_{113}-SH following a literature method reported previously for small organic molecules.[47] PEG_{113}-$SCOCH_3$ (200 mg, 3.80 mmol) was dissolved in methanol (10 mL) and acetyl chloride (80 mg, 1.0 mmol) was added to this solution. The reaction mixture was stirred at room temperature for 12 h, and then water (10 mL) was added to the crude mixture to quench the reaction. This was followed by the addition 10.0 mL of saturated aqueous $NaHCO_3$. The extraction was performed using dichloromethane (20 mL × 4). The combined organic layers were concentrated under reduced pressure to a volume of ~5 mL. The crude mixture was precipitated from diethyl ether (50 mL × 4) and was dried under vacuum overnight. ^{1}H NMR ($CDCl_3$ at 300 MHz): δ 3.9 (CH_3OCH_2-, 2H), 3.4-3.8 (-*m*, -OCH_2CH_2,456H), 2.23 (2H, -CH_2SH) ppm.

3.3.4 3-(Pyridin-2-yldisulfanyl)propyl 2-bromo-2-methylpropanoate (Py-S_2-Br)

The initiator 3-(pyridin-2-yldisulfanyl)propyl 2-bromo-2-methylpropanoate (Py-S_2-Br) was synthesized in a two-step synthesis following a literature procedure.[48] The overall yield of Py-S_2-Br was 55%. ^{1}H NMR ($CDCl_3$, 500 MHz): δ 8.6 (*m*, 1H), 7.7 (*m*, 2H), 7.10 (*m*, 1H), 4.3 (*t*, *J* = 6.0 Hz, 2H), 2.9 (*t*, *J* = 7.12 Hz, 2H), 2.1 (*m*, 2H), 1.94 (*s*, 6H) ppm.

3.3.5 Py-S_2-$PFOEMA_{12}$-Br

A typical FOEMA polymerization reaction with the initiator Py-S_2-Br is described below. FOEMA (0.78 mL, 2.3 mmol), Py-S_2-Br (54.6 mg, 0.160 mmol, as a 0.3 mL solution in anisole), trifluorotoluene (3.0 mL), bipyridine (75 mg, 0.44 mmol), and $CuBr_2$ (3.6 mg, 0.016 mmol) were added into a two neck round-bottom flask (100 mL). The mixture was bubbled

with N_2 for ~4 min before the addition of CuBr (24.0 mg, 0.167 mmol). The flask was subjected to four freeze-pump-thaw-N_2 refill cycles, and was immersed into a pre-heated oil bath at 85 ^oC. The reaction was monitored by ^1H NMR at various intervals. To perform ^1H NMR analysis, ~0.01 mL sample solutions were collected from the reaction mixture and subsequently diluted to 0.40 mL (0.08 mL TFT: 0.31 mL $CDCl_3$). A ~75% conversion was obtained within 70 min of polymerization. The reaction was quenched immediately by cooling the flask in a liquid nitrogen bath and subsequently exposing the contents to air. The crude mixture was diluted with TFT (10 mL) and was passed through a short alumina column. The alumina column was subsequently washed with 20 mL of TFT. The crude polymer solution (~12 mL) was concentrated to ~2 mL under reduced pressure. This crude homopolymer solution was precipitated from a THF/methanol mixture (45 mL, 20/80 v/v). The precipitate was re-dispersed into THF (2 mL) and precipitated again from a THF/methanol mixture (45 mL, 20/80 v/v). This process was repeated two more times, before the precipitate was dried in a vacuum oven at room temperature for 24 h. This provided 920 mg of the product as a white powder in a 69.5% yield. ^1H NMR (In $CDCl_3$:C_6F_6, v/v = 1/1, at 300 MHz): δ 4.4 (*br*, -OC*H*$_2$$CH_2$, 24H), 2.5 (*br*, -$OCH_2$*CH*$_2$$CF_2$, 24H), 2.0 (*br*, -$CH_2$, 24H), 1.2-0.9 (*br*, -$CH_3$, 36H).

3.3.6 Py-*S*$_2$-PFOEMA$_{12}$-*b*-P(HEMA-TMS)$_{60}$

The Py-*S*$_2$-PFOEMA$_{12}$-Br macroinitiator (0.33 g, 0.05 mmol) was transferred into a two neck Schlenk flask (100 mL) and placed under vacuum for 1 h. The flask was carefully backfilled with N_2. HEMA-TMS (0.55 mL, 2.5 mmol), TFT (1.2 mL), anisole (0.12 mL), bipyridine (24.0 mg, 0.153 mmol), and $CuBr_2$ (1.0 mg, 0.0050 mmol) were added into the flask. The mixture was bubbled with N_2 for 4-5 min before the addition of CuBr (7.9 mg, 0.055 mmol). The mixture was subjected to four freeze-pump-thaw-N_2 backfilling cycles. During

each cycle, the flask was placed briefly for 3-4 min in a water bath at ~35-38 ^{o}C. Finally, the mixture was stirred for 15 min at ~35 ^{o}C and then placed in a preheated oil bath at 82 ^{o}C. The color of the reaction mixture remained dark brown during the polymerization. ^{1}H NMR analysis was conducted at various intervals, such as 1, 3, and 5.5 h. An 80% monomer conversion was obtained in 5.5 h. The reaction was quenched by immersing the polymerization flask into a liquid nitrogen bath for ~1 min and subsequently the flask was purged with air. The crude polymer mixture was diluted with THF (20 mL) and was passed through a short pad of alumina. The column was washed with excess THF (100 mL). The eluted crude polymer was stirred in a THF/methanol/water (v/v/v = 6/1/0.2) solvent mixture overnight and was concentrated under reduced pressure to a volume of ~30 mL. This crude polymer was dialysed against THF for ~24 h by which was replaced with fresh THF (50 mL) every ~6 h. The dialysed sample was dried under reduced pressure, yielding 510 mg of the copolymer in 68.0% yield. ^{1}H NMR (In $CDCl_3$/TFT, v/v = 9/1, at 500 MHz): δ 4.2 (*br*, -O*CH*$_2$$CH_2CF_2$, 24H), 4.2 (*br*, -O*CH*$_2$$CH_2$, 120H), 3.85 (*br*, -$OCH_2$*CH*$_2$,120H), 2.5 (*br*, -$OCH_2$*CH*$_2$$CF_2$, 24H), 2.0 (*br*, -$CH_2$,144H), 1.2-0.9 (*br*, -$CH_3$, 216H) ppm.

3.3.7 PEG$_{113}$-*S*$_2$-PFOEMA$_{12}$-*b*-PHEMA$_{60}$

Py-*S*$_2$-PFOEMA$_{12}$-*b*-PHEMA$_{60}$ (50.0 mg, 0.003 mmol) was dissolved in anhydrous DMF (0.4 mL) in a 1.0 mL sealed vial. To this solution was added 10 µL of glacial acetic acid. A 0.2 mL DMF solution of PEG-SH (36.0 mg, 0.008 mmol) was subsequently added to the reaction mixture, which was stirred at room temperature. The reaction was monitored via UV-visible absorbance spectroscopy by measuring changes in the absorbance at 375 nm. Once the reaction was completed, DMF was removed via rotary evaporation. The crude mixture containing PEG-

S_2-PFOEMA-*b*-PHEMA and PEG-SH (some of which might have become oxidized to PEG-*S_2*-PEG) was washed with diethyl ether (3 × 2 mL) and subsequently dried under vacuum for 24 h.

3.3.8 PEG_{113}-*S_2*-$PFOEMA_{12}$-*b*-$PCEMA_{60}$ (P2)

PEG_{113}-*S_2*-$PFOEMA_{12}$-*b*-$PHEMA_{60}$ (62 mg of the copolymer containing 0.19 mmol of hydroxyl groups) was dissolved in dry pyridine (4 mL) and the solution was stirred for ~30 min before cinnamoyl chloride (60.1 mg, ~0.357 mmol, 1.90 equivalents) was added to the solution. The reaction mixture was stirred overnight at room temperature and kept in the dark. The pyridinium salt was removed via centrifugation at 3900 rpm (2600 *g*) for 10 min. The supernatant was subsequently concentrated via rotary evaporation to ~1 mL. This crude mixture was subsequently precipitated from diethyl ether (50 mL). The precipitates were again dissolved into 3 mL of THF and precipitated from diethyl ether (50 mL). This process of dissolving the copolymer into THF and subsequent precipitation with diethyl ether was repeated two more times. Finally, the obtained precipitates were washed twice with 2 mL of methanol. The resultant brown solid was dried at room temperature under vacuum for 24 h, yielding 66.1 mg of the copolymer. ^{1}H NMR (In $CDCl_3$, at 500 MHz): δ 8.0-6.6 (7H, Aromatic and C=C protons), 4.25 (*br*, -COO*CH_2*CH_2CF_2, 24H), 4.2-4.0 (*br*, -COO*CH_2* and CH_2*CH_2*OOC, 240H), δ 3.5-3.6 (*br*, -*CH_2CH_2*O, 456H), 2.4 (*br*, -*CH_2CF_2*, 24 H), 1.8-2.2 (*br*, -CH_2, 144H), 0.8-1.4 (*br*, -CH_3, 216H) ppm.

3.3.9 Kinetic Study of the Synthesis of PEG_{113}-*S_2*-$PFOEMA_{12}$-*b*-$PHEMA_{60}$

Py-*S_2*-$PFOEMA_{12}$-*b*-$PHEMA_{60}$ (~ 5.0 mg, ~2.2×10^{-4} mmol) was dissolved in anhydrous DMF (2.5 mL) within a sealed UV cuvette and loaded with a small magnetic stirring bar. To this solution was added 3 μL of glacial acetic acid. A 0.5 mL DMF solution of PEG-SH

(10 mg, 2.0 $\times 10^{-3}$ mmol) was subsequently added to the reaction mixture. UV-visible spectra were recorded at various intervals, as shown in results and discusion. Meanwhile, the reaction mixture was stirred at 300 rpm during the UV-visible measurements.

3.3.10 PEG_{113}-*S*$_2$-$PFOEMA_{12}$-*b*-$PCEMA_{60}$ (P2) Micelles

P2 (2.2 mg) was dissolved in THF (1.0 mL) and the solution was stirred for 2 h at room temperature. Deionized water was added dropwise at a rate of 6-7 drops per minute until the desired water volume fraction (f_{H2O}) of 80% was obtained. The final concentration of the micellar solution was 0.45 mg/mL. The solution was warmed to 40 ^{o}C for 15 min and magnetically stirred at 400 rpm. The solution was then stirred at room temperature for at least 12 h before performing AFM and TEM analysis.

3.3.11 AFM Measurements

Specimens were prepared for AFM analysis specimens by aero-spraying micellar solutions of the samples onto freshly cleft mica surfaces. Tapping mode AFM was performed using a Veeco Multimode microscope equipped with a Nanoscope IIIa controller. Silicon cantilevers were used that had a force constant of ~40 N/m and an oscillating frequency of ~300 kHz.

3.3.12 TEM Measurements

Specimens for TEM analysis were prepared by aero-spraying micellar solutions of the samples from a homemade atomizer onto cellulose-coated copper grids.[49] These sprayed samples were subsequently stained with OsO_4 vapour for 1.5 h. The specimens were analysed using a Hitachi H-7000 instrument operated at 75 kV.

3.3.13 Micellar Crosslinking

Micellar solutions of PEG_{113}-S_2-$PFOEMA_{12}$-*b*-$PCEMA_{60}$ (3 mL at 0.6 mg/mL in THF/water at f_{H2O} = 80%) were irradiated in a 1.00 cm thick Hellma quartz cell. The solution was magnetically stirred as this crosslinking process was performed. The focused beam was generated from a 500 W mercury lamp in an Oriel 6140 lamp housing powered by an Oriel 6128 power supply. This beam was passed through a 270 nm cut-off filter before it reached the sample. The sample was irradiated for 45 min to crosslink the PCEMA block. The irradiated polymer solution was subsequently concentrated via rotary evaporation and then dried overnight under vacuum at room temperature.

3.3.14 PEG Chain Cleavage from Crosslinked P2 Micelles.

Photo-crosslinked micelles (~1.2 mg) of P2 were dispersed in anhydrous DMF (0.2 mL). DTT ($5.2x10^{-3}$ mmol) was subsequently added to this solution, which was stirred at r.t. After 3 h, the suspended particles were centrifuged at 13,000 *g*. The settled particles were re-dispersed into methanol (1 mL) and subsequently centrifuged again. The process of rinsing the particles with methanol was repeated two more times. The obtained PEG-cleft particles were dried under vacuum for 12 h, thus yielding ~0.6 mg of the particles.

3.3.15 Film Casting and Contact Angle Measurements

PEG-cleft particles (~0.6 mg) were dispersed into TFT (0.3 mL), and 3-4 droplets of this dispersion were added one by one onto a glass plate to cover an area of ~10 mm^2 over a period of ~20 min. Each droplet was allowed to evaporate before the next droplet was applied onto the surface. The particulate film was allowed to dry for 2 h under ambient conditions. Subsequently, the film was annealed at 120 ^oC for 20 min. Liquid droplets of water impregnated

with Rhodamine B and droplets (5 μL) of diiodomethane were then placed onto the annealed film for the contact angle measurements. The images were collected after allowing the droplet to stay on the coated surface for at least two minutes

3.4 Results and Discussion

In this study, two doubly stimulable PEG-S_2-PFOEMA-*b*-PCEMA copolymers with various chain lengths were prepared by performing end-coupling reactions between PEG-SH and Py-S_2-PFOEMA-*b*-PHEMA, and subsequently modifying the PHEMA block. Initially, precursors for the triblock copolymer PEG-S_2-PFOEMA-*b*-PHEMA were synthesized. PEG-SH was synthesized from the commercially available polymer, PEG_{113}-OH. Meanwhile, *Py*-S_2-PFOEMA-*b*-PHEMA was synthesized via sequential ATRP of FOEMA and HEMA-TMS. Subsequently, PEG-SH and Py-S_2-PFOEMA-*b*-PHEMA were coupled together to obtain the triblock copolymer Py-S_2-PFOEMA-*b*-PHEMA. Cinnamation of the PHEMA block yielded the desired doubly-responsive triblock copolymer PEG-S_2-PFOEMA-*b*-PCEMA.

3.4.1 PEG_{113}-SH

In this study, PEG_{113}-SH was prepared by two different methods. Method 1 involved the direct synthesis of PEG_{113}-SH from the reaction of PEG-OTs with $NaSH{\cdot}H_2O$. Meanwhile, Method 2 was based on a three step synthesis of PEG-SH, as depicted in Scheme 3.2.

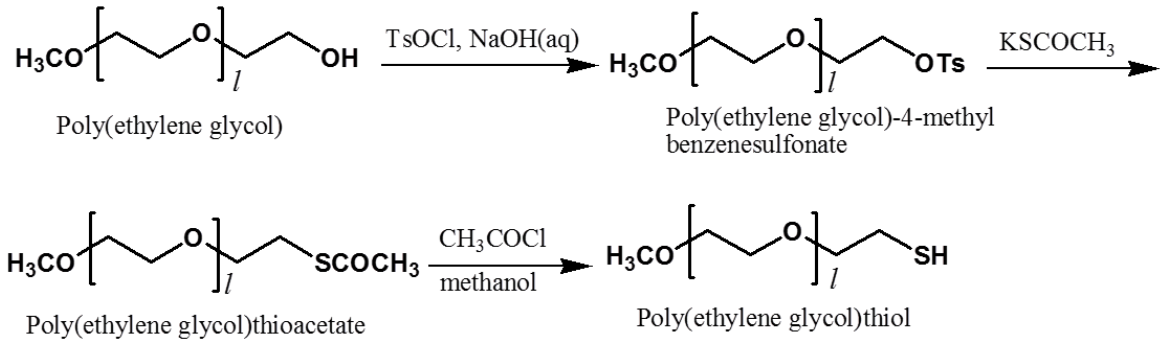

Scheme 3.2. Synthetic pathway toward PEG_{113}-SH via Method 2.

In both methods, the first step involved the synthesis of PEG_{113}-OTs. Firstly, PEG_{113}-OH was reacted with *p*-toluenesulfonyl chloride under basic conditions and low temperature to obtain α-methoxy-ω-toluenesulfonyl-PEG_{113} (PEG_{113}-OTs). The obtained PEG_{113}-OTs was characterized by ^{1}H NMR in $CDCl_3$, and peak assignments are shown in Figure 3.2. ^{1}H NMR analysis revealed that ~96% of the $PEG_{113}OH$ chains had been end-capped with OTs. This value was calculated from the peak integrations at 7.3 ppm and at 3.5-3.8 ppm corresponding to the aromatic protons of the tosyl group and the protons of the $PEG_{113}OH$ main chain, respectively (Figure 3.3).

Method 1: This method involved a single step substitution reaction between PEG_{113}-OTs and $NaSH{\cdot}H_2O$ to prepare the desired PEG_{113}-SH. For this purpose, the reactions mixture was refluxed at high temperature to force the substitution reaction. ^{1}H NMR analysis showed that the peak corresponding to the OTs group at 7.3 ppm had completely disappeared, indicating the displacement of OTs. Meanwhile, SEC analysis recorded on a DMF column revealed that the PEG_{113}-SH peak was accompanied by a dimer peak that possibly represented PEG_{113}-S_2-PEG_{113} (Figure 3.2). As it is well-understood that DTT is a highly efficient reagent for S_2 bond cleavage,[33] thus DTT was employed to rupture PEG_{113}-S_2-PEG_{113} to yield PEG_{113}-SH.

Although, the dimer peak eluting at 26.0 min diminished significantly after DTT treatment, but did not disappear completely (Figure 3.2). A partial cleavage with DTT indicated that the dimer peak may also contain PEG_{113}-*O*-PEG_{113} because PEG_{113}-*O*-PEG_{113} would remain unchanged upon reaction in the presence of DTT. We speculate that PEG_{113}-*O*-PEG_{113} would have been produced by the reaction of PEG_{113}-OTs with water at elevated temperatures to form PEG_{113}-OH, which could subsequently react with another molecule of PEG_{113}-OTs to form PEG_{113}-*O*-PEG_{113}. The presence of water in the system might have come from $NaSH.H_2O$. As SH is a stronger nucleophile than water itself, thus, $NaSH.H_2O$ was used. However, we did not investigate this method further, because an alternate method was used that worked best under mild conditions.

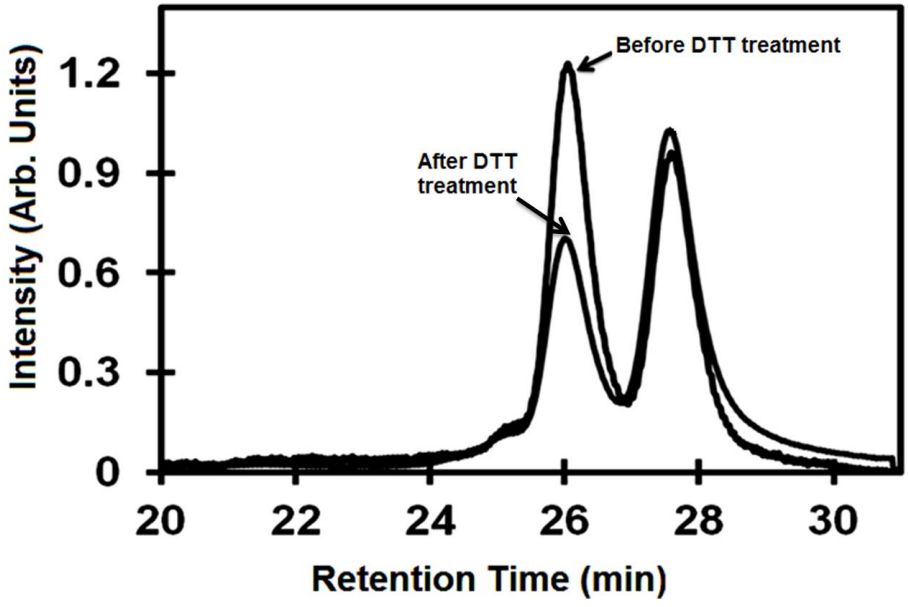

Figure 3.2. SEC traces of PEG_{113}-SH synthesized via Method 1. DMF salted with tetrabutylammonium bromide (0.25 wt.%) was used as the mobile phase.

Method 2: Due to the above mentioned complications in the synthesis of PEG_{113}-SH via method 1, a detour was taken as shown Scheme 3.2. Here, PEG_{113}-OTs was reacted with

potassium thioacetate under ambient conditions to yield poly(ethylene glycol)$_{113}$-thioacetate (PEG_{113}-SAc). A facile substitution reaction took place that yielded PEG_{113}-SAc. Figure 3.3B shows the ^{1}H NMR spectrum of PEG_{113}-SAc, in which the -OTs signals at 7.3 and 7.9 ppm had disappeared while a signal corresponding to -SAc emerged at 2.3 ppm. In the next step, the acetyl group of PEG_{113}-SAc was reacted with a 26 mol% (relative to the molar quantity of –SAc group) solution of acetyl chloride in methanol.[47] These mild conditions were used for the deprotection of SAc to suppress side reactions, such as thiol-thiol coupling. The resultant PEG_{113}-SH was characterized via ^{1}H NMR and SEC analysis. A labelled ^{1}H NMR spectrum for PEG_{113}-SH is shown in Figure 3.3C that revealed the formation of the desired product, as the signal at 2.3 ppm corresponding to SAc disappeared. An SEC trace of PEG_{113}-SH is shown in Figure 3.4, which consists of a main peak corresponding to PEG_{113}-SH eluting at ~28.0 min. A small shoulder peak at the high molecular weight side (26.5 min) of the main peak also appeared. This peak might be due to the auto-oxidation of PEG_{113}-SH in air, thus producing PEG_{113}-S_2-PEG_{113}. The polydispersity index (M_w/M_n) in terms of PS standards was low, at 1.05. Meanwhile M_w for PEG_{113}-SH in terms of PS standards was 14,000 g/mol, as shown in Table 3.1. This sample was used in the next step without further purification because PEG_{113}-S_2-PEG_{113} does not participate in the coupling reaction between Py-S_2-PFOEMA-*b*-PHEMA PEG_{113}-SH.

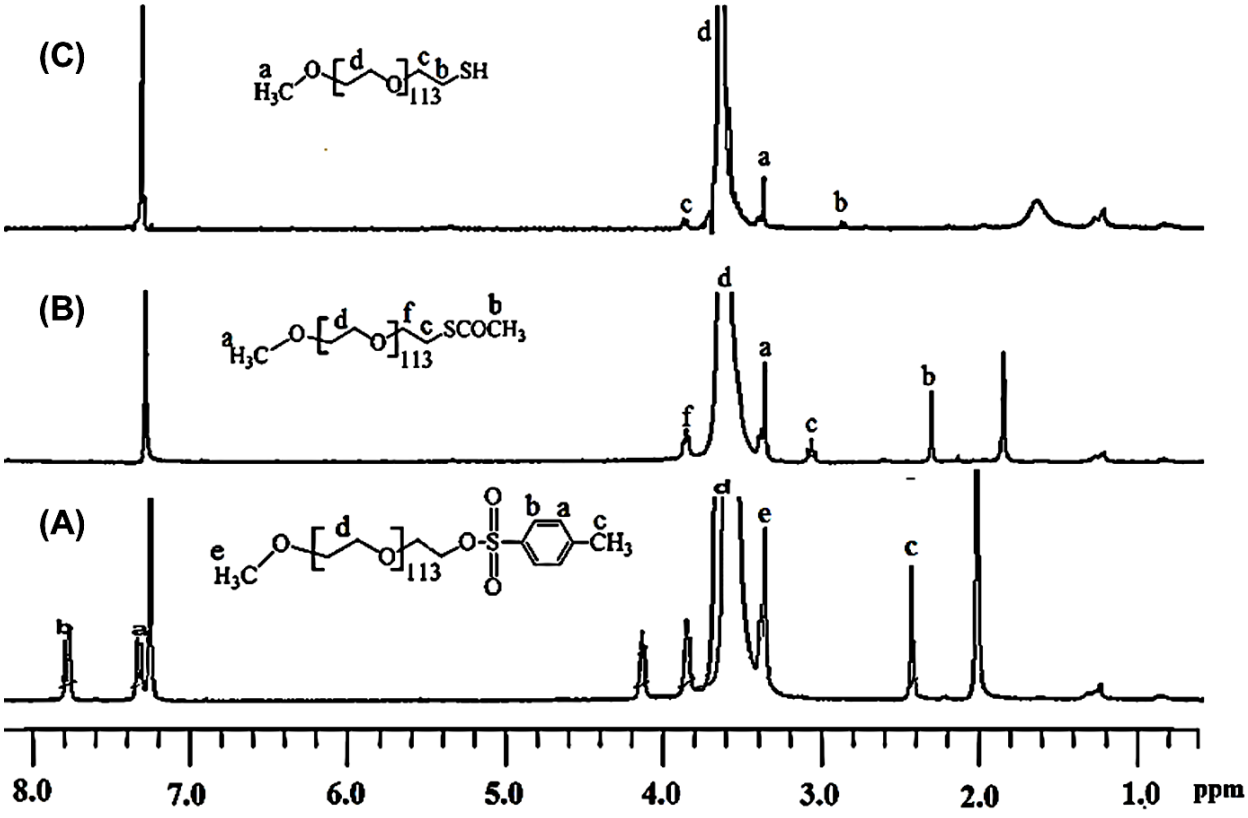

Figure 3.3. ^{1}H NMR (300 MHz, recorded in $CDCl_3$) spectra of PEG_{113}-OTs (A), PEG_{113}-SAc (B), and PEG_{113}-SH (C).

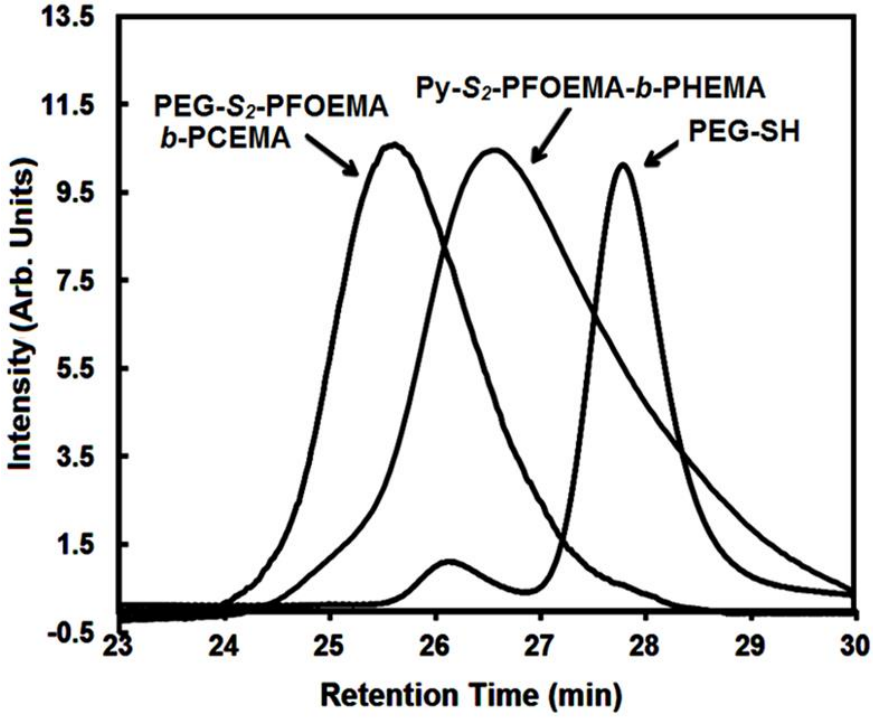

Figure 3.4. Combined SEC traces of P2 and its precursors, Py-S_2-PFOEMA$_{12}$-*b*-PHEMA$_{60}$ and PEG$_{113}$-SH. The SEC traces were recorded using DMF as the eluent.

3.4.2 3-(Pyridin-2-yldisulfanyl)propyl 2-bromo-2-methylpropanoate (Py-S_2-Br)

Py-S_2-Br was synthesized following a literature method as shown in Scheme 3.3.[48] In the first step, 3-(pyridine-2-yldisulfanyl)propan-1-ol was synthesized by reacting 2,2-dithiopyridine with mercaptopropanol in the presence of a catalytic amount of acetic acid. The reaction was performed at room temperature. Subsequently, 3-(pyridine-2-yldisulfanyl)propan-1-ol was reacted with 2-bromo-2-methylpropionic acid using coupling agents *N*,*N*'-dicyclohexylcarbodiimide (DCC) and 4-dimethylaminopyridine (DMAP) to form Py-S_2-Br. Figure 3.5 shows labelled ^{1}H NMR spectra of 3-(pyridine-2-yldisulfanyl)propan-1-ol and Py-S_2-Br, confirming the successful synthesis of Py-S_2-Br.

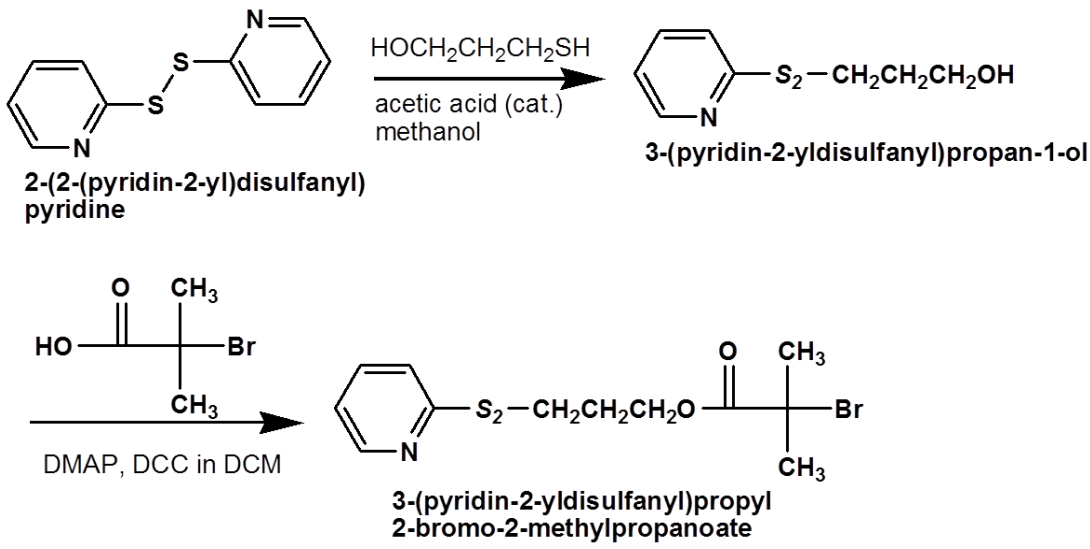

Scheme 3.3. Synthetic strategy for the preparation of the Py-S_2-Br initiator.

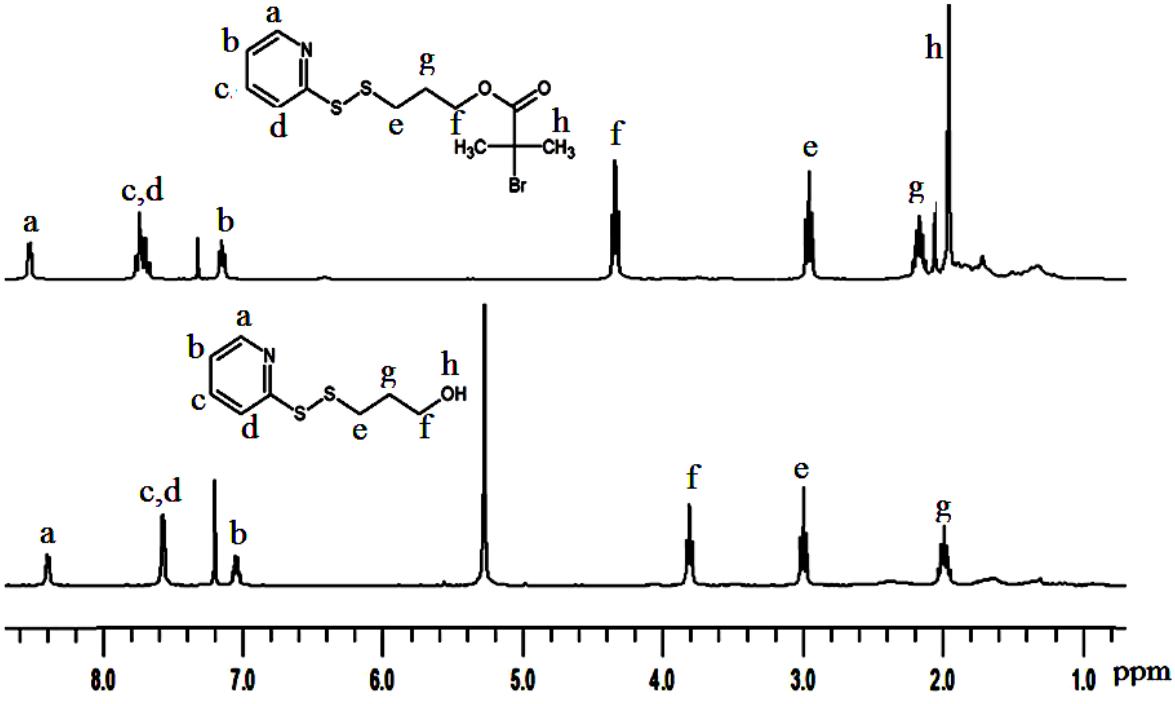

Figure 3.5. ^{1}H NMR (300 MHz in $CDCl_3$) spectra of 3-(pyridine-2-yldisulfanyl)propan-1-ol (bottom) and the initiator Py-S_2-Br (top).

3.4.3 Py-S_2-PFOEMA$_{12}$-*b*-PHEMA$_{60}$

The diblock copolymer Py-S_2-PFOEMA-*b*-PHEMA was synthesized by sequential ATRP polymerization of FOEMA and HEMA-TMS using Py-S_2-Br as the initiator (Scheme 3.4). During the first stage, Py-S_2-PFOEMA-Br was synthesized by ATRP of the FOEMA monomer. A detailed investigation on the optimization of the reaction conditions for PFOEMA synthesis eventually established that using TFT/anisole (9/1 v/v) at 85 ^{o}C provided the copolymers with the lowest polydispersities. The kinetics of the FOEMA polymerization was studied via ^{1}H NMR analysis by collecting samples at various time intervals (such as at 15, 45 and 70 min) during the polymerization. Based on the ^{1}H NMR analysis, it was found that a 75% monomer conversion was obtained in 70 min at 85 ^{o}C. The crude diblock copolymer was purified by passage through an alumina column to remove ligated copper. The column was washed with excess TFT to minimize the loss of the copolymer on the column. Py-S_2-PFOEMA$_{12}$-Br synthesis was obtained in good yield of ~70% when FOEMA monomer conversion reached 75%.

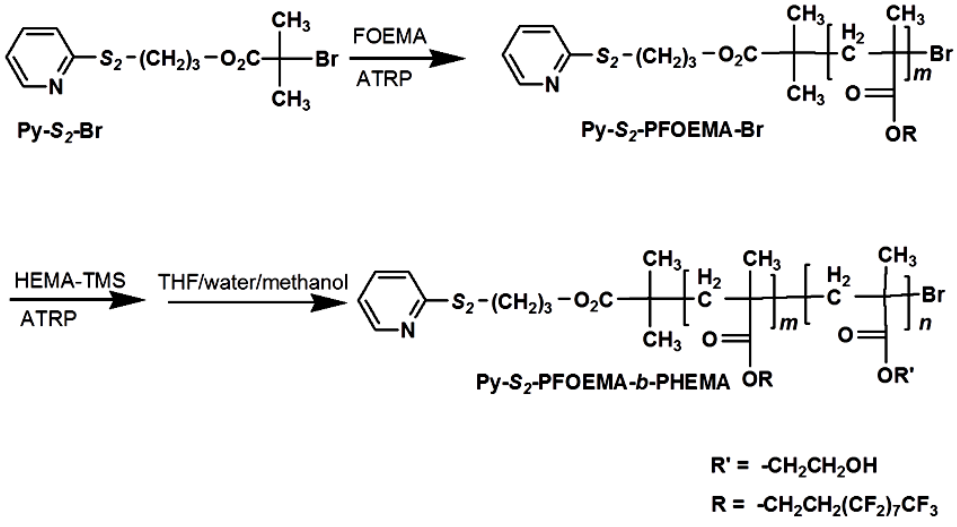

Scheme 3.4. Various reactions involved in the preparation of Py-S_2-PFOEMA$_{12}$-*b*-PHEMA$_{60}$.

In the next step, Py-S_2-PFOEMA$_{12}$-Br was used as a macroinitiator to polymerize HEMA-TMS. HEMA is difficult to polymerize directly by ATRP using Py-S_2-PFOEMA$_{12}$-Br. Therefore, HEMA-TMS was used as a monomer because HEMA-TMS and Py-S_2-PFOEMA$_{12}$-Br and the anticipated Py-S_2-PFOEMA$_{12}$-P(HEMA-TMS)$_{60}$-Br are all soluble in a TFT/anisole mixture used for this reaction. The reaction was monitored by ^{1}H NMR analysis by collecting samples from the reaction mixture at regular intervals. The degree of conversion of HEMA-TMS into the polymer P(HEMA-TMS) was calculated by matching peak integrations corresponding to P(HEMA-TMS) at ~4.0 to that of alkene protons of non-polymerized HEMA-TMS. As the polymerization proceeded, the integration of the P(HEMA-TMS) peak increased at the cost of the HEMA-TMS signal. The reaction was terminated after accomplishing ~80% monomer conversion in ~5.5 h. The crude diblock copolymer Py-S_2-FOEMA-*b*-P(HEMA-TMS) was freed of the ligated copper by passage through an alumina column. It is pertinent to mention that the use of excess THF for rinsing the column reduced the loss of the polymer to the column, and thus increased the overall yield for the polymerization reaction. The purification of Py-S_2-PFOEMA$_{12}$-*b*-P(HEMA-TMS)$_{60}$ from the copper residue was performed before TMS cleavage. Subsequently, the TMS group of Py-S_2-PFOEMA$_{12}$-*b*-P(HEMA-TMS)$_{60}$ was cleaved under mild conditions utilizing a mixture of THF/methanol/water. It was difficult to find a suitable solvent mixture for the precipitation of Py-S_2-PFOEMA$_{12}$-*b*-PHEMA$_{60}$. Therefore, the product was purified by dialysis against THF to remove small molecular impurities.

Figure 3.4 also shows an SEC trace of Py-S_2-PFOEMA$_{12}$-*b*-PHEMA$_{60}$. SEC analysis revealed that the copolymer had a monomodal and symmetrical Gaussian distribution,. The polydispersity index M_w/M_n in terms of PS standards was found to be 1.2. Meanwhile the M_w of Py-S_2-PFOEMA$_{12}$-*b*-PHEMA$_{60}$ in terms of PS standards was 24,480 g/mol. Further confirmation for the synthesis of Py-S_2-PFOEMA$_{12}$-*b*-PHEMA$_{60}$ was provided by ^{1}H NMR

analysis, as shown in Figure 3.6. The properties of these block copolymers determined by SEC and ^{1}H NMR analyses are summarized in Table 3.1.

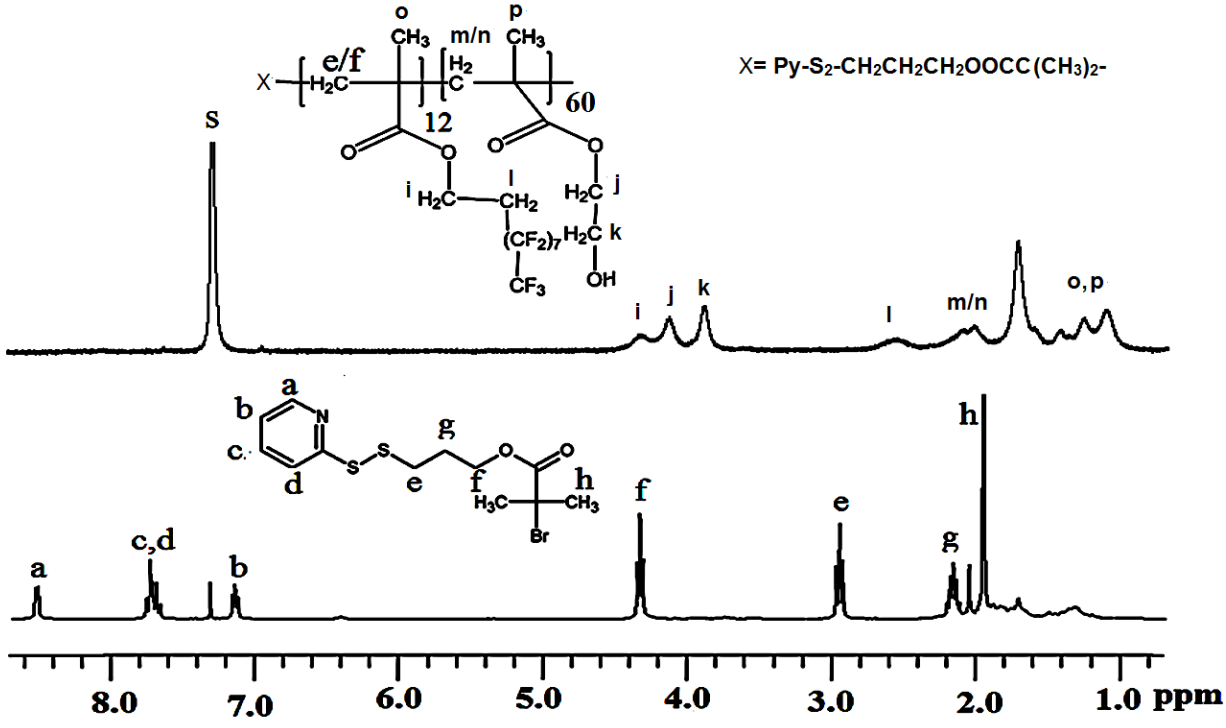

Figure 3.6. ^{1}H NMR spectra of the initiator Py-S_2-Br (bottom) and the diblock copolymer Py-S_2-PFOEMA$_{12}$-*b*-PHEMA$_{60}$ (top). The spectra were recorded in $CDCl_3$ using a 300 MHz ^{1}H NMR spectrometer.

3.4.4 Test for the Presence of Activated Sulfide (Py-S_2-) Among Batches of the Py-S_2-PFOEMA-*b*-PHEMA Copolymer

It was difficult to detect the presence of Py-S_2- end groups among batches of the synthesized Py-S_2-PFOEMA-*b*-PHEMA copolymer by ^{1}H NMR analysis. However, 2-pyridothione is produced as a by-product during the reduction of Py-S_2-PFOEMA-*b*-PHEMA with DTT (Scheme 3.5), which absorbs light at 375 nm.[29] Therefore, UV-Visible analysis was

better option to detect the presence of Py-S_2 in batches of Py-S_2-PFOEMA-*b*-PHEMA. For this purpose, Py-S_2-PFOEMA-*b*-PHEMA was reacted with DTT in DMF and was monitored by UV-Visible analysis. A facile reduction of Py-S_2-PFOEMA-*b*-PHEMA took place yielding HS-PFOEMA-*b*-PHEMA and 2-pyridothione. Peak at 375 nm appeared immediately after mixing the reagents, as shown Figure 3.7. The spectral analysis confirmed that the reaction requires ~4 min to reach to completion, as assessed by the peak intensity of 2-pyridothione. This clearly indicates the presence of an activated disulfide "Py-S_2" moiety in Py-S_2-PFOEMA$_{12}$-*b*-PHEMA$_{60}$.

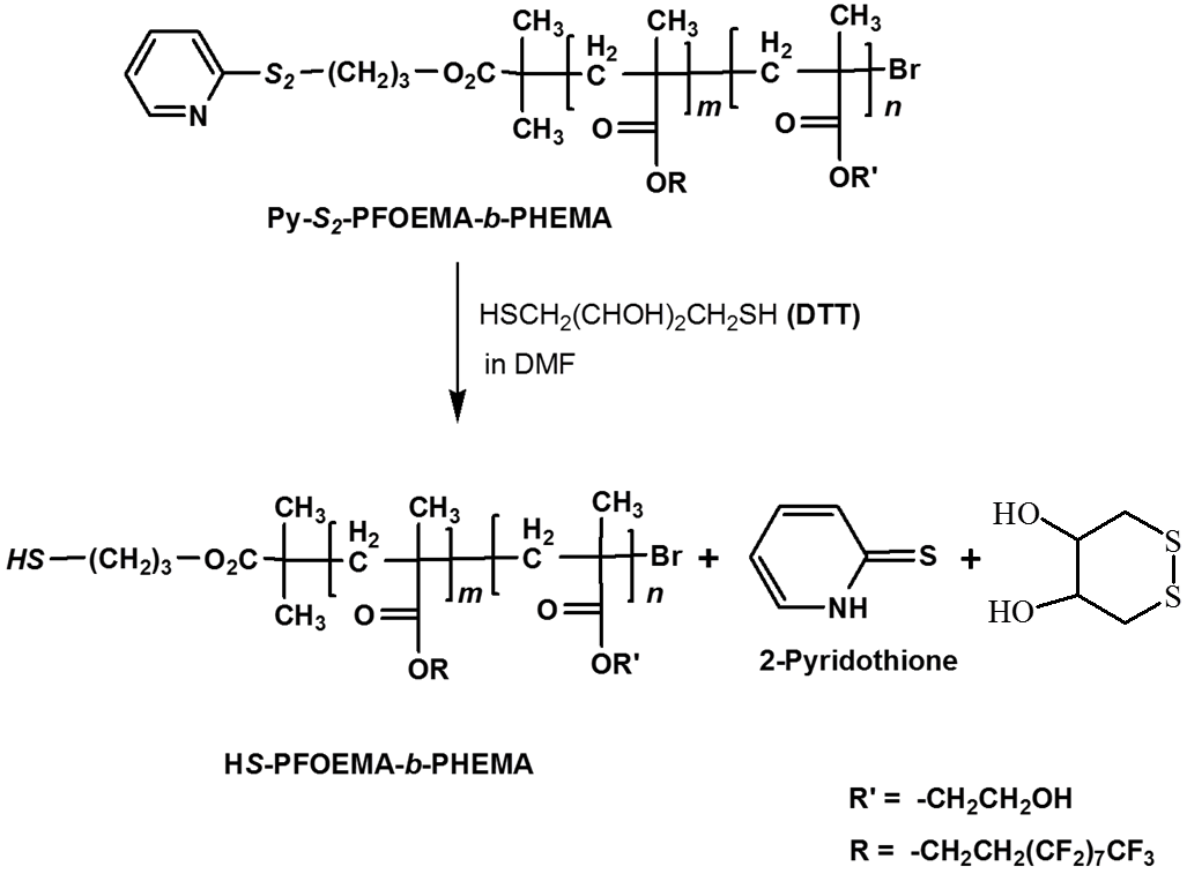

Scheme 3.5. Cleavage of Py-S_2-PFOEMA-*b*-PHEMA with DTT.

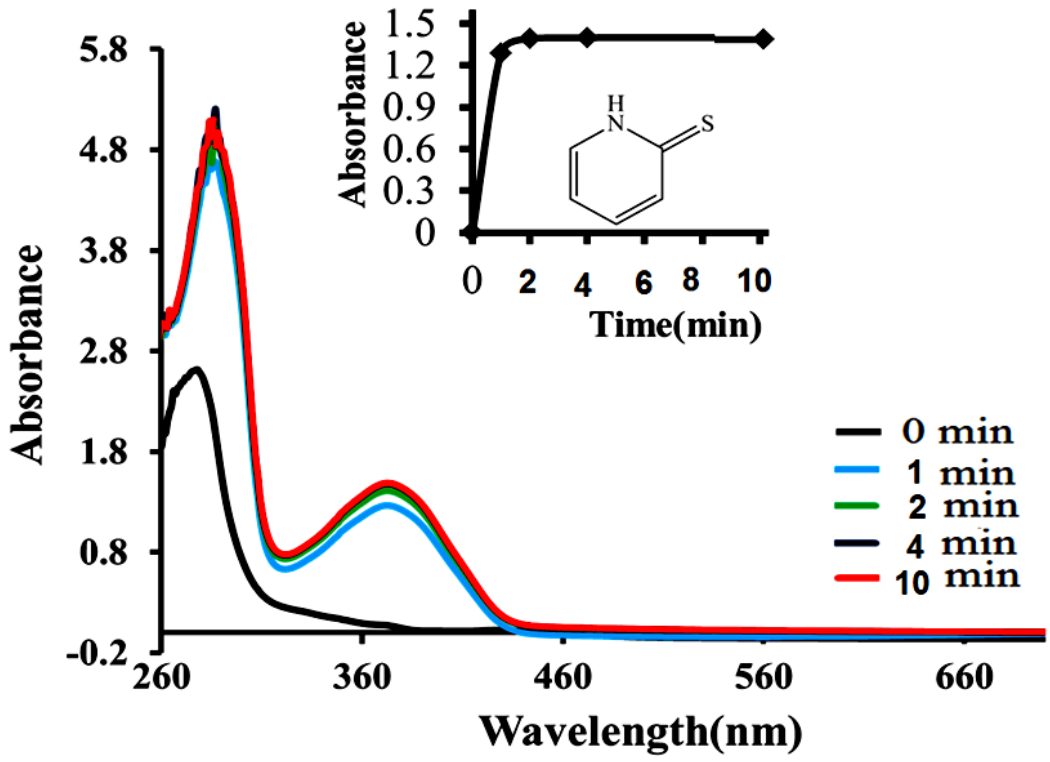

Figure 3.7. Plot of the absorbance vs. wavelength for the reduction of Py-S_2-PFOEMA$_{12}$-*b*-PHEMA$_{60}$ using DTT at various intervals. In the in-set, absorbance for 2-pyridothione at 375 nm vs. reaction time is shown. The UV-visible spectra were recorded in DMF.

3.4.5 PEG$_{113}$-S_2-PFOEMA$_{12}$-*b*-PHEMA$_{60}$

Scheme 3.6 depicts the end-coupling reaction between PEG$_{113}$-SH and Py-S_2-PFOEMA$_{12}$-*b*-PHEMA$_{60}$, which was performed according to a literature method.[29] Since PEG$_{113}$-SH undergoes auto-oxidation in air (Eq. 3.1), thus freshly prepared PEG$_{113}$-SH was used.[50] In anhydrous DMF, PEG$_{113}$-SH and Py-S_2-PFOEMA$_{12}$-*b*-PHEMA$_{60}$ were dissolved separately. The DMF solution of PEG$_{113}$-SH was mixed with that of Py-S_2-PFOEMA$_{12}$-*b*-PHEMA$_{60}$ in the presence of a catalytic amount of acetic acid. An excess of PEG$_{113}$-SH ensured the complete consumption of Py-S_2-PFOEMA$_{12}$-*b*-PHEMA$_{60}$.

$$2\ RSH \rightarrow RS\text{-}SR + 2\ H^+ + 2\ e^- \qquad \text{(Eq. 3.1)}$$

As shown in Scheme 3.6, a coupling reaction between PEG-SH and Py-S_2-PFOEMA$_{12}$-*b*-PHEMA$_{60}$ generates 2-pyridothione as a by-product that absorbs light at ~375 nm. The driving force for the reaction may have arisen from the aromatic stability of 2-pyridothione. Again, UV-Visible spectroscopy provides an ideal choice to monitor the progress of the reaction for triblock copolymer synthesis. In a controlled experiment, the kinetics of the coupling reaction was investigated. For this purpose, the reaction between PEG$_{113}$-SH and Py-S_2-PFOEMA$_{12}$-*b*-PHEMA$_{60}$ was performed in a sealed UV-visible quartz cuvette. The reaction was monitored by UV-visible spectroscopy. The UV-visible spectra recorded during the coupling reaction are shown in Figure 3.8a. The Py-S_2-PFOEMA$_{12}$-*b*-PHEMA$_{60}$ solution did not exhibit an absorption peak at ~375 nm. Similarly, PEG-SH does did not show any absorption in the UV-visible range. Upon mixing PEG$_{113}$-SH with the Py-S_2-PFOEMA$_{12}$-*b*-PHEMA$_{60}$ solution, a peak corresponding to 2-pyridothione appeared immediately. The spectra obtained at different time intervals indicated that ~90% of the reaction occurred in the first 30 min. Also, the absorbance at ~375 nm vs. the reaction time has been plotted in Figure 3.8b. Based on the UV-visible spectral data, it is evident that the coupling reaction between PEG$_{113}$-SH and Py-S_2-PFOEMA$_{12}$-*b*-PHEMA$_{60}$ is very efficient.

The coupling reaction between PEG$_{113}$-SH and Py-S_2-PFOEMA$_{12}$-*b*-PHEMA$_{60}$ was performed at different concentrations. It was observed that the reaction reaches completion in ~120 min, as there is no further increase in in the intensity of the 2-pyridothione peak at ~375 nm.

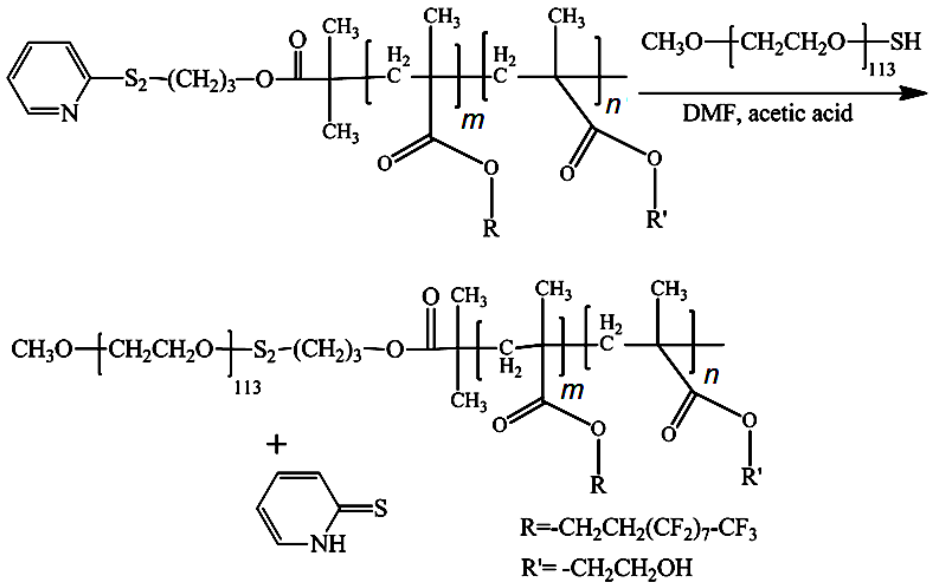

Scheme 3.6. Synthetic pathway for preparing PEG_{113}-S_2-$PFOEMA_{12}$-*b*-$PHEMA_{60}$ by the end-coupling of PEG_{113}-SH with Py-S_2-$PFOEMA_{12}$-*b*-$PHEMA_{60}$.

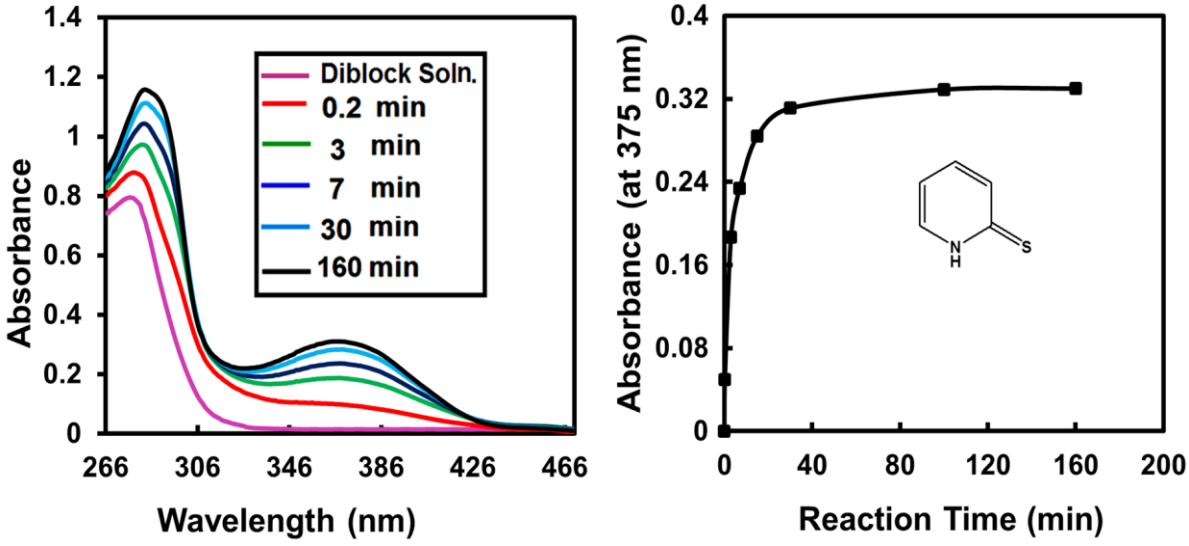

Figure 3.8. UV-visible spectra recorded during the coupling reaction between PEG-SH and Py-S_2-PFOEMA-*b*-PHEMA (a) and a plot of the absorbance at ~375 nm vs. reaction time (b).

3.4.6 PEG_{113}-S_2-$PFOEMA_{12}$-*b*-$PCEMA_{60}$ (P2)

Initially, we attempted to couple PEG-SH with Py-S_2-$PFOEMA_{12}$-*b*-$PCEMA_{60}$ instead of Py-S_2-$PFOEMA_{12}$-*b*-$PHEMA_{60}$. This procedure did not work, as the anticipated 2-pyridothione peak at 375 nm did not appear during the attempted end-coupling of Py-S_2-$PFOEMA_{12}$-*b*-$PCEMA_{60}$ and PEG_{113}SH. Alternatively, an initial coupling reaction was performed between Py-S_2-$PFOEMA_{12}$-*b*-$PHEMA_{60}$ and PEG_{113}-SH to prepare PEG-S_2-$PFOEMA_{12}$-*b*-$PHEMA_{60}$, which was followed by a cinnamation step. The hydroxyl groups of PEG_{113}-S_2-$PFOEMA_{12}$-*b*-$PHEMA_{60}$ were reacted with excess cinnamoyl chloride in dry pyridine, thus yielding PEG_{113}-S_2-$PFOEMA_{12}$-*b*-$PCEMA_{60}$ (P2). The pyridinium salt was removed from the reaction mixture by centrifugation and subsequent precipitation from diethyl ether. PEG-SH (which can become oxidized to PEG-S_2-PEG) was readily soluble in methanol while P2 remained as a solid precipitate. Thus, crude PEG_{113}-S_2-$PFOEMA_{12}$-*b*-$PCEMA_{60}$ was extracted with methanol to remove PEG-SH.

The weight average molecular weight (M_w), polydispersity index (PDI) and peak shapes of P2 were determined by SEC analysis. The SEC trace of PEG_{113}-S_2-$PFOEMA_{12}$-*b*-$PCEMA_{60}$ shown in Figure 3.4, consisted of a single and monomodal peak that eluted at 25.5 min. The polydispersity index (M_w/M_n) and M_w in terms of PS standards were 1.15 and 41,170 g/mol, respectively, as shown in Table 3.1. SEC analysis also revealed the purity of P2 from PEG_{113}-SH, which was initially used in excess.

Figure 3.9 shows the ^{1}H NMR spectrum of PEG_{113}-S_2-$PFOEMA_{12}$-*b*-$PCEMA_{60}$ along with peak assignments for each proton. Comparison of the integration of the PEG main chain protons at ~3.8 ppm to that of the PCEMA alkene protons observed at ~6.7 ppm was performed to determine the relative lengths of the PEG and PCEMA chains. Consideration of the

manufacturer's molecular weight of 5,000 g/mol for PEG indicated that the PEG and PCEMA blocks had repeat unit numbers of 113 and 60, respectively.

Table 3.1 provides a summary of the detailed characteristics of PEG_{113}-SH, Py-S_2-$PFOEMA_{12}$-*b*-$PHEMA_{60}$, and P2. These calculations are based on SEC and ^{1}H NMR analysis. The diblock Py-S_2-$PFOEMA_{12}$-*b*-$PHEMA_{60}$ copolymer has a wider distribution (1.2) than that of the triblock copolymer P2 (1.15). This decrease in the polydispersity of the triblock copolymer P2 is attributed to the subsequent attachment of the narrowly distributed homopolymer PEG_{113}-SH (1.05) to the diblock copolymer. The calculations based on SEC and ^{1}H NMR analysis are in agreement that the PEG/PFOEMA/PCEMA blocks have a respective repeat unit ratio of 113/12/60.

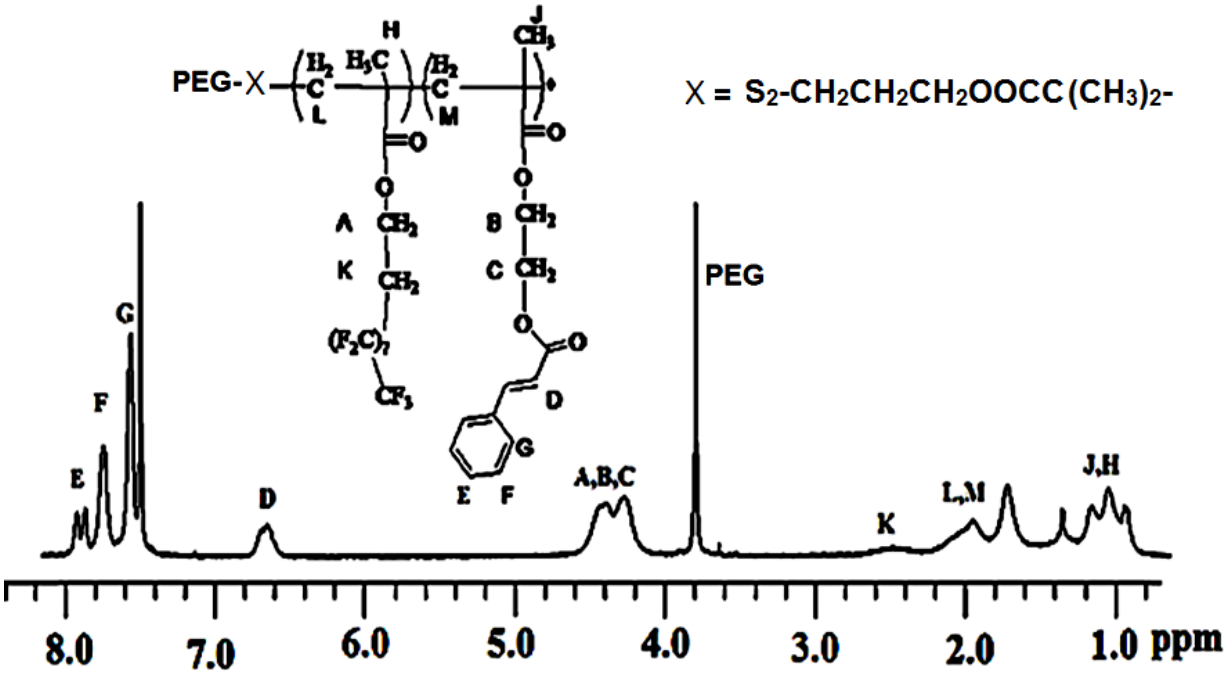

Figure 3.9. ^{1}H NMR (500 MHz, $CDCl_3$) spectrum of P2, with labelled peaks.

Table 3.1. Characterization of P2 and its precursors at various stages of the preparation.

Sample	M_w[a] (g/mol)	M_w/M_n[a]	$l/m/n$[b]	M_n[b]	l	m	N
PEG$_l$-SH	14,000	1.05		5,000[c]	113		
Py-S_2-PFOEMA$_m$-*b*-PHEMA$_n$-Br	24,480			13,120		12	60
Py-S_2-PFOEMA$_m$-*b*-PCEMA$_n$-Br	30,200	1.20		21,800		12	60
PEG$_l$-S_2-PFOEMA$_m$-*b*-PCEMA$_n$	41,170	1.15	113/12/60	26,800	113	12	60

[a]: Determined via SEC analysis in DMF.
[b]: Determined via ^{1}H NMR analysis.
[c]: Calculations based on the supplier's nominal molecular weight of 5,000 g/mol for PEG.

3.4.7 Synthesis of PEG$_{113}$-S_2-PFOEMA$_{10}$-*b*-PCEMA$_{20}$ (P3)

To further exploit this facile synthetic strategy for the preparation of doubly stimulable triblock copolymers, PEG$_{113}$-S_2-PFOEMA$_{10}$-*b*-PCEMA$_{20}$ (P3) was also synthesized. This P3 copolymer is similar to P2, except that it has shorter PFOEMA and PCEMA blocks. To prepare this copolymer, Py-S_2-PFOEMA$_{10}$-*b*-PHEMA$_{20}$ was initially synthesized by sequential ATRP. During the next step, Py-S_2-PFOEMA$_{10}$-*b*-PHEMA$_{20}$ was reacted with PEG$_{113}$-SH to yield the triblock copolymer PEG$_{113}$-S_2-PFOEMA$_{10}$-*b*-PHEMA$_{20}$. Upon cinnamation, the targeted doubly stimulable triblock copolymer P3 was obtained. Figure 3.10 shows combined SEC plots, including traces for P3, along with its precursors Py-S_2-PFOEMA$_{10}$-*b*-PHEMA$_{20}$ and PEG$_{113}$-SH. Peaks corresponding to the precursors PEG$_{113}$-SH and Py-S_2-PFOEMA$_{10}$-*b*-PCEMA$_{20}$ appeared at 28.0 and 28.4 min, respectively. The retention time for P3 was ~26.5 min, while the PDI was found to be 1.20 and M_w was 24,800 g/mol. ^{1}H NMR and SEC data established that P3 possessed PEG, PFOEMA and PCEMA blocks with 113, 10 and 20 repeat units, respectively. The characteristic features of P3 and its precursor determined by SEC and H NMR analysis are summarized in Table 3.2.

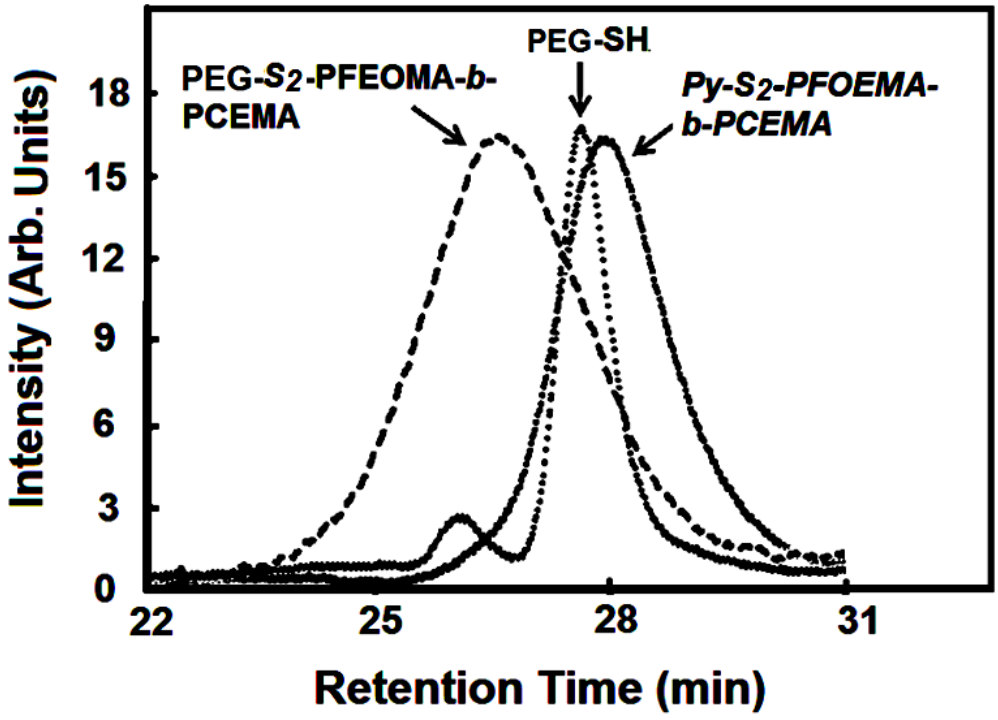

Figure 3.10. SEC traces for PEG_{113}-S_2-$PFOEMA_{10}$-*b*-$PCEMA_{20}$ (P3), PEG_{113}-SH, and Py-S_2-$PFOEMA_{10}$-*b*-$PCEMA_{20}$.

Table 3.2. Molecular properties of P3 and its precursors at various stages of the preparation.

Sample	M_w[a] (g/mol)	M_w/M_n[a] (PDI)	*l*/*m*/*n*[b]	M_n[b]	*l*	*m*	*n*
PEG_l-*SH*	14,000	1.05		5,000[c]	113		
Py-S_2-$PFOEMA_m$-*b*-$PHEMA_n$-Br				7,800		10	20
Py-S_2-$PFOEMA_m$-*b*-$PCEMA_n$				10,500		10	20
PEG_l-S_2-$PFOEMA_m$-*b*-$PCEMA_n$	24,800	1.20	113/10/20	15,500	113	10	20

[a]: Determined via SEC analysis.
[b]: Determined via ^{1}H NMR analysis.
[c]: Calculations based on the supplier's nominal molecular weight of 5,000 g/mol for PEG.

3.4.8 Reductive Cleavage of P2 and P3

It has been previously established that DTT induces disulfide bond cleavage at room temperature. Thus, P2 was dissolved in DMF and DTT was subsequently added to the P2 solution. The cleavage of P2 was analysed by SEC, as shown in Figure 3.11. Prior to DTT treatment, the SEC trace of a P2 solution displayed a single peak at an elution time of 25.5 min. After reaction with DTT, the triblock copolymer P2 had completely ruptured into two separate fragments. The SEC signal at ~28 min corresponded to the cleaved PEG_{113}-SH block, while the signal for HS-$PFOEMA_{12}$-*b*-$PCEMA_{60}$ appeared at 26.1 min.

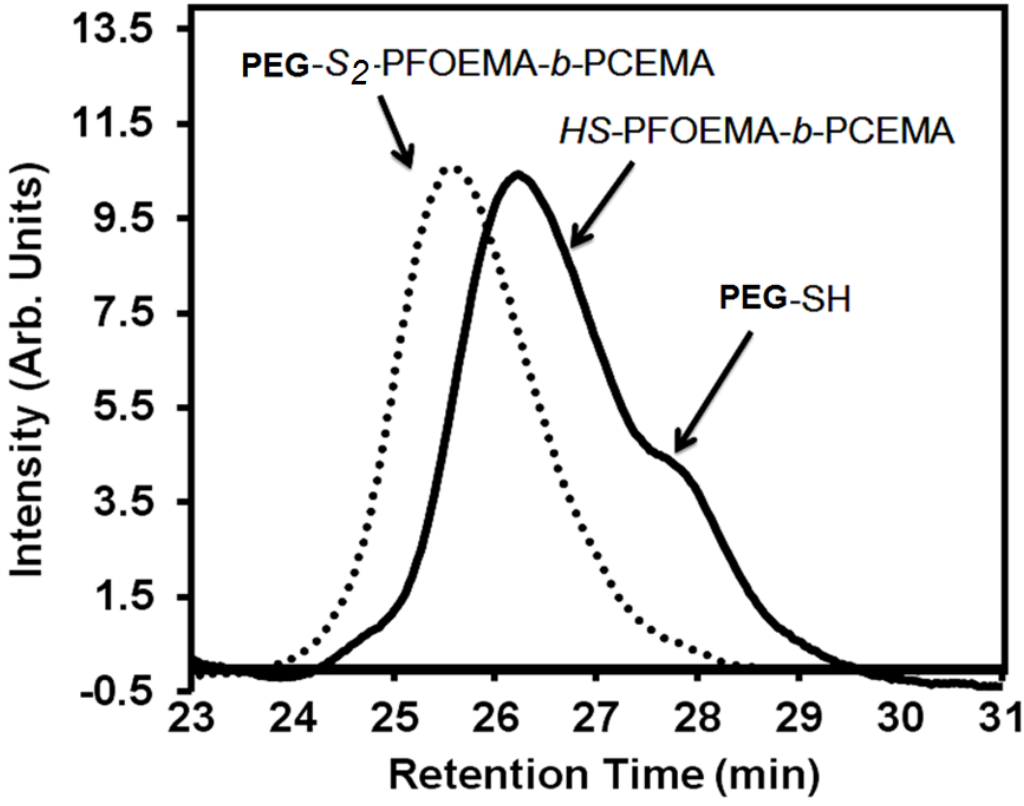

Figure 3.11. SEC plots of a P2 solution (in DMF) recorded before (dotted line) and after (solid line) DTT addition. After 3 h of reaction with DTT, the disulfide bond had been cleaved. Signals corresponding to PEG_{113}-SH and HS-$PFOEMA_{12}$-*b*-$PCEMA_{60}$ are also visible.

A further confirmation that the peak eluting at 26.1 min corresponded to HS-PFOEMA$_{12}$-*b*-PCEMA$_{60}$ was obtained through the SEC analysis of Py-*S*$_2$-PFOEMA$_{12}$-*b*-PCEMA$_{60}$. Therefore, the cinnamation of the diblock copolymer Py-*S*$_2$-PFOEMA$_{12}$-*b*-PHEMA$_{60}$ was firstly performed with cinnamoyl chloride to yield Py-*S*$_2$-PFOEMA$_{12}$-*b*-PCEMA$_{60}$. The SEC traces of Py-*S*$_2$-PFOEMA$_{12}$-*b*-PHEMA$_{60}$ and of Py-*S*$_2$-PFOEMA$_{12}$-*b*-PCEMA$_{60}$ were recorded, as shown in Figure 3.12. Both Py-*S*$_2$-PFOEMA$_{12}$-*b*-PCEMA$_{60}$ (obtained by cinnamation of Py-*S*$_2$-PFOEMA$_{12}$-*b*-PHEMA$_{60}$) and HS-PFOEMA-*b*-PCEMA (formed by the cleavage of P2) exhibited an identical retention time of 26.1 min, thus confirming the successful cleavage of P2.

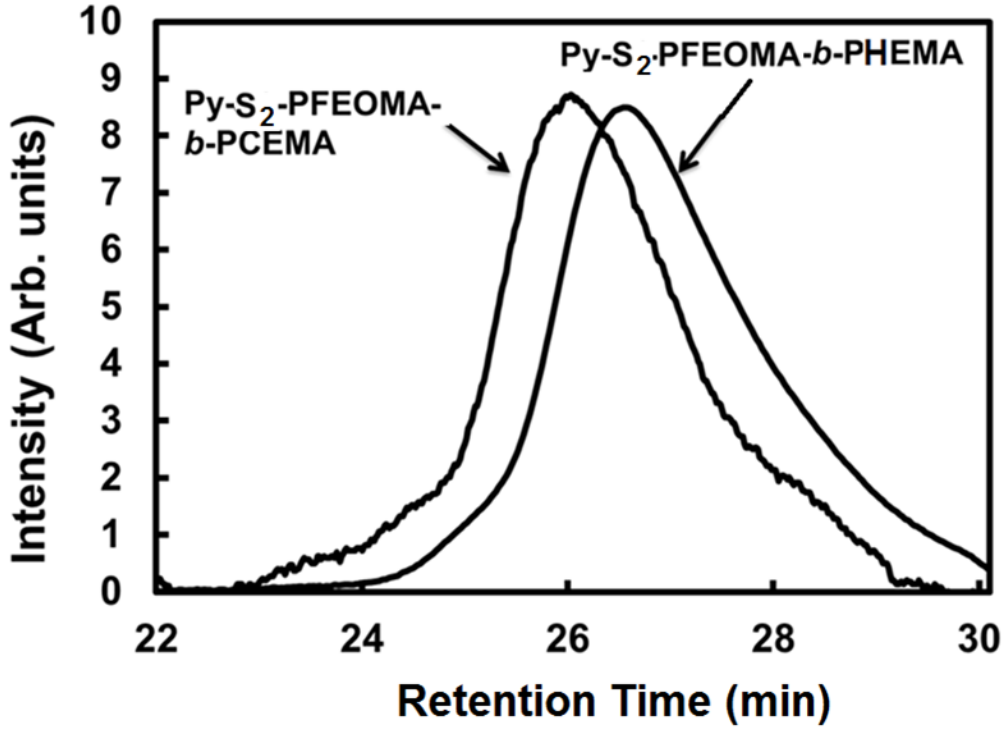

Figure 3.12. SEC traces of Py-*S*$_2$-PFOEMA$_{12}$-*b*-PHEMA$_{60}$ and Py-*S*$_2$-PFOEMA$_{12}$-*b*-PCEMA$_{60}$. The samples were recorded using DMF as the eluent at a flow rate of 0.9mL/min

Similarly, the stimuli-responsive properties of P3 were also examined by reaction of the triblock copolymer with DTT. SEC traces recorded during the cleavage test are shown in Figure

3.13, and demonstrate the successful cleavage of the PEG block from P3. Despite using a higher sample concentration of 20 mg/mL for the SEC analysis, the SEC traces of P3 still appeared noisy. This might be due to the higher PFOEMA content incorporated into P3, since PFOEMA has a smaller refractive index than the DMF eluent.

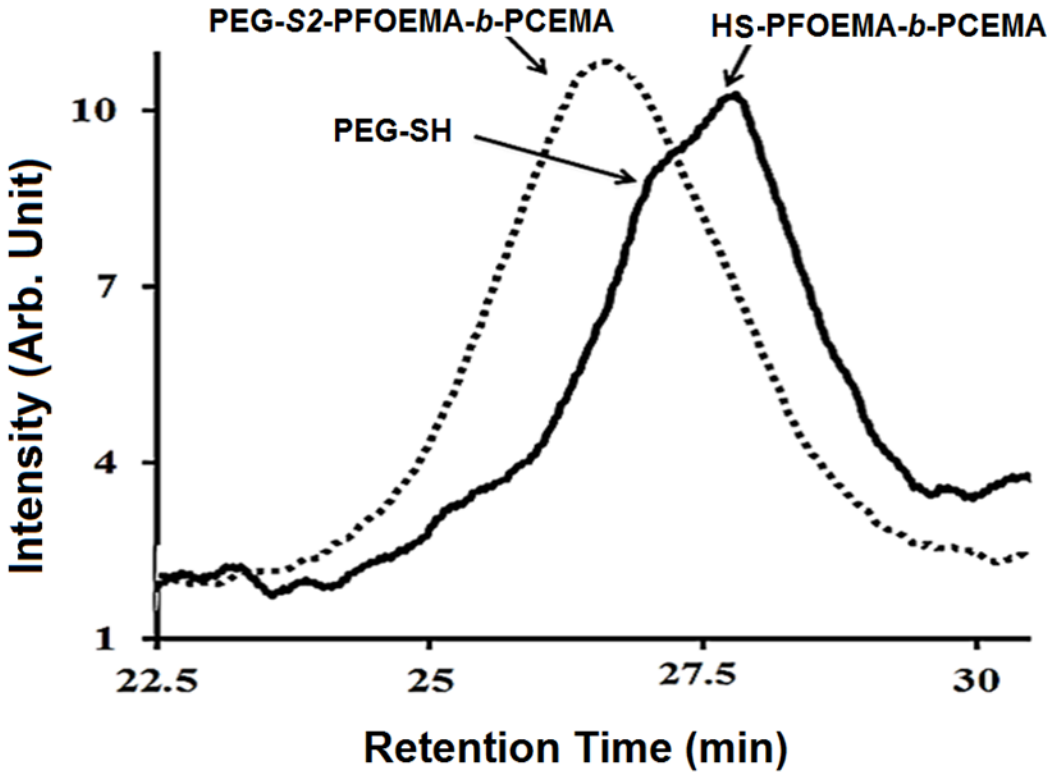

Figure 3.13. SEC traces of P3 before (dotted line) and after (solid line) reaction with DTT. The samples were recorded using DMF as the eluent.

3.4.9 Micellization of P2

Micelle formations by P2 in THF/water mixtures were studied. Firstly, P2 was dissolved in THF, which was a good solvent for all three blocks. PEG and PFOEMA were soluble in THF because of the low molecular weights utilized in P2. Water was slowly added (7-8 drops/min) as a selective solvent for PEG until f_{H2O} reached 80%. This solvent mixture yielded micelles

with PEG forming the corona, while PFOEMA and PCEMA formed the shell and core, respectively.

The P2 micelles were visualized via atomic force microscopy (AFM) and TEM analysis. For this purpose, specimens for AFM analysis were prepared by the aero-spraying the micellar solutions onto freshly-cleft mica surfaces using a home-built device. Aero-spraying of the sample helped to avoid morphological transitions during specimen preparation because of the fast evaporation of the solvent. Under these conditions, THF should have evaporated as it travelled from the spraying nozzle toward the silicon wafer. Meanwhile, water should have evaporated within ~3 s after the landing of the atomized aqueous droplets. Similarly, TEM samples were prepared by aero-spraying the micellar solutions onto thin films of cellulose supported copper grids. Before TEM analysis was performed, the specimens were stained with OsO_4, a selective staining agent for the PCEMA domains.

Figure 3.14a and 3.14b shows AFM height and TEM images of aero-sprayed P2 micelles at f_{H2O} = 80% in water/THF. P2 formed spherical micelles at this solvent composition. The average AFM diameter of these micelles was 60 ± 2 nm, while the average TEM diameter was 32 ± 3 nm. The AFM images (Figure 3.14a) revealed that the micelles possessed a uniform distribution. Meanwhile, a relatively broader distribution of the P2 micelles was observed in the TEM image (Figure 3.14b). For example, the TEM image showed the presence of some larger particles (highlighted with a white arrow in Figure 3.14b) that exceeded the average size of the micelles. Only core-shell particles will display a dark solid center after selective staining of the core-forming PCEMA block. Therefore, our suspicion is that the particles observed in the TEM image were core-shell-corona spherical micelles, where PCEMA, PFOEMA, and PEG formed the core, shell, and corona, respectively. Also, the AFM diameter was larger than the TEM diameter because AFM probed the whole particle including the PEG and PFOEMA layers in

addition to the core. Meanwhile, TEM only probed the OsO_4-stained PCEMA core. In addition, the AFM diameter was likely influenced by contributions from the finite size of the AFM tip. Evidently, spherical particles with core-shell-corona structures were obtained based on AFM and TEM studies. We also believe that the larger particles observed in the TEM image with an average diameter of 44 ± 2 nm are also core-shell-corona particles, because of their dark PCEMA core. These larger particles were not observed in the AFM image. However, this aspect is beyond the scope of the current investigation, but could be the subject of a future study.

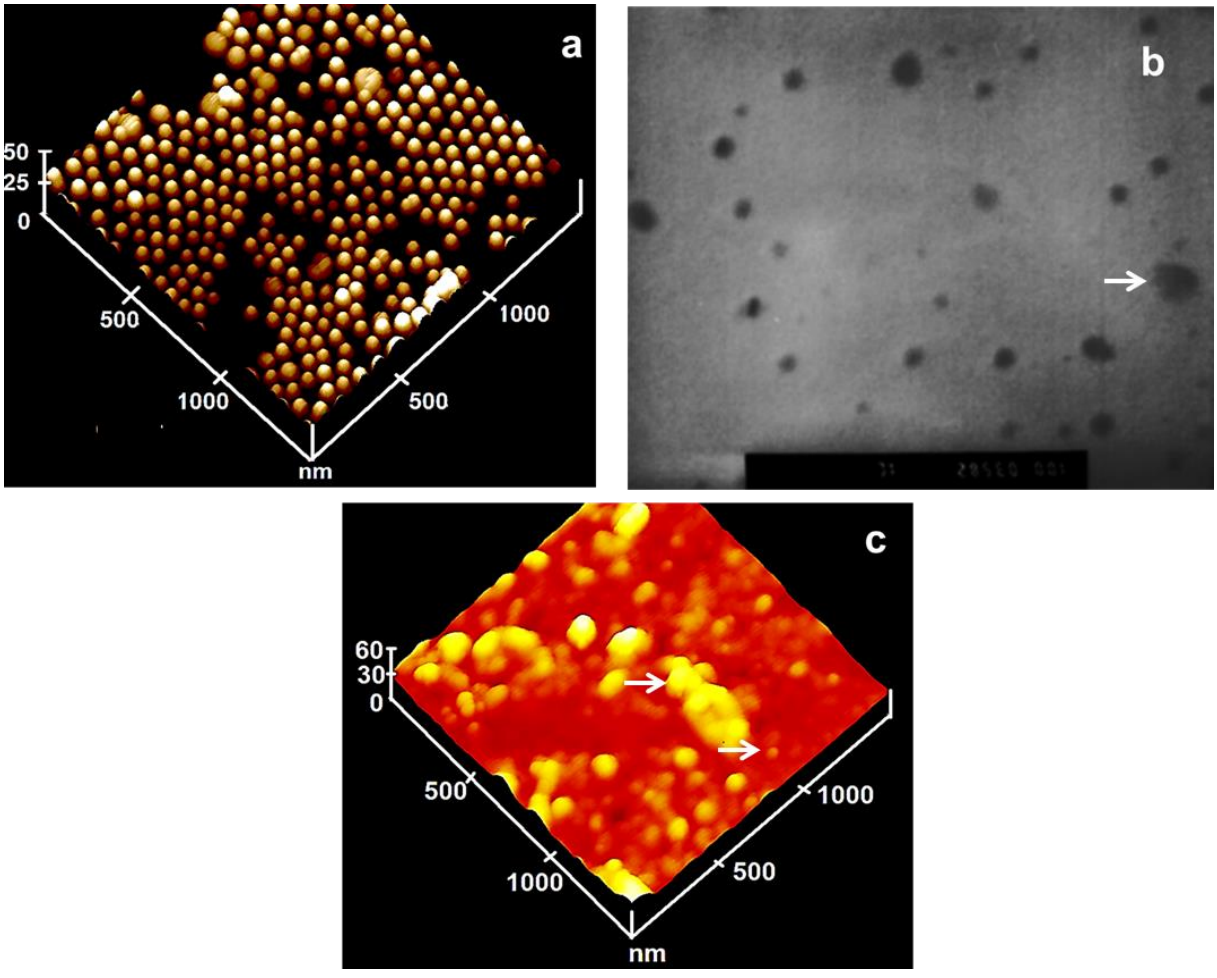

Figure 3.14. AFM topography (a) and TEM (b) images of P2 micelles obtained from a THF/water solution at f_{H2O} = 80%. An AFM topography image recorded after the P2 micelles underwent crosslinking and PEG-cleavage is also shown (c). The arrow in image (b) highlights a larger particle. The upper arrow in image (c) highlights an aggregate of smaller particles, while the lower arrow in that image highlights an individual particle.

3.4.10 Micellar Crosslinking and Coronal Chain Cleavage

PCEMA chains are crosslinkable due to the dimerization of CEMA units from different polymer chains.[45] To prepare stable nanoparticles with a crosslinked PCEMA core, the micellar solutions of P2 and P3 were photo-crosslinked in THF/water mixtures at f_{H2O} = 80%, as shown in Scheme 3.7. UV light was generated by a high-pressure mercury lamp that was passed through a 270 nm cut-off filter, since λ_{max} of PCEMA is 274 nm.[45] A focused UV beam was shined on the micellar P2 and P3 dispersions. Upon irradiation, initially clear P3 dispersions became turbid within ~10 min and this turbidity increased with further irradiation. This behaviour is partially attributed to disulfide bond cleavage upon exposure to UV light.[51] However, P2 dispersions did not show obvious turbidity upon irradiation with the UV beam. We believe that the longer PCEMA chains of P2 absorbed most of the light and thus shielded the disulfide bonds from the UV beam. After irradiation, the residual THF/water solvents were removed under vacuum before anhydrous DMF was added. The addition of DTT induced disulfide bond cleavage, thus causing the crosslinked particles to get rid of PEG chains. Meanwhile, the solution became turbid due to the loss of the corona-forming PEG chains. DMF was removed from the crude mixture and methanol was added to wash away the cleft PEG chains from the precipitates. The crude HS-PFOEMA$_{12}$-*b*-PCEMA$_{60}$ or PEG-cleft particles were rinsed with methanol and subsequently centrifuged. The supernatant contained the cleaved PEG chains, while the crosslinked PEG-cleft particles settled as precipitates.

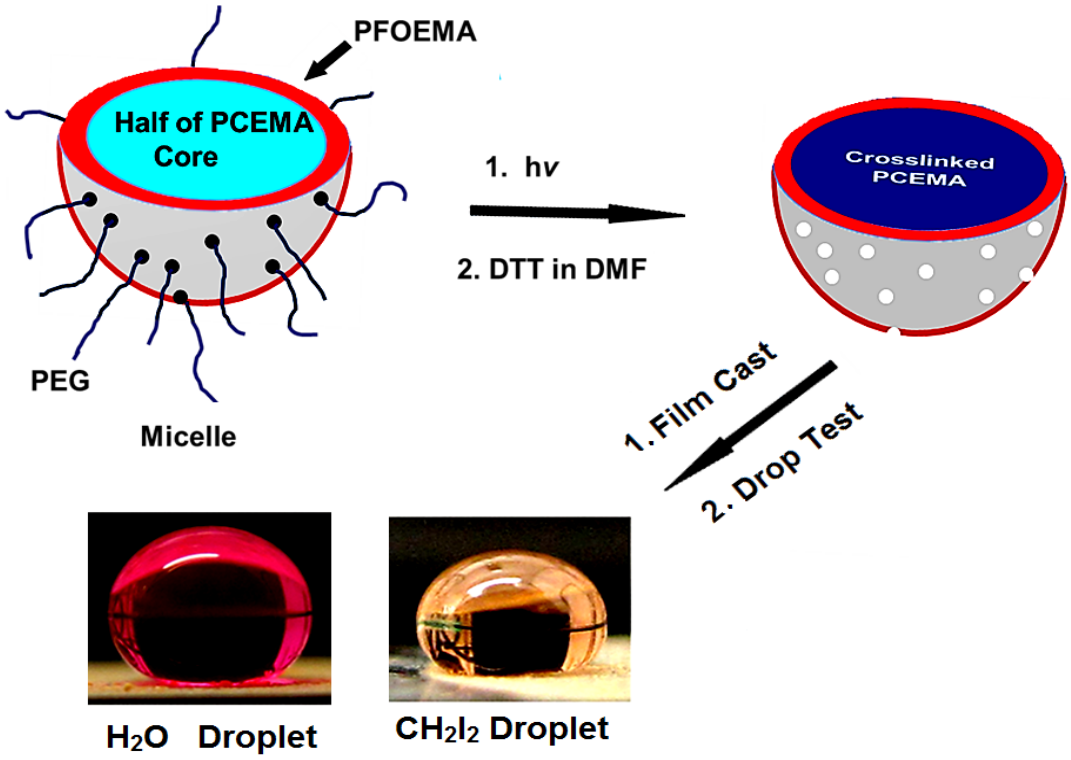

Scheme 3.7. Schematic representation of P3 micelles before and after crosslinking and DTT treatment. Water and diiodomethane droplets placed on a film cast from a dispersion of the PEG-cleft P3 particles are also shown.

3.4.11 PEG-Cleft Particles

The PEG-cleft particles were dispersed into $CDCl_3$ and aero-sprayed onto mica surfaces for AFM analysis. Figure 14c shows an AFM image of PEG-cleft P2 particles. Most of the particles were aggregates of smaller particles as highlighted with the top arrow in Figure 14c. The poor dispersibility of these particles strongly indicates that the particles are free of corona-forming PEG chains, which had provided dispersibility to their micellar precursors. However, some individual particles can also be seen in Figure 14c. The average AFM diameter of these individual particles was calculated as ~40 ± 5 nm. A decrease in the average AFM diameter for

the PEG-cleft particles (by ~20 nm) from that of the precursory P2 micelles (60 ± 2 nm) was observed that indicates the loss of PEG chains crosslinked particles.

We believe that the obtained PEG-cleft particles bear exposed PFOEMA chains on their surfaces that were initially masked by the PEG chains. ^{1}H NMR analysis (Figure 3.15) of the PEG-cleft particles obtained from P2 did not reveal any signals corresponding to the main PEG chain, which was otherwise observed at ~3.6 ppm before photolysis of P2. The absence of the PEG signal provided further evidence for the successful removal of the PEG chains from the crosslinked particles. Furthermore, proton signals for the pendent PCEMA protons normally observed between 4.0 and 5.0 ppm were absent due to crosslinking. However, very weak signals corresponding to the main chains of the PFOEMA and PCEMA blocks are visible, which are highlighted with the arrows shown in Figure 3.15.

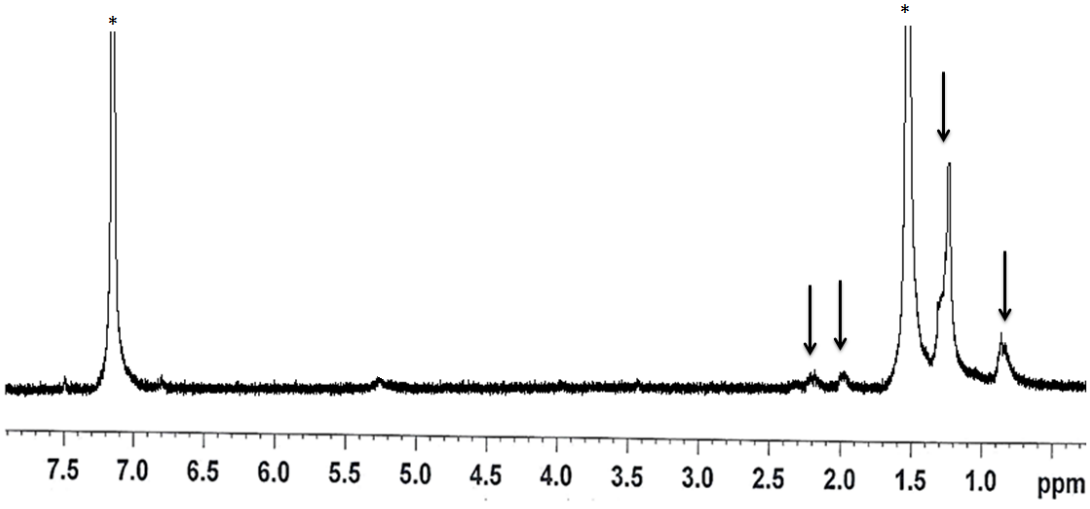

Figure 3.15. ^{1}H NMR (300 MHz in $CDCl_3$) spectrum of the PEG-cleft particles obtained from P2.

3.4.12 PEG-Cleft Particle Films

To probe the surface properties of these particles, films of the PEG-cleft particles were prepared using P2 and P3 as the precursors. For this purpose, PEG-cleft particles obtained from P2 and P3 were separately dispersed into trifluorotoluene (TFT) and applied onto glass surfaces. Droplet tests performed on films prepared from the PEG-cleft particles of P3 indicated that these films were highly water and oil repellent (Scheme 3.7). In particular, the contact angles of these films were 146 ± 3° and 133 ± 3° for water and diiodomethane droplets, respectively. These higher water and oil-repellent properties indicates that the crosslinked particles have exposed PFOEMA chains on their surfaces and also the particulate films were rough.[52-54] The films cast from TFT dispersions of PEG-cleft particles obtained from P2 were also amphiphobic, providing contact angles of 130 ± 3° and 112 ± 3° for water and diiodomethane droplets, respectively. A weaker amphiphobicity of the P2-derived films in comparison with those derived from the P3 precursors can be attributed to the lower PFOEMA content in P2 as compared to in P3.

3.4.13 AFM Analysis of P3-Derived Films Cast onto Glass

Glass surfaces were coated with films of the photolyzed P3 particles. These films were prepared by adding droplets of TFT dispersions containing the crosslinked P3 particles onto the glass surface. Cast films of the photolyzed P3 particles were characterized via AFM to measure the roughness of these films that had been cast onto glass substrates. The mean roughness of the film was automatically calculated and was found to be ~84.2 nm for an area covering 2.0 μm × 2.0 μm, as shown in Figure 3.16.

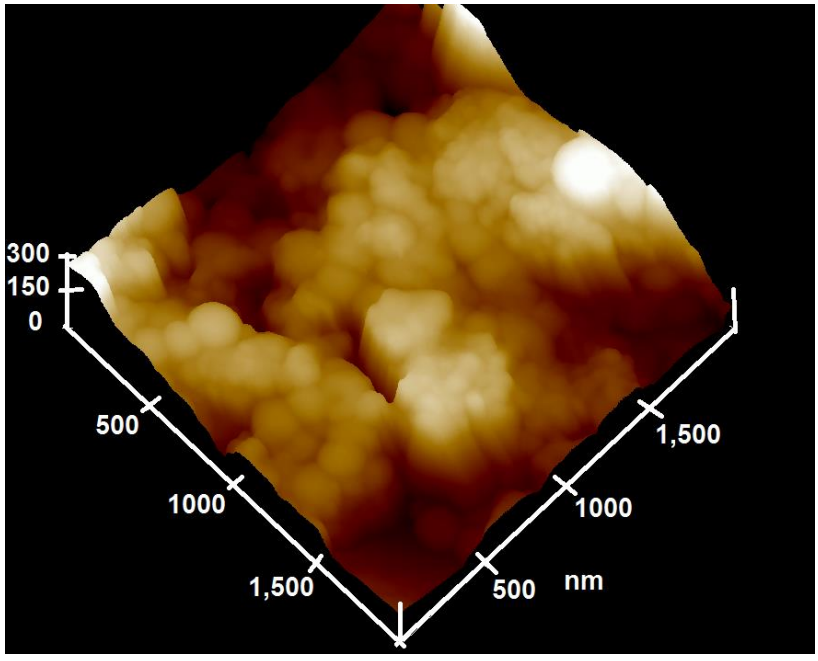

Figure 3.16. AFM analysis of glass surface coated with PEG-cleft P3 particles.

3.5 Conclusions

In this chapter, we report the facile synthesis of novel doubly stimulable P2 and P3 copolymers via ATRP and an end-coupling reaction. The structure and properties of the doubly stimulable copolymers PEG_{113}-*S*$_2$-$PFOEMA_{12}$-*b*-$PHEMA_{60}$ (P2) and PEG_{113}-*S*$_2$-$PFOEMA_{10}$-*b*-$PHEMA_{20}$ (P3) were determined via SEC and ^{1}H NMR analysis. The obtained triblock copolymers exhibited relatively low PDIs, such as 1.15 and 1.20 in terms of PS standards for P2 and P3, respectively. Spherical micelles of P2 were prepared in THF/water solutions at f_{H2O} = 80% and the micelles were characterized with AFM and TEM techniques. Micelles of P2 and P3 were crosslinked and their PEG corona chains were subsequently cleaved by the reducing agent DTT to expose the initially buried PFOEMA chains. Films cast from TFT dispersions of these particles rendered strong water and oil repellent properties.

3.6 References

1. Hu, J.; Liu. S. *Macromolecules,* **2010,** *43,* 8315.
2. de Silva, A. P.; Uchiyama, S.; Vance, T. P.; Wannalerse, B. *Coord. Chem. Rev.* **2007,** *251,* 1623.
3. de Las Heras, A. C.; Pennadam, S.; Alexander, C. *Chem. Soc. Rev.* **2005,** *34,* 276.
4. Qiu, Y.; Park, K. *Adv. Drug Delv. Rev.* **2001,** *53,* 321.
5. Mano, J. F. *Adv. Eng. Mater.* **2008,** *10,* 515.
6. Howse, J. R.; Topham, P.; Crook, C. J.; Gleeson, A. J.; Bras, W.; Jones R. A. L.; Ryan, A. J. *Nano Lett.* **2005,** *6,* 73.
7. Yerushalmi, R.; Scherz, A.; van der Boom, M. E.; Kraatz, H.B. *J. Mater. Chem.* **2005,** *15,* 4480.
8. Tokarev, I.; Minko, S. *Adv. Mater.* **2010,** *22,* 3446.
9. Olsen, B. D.; Segalman, R. A. *Mater. Sci. Eng.* **2008,** 62, 37.
10. Howarter, J. A.; Youngblood, J. P. *Adv. Mater.* **2007,** *19,* 3838.
11. Stratakis, E.; Mateescu, A.; Barberoglou, M.; Vamvakaki M.; Fotakis, C.; Anastasiadis, S. H. *Chem. Commun.* **2010,** *46,* 4136.
12. Pasparakis, G.; Vamvakaki, M. *Polym. Chem.* **2011,** *2,* 1234.
13. Dutta, N.K.; Truong, M.Y.; Mayavan, S.; Choudhury, N.R.; Elvin, C.M.; Kim, M.; Knott, R.; Nairn, K.M.; Hill, A.J. *Angew. Chem. Int. Ed.* **2011,** *50,* 4428.
14. Mart, R.J.; Osborne, R.D.; Stevens, M.M.; Ulijn, R.V. *Soft Matter.* **2006,** *2,* 822.
15. Howarter, J.A.; Youngblood, J.P. *Adv. Mater.* **2007**, *19,* 3838.
16. Liu, X.; Ye, Q.; Yu, B.; Liang, Y.; Liu, W.; Zhou, F. *Langmuir,* **2010,** *26,* 12377.
17. Schumers, J.M.; Fustin, C.; Gohy, J.F. *Macromol. Rap. Comm.* **2010,** *31,* 1588.

18. Guo, A.; Liu, G. J.; Tao, J. *Macromolecules,* **1996,** *29*, 2487.

19. Liu, G. J.; Qiao, L. J.; Guo, A. *Macromolecules,* **1996,** *29,* 5508.

20. Liu, G. J. *Adv. Polym. Sci.* **2008,** *220,* 29.

21. Njikang, G.; Liu, G.; Hong, L. *Langmuir*, **2011,** *27*, 7176.

22. Wyman, I.; Njikang, G.; Liu, G. *Progr. Polym. Sci.* **2011,** *36*, 1152.

23. Tao, J.; Stewart, S.; Liu, G. J.; Yang, M. L. *Macromolecules,* **1997,** *30,* 2738.

24. Stewart, S.; Liu, G. *Angew. Chem. Int. Ed.* **2000,** *39*, 340.

25. Chen, X.; Ding, X.; Zheng, Z.; Peng, Y. *New J. Chem*. **2006,** *30*, 577.

26. Liu, G.; Yan, X.H.; Li, Z.; Zhou, J. Y; Duncan, S. *J. Am. Chem. Soc.* **2003,** *125*, 14039.

27. a) Ding, J. F.; Liu, G. J. *Chem. Mater.* **1998,** *10*, 537. b) Stewart, S.; Liu, G. J. *Chem. Mater.* **1999,** *11*, 1048. c) Ding, J. F.; Liu, G. J. *J. Phys. Chem. B.* **1998,** *102*, 6107.

28. a) Han, D.; Tong, X.; Zhao, Y. *Langmuir,* **2012,** *28*, 2327. b) Sun. Y.; Yan, X. ; Yuan, T.; Liang, J.; Fan, Y.; Gu, Z.; Zhang, X. *Biomaterials,* **2010,** *31,* 7124.

29. Klaikherd, A.; Ghosh, S.; Thayumanavan, S. *Macromolecules,* **2007,** *40,* 8518.

30. Kang, M.; Moon, B. *Macromolecules,* **2009,** *42,* 455.

31. Johnson, J.A.; Lewis, D.R.; Az, D.D.D.U; Finn, M.G.; Koberstein, J.T.; Turro, N.J. *J. Am. Chem. Soc.* **2006,** 128, 6564.

32. a) Thambi, T.; Yoon, H. Y.; Kim, K.; Kwon, I.C.; Yoo, C. K.; Park, J.H. *Bioconjug. Chem.* **2011,** *22,* 1924. b) Tsarevsky, N. V., Matyjaszewski, K. *Macromolecules,* **2005,** *38*, 3087.

33. Lukesh, J. C.; Palte, M. J.; Raines, R. T. *J. Am. Chem. Soc.*, **2012,** *134*, 4057.

34. Khorsand, S. B.; Cunningham, A.; Zhang, Q.; Oh, J.K. *Biomacromolecules,*

2011, *12*, 3819.

35. Roth, P. J.; Boyer, C.; Lowe, A. B.; Davis, T.P. *Macromol. Rapid Commun.* **2011,** *32*, 1123.

36. Whittaker, M. R.; Goh, Y.K.; Gemici, H.; Legge, T. M.; Perrier, S.M.; Monteiro, M. J. *Macromolecules*, **2006,** *39*, 9028.

37. Xu, J.; He, J.; Fan, D.; Wang, X.; Yang, Y.; *Macromolecules,* **2006,** *39*, 8616.

38. a) Barner-Kowollik, C.; Davis, T. P.; Stenzel, M. H. *Aust. J. Chem.* **2006,** *59*, 719. b) Gao, H.; Matyjaszewski, K. *Prog. Polym. Sci.* **2009,** *34*, 317.

39. Klaikherd, A.; Nagamani, C.; Thayumanavan, S. *J. Am. Chem. Soc.* **2009,** *131*, 4830.

40. a) Wang, J. S.; Matyjaszewski, K. *J. Am. Chem. Soc.* **1995,** *117*, 5614. b) Matyjaszewski, K.; Xia, J. H. *Chem. Rev.* **2001,** *101*, 2921. c) Kato, M.; Kamigaito, M.; Sawamoto, M.; Higashimura, T. *Macromolecules,* **1995,** *28*, 1721.

41. a) Chiefari, J.; Chong, Y. K.; Ercole, F.; Krstina, J.; Jeffery, J.; Le, T. P. T.; Mayadunne, R. T. A.; Meijs, G. F.; Moad, C. L.; Moad, G.; Rizzardo, E.; Thang, S. H. *Macromolecules,* **1998,** *31*, 5559. b) Perrier, S.; Takolpuckdee, P. *J. Polym. Sci. A: Polym. Chem.* **2005,** *43*, 5347.

42. Marsat, J. N.; Heydenreich, M.; Kleinpeter, E.; Berlepsch, H. V.; Bottcher, C.; Laschewsky, A. *Macromolecules*, **2011,** *44*, 2092.

43. Li, K.; Wu, P. P.; Han, Z. W. *Polymer,* **2002,** *43*, 4079.

44. Xia, J. H.; Johnson, T.; Gaynor, S. G.; Matyjaszewski, K.; DeSimone, J. *Macromolecules*, **1999,** *32*, 4802.

45. Rabnawaz, M.; Liu, G. *Macromolecules,* **2012,** *45*, 5586.

46. Hirao, A.; Kato, H.; Yamaguchi, K.; Nakahama, S. *Macromolecules*, **1986,** *19*, 1294.

47. Tewari, N.; Hashim, N.; Avinash, M.; Vinoid, G..; Mohan, P. *Synth. Commun.* **2006,** *36*, 1911.

48. Bontempo, D.; Heredia, K. L.; Fish, B. A.; Maynard, H. D. *J. Am. Chem. Soc.* **2004,** *126*, 15372.

49. Ding, J. F.; Liu, G. J. *Macromolecules*, **1999,** *32*, 8413.

50. Witt, D. *Synthesis*, **2008,** 2491.

51. Wu, L.Z.; Sheng, Y.B.; Xie, J. B.; Wang, W. *J. Mol. Struct.* **2007,** *882*, 101.

52. Xiong, D.; Liu, G. J.; Hong, L. Z.; Duncan, E. J. S. *Chem. Mater.* **2011,** *23*, 4357.

53. Xia, F.; Jiang, L. *Adv. Mater.* **2008,** *20*, 2842.

54. Xiong, D.; Liu, G. J.; Zhang, J. G.; Duncan, S. *Chem. Mater.* **2011,** *23*, 2810.

Chapter 4 – Superhydrophobic and Oleophobic Cotton Coatings Prepared from Aqueous Micellar Solutions of Block Copolymers

4.1 Preface

The manuscript based on this research work is under preparation.

4.2 Introduction

The study of superhydrophobic surfaces, which are defined as surfaces that display contact angles greater than 150° for water droplets, has emerged as a very exciting area of research with many important applications such as corrosion-resistant coatings, self-cleaning surfaces.[1-8] It is well-established that the water- and oil-repellent properties of a surface depend on both its chemical composition and surface texture.[9-14] Consequently, the preparation of an oleophobic surface is more challenging due to the lower surface tension of oily substances than water at 25 ^{o}C.[15] For example, coatings adorned with long alkyl chains and roughly textured surfaces prepared via nanoparticle deposition have displayed superhydrophobic properties, but were not oleophobic.[16-17]

Cotton fabrics with water-proof properties have been studied since the 1930s.[18-19] However, in recent years, significant research attention has been focused on the fabrication of cotton fabrics that are both water- and oil-repellent.[8,20-25] Oleophobic surfaces are prepared via coatings of low surface energy materials, such as poly(perfluorinated) compounds, and blends of poly(vinyl phenol)/polybenzoxazine.[20-27] For example, copolymer consist of different poly(methacrylate) decorated with random fluorinated blocks,[28] and also fluorinated graft copolymers incorporating PAA[29] have been used for the preparation of superamphiphobic coatings. Recently, a block copolymer, poly(3-(triisopropyloxysilyl)propyl methacrylate)-*block*-

poly-(2-(perfluorooctyl)ethyl methacrylate) was used to prepare robust superamphiphobic cotton coatings.[20]

Generally, textiles are coated with fluorinated compounds by various methods. Common methods include electrospinning,[30] electrospinning in combination with chemical vaporization deposition,[31] sol-gel chemistry and condensation reactions,[20-21,32-33] plasma treatments,[34] sputtering techniques,[35] and the *in situ* growth of polymer chains from suitably functionalized textile surfaces.[36] However, some of these methods, such as the sputtering method, do not produce uniform coatings, and also require large amounts of polymer to generate superhydrophobicity. On the other hand, cotton coatings that are prepared via sol-gel chemistry can often display a uniform thickness as well as amphiphobic properties that can be achieved even with relative low polymer grafting densities (~1 wt.%).[20] However, if the sol-gel technique involves Si-O-Si bond formation, the resultant coating may be vulnerable to hydrolysis, and thus the coating may not be durable.

Micellar dispersions of block copolymers are used to form brush-like architectures on solid surfaces.[37-38] The preparation of brush-like architectures from block copolymers micellar solutions involves the adsorption of an insoluble block (the anchoring block) onto a solid support via van der Waals forces. Meanwhile, the corona-forming soluble chains acts as brush like bristles.[37-39] Although, PCEMA-based block copolymers have been used to coat glass surfaces with brush-like layers from block selective solvents where the PCEMA block was insoluble and acted as the anchoring block.[40-41] However, PCEMA has not been investigated as anchoring block for polymer grafting onto cotton. Similarly, there are no reports on the preparation of amphiphobic cotton coatings from aqueous polymer solutions. Also, the utilization of light, a clean and non-invasive method, to crosslink polymer coatings applied onto cotton has not been investigated.

In this chapter, we disclose a novel strategy to fabricate cotton from 100% aqueous solution using PEG-*ONB*-PFOEMA-*b*-PCEMA or P1. The PEG block of P1 is water soluble, and hence was used to prepare coating solutions in water. Meanwhile, the hydrophobic and crosslinkable PCEMA was used as an anchoring block that helped to prepare durable coatings. A light-sensitive *ONB* group is placed at the junction between the PEG and PFOEMA blocks, causing the PEG block to become cleaved from P1 upon exposure to light. Consequently, the PFOEMA chains became unmasked on the surface, and thus the cotton fabrics turned both water- and oil-repellent.

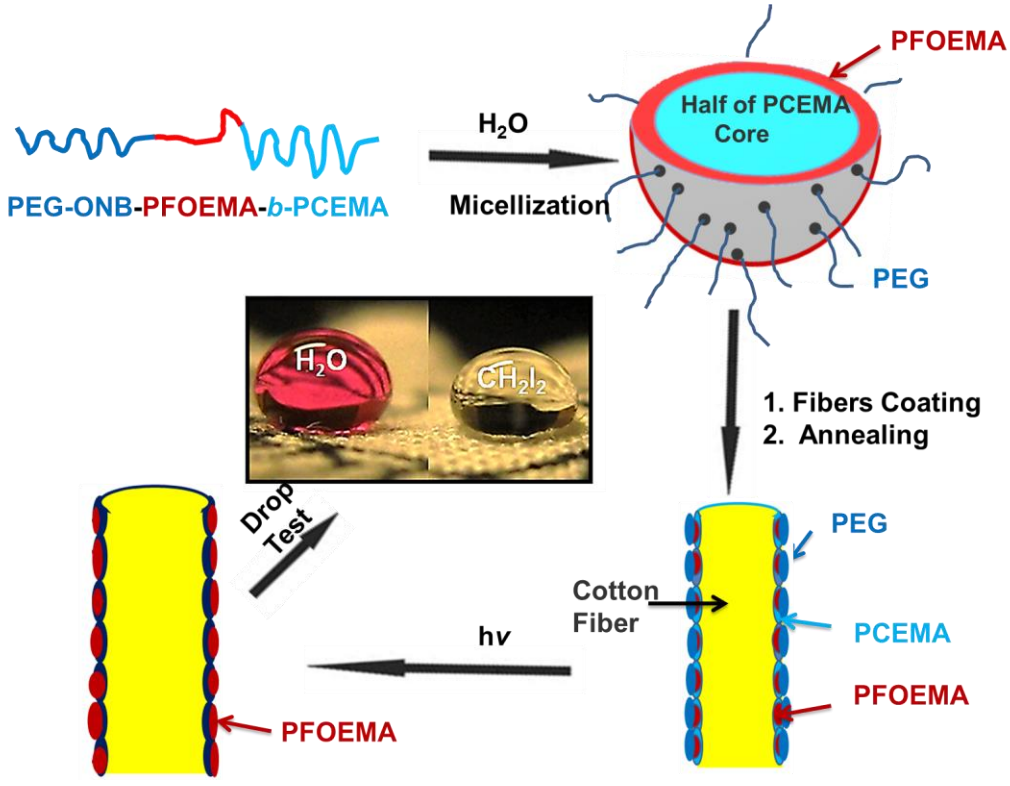

Scheme 4.1. Illustration of steps involved in the preparation of cotton coatings from micellar P1 solutions.

4.2.1 Objectives

The main purpose of this study was to develop a strategy for the preparation of stable amphiphobic cotton coatings from aqueous micellar block copolymer. This is the first approach for water- and oil-repellent cotton coatings from aqueous solutions. Also, PCEMA was examined for the first time as an anchoring block for attaching the copolymer chains onto cellulose fibers. This coating strategy is environmentally friendly, as the coating strategy involved aqueous micellar solution for the coatings. Both the crosslinking of PCEMA domains around the cotton fibers and the cleavage of PEG chains were driven by light, which is non-invasive, clean and environmentally benign method (stimulus).

4.2.2 Experimental Design Considerations

For the coating study, the micellar solutions of P1 were investigated. We selected P1 for this cotton coating study for numerous reasons. Firstly, P1 should form micelles in water because water selectively dissolves the PEG block. Secondly, PCEMA block is hydrophobic and thus will form compact chains in aqueous solution. These compact chains of the PCEMA block will be anchored onto the cotton fibers via photo-crosslinking. Also, light provides one of the least invasive and cleanest means to perform crosslinking. Finally, a photo-cleavable *ONB* unit placed at the junction between the PEG and PFOEMA blocks will become cleaved by exposure to light. Consequently, PFOEMA domains will become exposed after PEG cleavage to render superhydrophobicity and oleophobicity to the coated cotton samples.

4.3 Experimental

4.3.1 Materials

Plain-weaved cotton and semi-cotton textiles were purchased from a local vender and washed with detergents (Sparkleen) before use. Dimethyl phthalate (DMP, > 99%, Aldrich) and tetrahydrofuran were used as received. The preparation of PEG-*ONB*-PFOEMA-*b*-PCEMA (P1) was reported earlier in a different study that is described in Chapter 2, and P1 was used without any modification.[42]

4.3.2 Washing of the Blank Cotton Fabrics

Commercially available fabrics including cotton were cut into pieces of 27 cm × 27 cm and were soaked in a 5 wt.% detergent solution for 1 h. To remove the detergents after the soaking treatment, the fabric samples were washed with running water for 5-6 min and subsequently dried in an oven for 20-22 min at 120 ^{o}C.

4.3.3 Preparation of P1 Coating Solutions

P1 was dissolved in THF and stirred for 4-5 h. Subsequently, water was slowly added (7-8 drops/min) to the THF solution of P1 until the desired f_{H2O} value was reached. To prepare a P1 dispersion with f_{H2O} = 100%, initially a solution with f_{H2O} = 90% was prepared by the slow addition of water into a THF solution of P1. This was followed by the removal of the THF via gentle heating at 40 ^{o}C for 2 h. Dimethyl phthalate (DMP) was also added to certain coating solutions and stirred for at least 4 h before any coating treatment was performed.

4.3.4 Preparation of P1 Coating Solutions from Water/THF at Different f_{H2O}'s and Water/Ethanol at f_{H2O} at 5%

Standard solutions were prepared by dissolving P1 in THF and stirring the solution for 4-5 h. To achieve water/THF at different f_{H2O}'s, water was slowly added until the desired water fractions were achieved. Similarly, to prepare a water/ethanol solution at f_{H2O} at 5%, P1 was initially dissolved in THF and then ethanol (95 %, consisting of 5.0% water) was slowly added until the ethanol volume fraction ($f_{ethanol}$) reached 66%. THF was completely removed via evaporation at 40 °C, to leave behind a 5.0 mg/mL P1 solution in f_{H2O} at 5.0% in an ethanol/water mixture.

4.3.5 Preparation of Coating Solutions from P4, P5, and P6

Coatings were also prepared using the block copolymers PS-*b*-PCEMA (P4), P*t*BA-*b*-PCEMA (P5) and Py-S_2-PFOEMA-*b*-PCEMA (P6). The procedures involved with preparing solutions and coatings of P4, P5, and P6 are discussed in the Appendix A.

4.3.6 Coatings from P1 Solutions

Cotton samples (~1.0 cm^2) were soaked in aqueous solutions of P1 for various time intervals ranging from 2 to 90 min. These coated samples were taken out from the solution at the pre-designated time intervals and allowed to dry in the open atmosphere for 40 min before they were annealed for 20 min at 120 ^oC. The annealed samples were irradiated for 60 min on each side with a focused UV beam from a 500 W mercury lamp in an Oriel 6140 lamp housing powered by an Oriel 6128 power supply. The irradiated cotton samples were subsequently rinsed with water for 3 h. These samples were again dried at 120 ^oC for 20-25 min before contact angle measurements or any other analysis was performed.

4.3.7 UV Irradiation of the Cotton Samples

A focused beam generated by a 500 W mercury lamp placed in an Oriel 6140 lamp housing and powered by an Oriel 6128 power supply filter was shined onto the coated cotton samples. The cotton was held by a copper wire in the path of the focussed UV beam, and each side of a cotton sample was irradiated for ~60 min.

4.3.8 Durability Tests Against Washing

Three different pieces of coated fabrics were supported separately by copper wires and were forced to immerse into 50 mL of a 5.0 wt.% aqueous detergent solution contained in a 100 mL beaker. A magnetic stirring bar was used to stir the solution at 200 rpm. These samples were washed for different periods. After each washing cycle, the samples were removed from the aqueous detergent solution and then water was flushed over the samples for 5 min. The samples were dried for 25 min at 120 ^{o}C, before they were subjected to any contact angle measurements. The samples were subjected to numerous washing cycles over a total duration of 24 h.

4.3.9 SEM and AFM Analysis

A Philips XL-30 ESEM FEG instrument was used to obtain the scanning electron microscopy (SEM) images at 2 kV.[20] Two sets of samples were prepared for SEM and AFM analysis. One set was coated using an aqueous P1 solution, and the other set was coated from an aqueous P1 solution that also contained DMP. Both of these solutions had a final concentration of 5 mg/mL. In each case, cotton samples were equilibrated for 40 min. The coated samples were allowed to dry in the open atmosphere. Some of these samples were annealed at 120 ^{o}C. Both annealed and non-annealed samples were coated with gold and were analysed by SEM.

For AFM analysis, a coated cotton fiber was affixed onto a mica surface via double faced tape. AFM analysis was performed in the tapping mode using a Veeco multimode microscope equipped with a Nanoscope IIIa controller. (See Appendix B for AFM images).

4.3.10 Rinsing of Cleaved PEG Chains from Coated Samples

The crosslinked coated samples were forced to dip into water under constant stirring of 300 rpm at room temperature. Six rinsing cycles were performed of different period. During each cycle, the samples were rinsed with water and then dried in an oven for 25 min. Contact angles measurements were performed after each rinsing cycle. The sums of all rinsing cycles consist of 420 min.

4.3.11 Concentration Dependent Studies on Cotton Coating Performance

P1 (50.1 mg) was dissolved into THF (2.7 ml) by stirring the solution for 5 h at room temperature. Water was subsequently added drop wise to the THF solution until f_{H2O} = 70% was reached. DMP (5.0 mg) was added into the above solution and the solution was stirred for 20 min. This solution was distributed into six different vials. All of these solutions were placed in an oil bath at 50 ^{o}C. Consequently, six different solutions with final concentration ranging from 0.5 mg/mL to 20.0 mg/mL at f_{H2O} = 100% with 10 wt.% of DMP were obtained. All of these samples were stirred at room temperature for 4 h before any coating experiments were performed.

4.3.12 Contact Angle Measurements

Prior to contact angle measurements, the coated cotton samples were pressed using an auto-compressor for ~30 min to flatten the fabrics. Droplets of water (milli-Q with a surface

tension of 72.8 mN/m at 20 ^{o}C) and diiodomethane (>99%, Sigma-Aldrich, with a surface tension of 50.8 mN/m at 20 ^{o}C) were added onto coated samples as 5 µL droplets.[43] Images of these droplets were recorded after allowing the droplet to remain on the cotton sample for at least 2 min. For each contact angle measurements, an average of five different samples coated under identical conditions were used.

4.3.13 XPS Analysis

The surface chemical compositions of the coated and uncoated cotton samples were measured via X-Ray Photoelectron Spectroscopy (XPS). A Thermo Instruments Microlab 310F surface analysis system (Hastings, U.K.) was used following a literature method.[44] The samples for XPS analysis were prepared under standard conditions, in which coating solution concentrations of 5 mg/mL were used and each side of a coated samples was crosslinked for 1 h. Also, some of the samples were extracted with THF for at least 1 h before analysis.

4.3.14 TGA Characterization

A series of cotton fabrics were coated under standard conditions for the different periods of time and extracted with THF for 2 h before they were subjected to thermo gravimetric analysis (TGA). TGA experiments were performed using a TA Q500 Instrument. The samples were heated from room temperature to 600 °C at a rate of 10 ^{o}C/min, under N_2 atmosphere. During each TGA run, larger samples (~40-45 mg) of the samples were used to increase the accuracy of the measurements

4.4 Results and Discussion

4.4.1 Polymer Characteristics

In this study, P1 was primarily investigated for the preparation of cotton coatings under various conditions. The chemical structure of P1 is shown in Figure 4.1, while the molecular properties such as M_w, M_w/M_n, and the number of repeating units of each block of P1 are listed in Table 4.1. Other block copolymers used in this coating study included P4,[45] P5,[46] and P6 (Appendix A are also shown Table 4.1. (*Note:* The coating performance of P4, P5 and P6 are described in the Appendix A).

Table 4.1. Different polymers used in the coating studies

Polymer	M_w[a]	M_w/M_n	Number of repeating units
PEG-*ONB*-PFOEMA-*b*-PCEMA (P1)	16,500 g/mol	1.10	113/12/25
PS-*b*-PCEMA (P4)	36,100 g/mol	1.04	270/30
PtBA-*b*-PCEMA (P5)	48,100 g/mol	1.08	220/75
PFOEMA-*b*-PCEMA (P6)	16,000 g/mol	1.2	12/60

a: M_w were calculated based on SEC analysis.

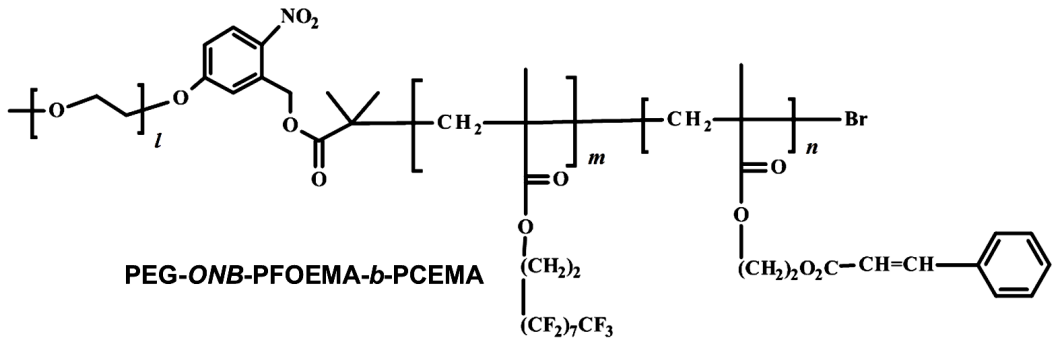

Figure 4.1. Chemical structure of P1.

4.4.2 Criteria for Selecting Polymers for the Coating Studies

In this study, PCEMA was chosen as an anchoring block, while PFOEMA was selected as a water- and oil-repellent block. In this new coating strategy, a desirable anchoring block should meet a number of requirements. Firstly, it must be crosslinkable to allow the copolymer chain to become firmly anchored onto the cotton fibers. Secondly, it must be insoluble in water and thus form collapsed chains in an aqueous medium so that the copolymer becomes adsorbed onto the fibers via the hydrophobic effect. Additionally, an anchoring block must occupy a terminal position in the copolymer chain to facilitate the direct contact of the collapsed anchoring block with cotton fibers. PCEMA meets all of these requirements. For example, PCEMA chains incorporate C=C functionalities that undergo [2+2] cycloaddition reactions upon exposure to light, and are thus photo-crosslinkable. Also, the PCEMA pendant groups consist of a hydrocarbon chain and an aromatic ring, and hence are hydrophobic. Additionally, as stipulated above, P1 incorporated a terminal PCEMA block.

Similarly, PFOEMA was strategically placed next to PCEMA, so that the perfluoroalkyl block should impart amphiphobic properties to the coated surface upon PEG cleavage. Meanwhile, the water-soluble PEG chains allowed dispersal of P1 into aqueous solution. The

placement of the photo-cleavable *ONB* unit at the junction of the PEG and PFOEMA blocks was a critical feature of P1. ONB group undergo rearrangement upon exposure to UV light. This arrangement yielded the cleavage of the PEG chains, thus leaving the PFOEMA chains exposed.

4.4.3 Preparation of Cotton Coatings and Assessment of their Properties

Various P1 coating solutions were prepared in various solvent systems including 100% aqueous solution (in both the presence and absence of DMP), water/THF (at various f_{H2O} compositions), and water/ethanol (at f_{H2O} = 5%). The cotton samples were immersed into the P1 dispersions and allowed to equilibrate for pre-designated time periods in the coating solutions. This equilibration allowed P1 become adsorbed onto the fibers as unimeric polymer chains and/or micelles, as shown in Scheme 4.1. These coated samples were then subjected to annealing at high temperature (120 ^{o}C) to facilitate the phase separation between the different blocks. Consequently, the initially collapsed PCEMA chains should form a smooth and uniform layer around a fiber after the annealing treatment. Similarly, PFOEMA chains will form an intermediate layer on the top of PCEMA layer, while the outermost layer will consist of PEG chains as shown in Scheme 4.1. Upon UV irradiation, PCEMA domains will become crosslinked around the fibers, and thus locked in place. Meanwhile, the *ONB* linker will undergo photo-cleavage, so that the PEG chains become separated from the copolymer. Consequently, upon subsequent rinsing the crosslinked PCEMA chains will remain firmly attached to the fiber, while the cleft PEG chains will be washed away to leave the PFOEMA domains exposed on the coated surfaces.

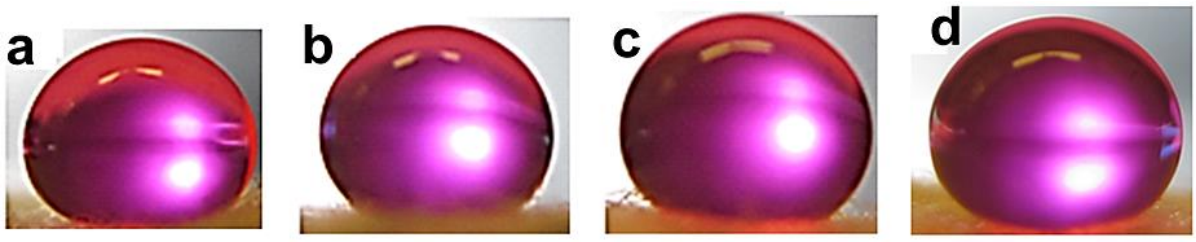

Figure 4.2. The images show water droplets that were placed on cotton samples that were coated with P1 using: (a) 100% aqueous solution (CA = 141 ± 1^{o}), (b) THF/water with f_{H2O} = 15 % (CA = 143 ± 1^{o}), (c) 95% ethanol (CA = 148^{o} ± 1^{o}), and (d) an aqueous DMP-containing solution (CA = 150 ± 1^{o}) as the dispersion solvent. The abbreviation CA refers to contact angles, while water droplets were impregnated with Rhodamine B for visual clarity.

Figure 4.2 shows images of water droplets that were placed on P1-coated cotton samples that were coated from various solvent systems. The water droplet tests showed that all of the coated samples were strongly hydrophobic. In addition, the sample coated with the aqueous P1 solution containing the DMP additive provided a contact angle that reached to 150^{o}, revealing its superhydrophobicity.

Besides the hydrophobic properties, droplet tests were also performed to screen the oleophobic properties of these samples. For this purpose, diiodomethane droplets were applied onto the coated samples and the contact angles were determined. The diiodomethane contact angles observed for P1-coated cotton samples that were prepared using 100% water, water/DMP, water/THF (at f_{H2O} = 15%), and water/ethanol (at f_{H2O} = 5%) as the solvent systems were 131 ± 1^{o}, 145 ± 1^{o}, 140 ± 1^{o}, and 141 ± 1^{o}, respectively. Due to better performance of the aqueous P1 solution incorporating the DMP additive, the contact angles of hexadecane (144 ± 1^{o}) and dichloromethane (137 ± 1^{o}) droplets were also tested for coatings prepared from this system.

4.4.4 Kinetics of P1-based Coatings from Different Solution Systems

The amphiphobic properties of cotton samples coated with P1 solutions utilizing various solvent systems were investigated and compared. These solvent systems included 100% water, water/DMP, water/THF (at f_{H2O} = 15%), and water/ethanol (at f_{H2O} = 5%). For comparison, coatings were first prepared from the above four solvent systems under identical conditions, with a P1 concentration of 5.0 mg/mL and 1 h of crosslinking treatment applied to each side of a given sample. The coated samples were rinsed with water to remove the cleaved PEG chains before the droplet tests. Figures 4.3 and 4.4 show the variation in contact angles for different coating solutions vs. equilibration time.

The contact angles observed among the samples coated from the P1 solution in 100% water for both H_2O and CH_2I_2 droplets are shown in Figures 4.3 and 4.4, respectively. It is apparent that the cotton samples immersed in the aqueous P1 solution for ~10 min were hydrophilic with 0.0 contact angles. As the soaking time was increased to 20 min, hydrophobicity began to appear. The contact angles continued to increase as the equilibration time was extended. The samples that were coated in the 100% aqueous solution for 100 min showed a water contact angle of 141 ± 1^o. Meanwhile, diiodomethane contact angles were also measured for the samples that were coated using the 100% aqueous system as shown in Figure 4.4. An essentially similar trend was observed during the diiodomethane droplet tests as was observed in the water droplet tests. For example, no oleophobicity was observed until the first 10 min of equilibration. However, after 20 min of immersion time the contact angles increased over the time. In general, the observed diiodomethane contact angles were lower than the corresponding water contact angles.

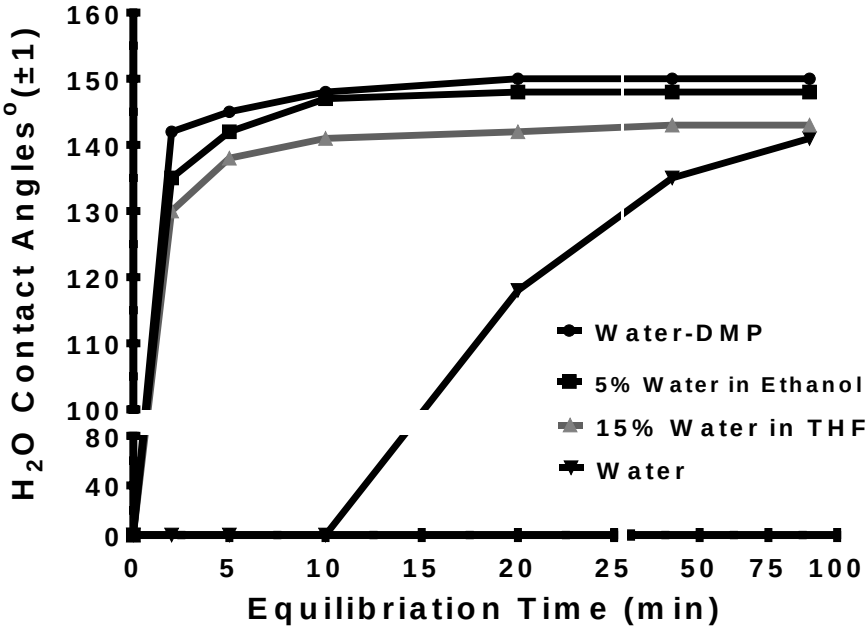

Figure 4.3. Water contact angles vs. equilibration time observed for P1 coatings prepared using 100% water, water/DMP, water/THF (at f_{H2O} = 15%), and water/ethanol (at f_{H2O} = 5%) as the solvent systems.

The contact angles of the P1 coatings prepared using water/THF at different f_{H2O}'s and water/ethanol at f_{H2O} = 5% were also measured. Interestingly, the water/THF system prepared at f_{H2O} = 15% provided moderate water- and oil-repellent properties after only ~2 min of immersion time, as shown in Figures 4.3 and 4.4. A further increase in the equilibration period, from 2 to 10 min, showed maximum contact angles of 143 ± 1° and 140 ± 1°, for water and diiodomethane droplets, respectively. However, a further increase in the equilibration time within this solvent system did not show any enhancement in the contact angles. We also investigated the effect of increase in the water content above f_{H2O} = 15% on water and oil repellency. Upon increasing the water content in the P1 coating solution to f_{H2O} = 25%, an identical behaviour to that encountered at f_{H2O} = 15% was observed, specifically facile coating

with high contact angles. However, when f_{H2O} was increased to 32%, the resultant coatings exhibited diminished performance comparable to that encountered among the coatings prepared from the 100% aqueous solutions. For example, the coating was not stable after 24 h detergent washing.

Meanwhile, P1 coatings prepared using from water/ethanol solutions at f_{H2O} = 5% reached their maximum oil and water repellencies in ~5 min (Figures 4.3 and 4.4). The maximum contact angle for water was found to be 148 ± 1^{o} while that for diiodomethane was 141 ± 1^{o}. The short equilibration time required revealed that it was relatively facile to prepare P1 coatings from the water/THF (at f_{H2O} = 15%) and water/ethanol (at f_{H2O} = 5%) solvent mixtures with high organic solvent content. This behaviour suggested that P1 underwent a faster grafting process onto the cotton fibers in these solutions that might be due to faster micellar dissociation into their unimers caused by presence of organic solvent.[47] Thus, an increase in the organic solvent content in the coating solution increases the rate at which P1 forms a coating.

The remarkable rate at which coatings were obtained in solutions with higher organic solvent contents prompted us to investigate the role of plasticizers as additives for the P1 coating solutions. Plasticizers are known to enhance the chain mobility of a micelle's core-forming block, and thus might increase the micellar dissociation rate as well. To increase the chain mobility of the core- and shell-forming PCEMA and PFOEMA chains, respectively, DMP was chosen as a plasticizer. As DMP is hydrophobic in nature, thus it will preferentially accumulate at the PCEMA core in 100% aqueous solution and consequently impart greater chain mobility to the core.[48] Therefore, DMP-containing aqueous dispersions of P1 were prepared by initially preparing 100% aqueous P1 dispersions, and subsequently adding DMP at ~10 wt.%. The 100% aqueous dispersions were obtained by the removal of residual THF, which was initially used to

solubilize P1 before water addition. Therefore, it was necessary to ensure that any residual THF was completely removed from the system to obtain the best results. THF is miscible with both DMP and water, and thus may interrupt the accumulation of the plasticizers at the micellar core.

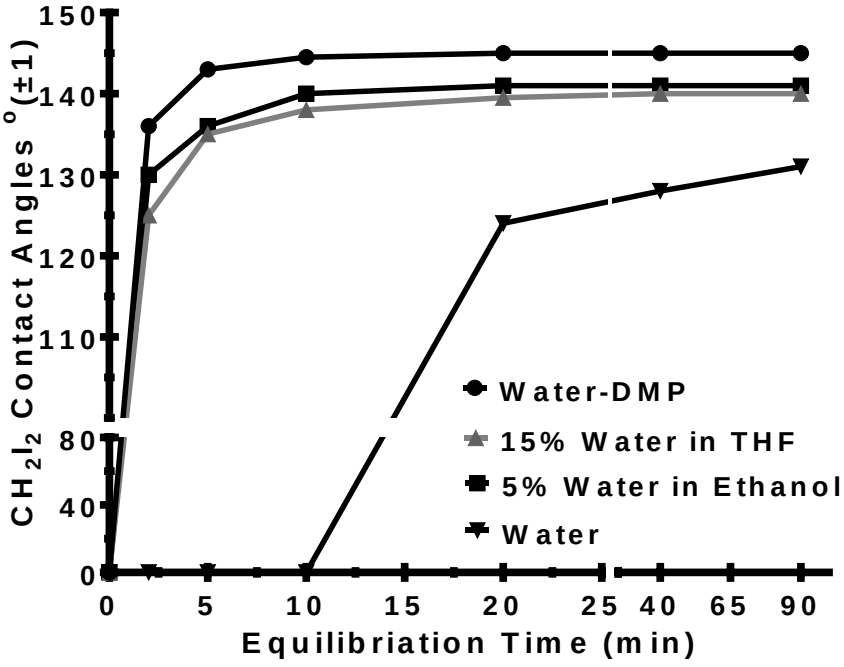

Figure 4.4. Plot of diiodomethane contact angles vs. equilibration time observed for P1 coatings prepared using 100% water, water/THF at f_{H2O} = 15%, water/ethanol at f_{H2O} = 5% and water/DMP as the solvent systems.

Cotton samples coated with 100% aqueous P1 dispersions containing DMP additives were photo-crosslinked and extracted with THF for 2 h prior to their examination via droplet tests. Figures 4.3 and 4.4 illustrate the variation of water and diiodomethane droplet contact angles vs. the coating time under standard coating conditions (5 mg/mL of P1 at room temperature). Data revealed that the largest improvements to the coating performance were witnessed during the first ~5 min of immersion in the DMP-containing coating solution.

Beyond 5 min of immersion in the coating solution, no significant increases in the contact angles were observed. In addition, the observed water droplet contact angles were very large 150 ± 1^{o}, indicating that the surfaces prepared using the DMP additive were superhydrophobic. Meanwhile, the diiodomethane droplet tests indicated that these surfaces were also strongly oleophobic 145 ± 1^{o}.

4.4.5 Coating Durability Tests against Washing

As textile fabrics are widely subjected to extensive laundry washing, the P1-coated samples stability under typical laundry conditions is very important for future applications. Therefore, the P1 coatings prepared from water, water/DMP, water/THF (at f_{H2O} = 15 %), and water/ethanol (at f_{H2O} = 5%) were washed with detergent to assess their durability. For washing purpose, the P1 coated samples were forcibly immersed into a 5 wt.% detergent (sparkleen) solution and gently stirred for various periods of time. Figure 4.5 depicts images of droplets placed on P1-coated samples that were prepared using various solvent systems. The images at the top and bottom were recorded before and after the washing treatment, respectively. P1-coated samples prepared from 100% aqueous solution lost their amphiphobic properties after the samples were washed with detergent wash for 24 h. Interestingly, the coatings prepared from the other three solvent systems remained stable, even after extensive washing of 24 h.

This stark contrast in the coating stabilities shows that only samples coated from 100% aqueous solutions lost the grafted P1, while P1 remained firmly attached to the fibers that were coated from the other solvent systems. This behaviour indicates that when 100% water was used, only physical grafting of P1 occurred, rather than covalent binding. A possible explanation for this behaviour is that P1 may have become adsorbed as micelles, rather than as unimers. Also, upon thermal annealing these micelles may not have dissociated very well for

uniform layer before the photo-crosslinking treatment. In such case, irradiation might cause PCEMA domains to undergo crosslinking within the micellar core, rather than directly on the surfaces of the cotton fibers. Consequently, these crosslinked micelles were easily removed from the coated surfaces during washing or extraction tests. On the contrary, the high resistance against washing exhibited by the other three systems strongly suggests that PCEMA underwent crosslinking around the fibers. This is only possible if unimeric P1 chains with collapsed PCEMA block, rather than micelles, are adsorbed onto the cotton, and crosslinked around the fiber.

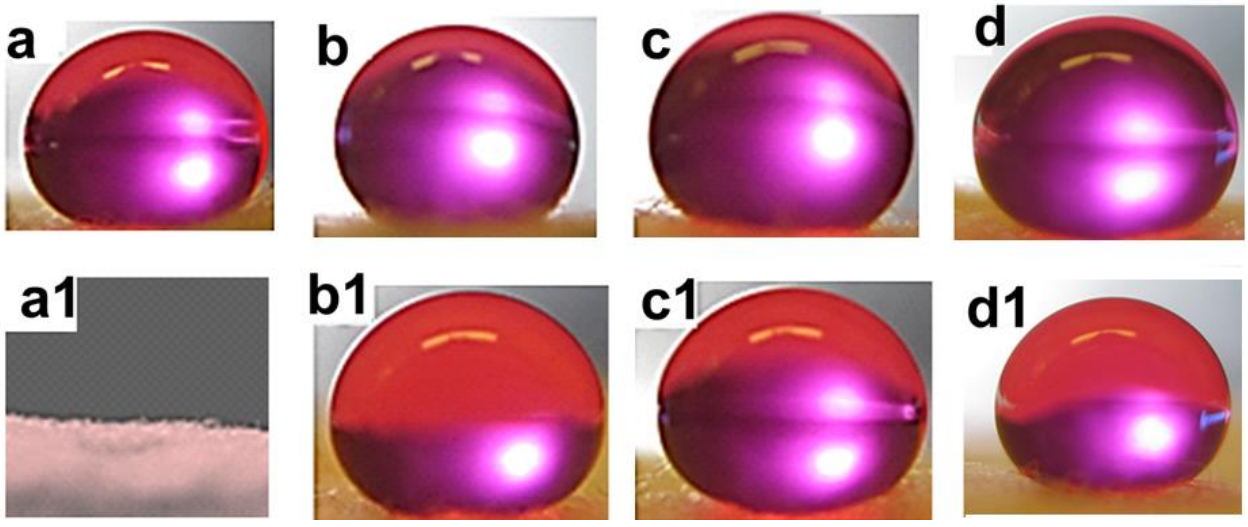

Figure 4.5. The images at the top show water droplets placed on cotton samples that were coated with P1 using (a) 100% aqueous solution (CA = 141 ± 1^{o}), (b) THF/water with f_{H2O} = 15 % (CA = 143 ± 1^{o}), (c) 95% ethanol (CA = 148 ± 1^{o}), and (d) water + 10 wt.% DMP (CA = 150 ± 1^{o}, d) as the dispersion solvent. The bottom images were recorded after 24 h washing cycles had been performed. They show water droplets placed on the washed cotton surfaces that were coated using (a1) 100% aqueous solution (CA = 0.0^{o}), (b1) THF/water with f_{H2O} = 15 %, (CA = 140 ± 1^{o}), (c1) 95% ethanol (CA = 144 ± 1^{o}), and (d1) water + 10 wt.% DMP (CA = 148 ± 1^{o}) as the P1 dispersion solvent.

A detailed study on the durability of the P1 coating from water + 10 wt.% DMP was performed and their water- and oil-repellent properties were recorded as shown in Figures 4.6A and 4.6B. Figure 4.6A shows two curves. One of these curves represents the water contact

angle measurements recorded before the cloth was washed; while the other curve represents measurements recorded after the samples had been washed for 24 h with detergent. A comparison between these curves revealed that only small decreases of less than 5^{o} in the contact angles for the water droplets was observed after washing. Also, the changes in diiodomethane contact angles after washing are shown in Figure 4.6B. Again, extensive washing resulted in a minor decrease in the contact angles for the diiodomethane droplets. Both the water and diiodomethane droplet tests exhibited similar trends upon washing. Our suspicion is that this small decrease in the contact angles may have been due to the detachment of weakly crosslinked P1 unimer chains from the cotton and the loss of physically adsorbed micelles. The stability of the P1 coating suggests that the presence of DMP in the system may have allowed P1 to become grafted to the cotton fibers as a uniform layer. Upon crosslinking, this uniform P1 layer became firmly attached to the fibers.

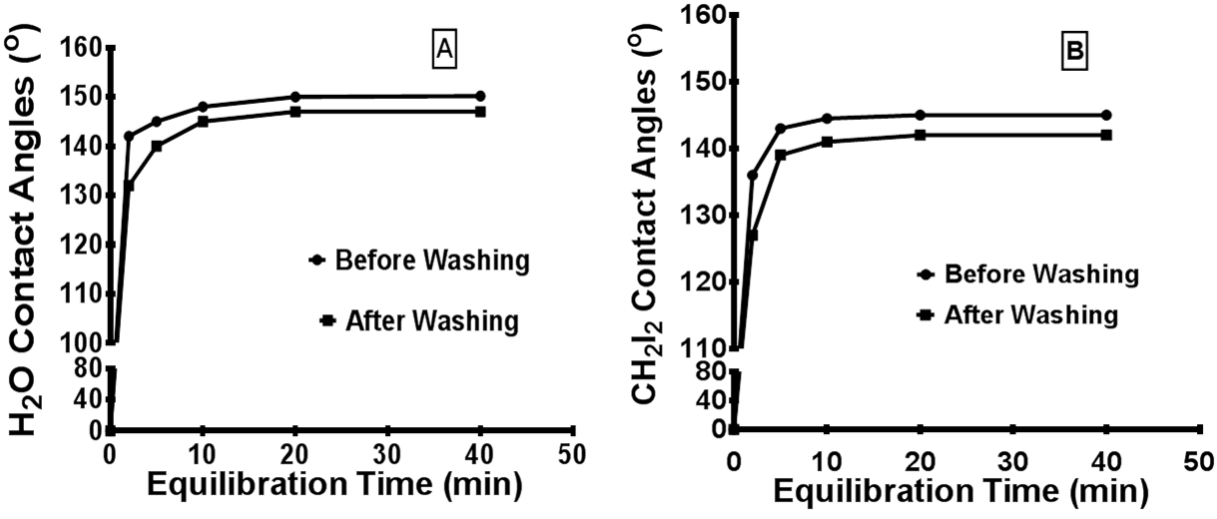

Figure 4.6. Plots comparing the contact angles of water (A) and diiodomethane (B) droplets placed on P1-coated cotton samples before and after washing treatment. These samples were coated using aqueous solutions of P1 containing the DMP additive (10 wt.%).

4.4.6 Reasons for the Poor Performance of the Coatings Prepared from Water

As mentioned above, a serious limitation of the coatings obtained from 100% aqueous P1 solutions was their instability against detergent washing. On the other hand, the P1 coatings prepared from the other three solvent systems, such as water/DMP, water/THF (at f_{H2O} = 15 %), and water/ethanol (at f_{H2O} = 5%), were remarkably stable. Additionally, the water- and oil-repellent properties in terms of their contact angles were also superior when these three systems were used. This prompted us to further investigate the coating formation mechanisms under different conditions. Thus, two systems were selected to be probed, one which exhibited poor performance and another in which the performance was very good. Therefore, SEM and AFM analysis was performed on coatings obtained for 100% aqueous solution (poor performance) and an aqueous solution containing the DMP additive (the best performance).

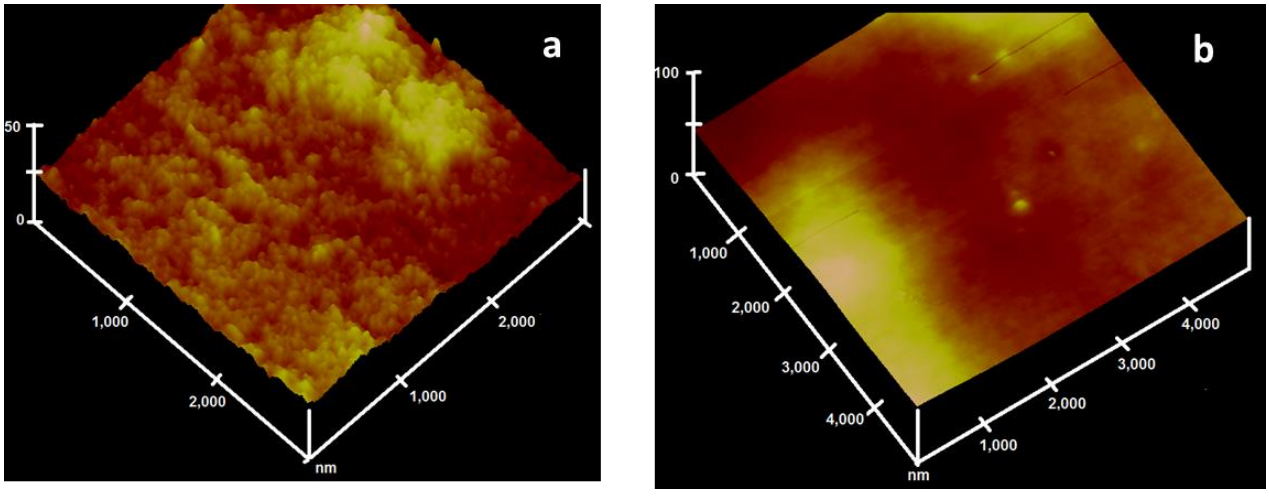

Figure 4.7: AFM image of P1 micelles from (a) 100% aqueous solution, and (b) aqueous solution with DMP.

Initially, two different P1 solutions were prepared at a concentration of 5 mg/mL. One of the solution contained P1 in 100% water, while the other one composed of P1 in water along

with DMP additive (10 wt.%). Before performing any coating, the micelles prepared in these two solvent systems were analysed with AFM as shown Figure 4.7. In 100% aqueous solutions, spherical micelles were formed as shown in Figure 4.7a. The large number of micelles appeared in the image corresponds to the higher concentration (5 mg/mL) of P1. Meanwhile, P1 solution in water with DMP additive did not show any micelles (Figure 4.7b). The absence of micelles in the latter system indicates P1 existed as unimers with collapsed chains of PFOEMA and PCEMA. These findings help to establish the role of DMP. For example, the polymer grafting from 100% aqueous solutions should involve micelles and unimers, while that from water with DMP as unimers. (For detailed AFM images at various stages of cotton coating preparation, see Appendix B).

Figure 4.8 shows SEM and AFM images of fabrics at various stages of their coating treatment. Both high and low resolution images of uncoated cotton fibers are shown in Figure 4.8A. It is apparent that the uncoated fibers at the given resolution are smooth and exhibit no apparent surface features. A higher magnification image is shown in the inset of Figure 4.8A, which confirmed that the uncoated cotton had a very smooth surface. Meanwhile, the P1-coated cotton sample that was coated using the aqueous DMP system showed rough texture on its surface before annealing treatment (Figure 4.8B). No micelles were visible on the surface of this non-annealed sample, even at the high resolution shown in the inset. However, after the sample was annealed, its surface became smooth again (Figure 4.7C). These observations suggest that P1 was adsorbed onto the cotton as unimers when the coating was performed using the aqueous DMP system, and upon annealing P1 formed a smooth and uniform layer.

On the other hand, samples coated from the 100% aqueous solution that lacked DMP were analysed by AFM (Figure 4.8D). The image is of an annealed sample that had been coated with an aqueous P1 solution. Micelles are clearly visible on the surface of this coated cotton

sample. This is also supported by detailed AFM analysis shown in Figure B1 in Appendix B, which depicts those micelles adsorption occurred on the fibers. This strongly suggests that P1 became adsorbed onto the cotton as micelles/unimers, rather than as exclusive unimers. Also, annealing does not help a lot to form uniform layer in case of coating from 100% aqueous P1 solutions. This also consistent with the slow grafting rate and poor stability of the cotton samples coated from 100% aqueous P1 solutions. Based on SEM and AFM analyses and the kinetic study of coatings, we are confident that P1 adsorption occurs on the surface of cotton when aqueous solutions lacking DMP are used, while unimer grafting occurs when the aqueous DMP solutions are used to coat the samples. The P1-coated samples prepared from water/THF (at f_{H2O} = 15 %) and water/ethanol (at f_{H2O} = 5%) closely resemble those coated with the aqueous DMP solution. Therefore, we assumed that P1 grafting took place in the unimer form in a similar manner to that observed among the aqueous DMP system, and thus these other two systems were not probed.

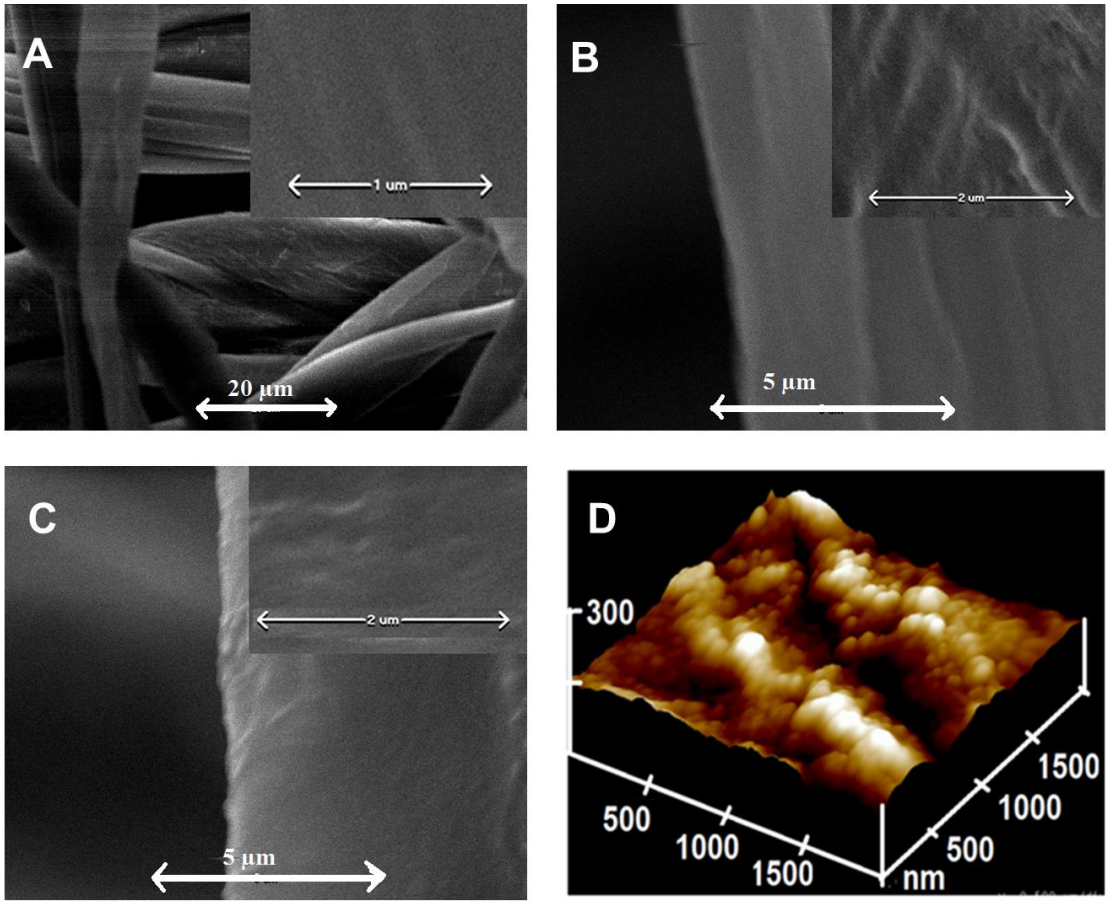

Figure 4.8. An SEM image of uncoated cotton (A). Also shown are SEM images of a cotton sample that had been coated with P1 using an aqueous solution containing the DMP additive both before (B) and after (C) annealing treatment. An AFM image is also shown of a cotton fiber that had been coated with an aqueous P1 solution containing no DMP and subsequently annealed (D).

4.4.7 Effect of Varying Polymer Concentration on Coating Performance

To study the effect of concentration on the coating performance, polymer solutions were prepared with P1 concentrations ranging from 0.5 to 20 mg/mL in aqueous solutions containing 10 wt.% DMP. Cotton samples were immersed into these solutions for 40 min, and photo-crosslinked for 1 h. Upon rinsing away the cleaved PEG chains with water for 3 h, these coated samples were subjected to droplet tests, and these results are plotted in Figure 4.9. Results shows that samples coated from the solution with lowest concentration of P1 (0.5 mg/mL) were

amphiphilic. Meanwhile, the samples coated from the 1 and 2 mg/mL P1 solutions were water repellent at certain locations on their surfaces. However, there were also weak spots on these surfaces where water drifted inside. These weak spots on the coated cotton samples indicated that an insufficient amount of P1 was available for grafting at low concentrations of ~2 mg/mL.

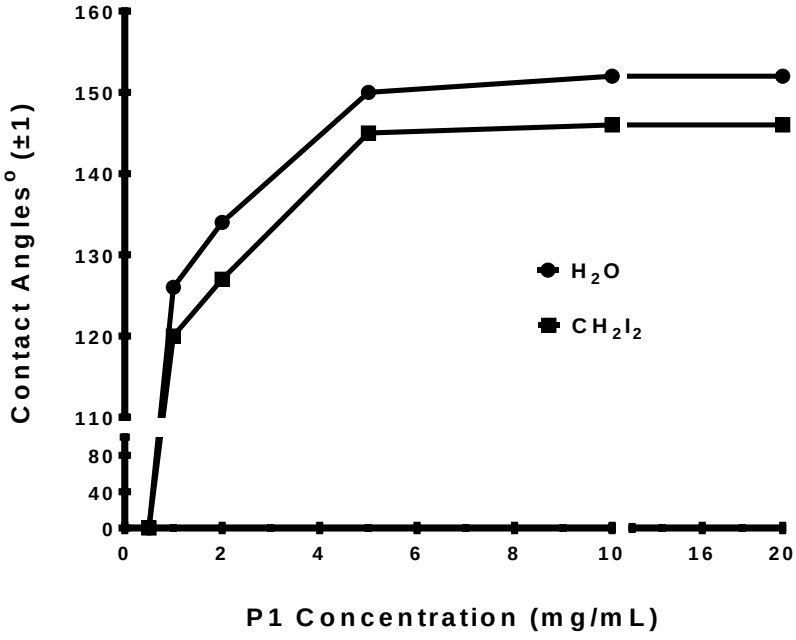

Figure 4.9. Plot showing the variation of the contact angles for water and diiodomethane droplets with changes in the concentrations of the P1 coating solutions. Cotton samples were immersed into different solutions for 40 min, and photo-crosslinked for 1 h.

However, the samples prepared from the 5 mg/mL of P1 solutions were both water- and oil-repellent. The contact angles for these samples were very high for both water and diiodomethane droplets as shown in Figure 4.9. Additionally, there were no weak spots on the coated cotton. A further increase in the coating solution concentration to 10 mg/mL of P1 showed a slight increase in the contact angles. However, no further increase in the water and oil

repellency was observed for the samples that were prepared using more concentrated P1 coating solutions, such as 20.0 mg/mL.

4.4.8 Effect of Varying Photolysis Time

We also investigated the effect of varying photolysis time on coating performance to establish optimum UV exposure time necessary to achieve maximum amphiphobicity. For this purpose, samples were first coated under standard conditions. These standard conditions included immersing the sample for 40 min in an aqueous coating solution (containing 5 mg/mL of P1 and 10 wt.% of DMP), and subsequently annealing the sample for 20 min. These coated cotton samples were irradiated on both sides for different periods of time such as 4, 10, 20, 40 and 100 min. The samples were then rinsed with water to remove the cleaved PEG chains before the contact angles were measured.

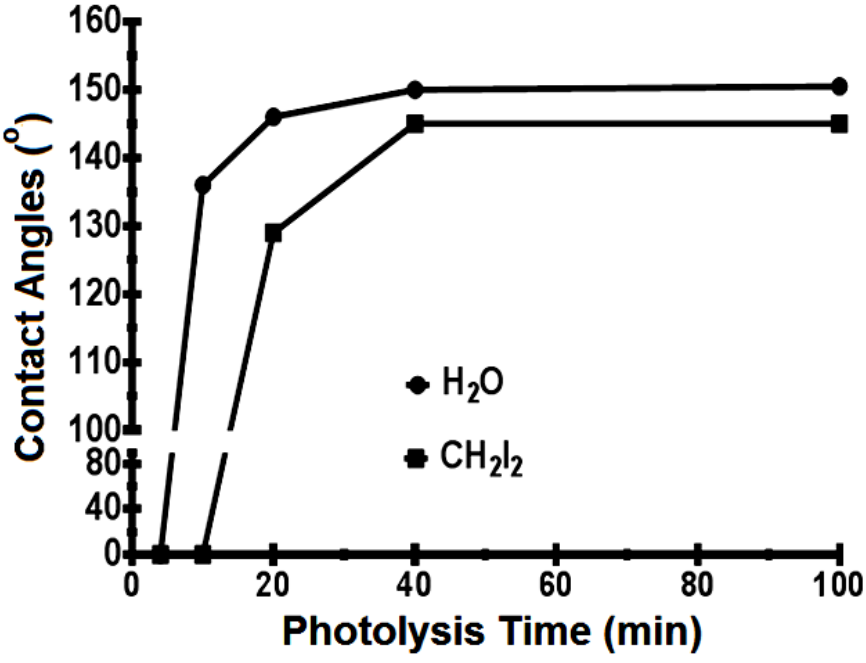

Figure 4.10. Plot of the changes in the contact angles of water and diiodomethane droplets vs. the duration of photo-crosslinking.

The results from this experiment are plotted in Figure 4.10. The samples irradiated for only 4 min were strongly amphiphilic. Meanwhile, those irradiated for 10 min were hydrophobic but not oleophobic. Also, the water droplets did not readily roll along the surfaces that were only irradiated for 10 min. However, the samples irradiated for 20 min or longer showed enhanced water and oil repellency. The samples irradiated for 40 and 100 min were almost identical in their high water- and oil-repellent properties, and hence the maximal contact angles for water and diiodomethane were obtained. This experiment shows that 40 min of crosslinking is sufficient for P1 to provide the desired coating properties.

4.4.9 Effect of PEG Rinsing on Contact Angles

As mentioned earlier, P1 consists of a photo-cleavable *ONB* junction. Therefore, the irradiation of P1 coated samples concurrently crosslinks the PCEMA chains and cleaves the PEG chains. As the PEG chains are hydrophilic in nature, thus it was necessary to remove these cleft chains. An experiment was performed to estimate the optimum rinsing time for the PEG chains to be removed. First, coated samples prepared under standard conditions were subjected to irradiation for 1 h. After irradiation, the samples were rinsed with water for different intervals of time. Meanwhile, the contact angles were measured after each rinsing interval (Figure 4.11). In the early stage, rinsing intervals were shorter in duration. Meanwhile, in the later stages longer rinsing intervals were employed. The first rinsing cycle was 2 min in duration, and this was followed by a 10 min rinsing cycle. After these two cycles (giving a total of 12 min of rinsing), the contact angles exceeded 140 $\pm 1^{o}$ and 130 $\pm 1^{o}$ for water and diiodomethane droplets, respectively. An additional 1 h cycle provided a further increase in the performance of coating with contact angles reached 148 $\pm$ 1^{o} and 137 $\pm$ 1^{o} for water and diiodomethane, respectively. The best results were achieved after 3 h where 150 $\pm$ 1^{o} and 145 $\pm$ 1^{o} for water and

diiodomethane, respectively, and beyond this point no further increase in the contact angles were observed. This established that ~3 h of washing was required for the complete removal of the cleaved PEG chains, thus providing the maximum amphiphobic character.

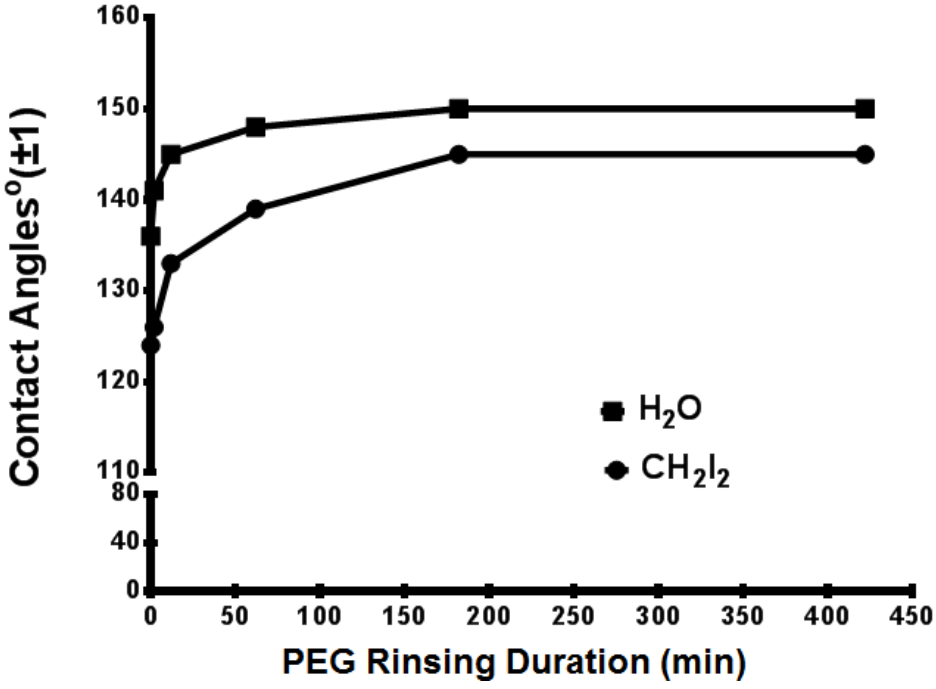

Figure 4.11. Plot of the water and diiodomethane contact angles vs. the rinsing time employed to remove the cleaved PEG chains from P1-coated cotton samples.

4.4.10 XPS Surface Analysis

Figure 4.12 compares the XPS spectra of a PFOEMA homopolymer, uncoated cotton, P1-coated cotton, and a "P1-coated-washed" cotton sample. The P1-coated-washed sample was coated with P1 and subsequently extracted with THF. In this study, the uncoated cotton fabric and the PFOEMA homopolymer were recorded as reference samples. Intense peaks corresponding to C1s and O1s signals were displayed by the uncoated cotton sample. Meanwhile, the PFOEMA spectrum consisted of four peaks, including two weak signals corresponding to C1s and O1s signals and two strong signals for F_{1S} and F_{KLL}. The spectrum of

the P1-coated sample had two additional peaks compared to that of the uncoated cotton sample. These newly emerged peaks were due to the presence of exposed PFOEMA domains on the surface, corresponding to the F_{1S} and F_{KLL} signals. These signals indicated that P1 was successfully grafted onto the surface. Interestingly, a significant increase in the intensity of the F_{1S} and F_{KLL} signals relative to the C_{1s} and O_{1s} peaks was observed for the P1-coated-washed sample. This phenomenon was observed due to the exposure of the PFOEMA block, which had initially been masked by PEG. XPS analysis suggested that P1 was successfully grafted onto the cotton, which was in agreement with the SEM analysis.

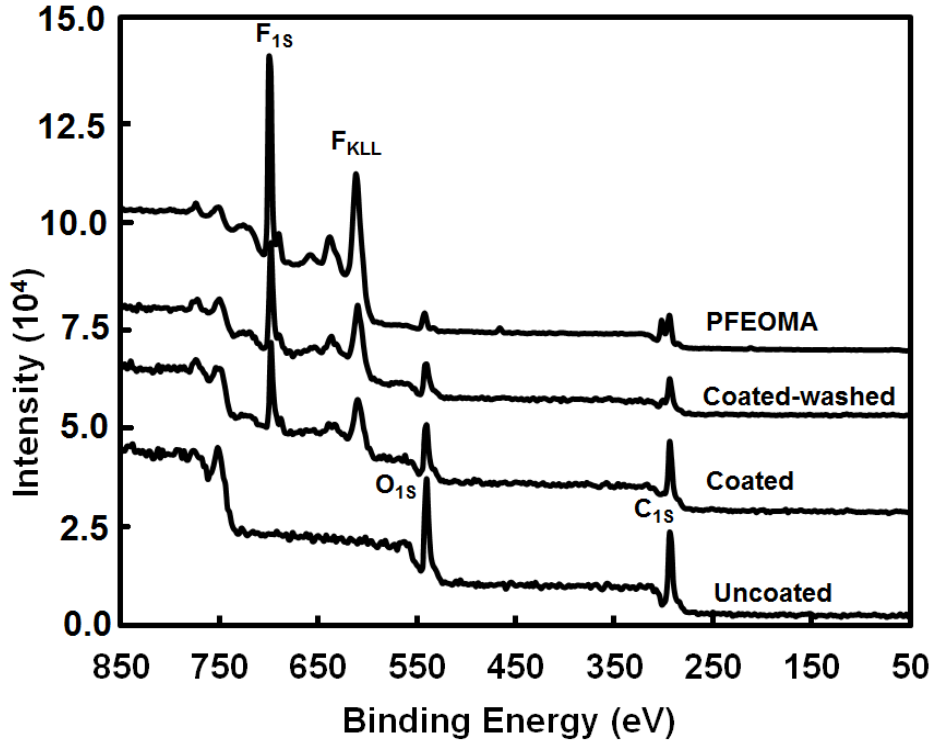

Figure 4.12. XPS spectra of PFOEMA, an uncoated cotton sample, a P1-coated cotton sample, and a "P1-coated-washed" cotton sample. The term P1-Coated-Washed means the samples had been coated with P1 and subsequently extracted with THF for 2 h to remove the cleft PEG chains and other loosely held polymer residues.

4.4.11 Determination of the Copolymer Grafting Densities

Two methods could be used to calculate the copolymer grafting densities of the cotton samples. Method 1 involved measuring the differences in the masses of the coated and uncoated cotton samples using a microbalance. Alternatively, Method 2 was based on TGA measurements of the coated samples. TGA analysis was chosen in our case, as TGA is used to successfully determine grafted amount as low as ~0.1 wt.%.

For this purpose, samples were prepared under standard coating conditions (using the aqueous DMP solution as the P1 coating solution) for TGA analysis. Figure 4.13 shows TGA curves that were recorded for uncoated cotton samples, cotton samples that were coated with P1 and subsequently washed with THF, and for the P1 copolymer. All of these curves were normalized at 150 ^{o}C. As shown in Figure 4.13, the TGA curve for the uncoated cotton sample did not exhibit a complete weight loss under the given experimental conditions, and 8.304 ± 0.005 wt.% of residue remained behind. Similarly, P1 lost 84.901 ± 0.005 wt.% of its composition during the TGA experiment, leaving behind a weight residue of 15.009 ± 0.005 wt.%. The TGA curve for the P1-coated cotton sample that was subsequently washed with THF lie between the traces obtained for the uncoated cotton sample and for P1. Also, the TGA curve of the uncoated sample showed a sharp transition at 300 ^{o}C, while that for P1 showed multiple transitions between 200 and 600 ^{o}C. The broad temperature range over which P1 exhibited weight loss is attributed to the copolymer incorporating three blocks that each had different decomposition temperatures.

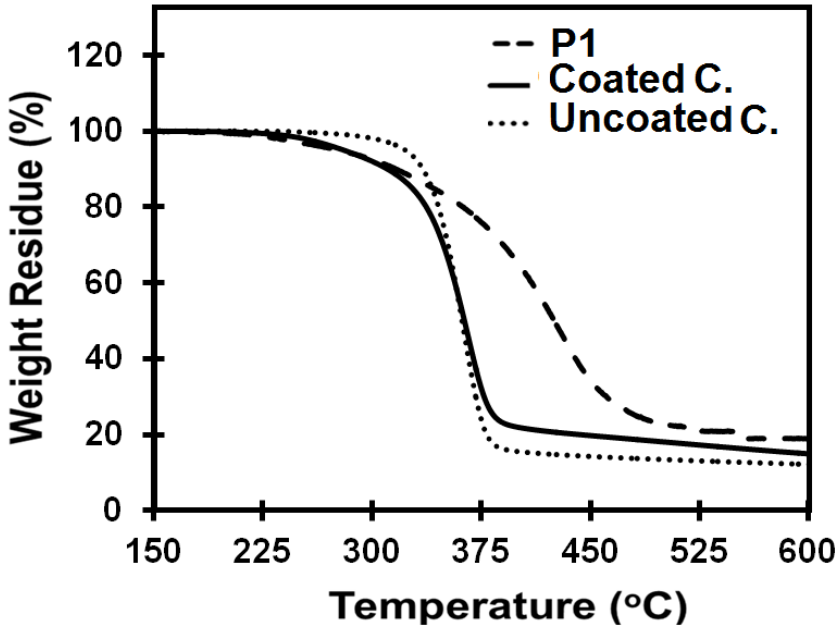

Figure 4.13. Comparison of TGA curves for P1, uncoated cotton, and cotton samples that were coated with P1 and subsequently washed with THF. In the legend above cotton is abbreviated as C.)

Following Eq. 4.1, the grafting densities of the cotton samples were calculated. In this equation, R_{PC} represents the weight residue of P1-coated cotton, R_P represents the weight residue of P1, R_C represents the weight residue of the uncoated cotton, and x is the grafting density. Rheology advantage data analysis (TA Instrument USA) was used to automatically measure the weight residues corresponding to the coated cotton, the uncoated cotton, and to P1. These values were then entered into Eq. 4.1.

$$(1-x)R_C + xR_P = R_{PC} \qquad \text{(Eq. 4.1)}$$

A sample calculation for determining the grafting density of a cotton sample coated for 22 min in a P1 solution is described here. Two cotton samples were independently coated under

standard conditions for 22 min. TGA was performed on both samples independently. The TGA curves were first normalized at 150 ^{o}C to 100% and the weight residues left behind were calculated as 10.670 ± 0.005 and 10.602 ± 0.005 wt. % for Samples 1 and 2, respectively. The values of 8.304 ± 0.005 % and 15.009 ± 0.005wt.% for R_C and R_P, respectively, were entered into Eq. 4.1 along with the weight residue measured for the coated cotton sample. For the cotton samples that were coated for a 22 min soaking period, the grafting densities were found to be 0.343 ± 0.005 and 0.351 ± 0.05 wt.% for the two different samples. This gave an average grafting density of 0.347 ± 0.005 %.

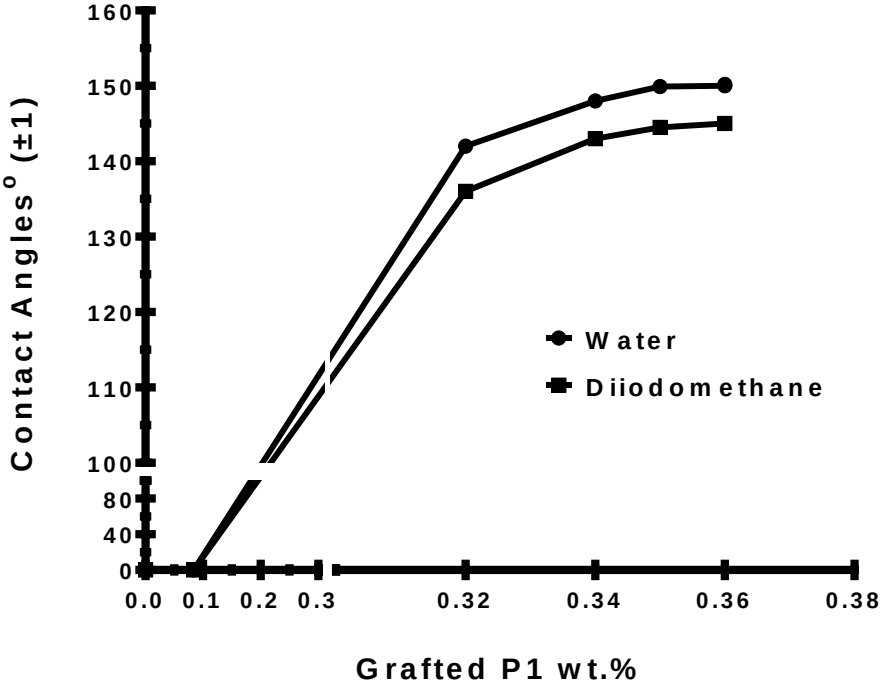

Figure 4.14. Plot comparing water and diiodomethane droplet contact angles vs. P1 content (wt.%) among cotton samples prepared using DMP-containing 100% aqueous P1 dispersions.

Figure 4.14 plots the grafting density of P1 against the contact angles for water and diiodomethane droplets. It is apparent that, the amphiphobic properties developed once the grafting density exceeded 0.320 ± 0.005 wt.%. The plot indicates that cotton samples with a grafting density of 0.370 ± 0.005 wt.% could provide water droplet contact angles that exceeded 150 ±1^{o} and diiodomethane droplet contact angles of 145 ±1^{o}.

4.4.12 Plastron Layer Formation

Figure 4.15 compares the images of ordinary cotton and superhydrophobic cotton (coated with P1) samples that had been immersed into water. Ordinary cotton is hydrophilic and thus easily becomes soaked with water (see Figure 4.15a). Meanwhile, superhydrophobic cotton repels water and thus floats on the surface of water. However, if the water-repellent cotton is forcibly immersed into water, a layer of air is formed at the interface between the superhydrophobic cotton and the surrounding water. This accumulation of air at the interface is known as a plastron layer, and prevents the cotton from undergoing wetting.[20] A plastron layer can be seen on the coated sample (Figure 4.15b) through the reflection of light because of the accumulation of air. The accumulated air layer remained on the cotton surface for hours without undergoing any changes.

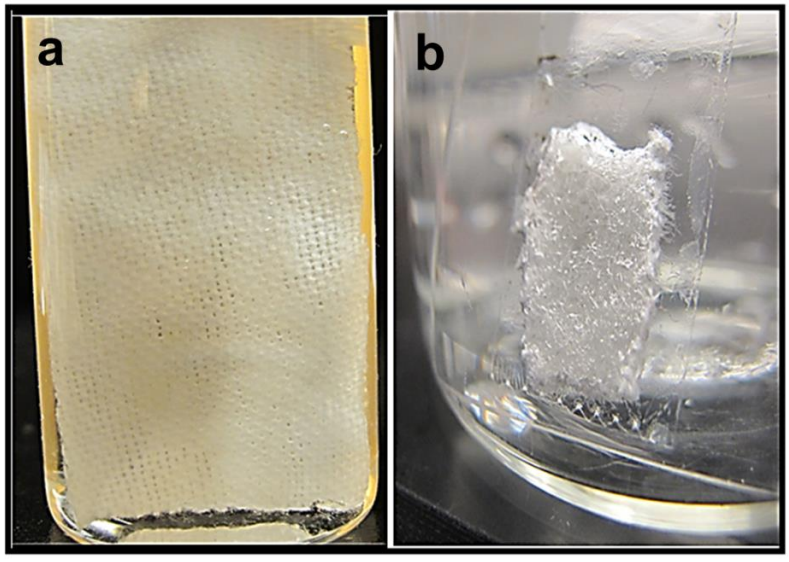

Figure 4.15. Pictures of an uncoated cotton fabric (a) and a P1-coated cotton sample (b) upon immersion into water. The coated cotton sample formed a plastron layer upon immersion into water, as evidenced by the reflections visible on its surface (b).

4.4.13 Application of P1 Coatings onto Semi-Cotton

We also demonstrated that the P1 coatings were not only limited to pure cotton but could also be successfully applied to semi-cotton that is roughly consisted of 45% cotton while 55% polyester. Here, the coatings were prepared under similar conditions as those described for pure cotton. The coated semi-cotton samples were subjected to 2 h of THF extraction, and subsequently subjected to water and diiodomethane droplets tests. Figure 4.16 compares photographs of water and diiodomethane droplets placed onto P1-coated pure cotton (Figure 4.16a) and P1-coated semi-cotton (Figure 4.16b). Both samples were highly water- and oil-repellent, and it was found that both the coated cotton and coated semi-cotton samples exhibited essentially identical amphiphobic properties. We did not examine other parameters such as the

grafting density, variation of contact angles with concentration, or XPS analysis for semi-cotton coatings. However, these properties will be investigated in the future.

Figure 4.16. Water (left) and diiodomethane (right) droplets placed onto coated samples of pure cotton (a) and semi-cotton (b). The pictures were taken 2 min after the droplets had been applied onto the surfaces. The P1 coatings were prepared using 100% aqueous dispersions containing DMP. The droplets were impregnated with Rhodamine B for visual clarity.

4.5 Conclusions

A facile, environmentally-friendly fabrication method for protecting cotton fabrics with superhydrophobic and oleophobic coatings has been developed. These coatings were prepared through the use of aqueous P1 dispersions containing a 10 wt.% DMP additive. The coating procedure is simple and involves the preparation of a micellar dispersion of P1 and subsequently immersing cotton fabrics into this dispersion for 5 min. The samples were annealed at 120 ^{o}C for 20 min few minutes before irradiation. After photo-crosslinking was performed, the cotton samples were washed with water to remove the cleft PEG chains. The obtained coated samples

displayed superhydrophobic and oleophobic properties with P1 grafting densities of ~0.35 wt.% when they were prepared from aqueous P1 dispersions containing the DMP additive. The surface properties of the uncoated and coated cotton samples were probed by XPS, SEM, and AFM techniques. XPS analysis suggested that the surface was enriched with PFOEMA, while SEM further support that P1 had been grafted as unimers instead of as micelles. The durability of the coated cotton samples were tested against 5 wt.% aqueous detergent solutions for 24 h washing cycles with no significant loss of their water- and oil-repellent properties. Furthermore, the P1 coatings were also successfully applied onto semi-cotton samples.

4.6 References

1. Feng, L.; Li, S.H.; Li, Y.S.; Li, H.J.; Zhang, L.J.; Zhai, J.; Song, Y.L.; Liu, B.Q.; Jiang, L.; Zhu, D. B.*Adv. Mater*. **2002,** *14*, 1857.
2. Quere, D. *Nat. Mater*. **2002,** *1*, 14.
3. Lafuma, A.; Quere, D. *Nat. Mater.* **2003,** *2*, 457.
4. Blossey, R. *Nat. Mater*. **2003,** *2*, 301.
5. Erbil, H. Y.; Demirel, A. L.; Avci, Y.; Mert, O. *Science,* **2003,** *299*, 1377.
6. Wang, S.; Jiang, L. *Adv. Mater*. **2007,** *19*, 3423.
7. Chen, W.; Fadeev, A. Y.; Hsieh, M. C.; Oner, D.; Youngblood, J.; McCarthy, T. J. *Langmuir,* **1999,** *15*, 3395.
8. Ma, W.; Higaki, Y.; Hideyuki, O.; Takahara, A. *Chem. Commun.* **2013,** *49*, 597.
9. Wenzel, R. N. *Ind. Eng. Chem.* **1936,** *28*, 988.
10. Cassie, A. B. D.; Baxter, S. *T. Faraday Soc.* **1944,** *40*, 546.
11. Chen, W.; Fadeev, A. Y.; Hsieh, M. C.; Youngblood, J.; McCarthy, T. J. *Langmuir,* **1999,** *15*, 3395.
12. Roach, P.; Shirtcliffe, N. J.; Newton, M. I. *Soft Matter,* **2008,** *4*, 224.
13. Barthlott, W.; Neinhuis, C. *Planta,* **1997,** *202,* 1.
14. Hikita, M.; Tanaka, K.; Nakamura, T.; Kajiyama T.; Takahara, A. *Langmuir,* **2005,** *21,* 7299.
15. Lide, D. R. *CRC Handbook of Chemistry and Physics.* 76th ed.; CRC Press: Boca Raton, FL, 1995.
16. Brandrup, J.; Immergut, E. H. *Polymer Handbook.* John Wiley & Sons: New York, 1989.
17. Hoefnagels, H. F.; Wu, D.; de With, G.; Ming, W. *Langmuir,* **2007,** *23*, 13158.

18. Schuyten, H. A.; Reid, J. D.; Weaver, J. W.; Frick, J. G. *Text. Res. J.* **1948,** *18,* 490.

19. Schuyten, H. A.; Reid, J. D.; Weaver, J. W.; Frick, J. G. *Text. Res. J.* **1948,** *18,* 396.

20. Xiong, D.; Liu, G.; Duncan, E. J. S. *Langmuir*, **2012,** *28*, 6911.

21. Vilcnik, A.; Jerman, I.; Vuk, A. S.; Kozelj, M.; Orel, B.; Tomsic, B.; Simonic, B.; Kovac, J. *Langmuir*, **2009,** *25*, 5869.

22. Yu, M.; Gu, G.; Meng, W. D.; Qing, F. L. *Appl. Surf. Sci.* **2007,** *253,* 3669.

23. Wi, D. Y.; Kim, W.; Kim, J. *Fiber Polym*. **2009,** *10*, 98.

24. Hirao, A.; Sugiyama, K.; Yokoyama, H. *Prog. Polym. Sci.* **2007,** *32,* 1393.

25. Qu, L.; Xin, Z. *Langmuir*, **2011,** *27,* 8365.

26. Ye, H.H.; Li, Z.X.; Chen, G.Q.; Fan, D. *J. Appl. Polym. Sci*. **2013,** *127,* 402.

27. Kuo S.W.: Wu, Y.C.: Wang, C.F.: Jeong, K.U. *J. Phys. Chem. C*. **2009,** *113,* 20666.

28. Luo, J.; Wu, Q.; Huang, H. C.; Chen, J.J. *Text. Res. J.* **2011,** *81,* 1702.

29. Tang, W. Y.; Huang, Y. G.; Qing, F. L.; *J. Applied. Polym. Sci.* **2010,** *119,* 84.

30. Ma, M. L.; Hill, R. M.; Lowery, J. L.; Fridrikh, S. V.; Rutledge, G. C. *Langmuir,* **2005,** *21*, 5549.

31. Ma, M. L.; Mao, Y.; Gupta, M.; Gleason, K. K.; Rutledge, G. C. *Macromolecules,* **2005,** *38*, 9742.

32. Yu, M.; Gu, G. T.; Meng, W. D.; Qing, F. L. *Appl. Surf. Sci.* **2007,** *253,* 3669.

33. Tang, W.; Huang, Y.; Qing, F. L. *J. Applied. Polym. Sci.* **2011,** *119,* 84.

34. Yang, S. H.; Liu, C. H.; Hsu, W. T.; Chen, H. *Surf. Coat. Technol.* **2009**, *203,* 1379.

35. Wi, D. Y.; Kim, I. W.; Kim, J. *Fib. Polym.* **2009,** *10,* 98.

36. Maity, J.; Kothary, P.; O'Rear, E. A.; Jacobi, C. *Ind. Eng. Chem. Res.* **2010,** *49*, 6075.

37. Milner, S.T. *Science,* **1991,** *251,* 905.

38. Halperin, A.; Tirrell, M.; Lodge, T. P. *Adv. Polym. Sci.* **1992,** *100*, 31.

39. Rizzardo, E.; Moad, G. *In Polymeric Materials Encyclopedia*: *Synthesis, Properties, and Applications*. Salamone, J. C., Ed.; CRC, Press: Boca Raton, FL, 1996.

40. Ding, J.F.; Tao, J.; Guo, A.; Stewart, S.; Hu, N.X.; Birss, V. I.; Liu, G.J. *Macromolecules*, **1996,** *29*, 5398.

41. Tao, J.; Guo, A.; Liu, G.J. *Macromolecules,* **1996,** *29,* 1618.

42. Rabnawaz, M.; Liu, G.; *Macromolecules,* **2012,** *45*, 5586.

43. a) Vogler, E. A. *Adv. Colloid. Interface Sci.* **1998,** *74*, 69.

b) Shimizu, R. N.; Demarquette, N. R. *J. Appl. Polym. Sci.* **2000,** *76*, 1831.

44. Liu, H. B.; Hamers, R. J. *Surf. Sci.* **1998,** *416*, 354.

45. Roy, X.; Hui, J. K. H.; Rabnawaz, M.; Liu, G.; Maclachlan, M. J. *J. Am. Chem. Soc.***2011,** *133,* 8420.

46. Li, X.; Liu, G. *Langmuir*, **2009**, *25,* 10811.

47. Riess, G. *Prog. Polym. Sci.* **2003,** *28,* 1107.

48. Ogliaruso, M.A.; Wolfe, J.F. *Synthesis of Carboxylic Acids Esters and their Derivatives.* Wiley, New York, 1991.

Chapter 5 - Synthesis of Poly(ethylene glycol)-*block*-poly(2-hydroxyethyl methacrylate) via Anionic Polymerization

5.1 Preface

The manuscript based on this research work is under preparation.

5.2 Introduction

Poly(ethylene oxide) (PEO)-based block copolymers are useful and interesting.[1-3] A striking example of their utility is the commercial scale production of PEO- and poly(propylene oxide) (PPO)-based triblock copolymers under the trade name Pluronic®.[4] Micelles of block copolymers in aqueous media bearing PEO as the corona have great potential as drug delivery agents for hydrophobic medicines.[5-6] Meanwhile, hydrogels formed from block copolymers incorporating PEO blocks can be useful as drug delivery systems for hydrophilic molecules.[7-8]

Despite the interest and usefulness of PEO-containing block copolymers and past efforts, the synthesis of PEO-based polymethacrylates by anionic polymerization has not been optimized.[9] Fetters has classified monomers for anionic polymerization based on their reactivity, that discloses the sequence in which monomers should undergo anionic polymerization.[10] According to this classification, methacrylate anions can initiate the nucleophilic ring opening of ethylene oxide (EO) because methacrylate anions are more basic than oxyanions. For this reason, methacrylate-based EO polymerization reactions must be performed at room temperature.[9,11] However, at room temperature side reactions can occur, such as trans-esterification from attack by an oxyanion of the methacrylate ester, thus yielding ill-defined polymers.[9,11]

Alternatively, a reverse order of this block copolymerization involving the polymerization of methacrylate and acrylate monomers using PEO-based oxyanions has been studied. For this purpose, the polymerization of methyl methacrylate (MMA)[12] and *tert*-butyl acrylate (*t*BA)[13] were reported with PEO–based macroinitiator at room temperature. Reportedly, these approaches yielded ill-defined block copolymers. This was especially the case for PEO-*b*-PMMA, due to the low steric hindrance involved. It has been established that the preparation of PEO-based methacrylate block copolymers encounters two problems. Firstly, PEO crystallizes from THF at a low temperature, while a low temperature is necessary to control the anionic polymerization of methacrylates. Secondly, a slow initiation of methacrylate double bonds occurs in the presence of PEO oxyanions because of the reactivity differences between these two reagents. However, the slow initiation problem was addressed in an effort to polymerise PEO-*b*-PDMAEMA using PEO oxyanion in the presence of the phosphazene base tBuP4 (IUPAC name: 1-*tert*-butyl-4,4,4-tris(dimethylamino)-2,2-bis[tris(dimethylamino)-phosphoranylidenamino]-2L5,4L5-catenadi(phosphazene)) at 10 ^{o}C.[14] The phosphazene base tBuP4 was used to allow a smooth cross-over by the PEO oxyanion toward the methacrylate double bond. However, besides an increase in the initiation rate, an increase in the propagation rate was also observed. Consequently, the block copolymers prepared by this approach had relatively wide molecular weight distributions (>1.40).

Therefore, a latent PEG macroinitiator was designed for methacrylate polymerization that can initiate methacrylate polymerization at low temperatures. Poly(ethylene glycol) (PEG) is referred to PEO if the average molecular weight of the polymer is less than 20,000 g/mol.[15] However, macroinitiators typically contain trace amounts of impurities. Therefore, the method had to allow the titration of the impurities before activation of the latent macroinitiator. In addition, the initiating functional group had to be sufficiently bulky and different from the PEG

backbone so that it would not be buried inside the PEG crystals at low temperatures. Based on these considerations, we decided to use diphenylethylene (DPE)-end-functionalized PEG (Figure 5.1) as the latent macroinitiator.

A superior property of DPE is that it can react with *sec*-butyllithium or other nucleophiles to produce an anion that can initiate the polymerization of many monomers, including styrene and methacrylate derivatives, but it does not undergo homopolymerization.[16-17] Therefore, the impurities in a PEG-DPE solution sample can be titrated with 3-methyl-1,1-diphenylpentyl lithium, which is produced by reacting an equimolar amount of DPE with *sec*-butyllithium. DPE is sufficiently bulky that its incorporation inside a PEG lattice should disrupt its crystalline packing. Therefore, the DPE group should remain exposed and reactive even at very low temperatures, such as -78 ^{o}C.

While there have not been any reports describing the preparation or use of PEG-DPE for block copolymer synthesis, other types of DPE-end-functionalized polymers have been prepared for block copolymer synthesis. The application of DPE chemistry has been reviewed by Roderick and coworkers.[18] The Hirao group is especially well-known for utilizing the DPE functionality for the preparation of block copolymers of various architectures.[19-20]

5.2.1 Objectives

This chapter will describe a novel method for the anionic polymerization of poly(ethylene glycol)-*b*-poly(2-trimethylsiloxyethyl methacrylate) (PEG-*b*-P(HEMA-TMS). This project was initiated to establish a long-sought-after anionic polymerization of a methacrylate using PEG-DPE as a latent macroinitiator.

5.2.2 Experimental Design Considerations

In this study, PEG_{113}-DPE was chosen as a potential macroinitiator for various reasons. Firstly, DPE is a non-homopolymerizable moiety that can initiate the polymerization of methacrylates. Secondly, THF solutions of PEG_{113}-DPE can be titrated with 3-methyl-1,1-diphenylpentyl lithium without reacting with PEG-DPE. Thirdly, DPE is a bulky species that can inhibit the chain packing of PEG at low temperatures.

HEMA-TMS was selected as a representative methacrylate in this proof of concept study, because HEMA-TMS is a less hindered methacrylate when compared to *tert*-butyl acrylate. Therefore, a successful block copolymerization of the HEMA-TMS monomer with PEG-DPE as the macroinitiator would indicate that this reaction should also be effective for other types of methacrylates.

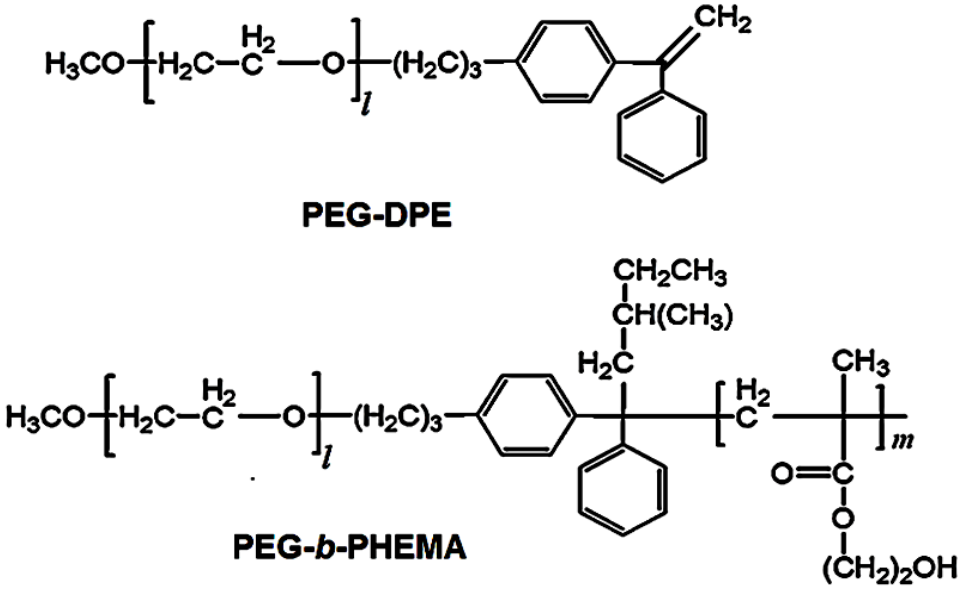

Figure 5.1. Chemical structures of PEG_{113}-DPE and PEG_{113}-*b*-$PHEMA_{260}$.

5.3 Experimental Section

5.3.1 Materials

1,1-Diphenylethylene (Aldrich, ≥ 95% purity) was distilled over calcium hydride and subsequently distilled over *n*-butyllithium. 2-Trimethylsiloxyethyl methacrylate (HEMA-TMS) was synthesized according to a literature method,[20] and was distilled over calcium hydride and in the presence of triethylaluminum (1.0 M in hexane) before use. Potassium *tert*-butoxide (Sigma-Aldrich, 95%) was purified via sublimation at high temperature (> 200 ^{o}C) under vacuum. THF was refluxed with sodium until a deep purple color developed, as indicated by benzophenone, before it was distilled. *sec*-Butyllithium (1.4 M in Hexane, Aldrich) was used as received. Polyethylene glycol monomethyl ether (5,000 g/mL, Scientific Polymer Products, Inc.) was dried under vacuum at 55 ^{o}C for three days. The end-capping reagent, 1-(4-(3-Bromopropyl)phenyl)-1-phenylethylene (DPE-Br) was prepared according to a literature procedure.[21]

5.3.2 Characterization

Size exclusion chromatography (SEC) was performed using a Waters 515 system equipped with a Waters 2410 refractive index detector. The three columns were packed by American Polymer Standards Corporation with 5-μm AM 1000, 10,000, and 100,000 Å gels. The system was calibrated using monodisperse polystyrene (PS) standards. The eluent used was *N*,*N*-dimethylformamide (DMF) containing 2.5 g/L of tetrabutylammonium bromide. The flow rate was set to 0.9 mL/min. ^{1}H NMR measurements were performed on Bruker Avance-300 or Avance-400 instruments using deuterated pyridine-d_5, methanol-d_4 or chloroform-*d* as solvents and a 3 s relaxation delay.

5.3.3 Synthesis of DPE-Br

5.3.3.1 Step 1: Synthesis of 4-(3-bromopropyl)benzophenone

Aluminum chloride (4.20 g, 160 mmol) was added to a THF solution of benzoyl chloride (5.10 g, 36.0 mmol) and the reaction mixture was stirred at 60 °C. After the mixture was stirred for 30 min at 60 ^{o}C, 3-bromopropylbenzene (25.0 g, 21.1 mmol) was added dropwise to the reaction mixture, and the mixture was subsequently stirred for 6 h at 60 °C. This reaction was terminated with 2 N aqueous HCl (10 mL). The crude reaction mixture was extracted with dichloromethane (3 × 10 mL). Subsequently, the combined organic layers were sequentially washed with 2.0 N aqueous NaOH (3 × 10 mL) and distilled water (1 × 10 mL). The organic layer was then dried over $MgSO_4$ for 1 h and was concentrated using a rotary evaporator. The oily crude product was purified by silica gel column chromatography with hexane:ethyl acetate (9:1) as the eluent. The product was vacuum dried overnight at room temperature, thus providing 25.1 g of product in a 67.0 % yield. ^{1}H NMR ($CDCl_3$, 300 MHz): δ 7.25-7.86 (*m*, 9H, Ar), 3.4 (*t*, *J* = 6.2 Hz, 2H, CH_2Br), 2.85 (*t*, *J* = 6.2 Hz, 2H, ArCH_2), 2.2 (*m*, 2H, $CH_2CH_2CH_2$) ppm.

5.3.3.2 Step 2: Synthesis of 1-(4-(3-bromopropyl)phenyl)-1-phenylethylene

Potassium *tert*-butoxide (8.27 g, 73.7 mmol) was added to a THF solution of methyltriphenylphosphonium bromide (26.1 g, 73.1 mmol), and the reaction mixture immediately turned yellow. 4-(3-Bromopropyl)benzophenone (18.0 g, 59.4 mmol) was added dropwise to the reaction mixture over a period of 15 min at 0 °C. As the reaction progressed, this solution gradually changed from a yellow solution to a brownish color. The reaction mixture was stirred overnight at room temperature and was subsequently quenched with distilled

water. The crude product was extracted with diethyl ether (3 × 50 mL) and the combined organic layers were sequentially washed with an aqueous $NaHCO_3$ solution (1.0 M, 3 × 10 mL) and then with a saturated brine solution (1 × 20 mL). The resultant solution was dried over Na_2SO_4. The organic layer was concentrated under reduced pressure using a rotary evaporator. The triphenylphosphine glycol by-product was removed as a precipitate from the crude mixture by adding the concentrated solution to excess hexane (50 mL). The crude product was purified via silica gel column chromatography using hexane:ethyl acetate (99:1) as the eluent yielding 11.5 g of 1-(4-(3-bromopropyl)phenyl)-1-phenylethylene in a 64.0 % yield. ^{1}H NMR ($CDCl_3$, 300 MHz): δ 7.2-7.4 (*m*, 9H, Ar), 5.5 (*d*, *J* = 7.2 Hz, 2H, CH_2=C(Ph)$_2$), 3.45 (*t*, *J* = 6.2 Hz, 2H, CH_2Br), 2.85 (*t*, *J* = 6.3 Hz, 2H, ArCH_2), 2.2 (*m*, 2H, $CH_2CH_2CH_2$) ppm.

5.3.4 Synthesis of PEG_{228} by Anionic Polymerization

Freshly distilled THF (300 mL) was placed into a three-neck (1 L) round-bottom flask. Gaseous ethylene oxide (Aldrich, ≥ 99.5% purity, 10.0 g or 0.250 moles) was condensed in an ampoule (50 mL) loaded with calcium hydride at -10 ^{o}C. The condensed ethylene oxide (EO) was distilled twice, once over calcium hydride and then over *n*-butyllithium. The ethylene oxide was distilled over *n*-butyllithium and transferred into a pre-cooled reaction flask at ~ -78 ^{o}C. The initiator, *tert*-butoxide (0.120 g, 1.00 × 10^{-3} mol) was transferred into the reaction mixture as a THF solution (3.0 mL) via syringe and the mixture was heated to 35 °C to initiate the polymerization reaction. The reaction mixture was stirred at 35 °C for three days. This reaction was subsequently terminated with 0.1 M HCl (2.0 mL). The crude mixture was concentrated to 15 mL using a rotary evaporator and was precipitated with diethyl ether (3 ×100 mL), which

yielded 9.2 g of PEG in 92% yield. ^{1}H NMR of PEG_{228} ($CDCl_3$, 300 MHz): δ 3.3-3.7 (*br*, 912 H, CH_2CH_2O), 1.2 (*s*, 9H, $OC(CH_3)_3$) ppm.

5.3.5 Synthesis of PEG_{113}-DPE

PEG_{113}-OH (9.8 g, 1.9 ×10^{-3} mol) was dissolved into THF (200 mL) and cooled to 8-10 °C using a cold water bath. Sodium hydride (0.188 g, 7.80 ×10^{-3} mol) was added to the reaction mixture, which was stirred for 30 min at this temperature. Subsequently, DPE-Br (2.94 g, 9.80 × 10^{-3} mol) was added dropwise into the reaction mixture at 8-10 °C. The reaction mixture was refluxed for 24 h at 70 °C. Distilled water (1 mL) was added at room temperature to terminate the reaction. The crude mixture was passed through a short pad of alumina before it was concentrated to a volume of ~6 mL using a rotary evaporator. The viscous solution was poured dropwise into diethyl ether (50 mL) to induce precipitation, and the precipitates were subsequently filtered off under vacuum. This precipitation procedure was repeated three more times (3 × 50 mL). PEG_{113}-DPE was obtained in 5.5 g in a 55% yield, of which 100% of the polymer chains were end-capped by DPE. ^{1}H NMR ($CDCl_3$, 300 MHz): δ 7.2-7.4 (*m*, 9H, Ar), 5.5 (*d*, *J* = 7.2 Hz, 2H, CH_2=C$(Ph)_2$), 4.0 (*s*, 3H, CH_3O-), 3.3-3.4 (br. *s*, 456 H, -CH_2CH_2O), 3.45 (*t*, *J* = 6.2 Hz, 2H, -OCH_2CH_2OPh), 2.85 (*t*, *J* = 7.5 Hz 2H, $ArCH_2$), 2.2 (*m*, 2H, $CH_2CH_2CH_2$) ppm.

5.3.6 PEG_{113}-DPE Initiated Anionic Polymerization of PEG_{113}-*b*-$PHEMA_{260}$

PEG_{113}-DPE (1.24 g, 2.44 × 10^{-1} mmol) was dissolved in 20 mL of THF and dialysed against distilled THF (6 × 150 mL) using a 3,500 g/mol cut-off membrane for ~24 h. The dialysed macroinitiator was added into a three-necked round-bottom flask (1 L) that was pre-

loaded with LiCl (43 mg, 4.0 equivalents). The residual THF was distilled from the reaction flask under vacuum and the macroinitiator, along with LiCl, were vacuum dried overnight. Subsequently, freshly distilled THF (300 mL) was added to the flask and the mixture was stirred at room temperature until the macroinitiator was completely dissolved. The reaction mixture was cooled to -78 °C using an acetone-dry ice bath, and the solution became turbid due to PEG crystallization. The resulting solution was titrated with a 3-methyl-1,1-diphenylpentyl lithium solution (0.2 M in THF). The 3-methyl-1,1-diphenylpentyl lithium solution was formed by the reaction between equimolar quantities of DPE and *sec*-butyllithium. The end-point of the titration was achieved once a persistent red color appeared due to the addition of 3-methyl-1,1-diphenylpentyl lithium. To the titrated system was added *sec*-butyllithium (0.17 mL, 1.4 M), which was provided in an equimolar amount to that of PEG_{113}-DPE (2.44×10^{-1} mmol) present in the mixture. The mixture was stirred for 15 min, and then 2-trimethylsiloxyethyl methacrylate (HEMA-TMS) (12.7 mL, $5.98 \times 10^{+1}$ mmol) was added dropwise via syringe over 5-6 min. The polymerization was allowed to continue for a total of 2.5 hours at -78 ^{o}C before 1.0 mL of degassed methanol was added to terminate the polymerization reaction. Subsequently, 60 mL of methanol/water at v/v = 50/10 was added to the resultant mixture. The mixture was stirred overnight at room temperature and was concentrated under reduced pressure to a volume of ~20 mL, yielding a viscous residue. The polymer was precipitated from diethyl ether (300 mL), and this precipitation process was repeated twice. After the product was dried under vacuum, 10.4 g of the polymer was obtained with an 87.0 % yield. ^{1}H NMR (CD_3OD, 300 MHz): δ 4.1(*m*, -$COOCH_2$, 520H), 3.8 (*m*, CH_2OH, 520H), 3.4-3.7 (*br. m*, -CH_2CH_2O, 456H), 2.1 (*m*, CH_2), 1.2-0.8 (*m*, CH_3) ppm.

5.3.7 Synthesis of PEG_{228}-VB

PEG_{228}-OH (10.1 g, 1.00×10^{-3} mol) was dissolved in 50 mL of THF and the solution was cooled down to 8-10 ^{o}C using an ice bath. Sodium hydride (0.15 g, 4.0×10^{-3} mol) was added at this temperature and the mixture was stirred for 30 min. Vinylbenzyl chloride (2.42 mL, 16.0×10^{-3} mol) was added into the reaction mixture, which was subsequently refluxed for 24 h at 70 ^{o}C. The reaction was cooled to room temperature and was quenched with distilled water (2 mL). The crude mixture was passed through a short-pad of alumina (neutral), using THF as the eluent. The obtained THF solution of the crude polymer was concentrated to 5 mL and was precipitated from diethyl ether (3 × 100 mL). The precipitate was subsequently dried under vacuum, providing 6.6 g of PEG_{228}-VB in a ~64% yield. ^{1}H NMR ($CDCl_3$, 300 MHz): δ 7.2-7.4 (*m*, 5H, Ar), 6.7 (*dd*, *J* = 8.2 Hz, 6.0 Hz, 1H, Ph*CH*=CH_2), 5.78 (*d*, *J* = 8.2 Hz, 1H, ArCH=*CH*$_2$), 5.33 (*dd*, *J* = 7.0 Hz, 2.0 Hz, 1H, ArCH=*CH*$_2$), 4.58 (*s*, 2H, Ar*CH*$_2$O-), 3.3-3.38 (*br*, 914 H, -*CH*$_2$*CH*$_2$O) ppm.

5.3.8 PEG_{228}-VB Initiated Anionic Polymerization of PEG-*b*-PHEMA

PEG_{228}-VB (2.32 g, 2.30 x 10^{-1} mmol) was dialysed against distilled THF with a dialysis membrane (12,000 g/mol cut-off molecular weight) and was transferred into a 1 L round-bottom flask containing LiCl (51.6 mg, 5 equivalents). The crude THF solution was distilled from this flask by connecting a vacuum pump to the polymerization flask. After the sample was dried overnight under vacuum, freshly distilled THF (300 mL) was transferred into the reaction flask, and the PEG-VB macroinitiator was allowed to completely dissolve. The reaction mixture was then cooled to -78 °C using an acetone-dry ice bath. The solution became turbid due to the poor solubility of PEG at this low temperature in THF. *sec*-Butyllithium (0.6 mL of a 1.4 M solution

in hexane) was added in a single shot to the reaction mixture, which immediately turned yellow. The temperature was raised to room temperature and the mixture was stirred for ~30 min at this temperature. Meanwhile, the yellow color began to fade and eventually disappeared to give a clear solution. This reaction was not continued further, as all of the active PEG-VB anions were terminated.

5.4 Results and Discussion

5.4.1 Diphenylethylene End-Capped Poly(ethylene glycol) (PEG_{113}-DPE) Macroinitiator

Scheme 5.1 illustrates the synthesis of the diphenylethylene end-capped polyethylene glycol (PEG_{113}-DPE) macroinitiator. First, 1-(4-(3-bromopropyl)phenyl)-1-phenylethylene was synthesized according to a procedure reported previously.[22] A Friedel-Crafts acylation reaction was conducted between 3-bromopropylbenzene and benzoyl chloride to yield 4-(3-bromopropyl)benzophenone. The product was purified via column chromatography and analysed by ^{1}H NMR spectroscopy. The labelled ^{1}H NMR spectrum (Figure 5.2) displayed the characteristic signals that would be anticipated for 4-(3-bromopropyl)benzophenone. In the next step, the carbonyl group of 4-(3-bromopropyl)benzophenone was transformed into an alkene group. A ^{1}H NMR spectrum of the product 1-(4-(3-bromopropyl)phenyl)-1-phenylethylene (DPE-Br) is also included in Figure 5.2. The signal appearing at 5.6 ppm corresponded to the alkene protons of DPE-Br, and thus confirmed the successful synthesis of the product. Further confirmation of the target compound was obtained from the characteristics peaks and peaks integration corresponding to each proton of DPE-Br.

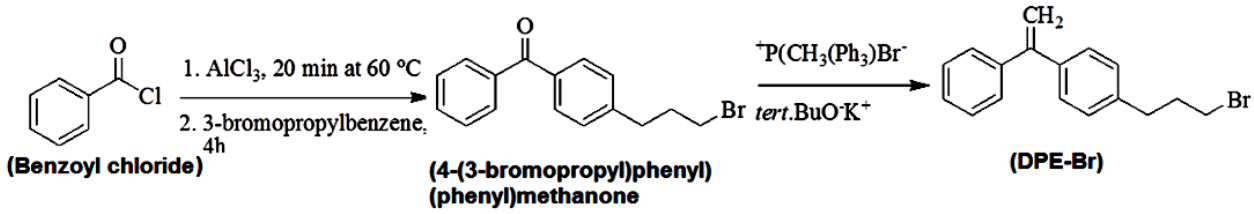

Scheme 5.1. Synthetic pathway for the preparation of 1-(4-(3-bromopropyl)phenyl)-1-phenylethylene (DPE-Br).

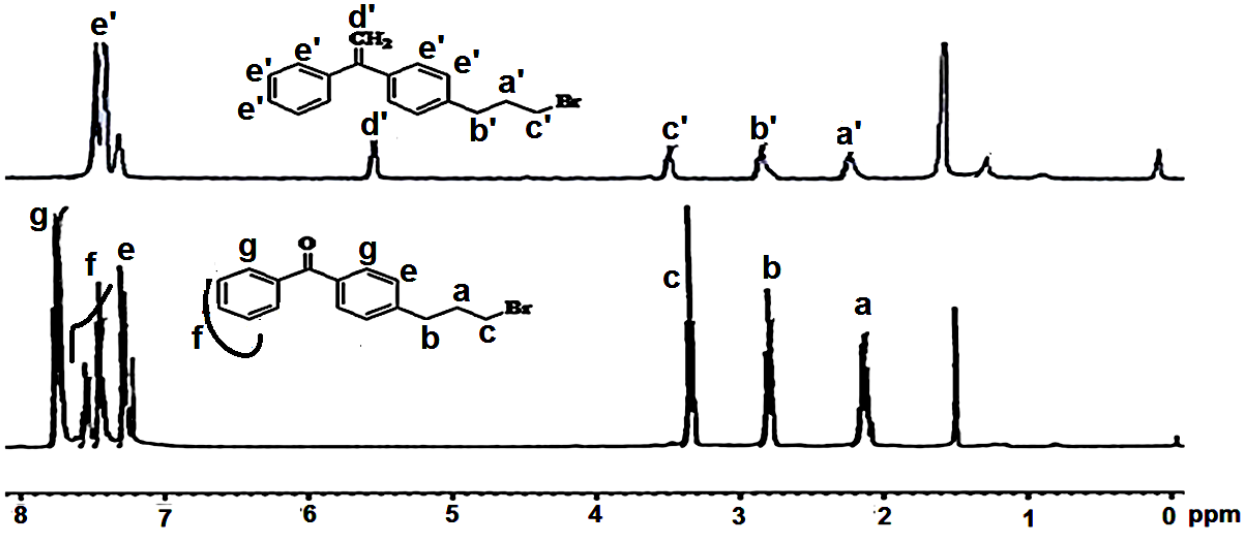

Figure 5.2. ^{1}H NMR spectra (recorded at 300 MHz in $CDCl_3$) of 4-(3-bromopropyl) benzophenone (bottom) and DPE-Br (top).

Scheme 5.2 highlights the synthetic pathway for the preparation of PEG_{113}-*b*-$PHEMA_{260}$. In general, three steps are required to synthesize the block copolymer. The first step involves the preparation of PEG_{113}-DPE by a substitution reaction. In the next step, the DPE end-group was reacted with *sec*-butyllithium, and subsequently HEMA-TMS was added to the mixture. Copolymerization with HEMA-TMS yielded PEG_{113}-*b*-$(PHEMA\text{-}TMs)_{260}$. In the final step, the hydrolysis of the $P(HEMA\text{-}TMS)_{260}$ block yielded PEG_{113}-*b*-$PHEMA_{260}$.

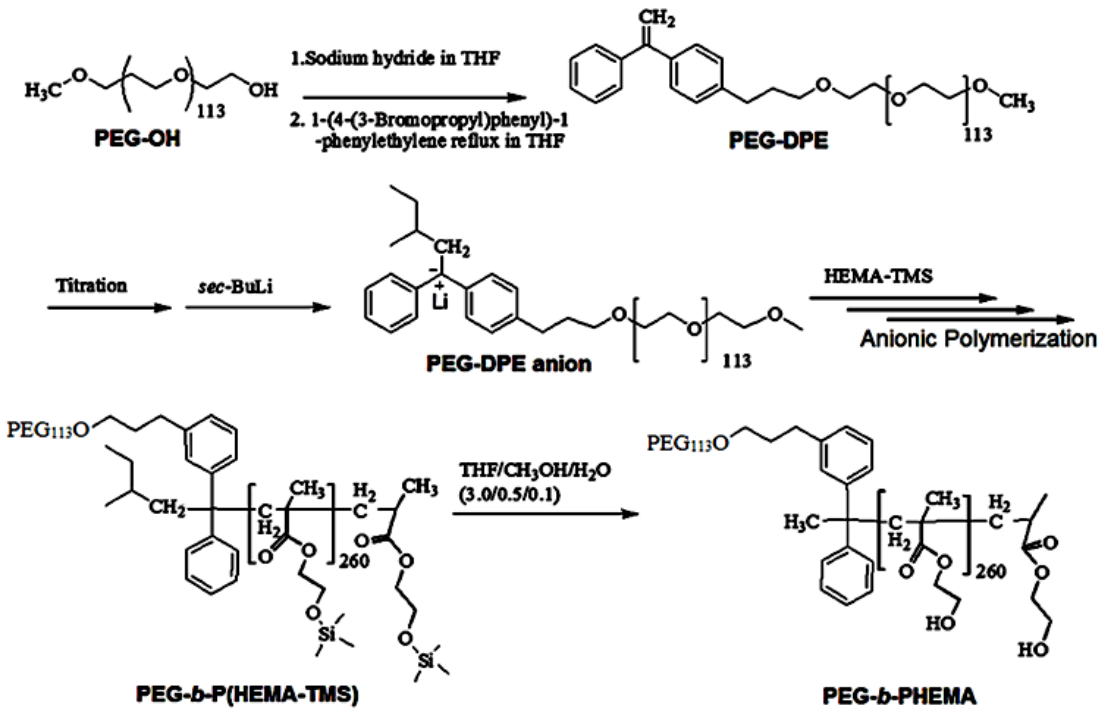

Scheme 5.2. Synthetic pathway followed for the preparation of PEG_{113}-*b*-$PHEMA_{260}$.

PEG_{113}-DPE could be prepared through two different methods. Method 1 involved the growth of the PEG oxyanion chain to react with DPE-Br. Consequently, oxyanions of the growing polymer chains displaced the bromide group of DPE-Br to yield PEG_{113}-DPE. Method 2 involved the reaction between monohydroxy PEG (PEG-OH) and DPE-Br in the presence of sodium hydride (NaH). NaH was used because of its strong basicity and weak nucleophilicity, which prevented it from participating in substitution reactions as a nucleophile. A careful ^{1}H NMR analysis confirmed the successful synthesis of PEG_{113}-DPE, as shown in Figure 5.3. Furthermore, the end-labelling of PEG chains with DPE was quantified by ^{1}H NMR spectroscopy. It was found that the DPE to PEG molar ratio was 1/113, which thus confirmed the quantitative labelling of the hydroxyl end-groups by DPE-Br.

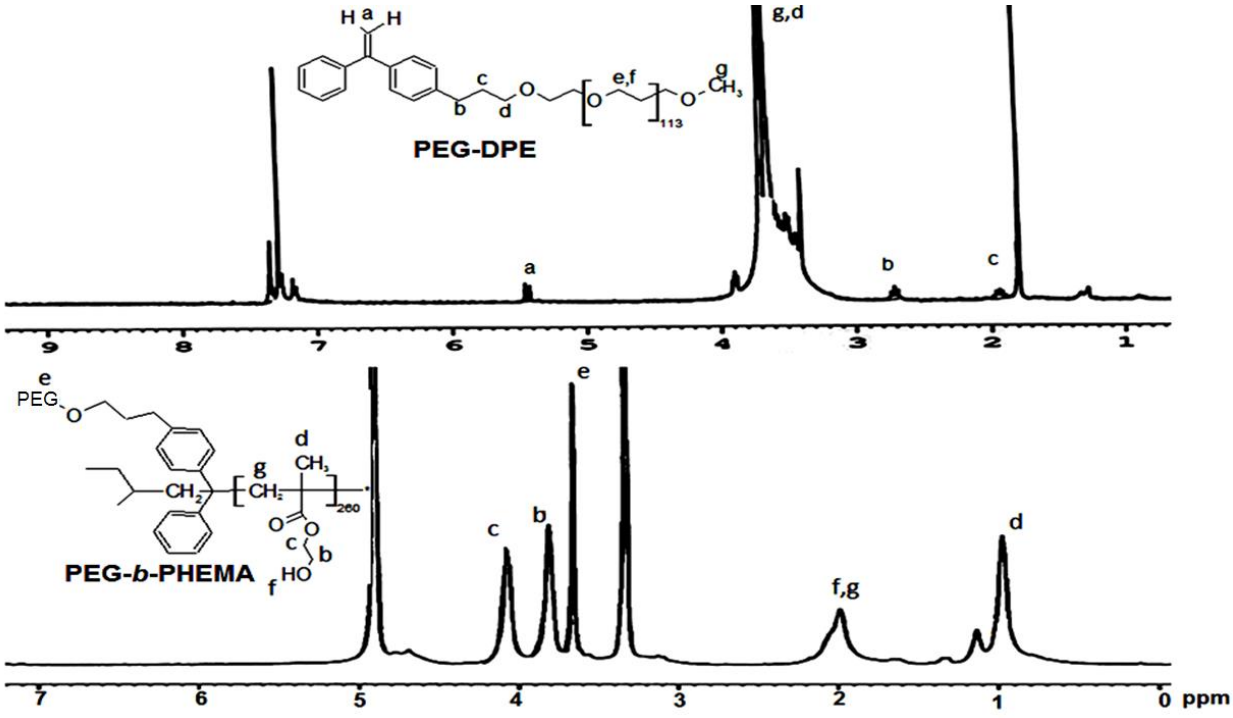

Figure 5.3. ^{1}H NMR spectra of PEG_{113}-DPE ($CDCl_3$, 300 MHz, top), and PEG_{113}-*b*-$PHEMA_{260}$ (CD_3OD, 300 MHz, bottom).

5.4.2 Synthesis of PEG_{113}-*b*-$PHEMA_{260}$ from the PEG_{113}-DPE Macroinitiator

Initially, the macroinitiator was dialysed against distilled THF to remove any possible impurities. The dialysed THF solution of PEG_{113}-DPE was transferred to a three necked polymerization flask containing LiCl salt. LiCl is used as an additive for the anionic polymerization of methacrylates to overcome side reactions and obtain monodisperse polymers.[22] Residual THF was removed via vacuum distillation, and the contents remaining in the flask were subsequently dried overnight under vacuum at room temperature to remove traces of THF and moisture. Subsequently, freshly distilled dry THF was added into the flask. Remaining impurities were quenched via titration with 3-methyl-1,1-diphenylpentyl lithium without affecting the integrity of the DPE initiating group. It was only after the impurities were

fully consumed by 3-methyl-1,1-diphenylpentyl lithium that an equimolar amount of *sec*-butyllithium was added to activate the DPE double bonds. The reaction between PEG_{113}-DPE and *sec*-butyllithium was relatively slow, and hence the red color of the reacted DPE group intensified only gradually over 3-4 min. To make sure that all of the DPE end-groups were activated, the reaction was allowed to stir for 15 min before the addition of HEMA-TMS. The addition of HEMA-TMS quickly dissipated the red color. As the block copolymerization progressed, the turbidity of the reaction mixture decreased. This reduced turbidity was likely due to micelle formation by the resultant PEG_{113}-*b*-$P(HEMA\text{-}TMS)_{260}$ copolymer in THF. The polymerization was terminated with degassed methanol. Stirring the resultant polymer in THF/methanol/water led to the hydrolysis of HEMA-TMS to yield PEG_{113}-*b*-$PHEMA_{260}$.

Figure 5.3 also includes a ^1H NMR spectrum of PEG_{113}-*b*-$PHEMA_{260}$ along the peak assignments for each individual proton of the diblock copolymer. From the relative integrations of signals corresponding to protons of the PEG and PHEMA blocks, the PEG/PHEMA repeat unit ratio was established as 113/260 for the block copolymer. This was in reasonable agreement with the ratio of 113/245 calculated from the PEG-DPE/HEMA-TMS molar feed ratio.

The SEC traces for PEG_{113}-*b*-$PHEMA_{260}$ and its precursor PEG_{113}-DPE are shown in Figure 5.4. The SEC peak for PEG_{113}-*b*-$PHEMA_{260}$ appeared at a retention time of 23.4 min. This retention time is significantly lower than that of the macroinitiator, PEG_{113}-DPE, which appeared at a retention time of 27.8 min. Furthermore, the PDI obtained for PEG_{113}-*b*-$PHEMA_{260}$ was 1.08 in terms of PS standard, which is a conclusive indication of livingness of the polymerization.

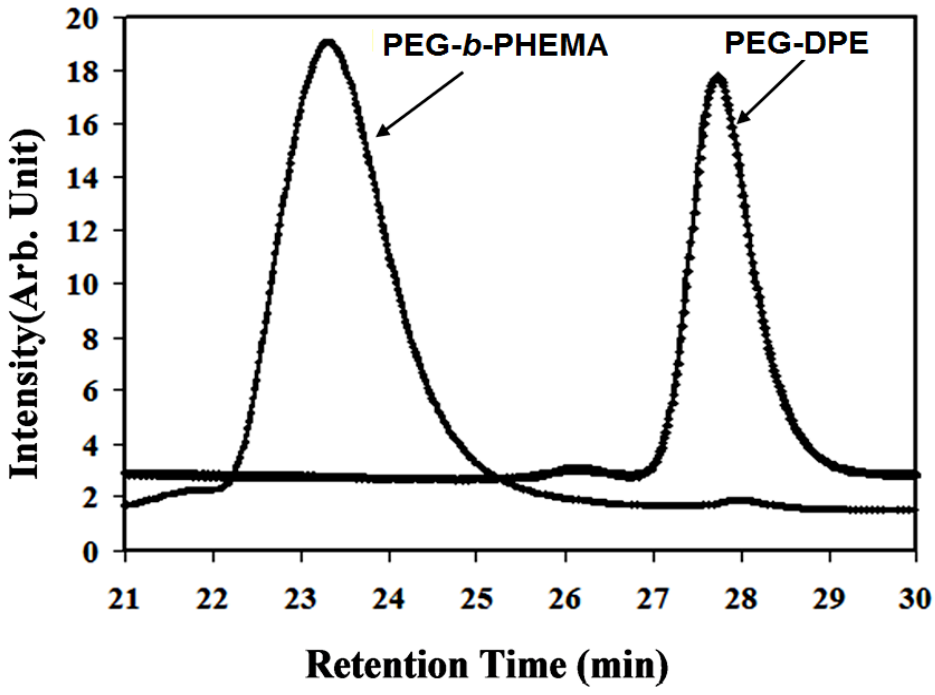

Figure 5.4. SEC traces for PEG_{113}-*b*-$PHEMA_{260}$ and PEG_{113}-DPE. The samples were recorded using DMF as the mobile phase at a flow rate of 0.9 mL/min.

Our investigations on the synthesis of PEG-bearing block copolymers can be extended to other polyacrylates and polymethacrylates, such as poly(methyl methacrylate) (PMMA), poly(*tert*-butyl acrylate) (P*t*BA), or poly(*N*,*N*-dimethylaminoethyl methacrylate) (PDMAEMA). In addition, this method is equally applicable for the preparation of ABC and ABA triblock copolymers such as PEG-*b*-P*t*BA-*b*-PMMA and P*t*BA-*b*-PEG-*b*-P*t*BA, respectively. Furthermore, there is no need to optimize the reaction conditions to accommodate the changing nature of the acrylates or their molecular weights because of the simplicity of the anionic polymerization.

Table 5.1. Molecular properties of polymers prepared in this study.

Sample	SEC M_w (g/mol)	SEC M_w/M_n (PDI)	NMR *l*/*m*	NMR M_n (g/mol)	*l*	*m*
PEG$_l$-*DPE*	14,000	1.04		5,000 [a]	113	
PEG$_l$-VB		1.04		10,000	228	
PEG$_l$-*b*-PHEMA$_m$ [a]		1.08	113/260	26,800	113	260
PEG$_l$-*b*-PHEMA$_m$ [b]	No Polymerization					

[a] Prepared using PEG-DPE as the macroinitiator.
[b.] Attempted by using PEG-VB as the macroinitiator.

5.4.3 Vinylbenzyl End-Capped Polyethylene Glycol (PEG_{228}-VB) Initiator

After successful utilization of the PEG_{113}-DPE macroinitiator, we decided to use poly(ethylene glycol)-vinylbenzene (PEG-VB) as the macroinitiator to further exploit the applicability of this new strategy. PEG_{228}-VB was chosen because vinyl benzyl chloride (VBC) and PEG are commercially available materials, and they are both relatively inexpensive. Consequently, successful strategies utilizing PEG macroinitiators that are end-capped with VB might be commercially viable. Additionally, the VB group of the latent macroinitiator PEG_{228}-VB can react with *sec*-butyllithium at low temperatures to form an active macroinitiator that can initiate a polymerization. Also, PEG_{228}-VB may display enhanced solubility at low temperatures, because the VB end-group can disturb the chain packing of PEG at low temperatures.

First, PEG_{228} was prepared by the polymerization of EO at room temperature, according to a literature procedure.[23] To ensure that all of the ethylene oxide monomer was consumed, the PEG polymerization was allowed to proceed for three days before VBC was added. The

obtained product was purified via precipitation prior to ^{1}H NMR analysis. Figure 5.5 shows the ^{1}H NMR spectrum of PEG_{228}-VB along with peak labelling, confirming the formation of PEG_{228}-VB. End-labelling efficiency was characterised by the comparison of integrals corresponding to the protons of the main PEG chain, VB group and the *tert*-butoxide end-group, indicating that all of the PEG chains had been end-capped as PEG_{228}-VB. Additionally, SEC analysis of PEG_{228}-VB indicated that the obtained PEG_{228}-VB polymer had a narrow molecular weight distribution (PDI = 1.04).

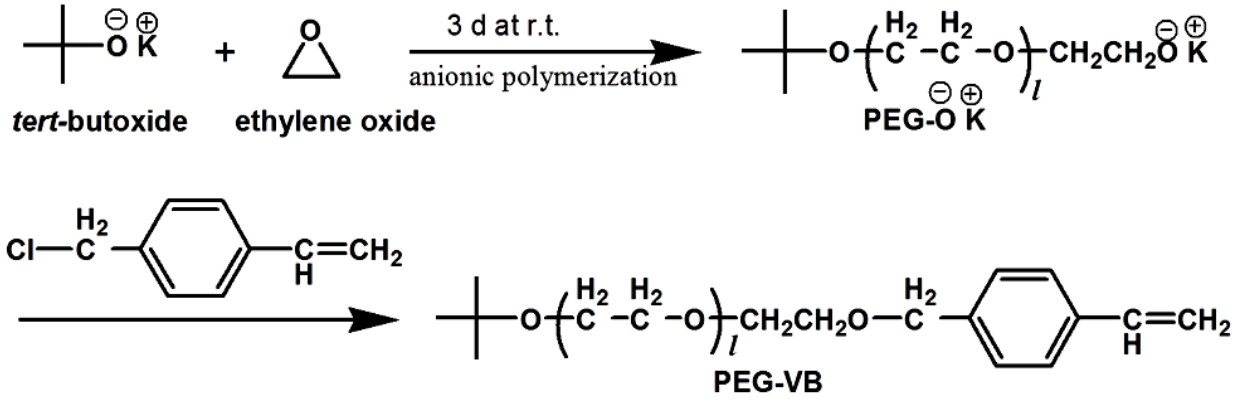

Scheme 5.3. Synthesis of PEG_{228}-OH from EO, and subsequent reaction with VBC.

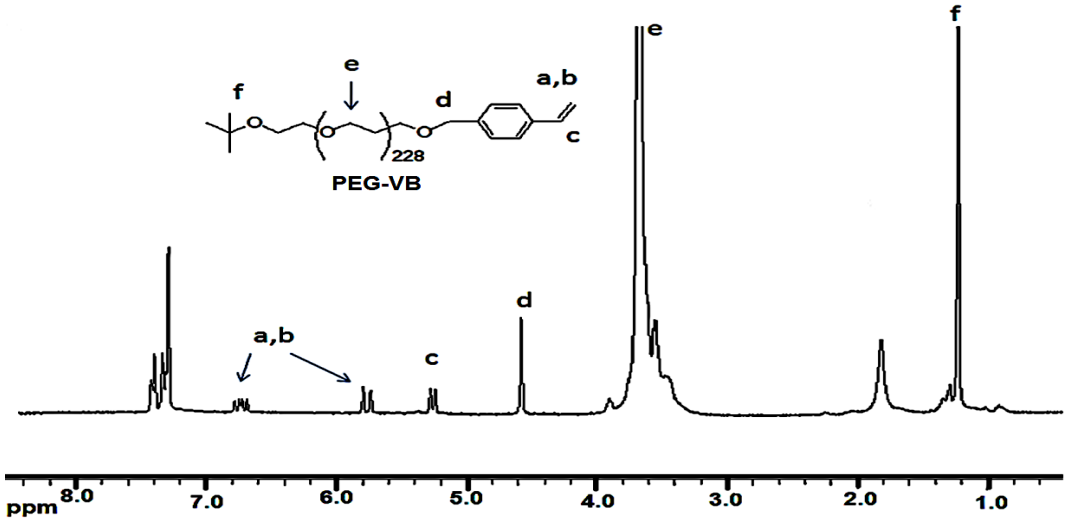

Figure 5.5. ^{1}H NMR spectrum (300 MHz in $CDCl_3$) of PEG_{228}-VB.

5.4.4 Synthesis of PEG_{228}-*b*-PHEMA from the PEG_{228}-VB Macroinitiator

Scheme 5.4 depicts synthetic route for the block copolymerization of HEMA-TMS using PEG_{228}-VB as the latent macroinitiator. A THF solution of PEG_{228}-VB was dialysed before use. The dialysed sample was transferred into a polymerization flask that was pre-loaded with LiCl. The contents of the flask were subsequently dried under vacuum overnight to remove residual THF. The next morning, freshly distilled THF was used to dissolve the PEG_{228}-VB and the solution was cooled to -78 °C using an acetone-dry ice bath. The solution became turbid as it was cooled. Despite this turbidity, we believe that the VB moieties of the PEG chains were still available to react with *sec*-butyllithium. Therefore, an excess of *sec*-butyllithium was added in a single-shot to kill any impurities within the system and also to activate the PEG_{228}-VB. A yellow color appeared immediately after this addition, indicating the formation of styryl anions from PEG_{228}-VB. The one-shot addition of *sec*-butyllithium was used to kill the impurities and also to produce anions from PEG-VB. Otherwise, if the *sec*-butyllithium had been added dropwise, it would have reacted with some of the PEG_{228}-VB chains to generate anions. These anions may have reacted further either with impurities or possibly could have become coupled with remaining PEG_{228}-VB. To remove the excess *sec*-butyllithium from the reaction mixture, the mixture was warmed to room temperature to react with THF. Meanwhile, the yellow color of the mixture gradually faded away, indicating the loss of the styryl anions. The reaction mixture was analysed via ^{1}H NMR spectroscopy, indicating the loss of vinyl groups. Clearly, PEG_{228}-VB was converted into an active initiator, but was destroyed in an attempt to quench excess *sec*-butyllithium. Furthermore, SEC analysis before and after the addition of *sec*-butyllithium to the PEG_{228}-VB solution did not show any change in the retention time for

PEG_{228}-VB, as shown in Figure 5.6. This demonstrated that the PEG chain remained intact after treatment with *sec*-butyllithium addition.

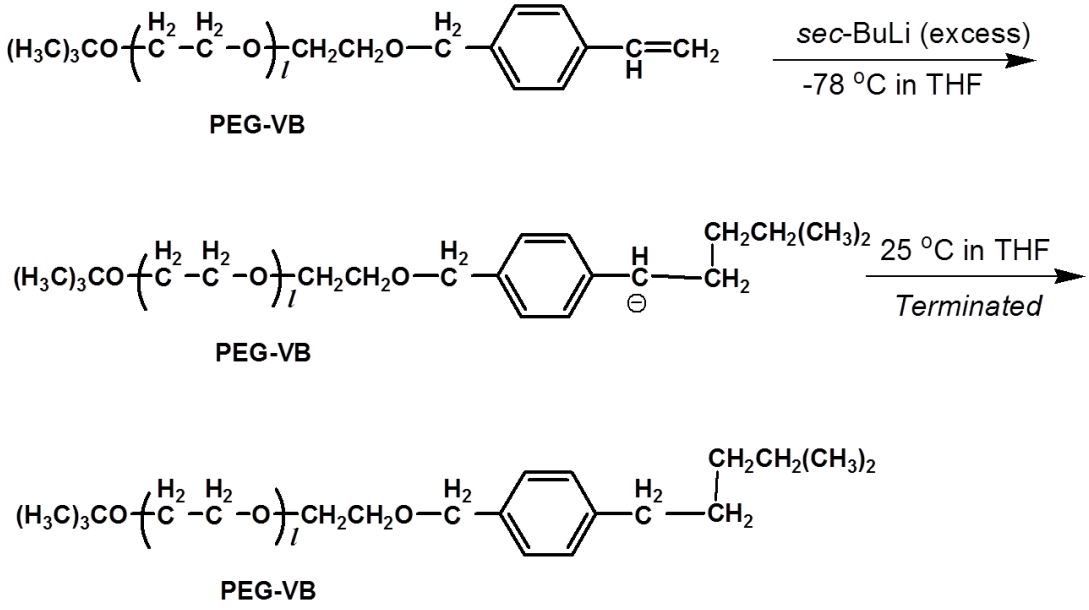

Scheme 5.4. Attempted synthesis of PEG_{228}-VB-*b*-PHEMA via anionic polymerization with PEG_{228}-VB as the macroinitiator.

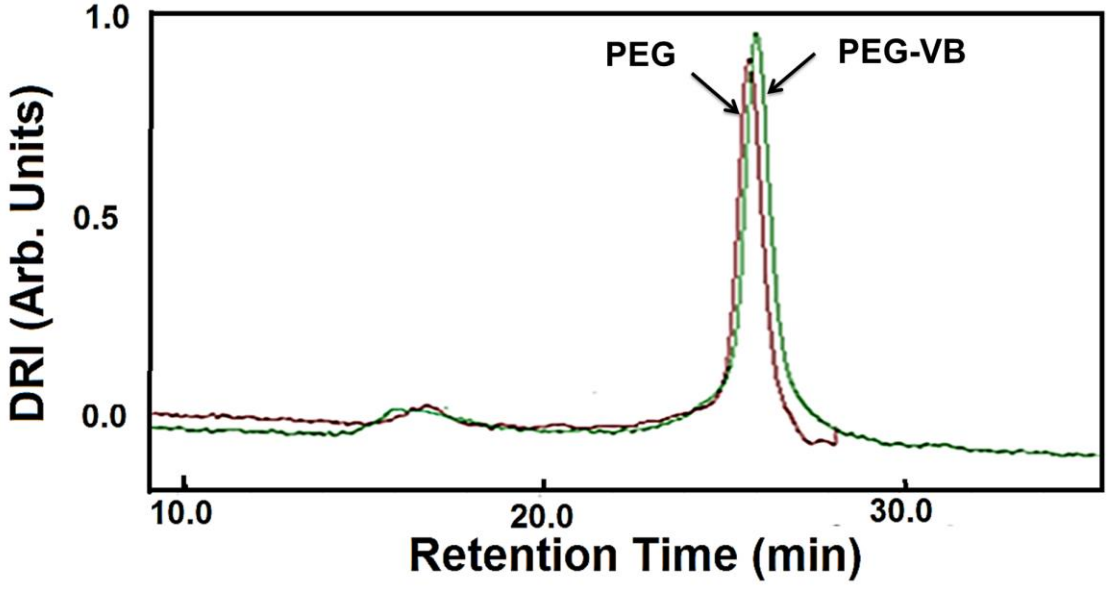

Figure 5.6. SEC traces of PEG_{228}-VB before the addition of *sec*-butyllithium addition and PEG_{228} after *sec*-butyllithium had been added and the VB group had been lost.

5.5 Conclusions

In this investigation, a new method has been developed for the synthesis of PEG-*b*-P(HEMA-TMS) by anionic polymerization. This method involves the preparation of the PEG-DPE macroinitiator by the reaction of the oxyanion at one end of the PEG chain with DPE-Br. Since the DPE group does not undergo homopolymerization, impurities in the initiation system were titrated with 3-methyl-1,1-diphenylpentyl lithium without affecting the integrity of the latent PEG-DPE macroinitiator. This titration process was followed by the *in situ* generation of the active macroinitiator, anionic PEG-DPE, by the reaction of the PEG-DPE with *sec*-butyllithium. This macroinitiator was subsequently reacted with HEMA-TMS to synthesize the diblock copolymer PEG-*b*-P(HEMA-TMS). Hydrolysis of the P(HEMA-TMS) block provided PEG-*b*-PHEMA. SEC analysis indicated that the resultant PEG-*b*-PHEMA samples had a PDI of 1.08, as expected of polymers prepared under optimized anionic polymerization conditions. While this method has been used to polymerize only one type of methacrylate monomer as a proof of concept, it could also be used to polymerize other methacrylates as well. In addition, we investigated that PEG-VB as a macroinitiator for the synthesis of the diblock copolymer PEG-*b*-P(HEMA-TMS) is not suitable.

5.6 References

1. van Vlerkin, L, E.; Tushar, K.V.; Mansoor, M. A. *Pharm. Res.* **2007,** *24*, 1405.
2. Inada, Y.; Furukawa, M.; Sasaki, H.; Kodera, Y.; Hiroto, M.; Nishimura, H.; Matsushima, A. *Trends Biotechnol.* **1995,** *13*, 86.
3. Finch, C.A. *Poly(ethylene glycol) Chemistry: Biotechnical and Biomedical Applications.* Plenum Press, New York, 1992.
4. Pluronic. Baden Aniline and Soda Factory -BASF Corporation Germany, accessed 2 February,2013.<http://worldaccount.basf.com/wa/NAFTA/Catalog/ChemicalsNAFTA/pi/BASF/Brand/pluronic>.
5. Attwood, D.; Zhou, Z. Y.; Booth, C. *Expert Opin. Drug Discovery*, **2007,** *4*, 533.
6. Zhou, Z.; D'Emanuele, A.; Lennon, K.; Attwood, D. *Macromolecules*, **2009,** *42*, 7936.
7. Anushree, Datta. (2007). *Characterization of Polythylene Glycol Hydrogels for Biomedical Applications*. Master Thesis, Louisiana State University.
8. Kissel, T.; Li, Y. X.; Unger, F. *Adv. Drug Deliv. Rev.* **2002,** *54*, 99.
9. Suzuki, T.; Muarakami, Y.; Takegami, Y. *Polym. J.* **1980,** *12*, 183.
10. Fetters, L. J. *J. Poly. Sci. pol. Sym.* **1969,** *26*, 1.
11. Seiler, E.; Fahrenbach, G.; Stein, D.; Ger. Pat. 2237954, BASF AG (1972), *Chem. Abstract*. 81, 13978x, **1974**.
12. Garg, D.; Horning, S.; Ulbricht, J. *Makromol. Chem. Rapid. Commun.* **1984,** *5*, 615.
13. Reuter, H.; Berlinova, I.V.; Horing, S.; Ulbricht, J. *Eur. Polym. J.* **1991,** *27*, 673.
14. Schacher, F.; Muller, M.; Schmalz, H.; Muller, A.H. *Macromol. Chem. Phys*. **2009,** *20*, 256.
15. Amiji, M.M. *Nanotechnology for Cancer Therapy*. CRC Press, USA, 2006.
16. Evans, A. G.; George, D. B. *J. Chem. Soc.* **1962,** 141.

17. Evans, A. G.; George, D. B. *J. Chem. Soc.* **1961,** 4653.

18. Quirk, R.P.; Yoo, T.; Lee, Y.; Kim, J.; Lee, B. *Adv. Polym. Sci.* **2000,** *153,* 67.

19. Zhao, Y.; Higashihara, T.; Sugiyama, K.; Hirao, A. *Macromolecules,* **2007,** *40,* 228.

20. Hirao, A.; Kato, H.; Yamaguchi, K.; Nakahama, S. *Macromolecules,* **1986,** *19,* 1294.

21. Kenji, S.; Yasunori, K.; Tomoya, H.; Youling, Z.; Akira, H. *Monatsh. Chem.* **2006,** *137,* 869.

22. Antoun, S.; Wang, J. S.; Jerome, R.; Teyssie, P. *Polymer*, **1996,** *37*, 5755.

23. a) Ito, K.; Tsuchida, H.; Hayashi, A.; Kitano, T.; Yamada, E.; Matsumoto, T. *Polym. J.* **1985,** *17,* 827. b) Mahajan, S.; Renker, S.; Simon, P. F. W.; Gutamann, J.S.; Jain, A.; Grunder, S. M.; Fetters, L. J.; Coates, G. W.; Weisner, U. *Macromol. Chem. Phys*. **2003,** *204*, 1047.

Chapter 6 – Conclusions and Future Work

6.1 Conclusions

The aim of this research was to develop new methodologies for the synthesis of novel block copolymers using ATRP and anionic polymerization techniques, along with post-polymerization modifications. Both multi-responsive and multiply stimulable block copolymers were prepared, and their stimuli-driven responses were investigated. We also prepared cotton coatings from the aqueous solutions of dual light-responsive block copolymers and investigated their water- and oil-repellent properties. Furthermore, a new method was developed for the preparation of poly(ethylene glycol)-*block*-poly(hydroxyethyl methacrylate) (PEG-*b*-PHEMA) via anionic polymerization.

In Chapter 2, we described the successful preparation of a novel dual light-responsive triblock copolymer, PEG-*ONB*-PFOEMA-*b*-PCEMA (P1). This triblock copolymer is exciting in several ways. Firstly, a dual light-responsive block copolymer incorporating both a photo-crosslinkable block and a photo-cleavable junction had never been reported before. Secondly, this triblock copolymer had a unique block sequence so that upon micellization in THF/water at f_{H2O} = 80%, the copolymer yielded spherical micelles consisting of PEG as the corona, PFOEMA as the shell and PCEMA as the micellar core. Upon photolysis, the PEG chains became cleaved at the *ONB* junction, so that the PFOEMA chains were left exposed. Thirdly, the synthesis of block copolymers incorporating a fluorinated polymer as the central block is highly challenging, and thus investigations of these copolymers are rare. In this study, ATRP was used to prepare P1, and the copolymer was obtained with a low PDI of 1.1 and at the designed molecular weight of 18,200 g/mol. Spherical micelles of the triblock copolymer were

prepared in THF/water at f_{H2O} = 80% and were probed via AFM and TEM techniques. These micelles had average AFM and TEM diameters of 31 ± 5 and 18 ± 4 nm, respectively. The stimuli-responsive behaviour was examined by exposing micellar solutions of P1 to light, which triggered the simultaneous crosslinking of the PCEMA block and cleavage of the PEG chains at the *ONB* junction. This cleavage of the PEG chains left these crosslinked particles with exposed PFOEMA chains on their surfaces. Consequently, films of these particles that were cast from a TFT dispersion exhibited both superhydrophobic and oleophobic properties.

Chapter 3 described the preparation of a series of two doubly stimulable PEG-*S*$_2$-PFOEMA-*b*-PCEMA block copolymers via a facile synthetic approach. First, two Py-*S*$_2$-PFOEMA-*b*-PHEMA copolymers with different block ratios were prepared via ATRP. In the next step, Py-*S*$_2$-PFOEMA-*b*-PHEMA was coupled with PEG-SH. The doubly stimulable triblock copolymers PEG_{113}-*S*$_2$-$PFOEMA_{12}$-*b*-$PCEMA_{60}$ (P2) and PEG_{113}-*S*$_2$-$PFOEMA_{12}$-*b*-$PCEMA_{60}$ (P3) were obtained upon the cinnamation of the PHEMA block. Both P2 and P3 were carefully characterized by ^{1}H NMR and SEC analysis. The PDIs of P2 and P3 were 1.15 and 1.2, respectively, in terms of PS standards. These low PDI values demonstrated the controlled synthesis of these triblock copolymers. Spherical micelles were prepared at f_{H2O} = 80% in THF/water and were characterized via AFM and TEM techniques. The average AFM diameter of these micelles was 60 ± 2 nm, while the average TEM diameter was 32 ± 3 nm. In addition, PEG-cleft particles were prepared by crosslinking the micelles and subsequently cleaving their PEG corona chains upon exposure to the reducing agent DTT. Subsequently, cast film of PEG-cleft particles was water- and oil-repellent for having exposed PFOEMA chains. It is noteworthy that P2 and P3 differed from the dual light-responsive triblock copolymer P1 in many aspects. Firstly, P2 and P3 were doubly stimulable on account of the PCEMA block and disulfide junction, which responded to light and reducing agents, respectively. In contrast, both

the PCEMA block and the *ONB* linker incorporated into P1 were light-responsive only. Secondly, PEG cleavage from P2 and P3 occurred within minutes under reducing conditions. In contrast, a slow cleavage of the PEG chains was observed upon irradiation of P1. This rapid cleavage of the PEG chains from P2 and P3 will help to enhance the viability of these doubly stimulable copolymers for large scale applications. In this study, we also explored PFOEMA as a macroinitiator for the synthesis of the diblock copolymer PFOEMA-*b*-PCEMA. This strategy will also help to open new synthetic routes for the preparation of multiply stimulable diblock and triblock copolymers incorporating a PFOEMA block.

Chapter 4 was focussed on the development of a new method for coating cotton fibers with P1 and other diblock copolymer for imparting them with water- and oil-repellent properties. In literature there are reports on cotton coatings prepared from solutions of fully dissolved block copolymers[1], but the concept of utilizing micellar block copolymer solutions to prepare cotton coatings is a new concept and has many advantages. Firstly, the coatings were prepared in aqueous solutions and thus this protocol was environmentally-friendly and cost-effective. Secondly, light was used as a clean and non-invasive triggering agent to crosslink P1 and anchor it onto the cotton. Thirdly, the coating procedures were simple and easy to perform. For example, they involved the preparation of micellar block copolymer dispersions, and subsequently soaking cotton samples in these dispersions for a few minutes, thus allowing P1 to graft onto the cotton fibers. Thermal annealing provided a uniform layer of PCEMA around the fiber so that upon UV exposure, the PCEMA block became crosslinked around the cellulose fibers. Meanwhile, the PEG chains were photo-cleaved, and thus left behind exposed PFOEMA domains on the surfaces of the cotton fabrics that rendered them highly water- and oil-repellent. Fourthly, remarkable superhydrophobic and oleophobic properties were obtained with a low

grafting density (~0.4 wt.%) of the coating material. Finally, the obtained coatings were durable against washing with aqueous detergents or extraction against organic solvents.

In Chapter 5, we discussed a new method for the synthesis of a very important class of block copolymers, PEG-*b*-P(HEMA-TMS). Various researchers had previously attempted to synthesize PEG-based block copolymers incorporating PMMA, PDMAEMA or other polyacrylates by anionic polymerization, but were unsuccessful for various reasons.[2] We developed a new method for the synthesis of PEG-*b*-P(HEMA-TMS) by anionic polymerization. A PEG-DPE macroinitiator was synthesized and subsequently converted into an active initiator by reaction with *sec*-butyl lithium. Consequently, the active initiator underwent polymerization with HEMA-TMS, to yield PEG-*b*-P(HEMA-TMS). Upon post-polymerization modifications, PEG-*b*-PHEMA was obtained with a low PDI value of 1.08. This method has great potential for the synthesis of PEG-based block copolymers bearing polyacrylate and polymethacrylate blocks. Also, this strategy can be used for the synthesis of BAB and ABC triblock copolymers by respectively using DPE-PEG-DPE and PEG-DPE as the macroinitiator, where A represents the PEG block. In addition, copolymers obtained via anionic polymerization do not have the foul odours or metallic residues typically encountered among copolymers prepared via RAFT or ATRP, respectively. This would also enhance the commercial viability of copolymers prepared through this strategy.

6.2 Future Work

As described in Chapter 4, the coatings prepared from aqueous solutions of P1 containing 10 wt.% of the DMP additive showed remarkable properties. However, the preparation of P1 involved a multi-step synthesis and thus was costly. To enhance the viability of these coatings for large scale applications, we attempted to utilize the diblock copolymer P6

as a coating material (see Appendix A). However, the resultant P6-based coatings showed poor performance. In particular, these coatings exhibited poor stability against detergent washings. Therefore, several new strategies are proposed in this section for the generation of stable and cost effective amphiphobic cotton coatings.

6.2.1 Facile Coating Strategy with Non-Cleavable PEG-*b*-PFOEMA-*b*-PCEMA and PCEMA-*b*-PEG-*b*-PFOEMA Copolymers

PEG-*b*-PFOEMA-*b*-PCEMA triblock copolymer that does not incorporate any cleavable blocks can be useful for the cotton coatings. We believe that the annealing treatment following the coating application is a crucial step, as it induces the phase separation of the PCEMA, PFOEMA, and PEG chains. The hydrophobic PCEMA domains will occupy the immediate layer surrounding the cotton fibers, since the coating application will have been performed from aqueous solutions. However, we expect that the PCEMA and PEG domains might approach one another due to the potential interactions between the ester bonds of PCEMA and ether linkages of PEG. In contrast, PFOEMA should show strong segregation from both the PEG and PCEMA domains. Thus, the anticipated chain packing after annealing treatment might resemble that displayed in Figure 6.1A.[3] Meanwhile, the PFOEMA chains will form the outer-most layer due to the low surface energy of the fluorinated materials.[4]

Alternatively, a triblock copolymer incorporating a central PEG block (i.e. PCEMA-*b*-PEG-*b*-PFOEMA) may also provide a promising candidate for coating applications. Here, the block sequence will further facilitate the appropriate chain packing that is crucial for amphiphobic coatings, by placing PFOEMA as the exposed layer in a similar manner to that depicted in Figure 6.1B.[3] A key advantage for using PCEMA-*b*-PEG-*b*-PFOEMA and PCEMA-*b*-PEG-*b*-PFOEMA is the low cost associated with these materials. These triblock copolymer

bearing conventional non-cleavable junctions require fewer synthetic steps than are needed to prepare P1. Therefore, the synthesis of these copolymers will easier and cheaper than that required for P1.

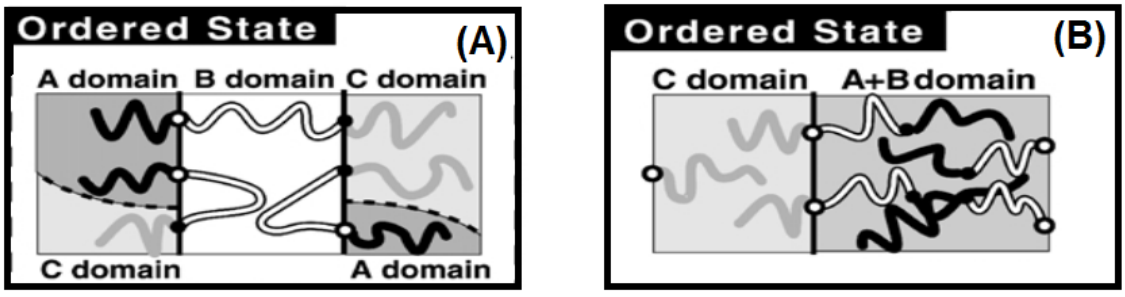

Figure 6.1. Possible chain packing patterns of two different systems. Scheme A depicts an ABC triblock copolymer in which the A and C blocks are more compatible with each other than with the middle B block. Scheme B depicts an ABC block copolymer in which the A and B blocks are more miscible with each other than with the terminal C block. Reprinted from Synthesis and morphological studies of polyisoprene-*b lock*-polystyrene-*b lock*-poly(vinylmethyl ether) triblock terpolymer, Yamauchi, K.; Hasegawa, H.; Hashimoto, T.; Kohler, N.; Knoll, K. *Polymer,* vol. 43, p. 3563, 2002, with permission from Elsevier.

6.2.2 Fabrication of Cotton Coatings using PEG_{113}-CH=N-$PFOEMA_{12}$-*b*-$PCEMA_{25}$ as a pH- and Light-Responsive Triblock Copolymer

This method involves the use of a pH-sensitive linker that will be strategically placed at the junction between the PEG and PFOEMA blocks in the copolymer PEG-CH=N-PFOEMA-*b*-PCEMA. As shown in Scheme 6.1, the preparation of NH_2-PFOEMA-*b*-PCEMA and PEG-CHO is required before they are coupled together in a basic solution (pH = 9.0) to yield a doubly stimulable triblock copolymer, PEG-CH=N-PFOEMA-*b*-PCEMA. This triblock copolymer should provide a promising candidate for amphiphobic cotton coatings that can be prepared from aqueous solutions. The PEG chains will eventually be cleaved from the coated samples via rinsing in an acidic medium (pH = 5.0). This cleavage would leave the PFOEMA chains exposed on the surface, and thus impart the coatings with amphiphobic properties.[5] This method

could be superior to the P1 based coating in terms of expected facile cleavage of PEG chains in an acidic medium.

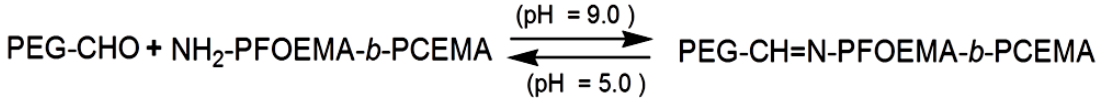

Scheme 6.1. The preparation of a dynamic pH- and light-responsive triblock terpolymer.

6.2.3 Non-Polymeric Substances as Potential Candidates for Cotton Coatings

We propose a new strategy that is based on the chemical grafting of non-polymeric coating materials through ester bond formation. Liu *et al.*[1] demonstrated the use of sol-gel chemistry for the preparation of amphiphobic coatings using PIPSMA-*b*-PFOEMA. However, the siloxane bonds are unstable in aqueous media at temperatures exceeding 40 ^{o}C.[6] Consequently, these coatings can become unstable under certain conditions. Therefore, a facile strategy (Scheme 6.2) is proposed here that may provide a potential remedy for this instability. This strategy involves the synthesis of a trisubstituted benzenoic acid that possesses long perfluoroalkyl chains.[7] In the next step, carboxylic acid functional group will be converted into its phthalimide derivative.[8] This reactive phthalimide derivative will subsequently undergo reaction with the OH groups of cellulose to anchor the coating material onto the cotton. This strategy has several potential advantageous over the P1 coating strategy described in Chapter 4. Firstly, the chemistry involved is simple and reproducible. Secondly, the anticipated coating will be very stable against washing on account of the stable ester bonds. Thirdly, the materials proposed for this project are very cheap, and thus this process can be readily scaled-up. Finally, benzene substituted with perfluoroalkyl chains at the 3, 4 and 5 positions should help to impart water- and oil-repellent properties because of their spatial orientations.

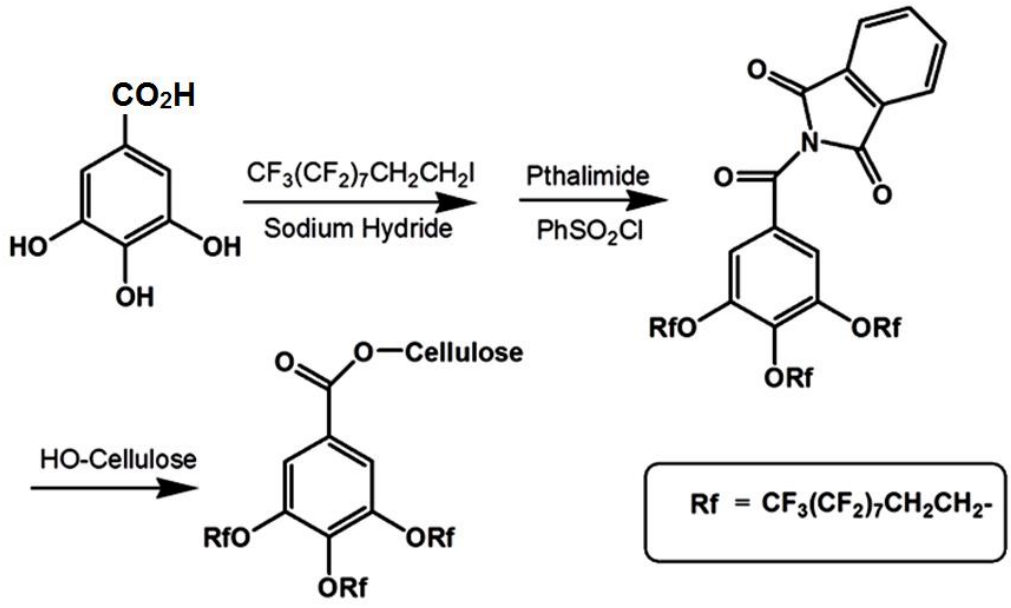

Scheme 6.2. Steps required for the synthesis and grafting of fluorinated molecules onto cellulose.

6.2.4 Proposed Chemical Grafting of PFOEMA onto Cotton using PAA as a Crosslinker

Another method that is of worth attempting involves the grafting of PFOEMA onto cellulose fibers in the presence of PAA as a crosslinker. The chemistry involved in this strategy is depicted in Scheme 6.3. This method has been adapted from the grafting of other substances onto cellulose using crosslinking agents endowed with many carboxylic acid groups.[9-11] The incorporation of many hydroxyl groups at the end of the PFOEMA homopolymer will help to obtain coatings from aqueous medium. Also, providing the homopolymer with numerous hydroxyl groups will increase the statistical probability that the PFOEMA chains will undergo efficient grafting to the cellulose via multiple bonds. The coatings prepared through this strategy will have several advantages. Firstly, the synthesis of PFOEMA and PAA homopolymers are more convenient than the preparation of diblock and/or triblock copolymers.

Secondly, a durable coating is expected because the anchoring would rely on ester bonds that should be stable against rigorous conditions such as hot aqueous detergent solutions.

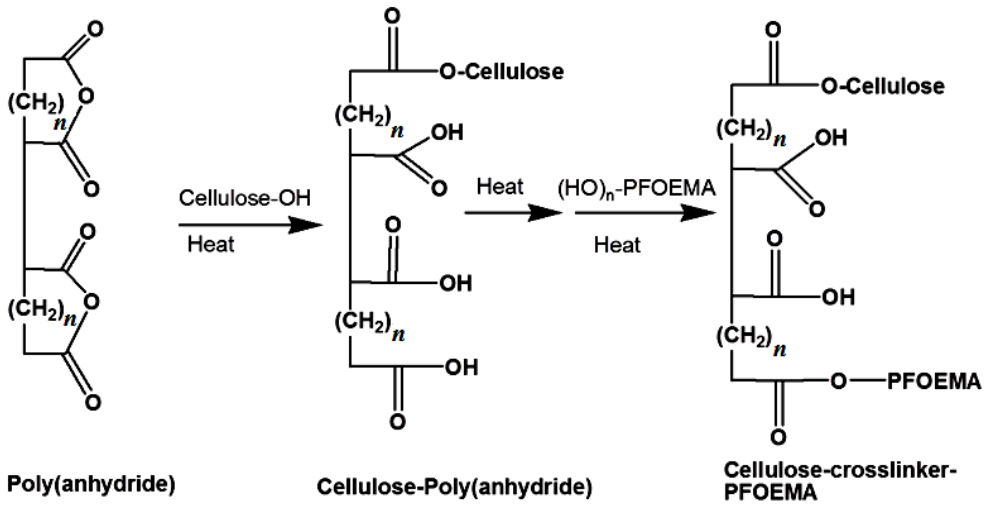

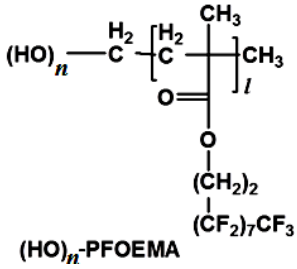

Scheme 6.3. Grafting of PFOEMA onto cellulose using PAA as a crosslinking reagent.

6.3 References

1. Xiong, D.; Liu, G.; Duncan, E. J. S. *Langmuir*, **2012,** *28*, 6911.
2. Suzuki, T.; Muarakami, Y.; Takegami, Y. *Polym. J.* **1980,** *12*, 183.
3. Yamauchi, K.; Hasegawa, H.; Hashimoto, T.; Kohler, N.; Knoll, K. *Polymer*, **2002,** *43*, 3563.
4. Li, K.; Wu, P.P; Han, Z.W. *Polymer*, **2002**, *43*, 4079.
5. Xu, X.; Flores, J. D.; McCormick, C.L. *Macromolecules,* **2011,** *44,* 1327.
6. Smith, E. A.; Chen, W. *Langmuir*, **2008,** *24,* 12405.
7. Lehmann, M. *Chem. Eur. J.* **2009,** *15*, 3638.
8. Chiriac, C. I. *Rev. Roum. Chim.* **1987,** *32,* 793.
9. Martel, B.; Weltrowski, M.; Ruffin, D.; Morcellet, M. *J. Appl. Polym. Sci.* **2002,** *83*, 1449.
10. Weltrowski, M.; Martel, B.; Morcellet, M. Patent PCT 00378, 2000.
11. Martel, B.; Morcellet, M.; Ruffin, D.; Weltrowski, M. *Proceedings of the 10th International Symposium on Cyclodextrins,* Ann Arbor, Michigan, 2000.

Appendix A – Cotton Coating with PS-*b*-PCEMA, P*t*BA-*b*-PCEMA and Py-S_2-PFOEMA-*b*-PCEMA

A1. PS-*b*-PCEMA (P4), P*t*BA-*b*-PCEMA (P5) and Py-S_2-PFOEMA-*b*-PCEMA (P6)

P4 and P5 Block copolymers have been reported in different studies, and used here without further modifications.[1,2] While, the third block copolymer Py-S_2-PFOEMA$_{12}$-*b*-PCEMA$_{60}$ (P6) was synthesized by a procedure described in Chapter 3, sections 3.3.5, 3.3.6 and 3.3.8. The molecular properties of all these polymers are shown in Table 4.1.

A2. Preparation of Cotton Coatings from P4 and P5

Micellar dispersions of P4 and P5 were prepared as follows. For P4, the copolymer was initially dissolved in THF and then cyclopentane was added, which is a block selective solvent for the PS. Micelles formed at a cyclopentane volume fraction (f_{cp}) of 75%. Similarly, the micellar solutions of P5 were prepared by initially dissolving the copolymer into THF. Methanol, a selective solvent for P*t*BA, was subsequently added until a ($f_{methanol}$) of 50% was obtained. The rest of coating procedure was identical to that used to prepare coatings from P1 aqueous solutions, described in the Chapter 4.

A3. Preparation of Cotton Coatings from P6

P6 (20 mg) was mixed with PEG monolaurate (2.0 mg, 10 wt.% with respect to the P6) and dimethylphtahalate (3.0 mg, 15 wt.%). Water was added until the final copolymer concentration reached the pre-designated concentrations of 5, 10, and 15 mg/mL. The mixture was stirred until most of the copolymer was dispersed and the solution turned milky in

appearance. The rest of coating procedure was identical to that used to prepare coatings from P1 aqueous solutions, described in the Chapter 4.

A4. Assessment of Coating Properties obtained from P4 and P5 Solutions

Two non-fluorinated copolymers, P4 and P5 were used to prepare cotton coatings. In the case of P4, the micelles were prepared in THF/cyclopentane solvent mixtures, where cyclopentane is a block selective solvent for PS. The PCEMA block was insoluble in THF/cyclopentane, and became attached to cellulosic fibers via van der Waal's forces. Following a similar procedure that was used for coating fabrics with P1 (described in the section 4.3.3 of the Chapter 4), the samples coated with PS-*b*-PCEMA were exposed to UV light. Similarly, micellar solutions of P*t*BA-*b*-PCEMA in THF/methanol were also used to coat cotton. Here, methanol is a block selective solvent for the P*t*BA block.

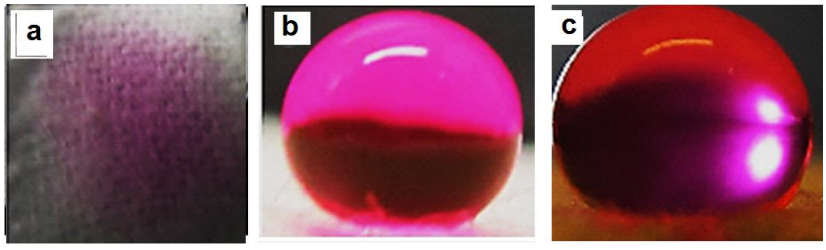

Figure A1. Images of water droplets placed on uncoated cotton (a), a cotton sample coated with P4 (b), and a cotton sample coated with P5. Images were recorded after 2 min of applying water droplet.

Figure A1 compares images recorded during wettability tests results involving water droplets. The results showed that the samples coated with P4 and P5 were hydrophobic. However, coated fabrics were not repellent to diiodomethane because of the oleophilic nature of the PS and P*t*BA chains. We did not investigate the coating properties of these two block

copolymers in detail as they were not the main focus of this research. Table A1 compares the water repellency for cotton samples coated with P4 and P5 before and after washing with detergents. It shows that the coating was hydrophobic before and after washing with detergents for 24 h.

Table A1. Properties of cotton samples that had been coated with P4 and P5.

Polymer	Water Repellency	Diidomethane Repellency	Washing Durability (after 24 h)
PS-*b*-PCMEA (P4)	Very high	0	No Obvious Change
PCEMA-*b*-PtBA (P5)	High	0	No Obvious change

A5. Assessment of Coating Properties of P6

P1 based coating described in the Chapter 4 of this thesis showed remarkable water and oil repellent properties. However, the synthesis of P1 is costly and challenging. Therefore, Py-S_2-PFOEMA-*b*-PCEMA or P6 was selected as new coating material to coat textiles. There are many reasons for using P6 as substitute to P1. Firstly, P6 incorporates a crosslinkable PCEMA block, which allows the stable grafting of this copolymer onto the cotton. Secondly, the PFOEMA block of P6 should remain on the surface of coated samples and render them with amphiphobic properties. Finally, the synthesis of P6 synthesis is relatively cheaper to perform on larger scales. However, P6 is insoluble in water but fully soluble in certain organic solvents such as THF. For coating purposes, a useful solvent would be one that could selectivity dissolve the PFOEMA block. This is technically possible with TFT and with supercritical CO_2 ($ScCO_2$). However, TFT is an expensive solvent and is thus not suitable. Meanwhile, $ScCO_2$ demands high pressure system that will make the coating difficult on larger scales.

Therefore, a detour was taken to solubilize P6 polymer in a mixture of water and PEG monolaurate, which was used as a surfactant. Also, DMP was added to increase the mobility of the polymer chains. For this purpose, three different solutions were prepared whose compositions are summarized in Table A2. The images of these solutions just before cotton soaking are displayed in Figure A2. Emulsions were formed by solutions **a** and **b** only. Notably, **a** and **c** varied only in the concentration of DMP, but the visual properties of these solutions differs greatly.

Table A2: Compositional analysis of the solutions prepared from P6

Sample	Surfactant[a]	Plasticizer[a]	Solution final conc.	Solvent composition
a	10%	15%	15 mg/ml	Aqueous solution
b	10%	15%	15 mg/ml	H_2O:THF(95/5)
c	10%	4%	15 mg/ml	Aqueous solution

[a]Relative to P6 by wt.%

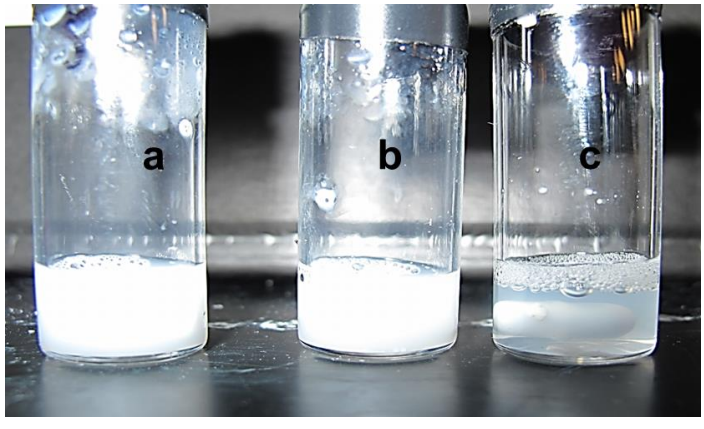

Figure A2. Images of solution **a**, **b**, and **c** prepared for coating using P6.

The above solutions were used for fabricating cotton by immersing the cotton samples into these solutions for different intervals of time, and the coated samples were brought to drop tests. The results from these tests are summarized in Table A3. The cotton samples coated with solution **c** were amphiphilic as water drop drifted-into cotton. Interestingly, the coatings obtained from solutions **a** and **b** were amphiphobic, showing higher contact angle for both water and diiodomethane. To examine the stabilities of these coatings, cotton samples coated with solutions **a** and **b** were subjected to a detergent washing test. After 12 h of washing with 5% detergent solutions, these samples lost the hydrophobicity as shown in Table A2. These findings suggest that the coatings obtained from the diblock copolymers via the current approach are not a desirable.

Table A3. Properties of P6-coated cotton samples those were prepared under various conditions.

Sample	Coating time (min)	Extracted with THF	Amphiphobicity Tests	After washing (12 h with 5% detergents)
a	3	2 hrs@50C	Amphiphilic	NA
	15	2 hrs@50C	Amphiphobic	**Amphiphilic**
b	3	2 hrs@50C	Amphiphobic	**Amphiphilic**
	15	2 hrs@50C	Amphiphobic	**Amphiphilic**
c	3	2 hrs@50C	Amphiphilic	NA
	15	2 hrs@50C	Amphiphilic	NA

A6. References:

1. Roy, X.; Hui, J. K. H.; Rabnawaz, M.; Liu, G.; Maclachlan, M. J. *J. Am. Chem. Soc.* **2011,** *133,* 8420.

2. Li, X.; Liu G. *Langmuir*, **2009,** *25,* 10811.

Appendix B – AFM Analysis of P1 Coated Fibers

Here, we describe the AFM analysis of P1 dispersions and of cotton samples during various stages of their coating with P1. Figure B1a shows an AFM image of micelles that had formed in a 100% aqueous solution and subsequently aero-sprayed on mica surface. The cotton samples that were coated with solutions of these P1 micelles were clearly visible on the surface of the coated fibers, as shown in Figure B1b. The presence of these micellar structures on the cotton surface demonstrates that the P1 micelles became adsorbed onto the fibers, as anticipated. Interestingly, after the coated cotton samples had been annealed, they were still covered with micelles, as demonstrated by the AFM image in Figure B1c. However, annealing did help to some extent to generate a partial layer, which was evident from the height of the grafted P1 layer, which was reduced from that visible before annealing treatment. These finding suggest that P1 had become grafted onto the cotton samples as micelles, but may have become partially dissociated during annealing treatment to yield a layer of unimers surrounding the cotton fibers.

Meanwhile, AFM samples that were dispersed from aqueous P1 solutions that contained 10 wt.% DMP did not show any micelles, as shown in Figure B2a. Similarly, cotton samples that were coated with these DMP-containing P1 solutions had smooth surfaces and did show any evidence of micelles, as seen in Figure B2b. This indicates that the DMP additive caused P1 to exist as individual unimer chains in these solutions with collapsed PFOEMA and PCEMA blocks. Consequently, P1 became adsorbed onto the cotton fibers as unimers rather than as micelles if DMP was present in the coating solution.

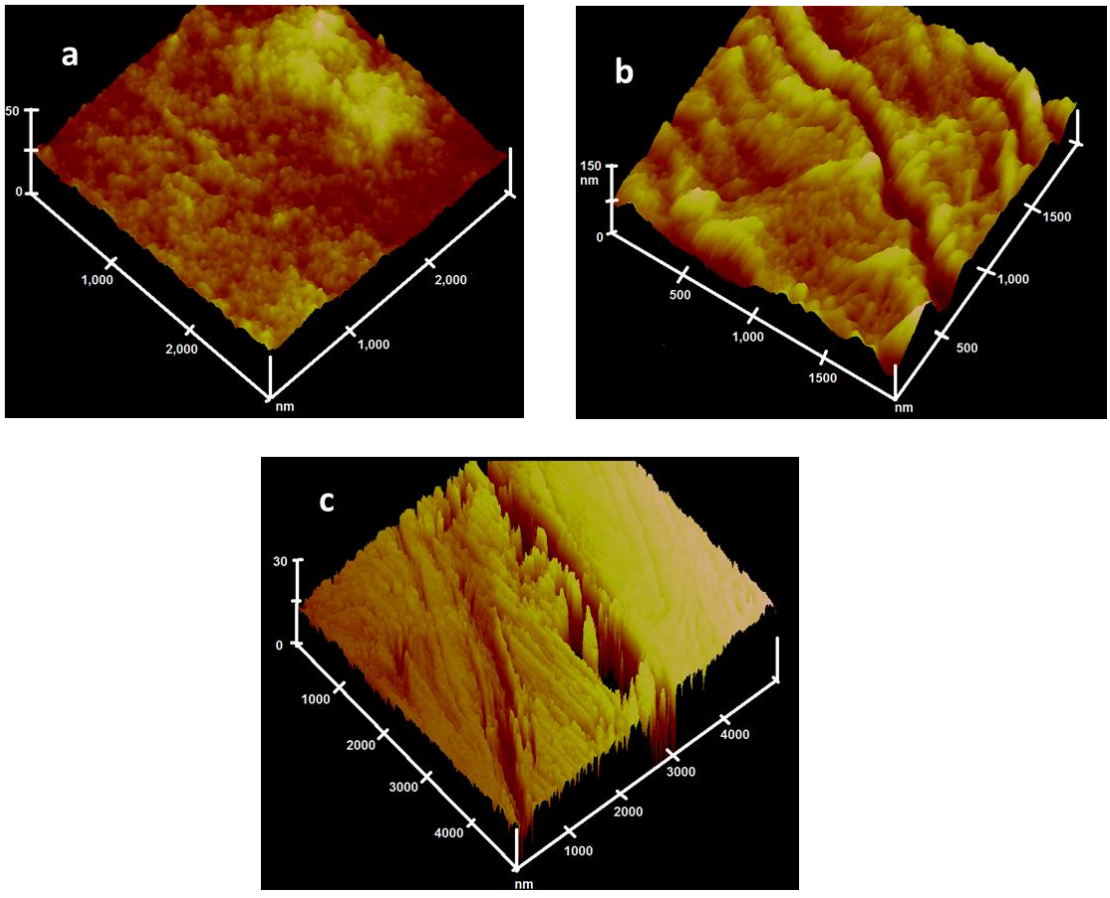

Figure B1. AFM images of aqueous P1 solutions (a), P1-coated cotton before annealing treatment (b), and a P1-coated cotton sample after annealing treatment (c).

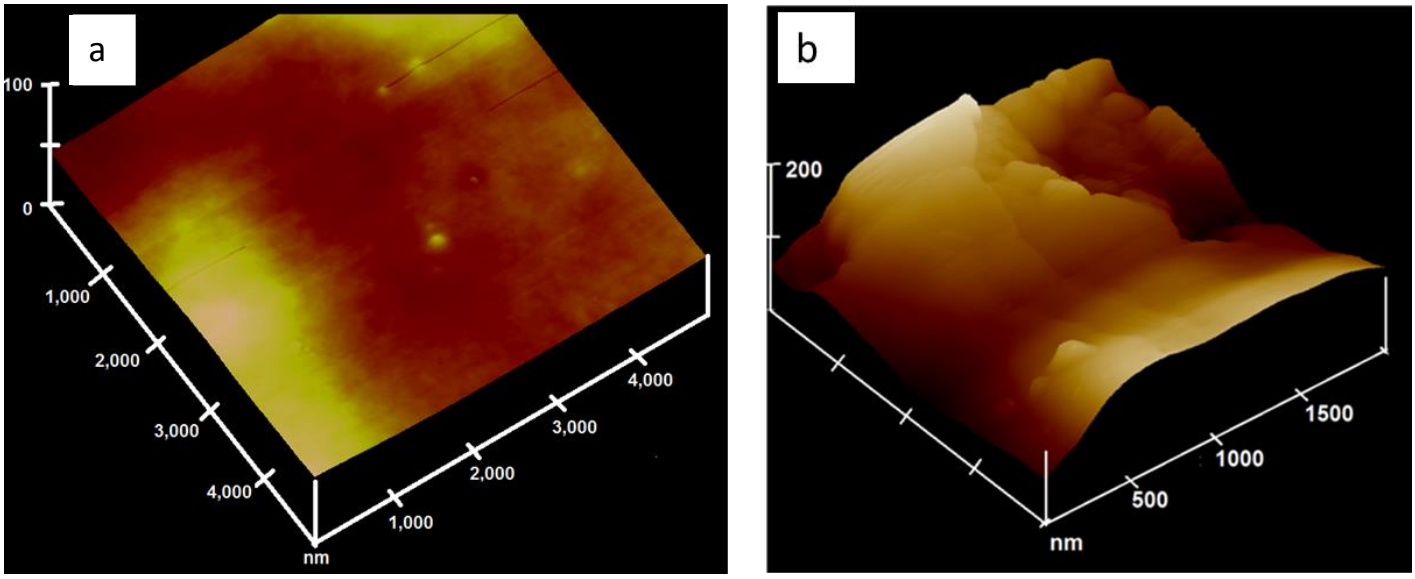

Figure B2. AFM images of samples collected from aqueous P1 aqueous solutions containing 10 wt.% DMP (a) and from a P1-coated cotton fiber after annealing treatment (b). This cotton sample had been coated by immersion into an aqueous P1 solution containing 10 wt.% DMP.

Appendix C - List of Publications

Articles under Preparation:

1. **Rabnawaz, M.;** Liu, G. "Poly(ethylene glycol) and Poly(methacrylate) Diblock Copolymer from Anionic Polymerization".
2. **Rabnawaz, M.;** Liu, G. "Synthesis and Application of Doubly Stimulable Triblock Terpolymers"
3. **Rabnawaz, M.;** Liu, G. "A Green Approach Towards Cotton Coatings: Superhydrophobic and Oleophobic Cotton Coatings Prepared from Aqueous Dispersions of a Dual Light Responsive Triblock Terpolymer"

Articles Published:

4. **Rabnawaz, M.;** Liu G. Preparation and application of a dual light-responsive triblock terpolymer. *Macromolecules*. **2012**;45(13). doi: 10.1021/ma3006476.
5. Roy, X.; Hui, J.K.; **Rabnawaz, M**.; Liu, G.; MacLachlan M.J. Prussian blue nanocontainers: Selectively permeable hollow metal-organic capsules from block lonomer emulsion-induced assembly. *J. Am. Chem. Soc*. **2011**;133(22). doi: 10.1021/ja2016075.
6. Roy, X.; Hui, J.K.; **Rabnawaz, M**.; Liu, G.; MacLachlan M.J. Soluble prussian blue nanoworms from the assembly of metal-organic block ionomers. *Angew. Chem. Int. Ed*. **2011;** 50(7). doi: 10.1002/anie.201005537.

7. **Rabnawaz, M.;** Ali, Q.; Shah, M.R.; Singh, K. 2,2 '-[biphenyl-2,2 '-diylbis(oxy)]diacetic acid monohydrate. *Acta Crystallographica Section E-Structure Reports Online*. **2008**, 64. doi: 10.1107/S160053680802833X.